eman ta zabal zazu

Universidad del País Vasco
Euskal Herriko Unibertsitatea

Universidad del País Vasco / Euskal Herriko Unibertsitatea
Facultad de Medicina y Enfermería
Departamento de Neurociencias

MICROGLIAL PHAGOCYTOSIS: UNRAVELING THE ROLE OF GPR34-LYSOPS SIGNALING AND PHAGOCYTIC MICROGLIA ON METABOLISM AND NEUROGENESIS

Tesis doctoral para optar al grado de Doctor, presentada por:

Víctor Sánchez Zafra

2019

Directora de Tesis:

Dra. Amanda Sierra Saavedra

TABLE OF CONTENTS

TABLE OF CONTENTS

1. ABBREVIATIONS 3

2. RESUMEN/SUMMARY 14

2.1. RESUMEN 14

2.2. SUMMARY 19

3. INTRODUCTION 27

3.1. INTRODUCTION TO MICROGLIA 27

3.1.1. Definition and origins 27

3.1.2. Microglial functions 27

Synapse monitoring 27

Myelination 28

Vasculogenesis 28

Neurogenesis 28

3.1.3. Immune response 28

3.2. INFLAMMATORY RESPONSE 29

3.2.1. Cytokines 30

3.2.1.1. Pro-inflammatory cytokines 30

TNF-α 31

3.2.1.2. Anti-inflammatory cytokines 33

3.2.2. Chemokines 33

CX3CL1 33

3.3. PHAGOCYTOSIS 35

3.3.1 Phagocytosis of apoptotic cells 37

3.3.2. Stages of phagocytosis 38

"Find-me" stage 39

"Eat-me" stage 39

"Digest-me" stage 40

3.3.3. Phagocytosis receptors 41

GPR34 42

3.3.3.1 GPR34 ligands 42

3.3.3.2 GPR34-related receptors 43

P2Y10 43

GPR174 43

G2A 43

3.3.4. Methods to quantify phagocytosis 45

3.3.5. Downstream consequences of phagocytosis of apoptotic cells 46

3.4. METABOLISM 48

3.4.1. Metabolic pathways in eukaryotic cells 49

3.4.1.1. Cytosolic metabolic pathways 49

Aerobic and anerobic glycolysis 49

Pentose phosphate pathway, gluconeogenesis and other cytosolic pathways 51

3.4.1.2. Mitochondrial metabolic pathways 51

TCA cycle 52

Oxidative phoshorylation (OXPHOS) 52

Other mitochondrial pathways 53

3.4.2. Mitochondria: definition, origin and functions 55

3.4.2.1. Mitochondrial dynamics 55

Fusion 56

Fission 56

Transport 56

Mitophagy 57

3.4.3. Cellular metabolism analysis methods 58

XF Cell Mito Stress Test Kit 59

XF Glycolysis Stress Test Kit 59

3.4.4. Metabolism regulation in macrophages and microglia 60

Metabolism regulation in macrophages 60

Metabolism regulation in microglia 60

3.5. ADULT HIPPOCAMPAL NEUROGENESIS 61

3.5.1. Neurogenic cascade in the SGZ of the hippocampus 62

3.5.2. Function of adult hippocampal neurogenesis 63

Learning and memory 64

Pattern separation 64

3.5.3. Regulation of adult hippocampal neurogenesis 65

Extrinsic regulation of neurogenesis 65

Intrinsic regulation of neurogenesis 66

3.5.4. The role of microglia in adult hippocampal neurogenesis 67

Microglial inflammation and adult hippocampal neurogenesis 68

Microglial phagocytosis and adult hippocampal neurogenesis 68

3.5.5. Methods to assess neurogenesis 68

Nucleotide analogs 69

Genetic tools 69

Specific markers 69

4. HYPOTHESIS AND OBJECTIVES 73

5. EXPERIMENTAL PROCEDURES 78

5.1. ANIMALS 78

5.2. CELL AND ORGANOTYPIC CULTURES 78

5.2.1. Primary microglia cultures 78

5.2.2. BV2 cell line 79

5.2.3. SH-SY5Y cell line 79

5.2.4. Vampire SH-SY5Y cell line 80

5.2.5. Organotypic hippocampal slice cultures 80

5.3. IN VITRO PHAGOCYTOSIS ASSAY 80

5.3.1. Primary microglia 80

5.3.2. BV2 cells 81

5.4. INTRAHIPPOCAMPAL INJECTIONS 81

5.4.1. LysoPS administration 81

5.4.2. Kainate administration 81

5.5. IMMUNOFLUORESCENCE 82

5.5.1. Antibodies 82

5.5.2. Primary microglia and BV2 cell cultures 82

5.5.3. Hippocampal organotypic cultures immunostaining 83

5.5.4. Brain tissue sections immunostaining 83

5.6. PGFP-MITO-7 PLASMID GENERATION 84

5.6.1. Plasmid transformation 84

5.7. TRANSFECTION 85

5.8. IMAGE ANALYSIS 86

5.8.1. Phagocytosis analysis 86

5.8.1.1. Phagocytosis in BV2 cells and primary microglial cultures 86

5.8.1.2. Phagocytosis in hippocampal sections and organotypic cultures 87

5.8.2. Mitochondrial morphology 88

5.9. FACS SORTING 88

5.10. RNA ISOLATION AND RETROTRANSCRIPTION 89

5.10.1. Primary microglia and BV2 cells 89

5.10.2. Tissue 89

5.10.3. FACS-sorted cells 90

5.11. qPCR 90

5.12. METABOLISM ANALYSIS 93

5.12.1. OXPHOS analysis 93

5.12.2. Glycolysis analysis 94

5.13. STATISTICAL ANALYSIS 94

6. RESULTS 99

6.1. MICROGLIAL PHAGOCYTOSIS IS NOT REGULATED BY IMMUNE MEDIATORS TNF-α AND CX3CL1 99

6.1.1. TNF-α microglial deficiency does not impair microglial phagocytosis nor reduce apoptosis in a mouse model of epilepsy 99

6.1.2. CX3CR1 deficiency does not impair microglial phagocytosis in physiological conditions 102

6.2. PHAGOCYTOSIS RECEPTOR GPR34 IS SPECIFIC OF MICROGLIA IN VIVO AND IN VITRO 103

6.2.1. GPR34 is highly expressed in microglia in vivo 103

6.2.2. GPR34 is the predominant lysoPS-associated receptor in microglia in vitro 105

6.3. MICROGLIA PHAGOCYTOSIS IS REGULATED BY GPR34 IN VIVO AND IN VITRO 107

6.3.1. GPR34 deficiency leads to microglial phagocytosis impairment in young mice in vivo 107

6.3.2. GPR34 ligand lysoPS impairs microglial phagocytosis in vitro 115

6.3.3. GPR34 ligand lysoPS impairs BV2 microglia phagocytosis in vitro 117

6.3.4. GPR34 ligand lysoPS impairs microglial phagocytosis in hippocampal organotypic slice cultures 119

6.3.5. GPR34 ligand lysoPS does not impair microglial phagocytosis in vivo 122

6.4. PHAGOCYTOSIS TRIGGERS METABOLIC ADAPTATIONS IN MICROGLIA IN VITRO 125

6.4.1. Glycolysis and OXPHOS genes are not altered in BV2 microglia after phagocytosis 125

6.4.2. Glycolysis is not increased whereas OXPHOS is decreased in BV2 microglia after phagocytosis 130

6.4.3. Mitochondrial morphology is affected in BV2 microglia after phagocytosis 136

6.4.4. Mitochondrial fusion genes remain unaltered but mitochondrial fission genes are affected in BV2 microglia after phagocytosis 138

6.5. PHAGOCYTOSIS IMPAIRMENT DOES NOT LEAD TO ALTERED NEUROGENESIS IN VIVO 141

6.5.1. GPR34 deficiency does not affect newborn cells proliferation in 1 month-old mice 141

6.5.2. GPR34 deficiency decreases mature neuroblasts in 3 month-old mice 148

7. DISCUSSION 155

7.1. CROSSTALK INFLAMMATION-PHAGOCYTOSIS IN MICROGLIA 156

7.1.1. TNF-α does not modulate neither apoptosis nor phagocytosis in vivo 156

7.1.2. CX3CL1 does not regulate phagocytosis of apoptotic cells in vivo 157

7.2. GPR34 AND LYSOPS ON MICROGLIA PHAGOCYTOSIS 159

7.2.1. GPR34 is the sole lysoPS receptor expressed in adult mouse microglia in vivo 159

7.2.2. GPR34 contributes to apoptotic cells clearance in young but not in adult mice 160

7.2.3. LysoPS inhibits microglial phagocytosis in cultures 162

7.2.4. Microglia do not respond to lysoPS in vivo 163

7.3. MICROGLIAL METABOLIC REWIREMENT UPON PHAGOCYTOSIS 164

7.3.1. Phagocytosis does not trigger a metabolic switch to glycolysis in BV2 microglia 165

7.3.2. Phagocytosis disrupts mitochondrial metabolism in BV2 microglia 167

7.4. MICROGLIA AND NEUROGENESIS 168

7.4.1. Phagocytosis does not regulate newborn cells production in the niche of the SGZ 169

8. CONCLUSIONS 176

9. BIBLIOGRAPHY 181

1. ABBREVIATIONS

ABBREVIATIONS

Aβ	Amyloid beta
Acetyl-CoA	Acetyl coenzyme A
Acyl-CoA	Acyl coenzyme A
AD	Alzheimer's disease
ADAM17	ADAM metallopeptidase domain 17
AMPA	α-amino-3-hydroxy-5-methyl-4-isoxazolepropionic acid
ANOVA	Analysis of variance
ANPs	Amplifying neural progenitors
ANXA1	Annexin 1
AP	Anteroposterior
ApoE	Apolipoprotein E
APP	Amyloid precursor protein
ATCC	American Type Culture Collection
ATP	Adenosine triphoshate
BAI-1	Brain-specific angiogenesis inhibitor 1
BBB	Blood brain barrier
Bcl-2	B-cell lymphoma 2
BDNF	Brain-derived neurotrophic factor
BLBP	Brain lipid-binding protein
BrdU	5-bromo-2-deoxyuridine
BSA	Bovine serum albumine
CA	Cornu ammonis
Ca^{+2}	Calcium
CAT	Carnitine translocase
Cd11b	Cluster of differentiation molecule 11b

CD68	Macrosialin
cDNA	complementary DNA
CHO	Chinese hamster ovary
CldU	5-Chloro-2'-deoxyuridine
CMLE	Classic Maximum Likelihood Estimation algorithm
CNS	Central nervous system
CPT-1	Carnitine palmitoyltransferase-1
CRT	Calreticulin
CSFs	Colony stimulating factors
CSF1R	Colony stimulating factor 1 receptor
Ct	Threshold cycle
CX3CL1	Fractalkine
CX3CR1	CX3C chemokine receptor 1
DAP12	DNAX-activation protein of 12 kD
DAPI	4',6-diamidino-2-phenylindole
DCX	Doublecortin
DG	Dentate gyrus
2-DG	2-deoxy-glucose
DMEM	Dulbecco's Modified Eagle Medium
DMSO	Dimethyl Sulfoxide
DNAse	Deoxyribonuclease
Dnm1l	Dynamin 1-like
Dock4	Dedicator of cytokinesis 4
dpi	Day post injection
Drp1	Dynamin-related protein 1
DV	Dorsoventral
E 7.5	Embryonic day 7.5

EBV	Epstein-Barr virus
ECAR	Extracellular acidification rate
ER	Estrogen receptor
ETC	Electron transport chain
F6P	Fructose-6-phosphate
FA	Formaldehyde
FACS	Fluorescence-activated cell sorting
FAD	Flavin adenine dinucleotide
$FADH_2$	Flavin adenine dinucleotide (hydroquinone form)
FBPase	Fructose biphosphatase
FBS	Fetal bovine serum
FCCP	Carbonyl cyanide-p-trifluoromethoxyphenylhydrazone
FIS1	Mitochondrial fission protein 1
G2A	G protein-coupled receptor 132
G3P	Glyceraldehyde-3-phosphate
G6P	Glucose-6-phosphate
G6Pase	Glucose-6-phosphatase
G6PDH	Glucose-6-phosphate dehydrogenase
GABA	Gamma-Aminobutyric acid
GAS6	Growth arrest-specific protein 6
GFAP	Glial fibrillary acidic protein
GFP	Green fluorescent protein
GlycoPER	Glycolytic proton efflux rate
GM-CSF	Granulocyte-macrophage colony stimulating factor
GPR34	G protein-coupled receptor 34
Gpr75	Glucose-regulated protein 75
GPR174	G protein-coupled receptor 174

GTP	Guanosine triphosphate
GTPases	Guanosine triphosphate hydrolases
HAP1	Huntingtin-associate protein 1
HBSS	Hank's Balanced Solution
H_2O	Water
HIF-1	Hypoxia induced factor-1
HIF-1α	Hypoxia induced factor-1 alpha
HSCs	Hematopoietic stem cells
Iba1	Calcium-binding adapter molecule 1
ICAM3	Intercellular adhesion molecule 3
IDH3G	Isocitrate dehydrogenase 3 gamma
IdU	5-iodo-2'-deoxyuridine
IFNs	Interferons
IFN-γ	Interferon gamma
IGF-1	Insulin growth factor 1
ILs	Interleukins
IL-1β	Interleukin 1 beta
IL-4	Interleukin 4
IL-6	Interleukin 6
IL-10	Interleukin 10
IMM	Inner mitochondria membrane
IMS	Intermembrane space
ISCs	Intestinal stem cells
KA	Kainate
KO	Knockout
LB	Lysogeny Broth
LBD	Long-binding domain

LL	Laterolateral
LPA	Lysophosphatidic acid
LPC	Lysophosphatidylcholine
LPS	Lipopolysaccharide
LTP	Long term potentiation
LysoPS	Lysophosphatidylserine
MAM	Methylazoxymeathanol
MCP-1	Monocyte chemotactic protein 1
MEFs	Mouse embryonic fibroblasts
MerTK	Mer tyrosine kinase
MFF	Mitochondrial fission factor
MFG-E8	Milk fat globule-EGF factor 8
MFN1	Mitofusin 1
MFN2	Mitofusin 2
MIC-1	Macrophage inhibitory cytokine 1
MIP-1A	Macrophage-inflammatory protein 1A
MitoPER	Mitochondrial proton efflux rate
MPC1	Mitochondrial pyruvate carrier 1
MS	Multiple sclerosis
mtDNA	Mitochondrial DNA
MTLE	Mesial lobe temporal epilepsy
NAD^+	Nicotinamide adenine dinucleotide (oxidized form)
NADH	Nicotinamide adenine dinucleotide (reduced form)
$NADH_2$	Nicotinamide adenine dinucleotide (reduced form)
NADPH	Nicotinamide adenine dinucleotide phosphate
NDUFAF4	NADH ubiquinone oxidoreductase complex assembly factor 4
NGF	Nerve growth factor

NMDA	N-methyl-D-aspartate
NO	Nitric oxide
NPCs	Neuroprogenitor cells
NSCs	Neural stem cells
OAZ-1	Ornithine decarboxylase antizyme 1
OB	Olfactory bulb
OCR	Oxygen consumption rate
O/N	Overnight
OPA1	Optic atrophy 1
OXPHOS	Oxidative phosphorylation
PBS	Phosphate buffer solution
PC	Pyruvate carboxylase
PCNA	Proliferating cell nuclear antigen
PD	Parkinson's disease
PDH	Pyruvate dehydrogenase
PDHB	Pyruvate dehydrogenase beta
PEPCK	Phosphoenolpyruvate carboxykinase
PER	Proton efflux rate
PFA	Paraformaldehyde
PFKFB3	6-phosphofructo-2-kinase/fructose-2,6-biphosphatase 3
PFKM	6-phosphofructokinase muscle
6PGDH	6-phosphogluconate dehydrogenase
6PGL	6-phosphogluconolactonase
PKC	Protein kinase C
PLAs	Phospholipases
PLA1	Phospholipase A1
PLA2	Phospholipase A2

PND	Postnatal day
PPP	Pentose phosphate pathway
ppu	Parts per unit
PS	Phosphatidylserine
PSA-NCAM	Polysialylated neuronal cell adhesion molecule
Q	Coenzyme Q
Rack1	Receptor for activated C kinase 1
RANTES	Chemokine ligand 5
RFU	Relative fluorescence unit
RMS	Rostral migratory stream
rNSCs	Radial neural stem cells
ROS	Reactive oxygen species
R5P	Ribose-5-phosphate
RT	Room temperature
RT-qPCR	Real Time-Quantitative Polymerase Chain Reaction
Ru5P	Ribulose-5-phosphate
SDHB	Succinate dehydrogenase beta
SEM	Standard error of the mean
SGZ	Subgranular zone
SOC	Super optimal catabolite
S1P	Sphingosine-1-phosphate
SPC	Shingosylphosphorylcholine
STP	Staurosporine
Succinyl-CoA	Succinyl-coenzyme A
SVZ	Subventricular zone
TAE	Tris-acetate-EDTA
TCA	Tricarboxylic acid

TGFs	Transforming growth factors
TGF-β	Transforming growth factor beta
Th1	T helper 1
Th2	T helper 2
TIM-4	T-cell immunoglobulin domain-containing 4
Tm	Melting temperature
TNFs	Tumor necrosis factors
TNF-α	Tumor necrosis factor alpha
TNFR1	Tumor necrosis factor receptor 1
TNFR2	Tumor necrosis factor receptor 2
TREM2	Triggering receptor expressed on myeloid cells-2
UQCRQ	Ubiquinol-Cytochrome C Reductase Complex III Subunit VII
UTP	Uridine triphosphate
UV	Ultraviolet
vATPase	Vacuolar adenosin triphosphatase
VEGF	Vascular endothelial growth factor
VNRs	Vitronectin receptors
VZ	Ventricular zone
Wnt3a	Wingless/integrated 3a protein
WT	Wild type

2. RESUMEN/SUMMARY

2.RESUMEN/SUMMARY

2.1 RESUMEN

Las células de microglía constituyen los macrófagos residentes del sistema nervioso central (CNS). Estas células vigilan constantemente el parénquima cerebral con sus procesos altamente móviles y ayudan a mantener la homeostasis en el tejido cerebral ejerciendo una de sus principales funciones, que es la fagocitosis.

Las células de microglía están consideradas como los fagocitos profesionales del cerebro. Sin embargo, el papel de la microglía en la fagocitosis es en gran medida desconocido. La fagocitosis es el proceso celular de comer y supone un fenómeno crucial durante el desarrollo cerebral y en contextos patológicos. Se ha visto que las células de microglía fagocitan muy diferentes cargas tanto en condiciones fisiológicas como en condiciones patológicas, y en esta tesis, nos hemos centrado en la fagocitosis de células apoptóticas.

La apoptosis o "muerte celular programada" es un fenómeno ubicuo que lleva al mantenimiento de una población celular, como parte normal del desarrollo, que ayuda a preservar la homeostasis tisular y que ha sido visto también en patología. Una limpieza eficiente de células apoptóticas resulta fundamental para evitar la liberación de contenidos intracelulares tóxicos. Para posibilitar una limpieza eficaz de células apoptóticas, las células de microglía presentan una gran variedad de receptores anclados a la membrana que ayudan a detectar y reconocer las diferentes moléculas liberadas por las dianas apoptóticas, incluyendo señales "encuéntrame" y "cómeme". Una vez esas señales son reconocidas por la microglía, las células apoptóticas son englobadas en un fagosoma que en última instancia se fusiona con lisosomas, permitiendo la degradación completa de la carga por el fagocito.

Durante los últimos años, el papel de la microglía en la fagocitosis ha sido estudiado muy bien en la región subgranular (SGZ) del giro dentado (DG) del hipocampo. Aquí, la gran mayoría de las células recién nacidas experimentan apoptosis durante sus primeros días de vida y son eficientemente retiradas por la microglía en condiciones fisiológicas. Por tanto, en esta tesis nos hemos centrado en el uso de la SGZ del hipocampo como modelo para valorar la eficiencia de las células de microglía en retirar las células apoptóticas bajo diferentes condiciones así como evaluar su capacidad para potenciar la respuesta fagocítica según el contexto.

Por otra parte, las células de microglía son responsables de orquestar la respuesta inflamatoria. Al contrario que en la fagocitosis, el papel de la microglía en la inflamación ha

sido bien caracterizado. La inflamación constituye una respuesta desencadenada por el sistema inmune contra cualquier estímulo dañino para el organismo. Durante la inflamación, la microglía, como componente relevante del sistema inmune, se activa e inicia el reclutamiento de otras células inmunes que contribuyen a la protección y reparación del tejido afectado. En un contexto inflamatorio, las células de microglía liberan diferentes moléculas, principalmente citoquinas y quimioquinas. En esta tesis hemos estudiado dos mediadores inflamatorios diferentes: el factor alfa de necrosis tumoral (TNF-α), que es una de las citoquinas pro-inflamatorias mejor caracterizadas y la quimioquina fractalquina (CX3CL1).

En las últimas décadas, se ha visto que tanto la inflamación como la fagocitosis están relacionadas. Se ha mostrado que las células de microglía mejoran su respuesta fagocítica tras la inflamación, aunque la fagocitosis también se ha mostrado capaz de alterar la respuesta inflamatoria, evidenciado una comunicación cruzada entre la inflamación y la fagocitosis que inevitablemente influencia la respuesta inmune de la microglía y su capacidad de preservar la homeostasis cerebral. A pesar de que los papeles tanto de TNF-α como de CX3CL1 en inflamación han sido bien definidos, su posible papel en la fagocitosis microglial no ha sido evaluado aún.

Por tanto, nuestro **Objetivo 1.1** en esta tesis fue examinar el posible papel de TNF-α en la fagocitosis microglial (y también en la neurotoxicidad) de las células apoptóticas en la SGZ del hipocampo. Para examinar esto, llevamos a cabo un análisis de la eficiencia fagocítica en ratones cuya microglía es deficiente en la expresión de TNF-α comparado con ratones control, ambos inyectados con el análogo de glutamato kainato (KA), conocido por causar excitotoxicidad en un modelo murino de epilepsia mesial del lóbulo temporal (MTLE). El número de células apoptóticas fagocitadas por la microglía (índice fagocítico (Ph index)) era similar en ratones con microglía deficiente en la expresión de TNF-α comparado con ratones control, sugiriendo que el TNF-α secretado por la microglía no influenciaba la conducta fagocítica microglial. Además, el TNF-α microglial tampoco afectaba a la apoptosis, ya que la cantidad de células apoptóticas observadas en ambos ratones era similar.

Con relación a CX3CL1, nuestro **Objetivo 1.2** en esta tesis fue estudiar la conducta fagocítica microglial a través del estudio de su receptor, el receptor 1 de la quimioquina CX3C (CX3CR1), en ratones deficientes en dicho receptor comparado con ratones control en la SGZ del hipocampo. Los análisis revelaron que los ratones deficientes en CX3CR1 presentaban un Ph index similar comparado con los ratones control, sugiriendo que, al igual que TNF-α, CX3CL1 no mostraba ninguna evidencia de regular la fagocitosis microglial, ya que la interacción de

CX3CL1 con CX3CR1 o la ausencia de ella no suponía una alteración en la eficiencia fagocítica para retirar las células apoptóticas por parte de la microglía.

Entonces nos centramos en receptores fagocíticos alternativos. En concreto, en esta tesis nos enfocamos en el receptor 34 acoplado a proteína G (GPR34). Se sabe que GPR34 está muy expresado en microglía, aunque también se expresa en otras células inmunes, tales como macrófagos, células dendríticas o linfocitos, entre otras. En los últimos años, GPR34 ha sido postulado como un potencial regulador de la fagocitosis microglial de células apoptóticas, particularmente in vitro.

Por tanto, el **Objetivo 2** en esta tesis consistió en valorar el papel de GPR34 en la fagocitosis microglial de células apoptóticas in vivo. Con este propósito, nos enfocamos en evaluar la respuesta fagocítica de la microglía en ratones jóvenes y adultos deficientes en GPR34 en la SGZ del hipocampo. El estudio de la conducta fagocítica en ratones jóvenes deficientes en GPR34 mostró que había un gran descenso en el Ph index comparado con ratones control, acompañado de una disminución en el porcentaje de microglía fagocítica (capacidad fagocítica (Ph capacity)). En consecuencia, existía un desacoplamiento entre los eventos de fagocitosis y apoptosis (acoplamiento fagocitosis/apoptosis (Ph/A coupling)), poniendo de manifiesto el papel de GPR34 en la regulación de la fagocitosis microglial in vivo, como se mostró previamente in vitro. Por el contrario, los ratones adultos deficientes en GPR34 no mostraron ninguna diferencia en el Ph index ni en Ph capacity y por tanto el Ph/A coupling se mantuvo inalterado.

El receptor GPR34 fue inicialmente considerado un receptor huérfano. Sin embargo, recientemente se demostró que presenta afinidad por un ligando: lisofosfatidilserina (lysoPS). LysoPS es una molécula lipídica que deriva de la fosfatidilserina (PS), el marcador clásico de las células apoptóticas. LysoPS se ha asociado a varias respuestas celulares. De manera interesante, una de esas respuestas consiste en la potenciación de la respuesta fagocítica a neutrófilos apoptóticos por parte de macrófagos in vitro.

Por tanto, con el propósito de profundizar en el estudio de la señalización GPR34-lysoPS sobre la fagocitosis microglial, el **Objetivo 3** de esta tesis fue dirigido a evaluar el papel de lysoPS en la fagocitosis microglial tanto in vitro como in vivo. Con este objetivo, tratamos cultivos de microglía con lysoPS en presencia de células apoptóticas. Los datos referidos a la fagocitosis microglial reflejaron que lysoPS añadida a los cultivos de microglía producía una caída perceptible e importante en la Ph capacity de las células de microglía. Después, tratamos cultivos organotípicos de hipocampo con lysoPS, encontrando un Ph index reducido,

acompañado de una Ph capacity disminuida, al igual que en los cultivos de microglía, dando fe de la influencia de lysoPS en la fagocitosis microglial in vitro.

Por otra parte, lysoPS se ha demostrado que presenta afinidad por otros tres receptores además de por GPR34: P2Y10, el receptor 174 acoplado a proteína G (GPR174) y G2A. Por consiguiente, para asegurar que los efectos de lysoPS sobre la fagocitosis microglial in vitro fueron solo debidos a su interacción con GPR34, analizamos la expresión de esos receptores en microglía. GPR34 era predominante en cultivos de microglia (con escasa expresión de G2A). Por el contrario, GPR34 fue el único receptor de lysoPS expresado por microglía in vivo. Finalmente, analizamos el impacto de lysoPS en la fagocitosis microglial in vivo mediante la inyección de lysoPS en el hipocampo de ratones. Los resultados reflejaron que tanto el Ph index como la Ph capacity de la microglía permanecían inalterados de modo que lysoPS presumiblemente no tenía efecto regulador alguno in vivo, al contrario de lo registrado in vitro.

Para terminar, nos centramos en las consecuencias funcionales de la fagocitosis. La fagocitosis microglial es una tarea compleja cuyas consecuencias pueden extenderse a otros procesos celulares como el metabolismo, como fue relatado en macrófagos, en los que varias modificaciones en rutas metabólicas se observaron tras el englobamiento de residuos. Considerando eso, es posible que un fenómeno similar pudiera ocurrir en células de microglía.

Por consiguiente, el **Objetivo 4** de esta tesis fue el estudio de las posibles consecuencias de la fagocitosis de células apoptóticas sobre el metabolismo microglial. Para valorar esto, en primer lugar analizamos la expresión de varios tránscritos importantes relativos a la fosforilación oxidativa (OXPHOS) y la glicólisis, las dos principales rutas metabólicas en células eucariotas, revelando en general una expresión inalterada en microglía fagocítica comparada con microglía control. Después, evaluamos directamente las rutas de la OXPHOS y la glicólisis. Los análisis metabólicos dieron evidencia de una regulación a la baja de la OXPHOS en la microglía fagocítica mientras la glicólisis se mantenía inalterada tras la fagocitosis. Por si esto fuera poco, un análisis más profundo de las mitocondrias reveló diferencias morfológicas en la microglía fagocítica comparada con la microglía control así como varias alteraciones en genes de fisión (división) mitocondrial mientras los genes de fusión (unión) analizados no mostraron diferencias en la microglía fagocítica comparada con la microglía control.

La fagocitosis microglial puede implicar cambios en otros procesos, como la neurogénesis hipocampal adulta, ya que la microglía engloba el exceso de células recién nacidas. El **Objetivo 5** en esta tesis fue evaluar si las alteraciones en la fagocitosis microglial podrían dar lugar a

algunos cambios en la neurogénesis. Considerando el potencial de GPR34 en la regulación de la fagocitosis microglial, examinamos si la deficiencia en la fagocitosis microglía observada en ratones jóvenes deficientes en GPR34 podría impactar sobre el proceso neurogénico. Evaluamos las poblaciones de células madre (NSCs) y de neuroblastos en la SGZ del hipocampo de ratones jóvenes y adultos deficientes en GPR34. Los resultados descartaron alteración alguna en la población de NSCs en ambos ratones. Sin embargo, se produjo una disminución evidente en el número de neuroblastos en los ratones adultos deficientes en GPR34, no afectados por la deficiencia fagocítica, comparado con ratones control, que no se reprodujo en ratones jóvenes, descartando la posibilidad de que la fagocitosis microglial pudiera influir en la neurogénesis durante la etapa adulta.

En conclusión, todos estos resultados destacan la relevancia de la fagocitosis microglial en la homeostasis cerebral, y particularmente el papel de GPR34 y su ligando lysoPS durante este proceso. Además, la fagocitosis de células apoptóticas implica efectos en el metabolismo de la microglía, especialmente en las mitocondrias, a través de la regulación a la baja de la OXPHOS y cambios morfológicos. Sin embargo, los datos obtenidos no apuntan a un nexo entre la fagocitosis de células apoptóticas y cambios en neurogénesis en el nicho neurogénico de la SGZ.

2.2 SUMMARY

Microglial cells constitute the resident macrophages of the central nervous system (CNS). They constantly surveil the brain parenchyma with their highly motile processes and help maintain the brain tissue homeostasis by exerting one of their main functions, which is phagocytosis.

Microglia are considered the professional phagocytes in brain. However, the role of microglial cells in phagocytosis is largely unknown. Phagocytosis is the cellular process of eating and supposes a crucial phenomenon during brain development and pathological contexts. Microglia have been shown to phagocytose many different cargo in both physiological and pathological conditions, and in this PhD Thesis, we have focused in the phagocytosis of apoptotic cells.

Apoptosis or "programmed cell death" is an ubiquitous phenomenon that leads to the maintenance of a cell population, as a normal part of development, which helps preserving tissue homeostasis and also seen in pathology. An efficient clearance of apoptotic cells results fundamental for avoiding the leakage of intracellular toxic contents. In order to enabling a rapid clearance of apoptotic cells, microglial cells present a great variety of receptors attached to the membrane that help detect and recognize the different molecules released by apoptotic targets, including "find-me" and "eat-me" signals. Once these signals are recognized by microglia, apoptotic cells are engulfed in a phagosome that in the last term fuses with lysosomes, allowing the complete degradation of the cargo by the phagocyte.

In the last few years, the role of microglia in phagocytosis has been studied very well in the subgranular zone (SGZ) of the dentate gyrus (DG) of the hippocampus. Here, the vast majority of the newborn cells undergo apoptosis during their first days of life and they are efficiently removed by microglia in physiological conditions. Therefore, this PhD Thesis has been focused on the use of the SGZ of hippocampus as a model to assess microglial cells efficiency in removing apoptotic cells under different conditions just as evaluate their capacity to enhance the phagocytic response depending on the context.

Furthermore, microglial cells are responsible for orchestrating the inflammatory response. In contrast to phagocytosis, the role of microglia in inflammation has been well characterized. Inflammation constitutes a response triggered by the immune system against any harmful stimulus for the organism. During inflammation, microglia, as relevant components of the immune system, become activated and trigger the recruitment of other immune cell types that contribute to the protection and reparation of the affected tissue. In an inflammatory context,

microglia release different molecules, mainly cytokines and chemokines. In this PhD Thesis we have studied two different inflammatory mediators: tumor necrosis factor alpha (TNF-α), which is one of the best characterized pro-inflammatory cytokines and the chemokine fractalkine (CX3CL1).

In the last decades, it has been shown that both inflammation and phagocytosis processes are related each other. Microglia cells have been shown to improve its phagocytic response upon inflammation, but microglial phagocytosis has been also revealed to alter the inflammatory response, thus evidencing a crosstalk inflammation-phagocytosis which inevitably influences the immune response of microglial cells and their capacity to preserve brain homeostasis. Despite that TNF-α and CX3CL1 roles in inflammation have been well defined, their possible roles in microglia phagocytosis have not been assessed yet.

Thereby, our **Objective 1.1** in this PhD Thesis was to examine the possible role of TNF-α in microglial phagocytosis (and also neurotoxicity) of apoptotic cells in the SGZ of the hippocampus. In order to test it, we performed an analysis of the phagocytic efficiency in microglial TNF-α deficient mice versus control mice, both injected with the glutamate analog kainate (KA), known for causing excitotoxicity in a mouse model of mesial lobe temporal epilepsy (MTLE). The number of apoptotic cells phagocytosed by microglia (Ph index) was similar in microglial TNF-α-deficient mice compared to control mice, suggesting that TNF-α secreted by microglia did not influence microglial phagocytic behavior. Besides, microglial TNF-α by did not affect apoptosis either, since the amount of apoptotic cells observed in microglial TNF-α deficient mice was similar to observed in control mice.

Regarding CX3CL1, our **Objective 1.2** in this PhD Thesis was to study microglial phagocytic behavior through the study of its receptor CX3C chemokine receptor 1 (CX3CR1) in CX3CR1-deficient versus control mice in the SGZ of the hippocampus. Analyses revealed that CX3CR1-deficient mice presented a similar Ph index than control mice did, suggesting that, similar to TNF-α, CX3CL1 did not show any evidence of regulating microglial phagocytosis, since its interaction with CX3CR1 or the lack of it did not suppose an alteration in the phagocytic efficiency to remove apoptotic cells by microglia.

We then focused on alternative phagocytosis receptors. Specifically, in this PhD Thesis we focused on G protein-coupled receptor 34 (GPR34). GPR34 is known for being highly expressed in microglia, although it is also expressed in other immune cells types, such as macrophages, dendritic cells or lymphocytes, among others. In the last few years, GPR34 has been postulated as a potential regulator of microglial phagocytosis of apoptotic cells, particularly in vitro.

Thus, the **Objective 2** in this PhD Thesis was to assess the role of GPR34 in microglial phagocytosis of apoptotic cells in vivo. For this purpose, we focused on evaluating phagocytic response of microglia in GPR34-deficient young and adult mice in the SGZ of the hippocampus. The study of microglial behavior in young GPR34-deficient mice showed that there was a great drop in the Ph index compared to control mice, accompanied by a decrease in the percentage of phagocytic microglia (Ph capacity). Consequently, there was an uncoupling between phagocytosis and apoptosis (Ph/A coupling) events, evidencing the role of GPR34 in the regulation of microglial phagocytosis in vivo, as previously shown in vitro. In contrast, adult GPR34-deficient mice did not show any differences neither in the Ph index or Ph capacity and thus Ph/A coupling was unaltered.

GPR34 receptor was initially considered an orphan receptor. However, it has been recently shown that GPR34 presents affinity for one ligand: lysophosphatidylserine (lysoPS). LysoPS is a lipidic molecule derived from phosphatidylserine (PS), the classical marker of apoptotic cells. LysoPS has been shown to elicit several cellular responses. Interestingly, one of these responses is the enhancement of phagocytic response to apoptotic neutrophils by macrophages in vitro.

Thereby, with the purpose to delve into the study of GPR34-lysoPS signaling on microglial phagocytosis, the **Objective 3** of this PhD Thesis was focused on assessing the role of lysoPS in microglial phagocytosis both in vitro and in vivo. For this purpose, we challenged microglia to the addition of lysoPS in microglia cultures with apoptotic cells. Data referred to microglial phagocytosis reflected that lysoPS added to microglia cultures produced a perceptible and important drop in the Ph Capacity of microglial cells. Next, we treated hippocampal organotypic cultures with lysoPS, finding a reduced Ph index of microglia, accompanied by a decreased Ph capacity, as found in microglial cultures, giving evidence of the influence of lysoPS on microglial phagocytosis in vitro.

Furthermore, lysoPS has been shown to have affinity for other three receptors apart from GPR34: P2Y10, G protein-coupled receptor 174 (GPR174) and G2A. Therefore, to ensure that lysoPS effects on microglial phagocytosis in vitro were only due to its interaction with GPR34, we analyzed the expression of these receptors in microglia. GPR34 was predominant in cultured microglia (with a scarce expression of G2A). In contrast, GPR34 was the unique lysoPS-receptor expressed in microglia in vivo. Finally, we analyzed lysoPS impact on microglial phagocytosis in vivo by injecting mice hippocampi with lysoPS. Results reflected that both Ph

index and Ph capacity of microglia remained unaltered so that lysoPS did not presumably have any regulatory effect in vivo, contrary to registered in vitro.

Lastly, we focused on the functional consequences of phagocytosis. Microglial phagocytosis is a complex task whose consequences can be extended to other cellular processes such as metabolism, as clearly reported in macrophages, in which several modifications in metabolic pathways have been observed upon engulfment of debris. Regarding that, it is possible that a similar phenomenon could occur in microglial cells.

Thus, the **Objective 4** of this PhD Thesis was to study the possible downstream consequences of apoptotic cells phagocytosis on microglial metabolism. To assess this, we first analyzed the expression of several important transcripts of genes related to oxidative phosphorylation (OXPHOS) and glycolytic pathways, the two main metabolic routes in eukaryotic cells, revealing an overall unaltered expression in phagocytic microglia compared to naïve microglia. Next, we directly evaluated OXPHOS and glycolysis pathways. Metabolic assays gave evidence of a downregulation of OXPHOS in phagocytic microglia whereas glycolysis was unaltered upon phagocytosis. On top of that, a deeper analysis of mitochondria revealed morphological differences in phagocytic microglia compared to naïve microglia just as several alterations in mitochondrial fission (division) genes whereas mitochondrial fusion (joint) genes analyzed showed no differences in phagocytic microglia compared to naïve microglia.

Microglial phagocytosis can involve changes in other processes, such as adult hippocampal neurogenesis, as microglia engulf the excess of newborn cells. The **Objective 5** in this PhD Thesis was to evaluate whether alterations in microglial phagocytosis could lead to any changes in neurogenesis. Considering the potential role of GPR34 in microglial phagocytosis regulation, we tested whether microglial phagocytosis impairment previously observed in young GPR34-deficient mice could have some impact on neurogenic process. We evaluated the neural stem cells (NSCs) as well as neuroblasts in the SGZ of the hippocampus of young and adult GPR34-deficient mice. Results discarded any alteration in the NSCs population in both young and adult mice. However, there was an evident decline in neuroblasts numbers in adult GPR34-deficient mice, not affected by phagocytic impairment, compared to control mice, that was not reproduced in young mice, discarding the possibility that microglial phagocytosis may influence neurogenesis in adulthood.

In conclusion, all these results remark the relevance of microglial phagocytosis in brain homeostasis, and particularly the role of GPR34 receptor and its ligand lysoPS during this process. Besides, phagocytosis of apoptotic cells involves downstream effects on microglia

metabolism, especially on mitochondria, through the downregulation of OXPHOS and changes in mitochondrial morphology. Nevertheless, data obtained do not point towards a link between phagocytosis of apoptotic cells and changes in neurogenesis in the neurogenic niche of the SGZ.

3. INTRODUCTION

3. INTRODUCTION

3.1. INTRODUCTION TO MICROGLIA

3.1.1. Definition and origins

Microglia constitute the resident macrophages of the CNS, acting as professional phagocytes and coordinators of the innate immune response [1]. Microglia were first described by Pío Del Río-Hortega in 1919 [2] and they comprise around 10-15 % of the glial cells in brain [3].

Microglia belong to the monocytic-macrophage lineage [4], having a different origin with respect of other glial cells during embryonic development that makes them unique. Whereas the other glial cells originate from the ectoderm, microglia originate from the mesoderm. More specifically, they originate from the yolk sac at the embryonic day 7.5 (E7.5) in the mouse [5]. In that stage, hematopoietic stem cells become primitive macrophages and migrate into the developing CNS to finally become microglia [6, 7].

3.1.2. Microglial functions

Microglia have been revealed as great sensor cells in the brain tissue. They possess a remarkable surveillance capacity, which is supported by the unique motility of their fine processes, whose dynamics allow to scan the whole brain parenchyma with high frequency [8, 9]. Microglia are able to respond to many changes of their surroundings by modifying their morphology and gene expression [6, 10]. This particular feature helps maintain the CNS homeostasis in health and disease and thus it allows fulfilling a wide range of functions [11, 12]. Some of the most important renowned functions of microglia are synapse monitoring, myelination, vasculogenesis, and neurogenesis during both development and adulthood in health and disease, as we will briefly summarize:

Synapse monitoring: during CNS development, more synapses are produced than are lastly required, so a remodeling of neuronal circuit is needed. In order to exert the synapse remodeling, microglia eliminate the immature ones while the mature ones are strengthened [13-16]. It has been shown that microglia have a role in synapse remodeling by engulfing pre-synaptic elements in the postnatal brain [17]. Additionally, in the adult CNS, microglia have been involved in reshaping neuronal circuit via trogocytosis (partial elimination) of pre-synaptic elements [18]. Importantly, synapse remodeling has to be under control since an excessive removal of synapses may worsen several neurodegenerative diseases like Alzheimer's Disease (AD) [19].

Myelination: Microglia have been also related to myelination through the production of growth factors that regulate the proliferation and survival of oligodendrocytes [20]. Additionally, microglial activity is crucial for remyelination, since their phagocytosis of myelin debris when demyelination occurs facilitates the recruitment and differentiation of olygodendrocyte precursors [21, 22]. Contrary to this, it has been also reported that microglia release pro-inflammatory cytokines in pathological conditions which could be detrimental for remyelination [23].

Vasculogenesis: Furthermore, some other evidences point towards a role of microglial cells in embryonic vasculogenesis. Microglia have been observed in close association with developing vessels [24]. Likewise, the lack of microglia is linked to a decrease in the developing vasculature [25]. On top of that, some studies suggest that microglia could exert a role in alterations of the vasculature in pathologies like AD or Parkinson's Disease (PD) [26].

Neurogenesis: During development, it has been suggested that microglia modulate the amount of neuroprogenitors in the subventricular zone (SVZ) of rats [27]. Nevertheless, during adulthood, microglia have been shown to regulate neurogenesis through the phagocytosis of apoptotic newborn neurons in the hippocampus [28] and in the SVZ as well [29]. Besides, microglia can also act as a detrimental factor in neurogenesis. In pathological conditions, aging or neurodegenerative diseases, microglia are able to release pro-inflammatory cytokines triggering negative consequences for neurogenesis [30]. Consequently, one of the aims of this PhD Thesis will be to assess whether microglial release of pro-inflammatory cytokine TNF-α may impact on neuronal apoptosis. The role of microglial cells on neurogenesis will be described below **(Section 3.5.4)**.

This variety of microglial functions and others are linked to the two main abilities of microglia, which highlight their relevance in the CNS: the control of the inflammatory response and the phagocytosis of debris, which are essential for the maintenance of brain tissue homeostasis and will be described next.

3.1.3. Immune response

Microglial cells constitute the main immune cells in the CNS [31]. Microglia modulate innate immunity and also participate in the adaptive immune response. Innate immunity represents the immediate response of the organism against any harmful stimulus, such as pathogens or apoptosis, by developing an inflammatory response [32]. In contrast to adaptive immunity system, which is specific to each pathogen, the innate immunity has been classically shown to

recognize pathogens non-specifically and may not provide long-lasting immunity to the organism [33].

In response to CNS injury or in neurodegenerative diseases, microglia undergo activation. Concomitantly, the infiltration of other immune cells from the peripheral blood is produced [34] to protect and initiate the reparation of the organism by performing an inflammatory response. Once the inflammatory response is performed and infection is contained, microglia proceed to the removal of infective agents by exerting phagocytosis. Phagocytosis constitutes, together with inflammation, the fundamental component of the innate immune response [35]. Microglia engulf pathogens/cell debris or present them to T cells that traffic in and out of the CNS to develop an adaptive immune response [34]. Microglial phagocytosis is the main goal of this PhD Thesis and will be described in detail below **(Section 3.3)**.

Inflammation and phagocytosis are processes related to each other. It is known that inflammatory stimuli, such as lipopolysaccharide (LPS) or amyloid beta (Aβ) give rise to morphological alterations in cultured microglia, by inhibiting their cytokinesis, directly affecting their potential to phagocytose dead cells [36]. Nevertheless, when challenged with inflammation in vivo (via LPS administration or omega 3 fatty acid deficient diets) microglia maintained their phagocytic potential unaltered [37]. Furthermore, it has been shown that defects in the clearance of apoptotic cells by macrophages are directly linked to the development of an inflammatory response, persistent inflammatory disorders and also autoimmunity [38-41]. In contrast, the accurate clearance of these corpses by macrophages involves the secretion of anti-inflammatory cytokines, preventing inflammation [42]. In microglia, in vitro evidences have shown that phagocytosis triggers the secretion of anti-inflammatory cytokines, such as transforming growth factor beta (TGF-β) and neuroprotective factors such as nerve growth factor (NGF) [43, 44]. Consequently, the crosstalk between inflammation and phagocytosis guarantees an accurate immune response by the organism.

Therefore, our **Objective 1** in this PhD Thesis was to assess the role of two of the most important inflammatory mediators (TNF-α and CX3CL1) in phagocytosis regulation. Both inflammatory and phagocytic responses will be described in more detail below.

3.2. INFLAMMATORY RESPONSE

In the brain, microglia are in charge of developing the inflammatory response. Inflammation is a mechanism triggered by the immune system in response to noxious stimuli, such as

pathogens or excessive cell death. Inflammatory responses have been also reported in all neurodegenerative diseases [45]. In response to damage, the inflammatory response generates heat, redness and swelling, which converge into fever with the aim to control the proliferation of pathogenic molecules [46]. Upon an inflammatory stimulus, microglia respond by releasing pro and anti-inflammatory cytokines, chemokines and complement proteins [12].

3.2.1. Cytokines

Several factors are released during an inflammatory insult but cytokines are the major orchestrators of the inflammatory response by microglia. Remarkably, microglia are not the only source of these cytokines, since they are also released by astrocytes, oligodendrocytes, endothelial cells and neurons [47, 48]. Cytokines are proteins that coordinate the immune response by triggering cell proliferation, differentiation, apoptosis or release of other cytokines, among others [49]. Several groups of cytokines have been defined, such as interleukins (ILs), which help activate several cells of the immune system and facilitate their migration to the affected tissue [50]. Other group of cytokines are transforming growth factors (TGFs), needed for repairing the injury site [51]. Furthermore, interferons (IFNs) are crucial during the innate immune response to viruses [52]. Colony-stimulating factors (CSFs) are related to the production of other cytokines and have been also shown to stimulate the proliferation and differentiation of stem cells to immune cells [53]. Lastly, tumor necrosis factors (TNFs) are relevant cytokines during the initiation of the inflammatory response which have been shown to play an important role in cell processes like proliferation and apoptosis [54].

Since cytokines modulate inflammation towards a pro or an anti-inflammatory response, they can be divided into two different categories: pro-inflammatory and anti-inflammatory cytokines.

3.2.1.1. Pro-inflammatory cytokines

Pro-inflammatory cytokines are essential for the initiation of the inflammatory response. Although their main role is to defend the organism, it is important to state that an excessive and continuous release of pro-inflammatory cytokines results detrimental in pathological conditions, aggravating several neurodegenerative diseases like AD, multiple sclerosis (MS) or epilepsy [45, 55]. A continuous production of pro-inflammatory cytokines enhances the permeability of the blood brain barrier (BBB), which involves migration of peripheral immune cells into the CNS, increasing neuronal damage through the release of neurotoxic factors such

as reactive oxygen species (ROS) or nitric oxide (NO) [56, 57]. The most characterized pro-inflammatory cytokines are interleukin 1 beta (IL-1β), interleukin 6 (IL-6), interferon gamma (IFN-γ) and TNF-α [58].

TNF-α: TNF-α belongs to TNF ligand superfamily. TNF-α is generated from a transmembrane precursor which is finally cleaved into a soluble homotrimer [59]. TNF-α is produced by many cell types such as endothelial cells, fibroblasts and also by microglia, astrocytes and neurons in the CNS [60, 61] **(Figure 1)**. It has been shown that microglial production of TNF-α is increased after immunological stimulus both in vivo and in vitro [34, 62]. TNF-α has been shown to influence CNS development through its role on neuroprogenitor cells (NPCs) differentiation and maturation. TNF-α acts as anti-neurogenic agent during cell lineage fate determination, increasing the amount of astrocytes [63]. Nonetheless, TNF-α exhibits pro-neurogenic activity in SVZ cultures [64] and has a relevant role in neurons maturation [65]. Furthermore, it has been reported the role of TNF-α in synaptic plasticity, since it enhances α-amino-3-hydroxy-5-methyl-4-isoxazolepropionic acid (AMPA) receptor expression, thus increasing synaptic transmission [66] and consequently long term potentiation (LTP). Indeed, synaptic connectivity is affected by TNF-α ablation, impacting on plasticity [67]. Remarkably, TNF-α has been revealed as a neuroprotective agent. The neuroprotective role of TNF-α [68-70] is attributed to its affinity for TNF receptor 2 (TNFR2) [71], whose expression is restricted to hematopoietic cells [72]. In contrast, TNF-α has been also shown a neurotoxic function. The neurotoxic effect of TNF-α [73-75] has been traditionally linked to its binding to TNF receptor 1 (TNFR1) [76]. TNFR1 is expressed in almost every cell type (except for erythrocytes) [72]. TNF-α has been also related to some neurodegenerative diseases, such as MS, where its expression levels correlate with the progression of the disease [77]. Likewise, together with IL-6 and IL-1β, TNF-α has been found to be overexpressed in models of seizures, specially by glia [78]. Lastly, it is known that TNF-α constitutes one of the most important cytokines released during inflammation [78]. This fact, together with the evidences pointing towards a link between inflammation and microglial phagocytosis mentioned before [36, 37, 43, 44] raises the possibility that microglial TNF-α exerts some regulation in the phagocytosis of apoptotic cells. For instance, in vitro data have reported that TNF-α addition to neuron-glial cultures triggers microglial activation and phagocytosis of viable neurons (phagoptosis, which will be explained in more detail in **Section 3.3**). In order to evaluate whether microglial release of TNF-α could play a role in phagocytosis of apoptotic neurons, we first aimed **(Objective 1.1)** at assessing both apoptosis and phagocytic behavior in microglial-specific TNF-α knockout (KO) mice.

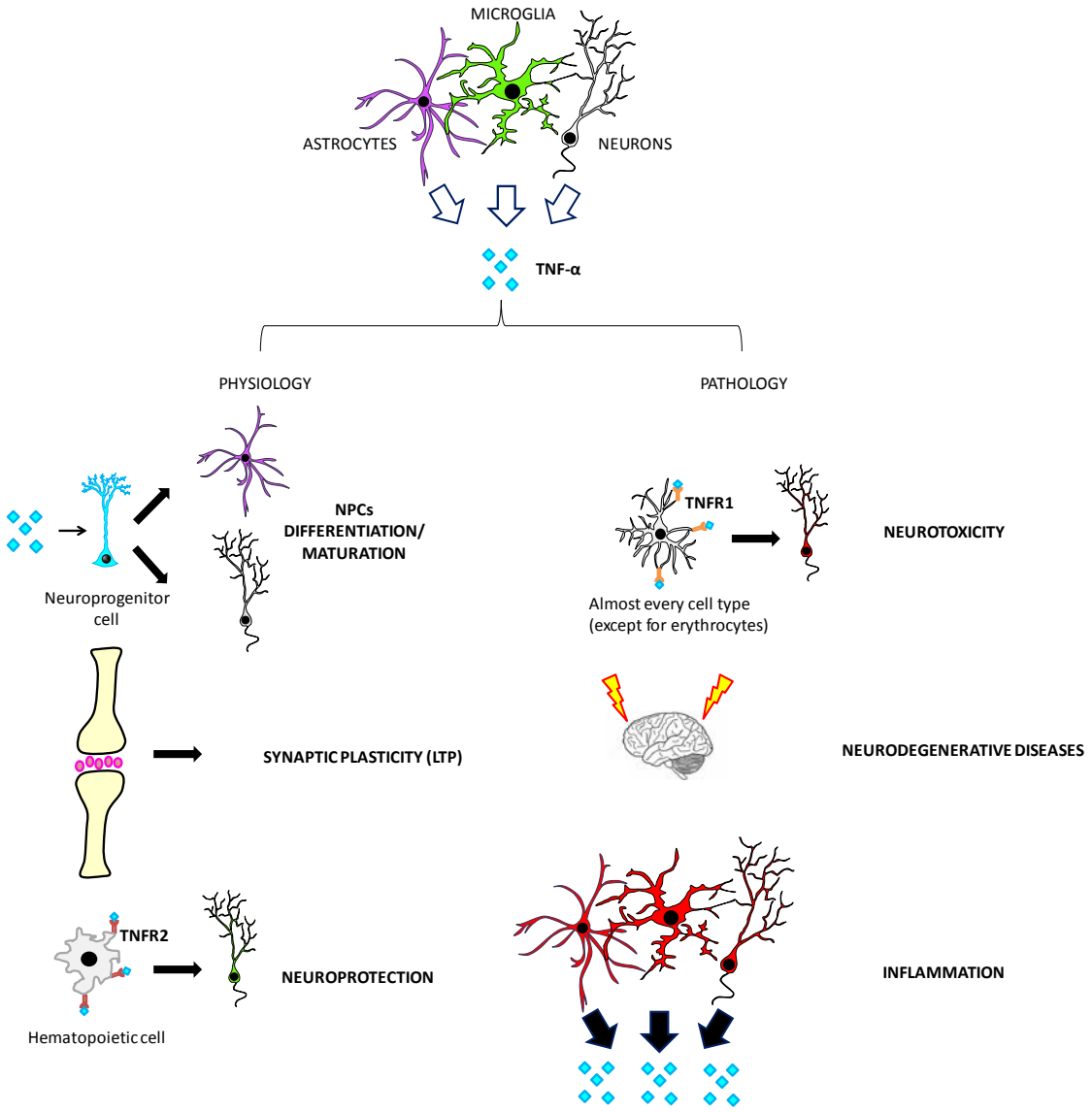

Figure 1. Different roles of cytokine TNF-α in the CNS*. Microglia, in conjunction with other cell types in the CNS, such as astrocytes and neurons, are able to release several cytokines. Among them, one of the most important ones is tumor necrosis factor alpha (TNF-α), which plays a relevant role in both physiological and pathological conditions. TNF-α can determine neuroprogenitor cells (NPCs) destination, giving rise to astrocytes [63] or newborn neurons [65]. Additionally, it influences synaptic plasticity, increasing synaptic transmission [66] and also impacting on long term potentiation (LTP). On top of that, TNF-α can act as a neuroprotective factor through its binding to tumor necrosis factor receptor 2 (TNFR2) [71], whereas it exerts a neurotoxic effect through its binding to tumor necrosis factor receptor 1 (TNFR1) [76]. Furthermore, TNF-α is also implicated in the progression of neurodegenerative diseases [77]. Besides, it is known that TNF-α is one of the most important cytokines released upon inflammation occurs [78].*

3.2.1.2. Anti-inflammatory cytokines

Anti-inflammatory cytokines act as a mechanism to control the duration of the inflammatory response since they regulate the pro-inflammatory cytokines response [79] and determine the resolution of inflammatory processes, avoiding complications linked to chronic inflammation [80]. The most defined cytokines in this category are TGF-β, interleukin 4 (IL-4) and interleukin 10 (IL-10) [58]. However, sometimes the role of anti-inflammatory cytokines as facilitators of tissue repair and "brake" for the pro-inflammatory cytokines production [81] does not prevent them to also exert detrimental effects. For example, TGF-β has been related to epileptogenesis [80]. Additionally, another less known anti-inflammatory cytokine, macrophage inhibitory cytokine 1 (MIC-1), is associated with microglial phagocytosis impairment in brain tumors [82].

3.2.2. Chemokines

Chemokines constitute one of the different types of molecules secreted during the inflammatory response. They present an amino acid sequence and several cysteine residues [83]. These residues form disulfide bonds to maintain a complex structure composed of a three stranded β-sheet, a C-terminal helix and an N terminus, fundamental for chemokine receptor activation [84]. Depending on the position of the cysteine residues closest to the N terminus, chemokines are divided in four families: CC, CXC, CX3C and XC. Contrary to cytokines, responsible for initiating inflammation [46], chemokines are in charge of mediating the motility of immune cells, most notably leukocytes, towards the infection site in a process called chemotaxis [83].

It is known that during an inflammatory challenge, microglial cells secrete several chemokines, such as macrophage-inflammatory protein 1A (MIP-1A), monocyte chemotactic protein 1 (MCP-1) and chemokine ligand 5 (RANTES) [85]. Furthermore, chemokines are involved in other immune processes, such as phagocytosis. One of the best characterized chemokines is CX3CL1, detailed next:

CX3CL1: It is the only reported member of CX3C family [86]. CX3CL1 is highly expressed in neurons. CX3CL1 can be anchored to the cell membrane or being cleaved into a soluble form (via ADAM metallopeptidase domain 17 (ADAM17) protease) when apoptosis occurs **(Figure 2)**. Its receptor, called CX3CR1, is specifically expressed in microglia in the healthy brain [87, 88].

CX3CL1-CX3CR1 signaling has implications in physiological conditions. It has been suggested that it plays a role in coordinating microglial processes motility, since CX3CR1-deficient mice

have shown lower processes velocity in retinal explants [89]. Besides, CX3CL1/CX3CR1 signaling is involved in synaptic transmission. It has been established that application of CX3CL1 diminishes the amplitude of the AMPA receptor-mediated excitatory postsynaptic currents in *Cornu ammonis* (CA) pyramidal neurons of the hippocampus in vitro [90] whereas it potentiates the amplitude of the N-methyl-D-aspartate (NMDA) receptor-mediated component of these currents [91]. On top of that, CX3CL1 is upregulated in the hippocampus during synaptic plasticity [92]. Lastly, CX3CR1 has been linked to LTP, although some authors establish that the lack of the receptor inhibits LTP [93] whereas other authors state the opposite [94].

Furthermore, CX3CL1-CX3CR1 signaling is known to regulate microglial activation [95]. Indeed, it is known that CX3CL1-CX3CR1 signaling maintains microglia in a resting state [96], thus inhibiting the release of pro-inflammatory cytokines [95, 97]. Nevertheless, in several mice models of neurodegenerative diseases, the absence of CX3CL1 or its receptor has been shown to increase the release of these cytokines [98]. Remarkably, in some of these diseases, like AD, CX3CL1-CX3CR1 signaling can involve neurotoxic effects, which are abolished by inactivating this signaling pathway through CX3CR1 abolishment [99]. Nonetheless, CX3CR1 is protective in other pathologies, such as ischemia [100]. These evidences show that implications of CX3CL1-CX3CR1 interaction depend on the microglial activation stimuli as well as the pathological context.

Formerly mentioned evidences show the impact of CX3CL1-CX3CR1 signaling during inflammation [95, 97]. Nevertheless, its role on phagocytosis regulation has only started to be elucidated. Several authors have shown that apoptotic cells release CX3CL1, which binds to microglial CX3CR1 and a chemotaxic response is triggered, acting as a “find-me” signal **(see Section 3.3.2)** [101, 102]. Besides, other studies have established that CX3CL1-CX3CR1 signaling modulates microglial phagocytosis and activation in a mouse model of retinitis pigmentosa [103]. Therefore, our next aim **(Objective 1.2)** will be focused on assessing the role of CX3CL1 on microglial phagocytosis in a mouse model of genetic CX3CR1 deficiency.

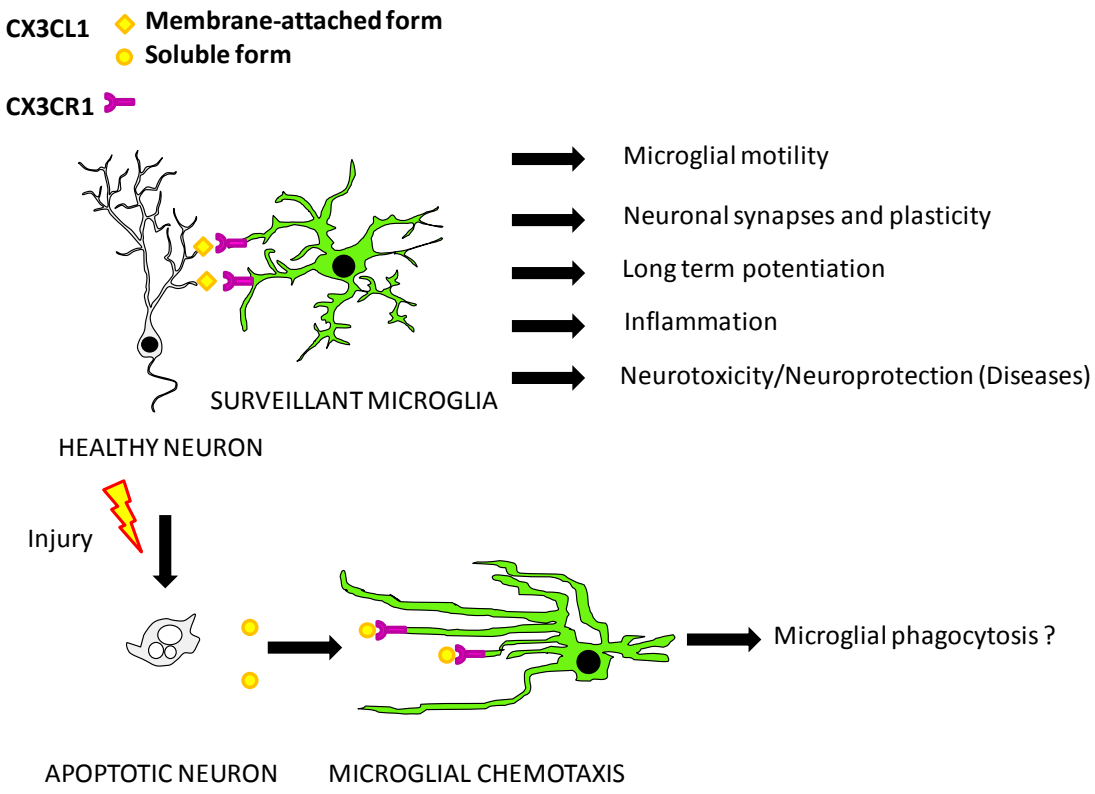

Figure 2. The role of CX3CL1-CX3CR1 signaling in the CNS. *The chemokine fractalkine (CX3CL1) is highly expressed by neurons. CX3CL1 is recognized by CX3C chemokine receptor 1 (CX3CR1) (Y-shaped), expressed by surveillant microglia. Signaling between neurons and microglia has been related to many cell processes, such as microglial processes motility [89], synaptic integration and plasticity [92] and even long term potentiation [93, 94]. In addition to this, CX3CL1-CX3CR1 signaling is involved in the microglia activation state [95]. It can maintain microglia in a resting state by inhibiting the production of pro-inflammatory cytokines, and thus inflammation. CX3CL1-CX3CR1 signaling also determines the secretion of neurotoxic or neuroprotective factors, seen in some neurodegenerative diseases models [98]. On top of that, it exerts a relevant role in the inflammatory response* [95, 97]. *Remarkably, when neurons become apoptotic, CX3CL1 is cleaved from their membrane (diamond-shaped). Then microglia suffer chemotaxis, being attracted to soluble CX3CL1 (sphere-shaped), behaving as a "find-me" signal emitted by apoptotic neurons [101, 102], suggesting a possible role in phagocytosis.*

3.3. PHAGOCYTOSIS

Phagocytosis is referred to the process of recognition, engulfment and degradation of a particle or solid structure (>0.5 µm) by a cell [104]. It constitutes the first line of defense against pathogens and clearance mechanism for cell debris triggered during normal brain development and injuries [105, 106]. In the brain, phagocytosis is mostly performed by microglia, the professional phagocytes. Other cell types are able to exert phagocytosis, such as

dendritic cells, neutrophils and also astrocytes [107] or neuroblasts [28, 108] but these are not as efficient as microglia in removing apoptotic bodies, and are therefore referred to as non-professional phagocytes [107, 109]. Microglia have been shown to phagocytose a wide variety of cargo during physiological and pathological conditions. These phagocytosed targets can include synapses **(see Section 3.1.2)**, microbes, axonal and myelin debris, pathogenesis-related proteins such as Aβ, living cells (phagoptosis) and also apoptotic cells [1], which is the focus of this PhD Thesis.

Microbes: several evidences highlight the role of microglial cells in the clearance of microbial targets such as bacteria or fungi. Both microglia and astrocytes activation is immediately following the entry of bacteria into the CNS [110]. Specifically, it has been shown that microglia can phagocytose and kill *Staphylococcus aureus* [111], although in a minor proportion than neutrophils and macrophages. Furthermore, other studies have shown that microglia can also phagocytose fungal targets. In vitro experiments have revealed that the addition of IFN-γ enhances microglial phagocytosis of *Cryptococcus neoformans* [112]. The effect of microglial activation in response to microbes enables the recruitment of infiltrating immune cells, thus microglia impact on both innate and adaptative immune response during an infection.

Axonal and myelin debris: microglial cells have been shown to remove other neuronal components, such as axonal debris, in order to permit the axonal outgrowth during brain injury. Microglia have been shown to phagocytose axonal debris in rat cortical explants in which neurites were sectioned [113]. Additionally, microglia have been able to eliminate the axonal debris in a co-culture model with induced axonal degeneration [114]. Besides, microglia have been shown to exert a role in the removal of myelin debris [115]. In physiological conditions, microglia phagocytose myelin residues released from aging myelin sheaths [116]. Moreover, the elimination of myelin debris is crucial in some demyelinating diseases like MS and nerve or spinal cord injuries. Therefore, the efficient removal of myelin remains essential for the remyelination process of demyelinating sites.

Aβ plaques: several studies suggest that microglia also phagocytose Aβ residues. Aβ is a peptide generated by the cleavage of the amyloid precursor protein (APP) by β and γ-secretases [117]. Aβ peptide can give rise to aggregates in amyloid plaques, as observed in AD [118]. Microglia have been shown to surround amyloid plaques in AD brains [119]. This leads to propose microglia as phagocytes of Aβ debris [120] but this is still not clear yet. Several reports support the phagocytosis of Aβ in vitro [121, 122]. Furthermore, Aβ internalization by microglia has been shown both in organotypic hippocampal slices [123] and in vivo [124].

However, several studies report incomplete processing of Aβ residues [120]. Thus, there are no strong evidences of microglial processing of Aβ in vivo yet.

Living cells (phagoptosis): Phagoptosis is a type of cell death in which a living cell dies as a result of being phagocytosed for another cell. Phagoptosis is initiated when PS and other considered "eat-me" signals are reversibly exposed on the surface of viable cells **(for more details on "eat-me" signals see Section 3.3.2)** , triggering its engulfment [125]. Therefore, cell death by phagoptosis can be prevented by inhibiting phagocytosis [126].

Several studies have reported that living neurons are phagocytosed by microglia activated via LPS or Aβ [127, 128]. In vitro experiments with microglia defective for annexin 1 (ANXA1) protein have shown that microglial activation via inflammation impedes them to distinguish between apoptotic and viable neurons, giving rise to phagoptosis. These results highlighted the role of microglial ANXA1 protein in identifying apoptotic cells, since they serve as a bridge molecule between PS exposed by apoptotic cell and the phagocyte [129]. An inflammatory context increases the phagocytic capacity of microglia through the release of the adaptor protein milk fat globule-EGF factor 8 (MFG-E8), inducing the reversible exposure of PS on neurons to be phagocytosed via phagoptosis [127, 128]. Microglial phagocytosis of viable neurons by phagoptosis has been shown in a model of retinitis pigmentosa, in which retinal rod cells are removed by microglial phagocytosis, prevented by removing microglial cells or blocking vitronectin receptors (VNRs) [103]. In addition, phagoptosis has been demonstrated in other pathological contexts, such as ischemia [130] and epilepsy [37]. Other studies have revealed that, apart from removing viable neurons, microglia can remove neuronal processes in vitro [131].

In this PhD Thesis, we have focused on microglial phagocytosis of apoptotic cells.

3.3.1. Phagocytosis of apoptotic cells

Apoptosis or programmed cell death is a frequent phenomenon that occurs throughout life in almost every tissue, including brain, as a normal part of development, in homeostasis and in pathogenic processes [132].

Apoptosis can be initiated by two different mechanisms, the extrinsic and intrinsic pathways [133, 134]. The extrinsic pathway is activated by death signals mediated by death receptor ligands [135], whereas the intrinsic pathway is activated by cell stress, leading to the release of cytochrome C from mitochondria via B-cell lymphoma 2 (Bcl-2) proteins [135]. Both pathways are different in the involved initiator caspases but both share the executioner caspases (3, 6

and 7), which are responsible for the morphological and biochemical cell changes derived from apoptosis [134]. The most evident changes are the condensation of the cytoplasm as a consequence of the cell shrinkage, followed by nuclei condensation (pyknosis) and subsequent fragmentation (karyorrhexis), as well as the formation of membrane-encapsulated apoptotic bodies with portions of cytoplasm and nuclei [132, 136, 137]. The most relevant feature of apoptosis, contrary to necrosis, another mechanism of cell death [137], is that it leads to the recognition and engulfment of apoptotic bodies by phagocytes [42].

3.3.2. Stages of phagocytosis

Phagocytosis process is composed of three different stages ("find-me", "eat-me" and "digest-me") **(Figure 3),** which allow the internalization and degradation of the cell corpses, maintaining the tissue homeostasis. Microglia need to receive some stimuli called "find-me", "eat-me" and "digest-me" signals to perform phagocytosis [42]. First of all, apoptotic cells emit "find-me" signals that act as chemoattractors for microglial cells [138]. Second, microglia engulf apoptotic cells via "eat-me" signals detected by engulfing receptors, which imply cytoskeletal modifications in the microglial membrane [139]. Finally, engulfed particles are degraded with the aid of "digest-me" signals, which enable the formation of the phagosome, once the phagocytic pouch is sealed, and the posterior degradation of the cargo in the lysosome [1, 140, 141].

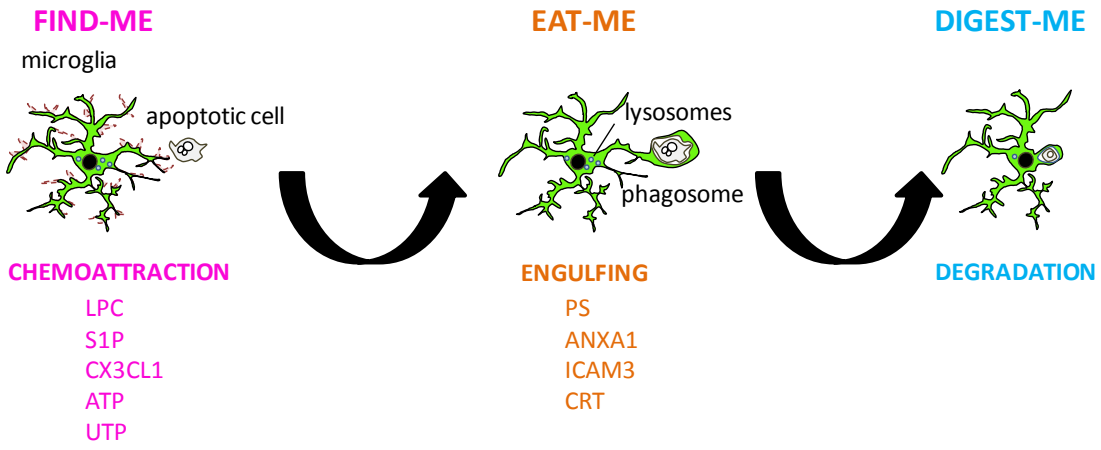

Figure 3. Phagocytosis of apoptotic cells by microglial cells. *Microglial phagocytosis is initiated with the "find-me" stage, in which microglia find its target cell. Chemoattraction is mediated by several molecules such as* lysophosphatidylcholine *(LPC),* sphingosine-1-phosphate *(S1P), fractalkine (CX3CL1), adenosine triphosphate (ATP) or uridine triphosphate (UTP). Next, in the "eat-me" stage, microglia and the target cell interact through microglial engulfment receptors allowing the recognition and engulfment of the cargo. Engulfment is*

mainly mediated by phosphatidylserine (PS). Other molecules involved are annexin 1 (ANXA1), intercellular adhesion molecule 3 *(ICAM3) and calreticulin (CRT). Finally, in the "digest-me" stage, the engulfed target cell will be degraded by microglial phagolysosome. Adapted from [1]*.

"Find-me" stage

Microglial cells are able to find apoptotic bodies to phagocytose due to their highly motile processes [8, 9]. Motility allows microglia to scan the whole brain parenchyma in search for targets which emit signals to be phagocytosed. These signals are known as "find-me" signals, recruiting microglia to the apoptotic cells. There are many "find-me" signals such as CX3CL1, lysophosphatidylcholine (LPC), sphingosine-1-phosphate (S1P), and extracellular nucleotides that include adenosine triphosphate (ATP) and uridine triphosphate (UTP) [1, 38, 142-145].

- CX3CL1 was shown to act as a chemotactic factor for microglia, as mentioned before **(See Section 3.2.2)** [101, 102]. Moreover, CX3CL1 released from apoptotic cells was shown to induce the migration of macrophages in vivo and in vitro [144].

- LPC is known to be secreted by apoptotic cells through a mechanism dependent on caspase-3-induced activation of phospholipase A2 (PLA2) [146], enabling phagocyte recruitment via interaction with G protein-coupled receptor 132, also known as G2A receptor [147]. Additionally, LPC promotes microglial colonization in the developing zebrafish midbrain [148].

- S1P is another molecule released by apoptotic cells [145]. However, it has never been directly shown that S1P acts as a chemotactic factor. There are well characterized receptors for S1P and it has been demonstrated the presence of a S1P receptor in microglia [149]. However, the role of S1P interaction with this receptor and its possible influence in phagocytes recruitment has not been elucidated yet.

- ATP and UTP have been shown to be released from apoptotic cells to attract phagocytes [143]. In the last few years, pannexin 1 channels have been revealed as one of the mechanisms in charge of releasing these nucleotides from apoptotic cells [150]. Once "find-me" signals manage to generate the contact between phagocytes and apoptotic targets, the next step in phagocytosis is the "eat-me" stage [1].

"Eat-me" stage

The "eat-me" stage comprises the accurate recognition and posterior engulfment of the apoptotic cell by microglia [1].

When the apoptotic cell or target is committed to be phagocytosed, “eat-me” signals are produced. A plethora of molecules have been described as mediators of “eat-me” stage. One of them and maybe the best characterized one is PS [151]. PS translocation from the inner to the outer leaflet of the cell membrane is commonly determined as an initiator of apoptotic process [137, 152]. Once the exposure is produced, PS manages to interact with several receptors **(See Section 3.3.3)** attached to the phagocyte membrane facilitating the internalization of the cargo [42, 153, 154].

Several molecules are capable of eliciting “eat-me” signaling process other than PS, such as ANXA1, intercellular adhesion molecule 3 (ICAM3) or calreticulin (CRT) [155-157]. Once “eat-me” signals and their respective receptors contact each other, the activation of the guanosine triphosphate (GTP)ase Rac is initiated within the phagocytes, which implies the reorganization of the phagocyte cytoskeleton giving rise to the formation of the phagocytic cup, a modification of the membrane in charge of internalizing the corpse [158, 159].

“Digest-me” stage

After engulfment of the apoptotic cargo by the phagocytic pouch, the phagosome begins to take shape surrounding the ingested particle. From that moment on, degradation can occur. For that purpose, the phagosome suffers several maturation steps through fusion of endosomes and lysosomes [160]. In these new formed structures, called phagolysosomes, several ATPases maintain an acid pH for ensuring the degradation of the cargo through hydrolases [161]. Studies performed in *Caenorhabditis elegans* served to identify a convergence in respect to the intracellular signaling in phagocytes for the degradation of apoptotic bodies. Both nematodes and mammals share the involvement of the Rho GTPase CED10/Rac1 giving rise to the actin nucleation and cytoskeleton rearrangement needed for corpse removal [162]. Other studies have proposed that the signaling triggered after internalizing the cargo might regulate the phagocytic capacity of microglia to engulf additional corpses [163, 164]. Nevertheless, the process of phagosome formation and cargo degradation has been barely addressed in microglia. Live imaging experiments have shown that microglial vacuolar (v)ATPases are needed for these mentioned processes in *C. elegans* [165]. On top of that, the location where the cargo is degraded remains unknown. Microglial phagocytosis is usually carried out by terminal or en passant branches of ramified surveillant microglia [28, 165]. Interestingly, it has been shown that phagocytic pouches are retrogradely transported to the cell soma in the mouse neocortex [9] and in *C. elegans* [165], suggesting a role of

cytoskeleton in phagosome transportation to finally degrade the cargo. Further research is needed to completely unravel the mechanisms of degradation of apoptotic cells by microglia.

3.3.3. Phagocytosis receptors

Phagocytes present diverse receptors attached to their membranes in order to initiate the engulfment of the cargo **(Figure 4)**. Some of these engulfment receptors are T-cell immunoglobulin domain-containing 4 (TIM-4) [166] and MER proteins, both implicated in the clearance of apoptotic bodies by peritoneal macrophages via interaction with PS [167]. Receptor Mer tyrosine kinase (MerTK) was described as a mediator of clearance of apoptotic cells both in vivo and in vitro [168]. MerTK is able to bind to growth arrest-specific protein 6 (GAS6) or protein S, mediating its interaction with PS on apoptotic cells in vitro [169]. Moreover, VNR can mediate phagocytosis via MFG-E8 protein in vivo and in vitro [170]. Curiously, a crossktalk between MerTK and VNR signaling pathways have been shown in cell lines, involving an enhancement of phagocytosis in vitro [169]. Another well-known engulfment receptor is Brain-specific Angiogenesis Inhibitor 1 (BAI-1), involved in the removal of dying neurons by microglia [171]. Another relevant receptor is Triggering Receptor Expressed on Myeloid cells-2 (TREM2), preferentially expressed in brain microglia [172] and also involved in phagocytosis, since it mediates apoptotic cell engulfment by microglia in vitro by forming a complex with the adapter protein DNAX-activation protein of 12 kD (DAP12) [173]. Recently, it has been proposed that apolipoprotein E (apoE) is the ligand for TREM2 [174]. In this PhD Thesis we will focus on a novel phagocytosis receptor, GPR34.

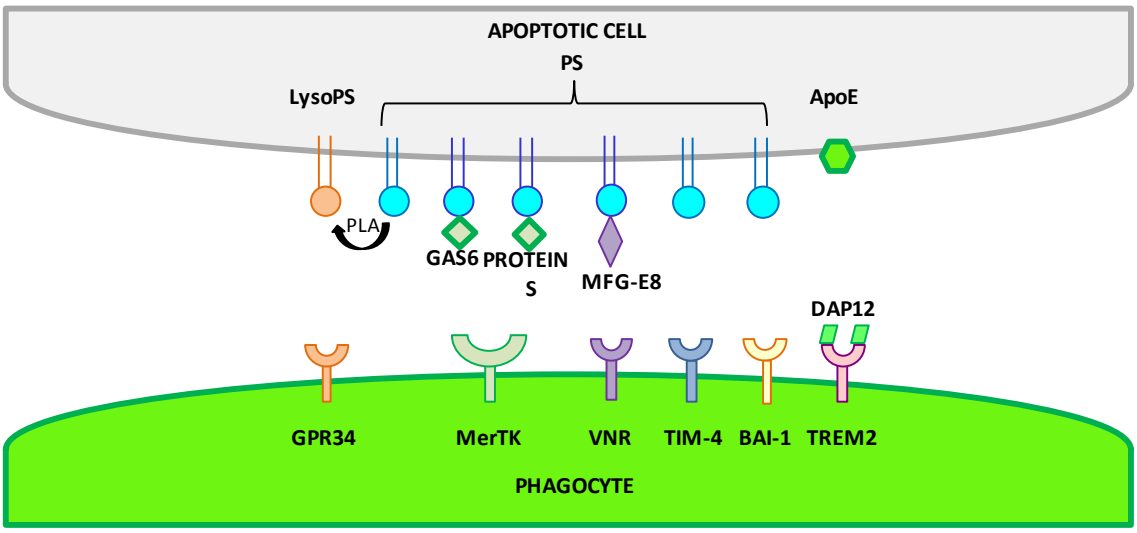

Figure 4. Receptors related to phagocytosis of apoptotic cells*. Schematic representation of transmembrane phagocytic receptors and their respective ligands exposed by apoptotic cells. Several receptors, such as Mer tyrosine kinase (MerTK), vitronectin receptor (VNR), T-cell immunoglobulin domain-containing 4 (TIM-4) or Brain-specific Angiogenesis Inhibitor 1 (BAI-1) recognize phosphatidylserine (PS), the most characterized signal of apoptosis [151], prior to phagocytose the corpse. In the case of MerTK, it needs the aid of several mediators such as growth arrest-specific protein 6 (GAS6) or protein S [169].Regarding VNR, it also needs an intermediate, such as milk fat globule-EGF factor 8 protein (MFG-E8), to engulf the cargo [170]. Another phagocytic receptor, such as G protein-coupled receptor 34 (GPR34), presents affinity for lysophosphatidylserine (lysoPS), derived from PS via phospholipase enzyme (PLA) [175], serving as signal for phagocytosing the apoptotic cell. Furthermore, Triggering Receptor Expressed on Myeloid cells-2 (TREM2), which creates a complex with DNAX-activation protein of 12 kD (DAP12) [173], exerts its phagocytic function by binding to apolipoprotein E (apoE) [174].*

GPR34: It belongs to the P2Y12-line receptor family [176]. GPR34 is highly expressed in microglia [177, 178], constituting a key marker for this population [177]. In addition, it is expressed in macrophages, monocytes, dendritic cells, natural killer cells, megacaryocites, thymocytes and B cells [179, 180]. GPR34 has a role in the cellular response to immunological challenges [181] and it has been shown to mediate microglial phagocytosis, since GPR34-deficient microglia present a decreased capacity for clearance in vitro [182]. This raises the possibility that GPR34 also mediates microglial phagocytosis in vivo. Therefore, the **Objective 2** of this PhD Thesis will be to assess whether GPR34 mediates microglial phagocytosis in vivo by the use of GPR34-deficient mice.

3.3.3.1. GPR34 ligands

GPR34 is activated by binding to its specific ligand lysoPS [183], the deacylated form of PS, via enzymes called phospholipases (PLAs) [175]. LysoPS has a complex structure. It consists of a single fatty acid bind to glycerol by an ester linkage, and L-serine residue connected to glycerol by a phosphodiester linkage [180]. LysoPS has been shown to elicit several cellular responses: to stimulate degranulation of mast cells [184]; to induce neurite outgrowth in PC12 cells [185]; to suppress the proliferation of T lymphocytes [186]; and to facilitate the migration of fibroblasts [187]. More interestingly, lysoPS has been implicated in the enhancement of macrophage-mediated phagocytosis of aged neutrophils in vitro [188]. Considering the involvement of lysoPS in phagocytosis in vitro, the **Objective 3** in this PhD Thesis will be to assess its possible role on microglial phagocytosis both in vitro and in vivo.

3.3.3.2. GPR34-related receptors

LysoPS recognition is not restricted to GPR34. It is shared with other three known receptors: P2Y10, GPR174 [189], and G2A [190] **(Figure 5)**. Among these three receptors, only G2A has been linked to phagocytosis [190, 191], similar to GPR34 [182].

-P2Y10: P2Y10 expression has been demonstrated to be restricted to the spleen and thymus [192]. Recent qPCR analyses have shown no expression in cultured microglial cells [193]. Additionally, recent studies have shown that P2Y10 is highly enriched in eosinophils compared to other leucocytes, being the only lysoPS receptor expressed by eosinophils as well [194]. It is known that P2Y10 interaction with lysoPS determines eosinophils degranulation [195]. Furthermore, in vitro studies with chinese hamster ovary (CHO) cells allowed to demonstrate that P2Y10 recognizes two ligands other than lysoPS, S1P and lysophosphatidic acid (LPA), both related to intracellular calcium (Ca^{+2}) increases [196].

- GPR174: GPR174 receptor expression is also restricted to spleen and thymus, and no expression is detected in microglial cells at all [193]. This receptor has been involved in the suppression of T lymphocytes activation via lysoPS [197].

- G2A: is highly expressed in B and T cells, although is predominant in macrophages [198, 199]. Its expression in microglia remains unknown. Studies in T lymphocytes allowed to identify sphingosylphosphorylcholine (SPC) as G2A receptor ligand [200]. SPC has been shown to induce intracellular signaling such as intracellular Ca^{+2} levels increase [200]. In spite of being initially defined as a proton sensor very sensitive to pH variations [201], G2A has been revealed as an enhancer of phagocytosis in macrophages as well. In the last few years, G2A has been shown to have affinity for a second ligand, lysoPS. Consequently, lysoPS-G2A interaction has been stated to influence the phagocytosis of apoptotic neutrophils by peritoneal macrophages [190, 191].

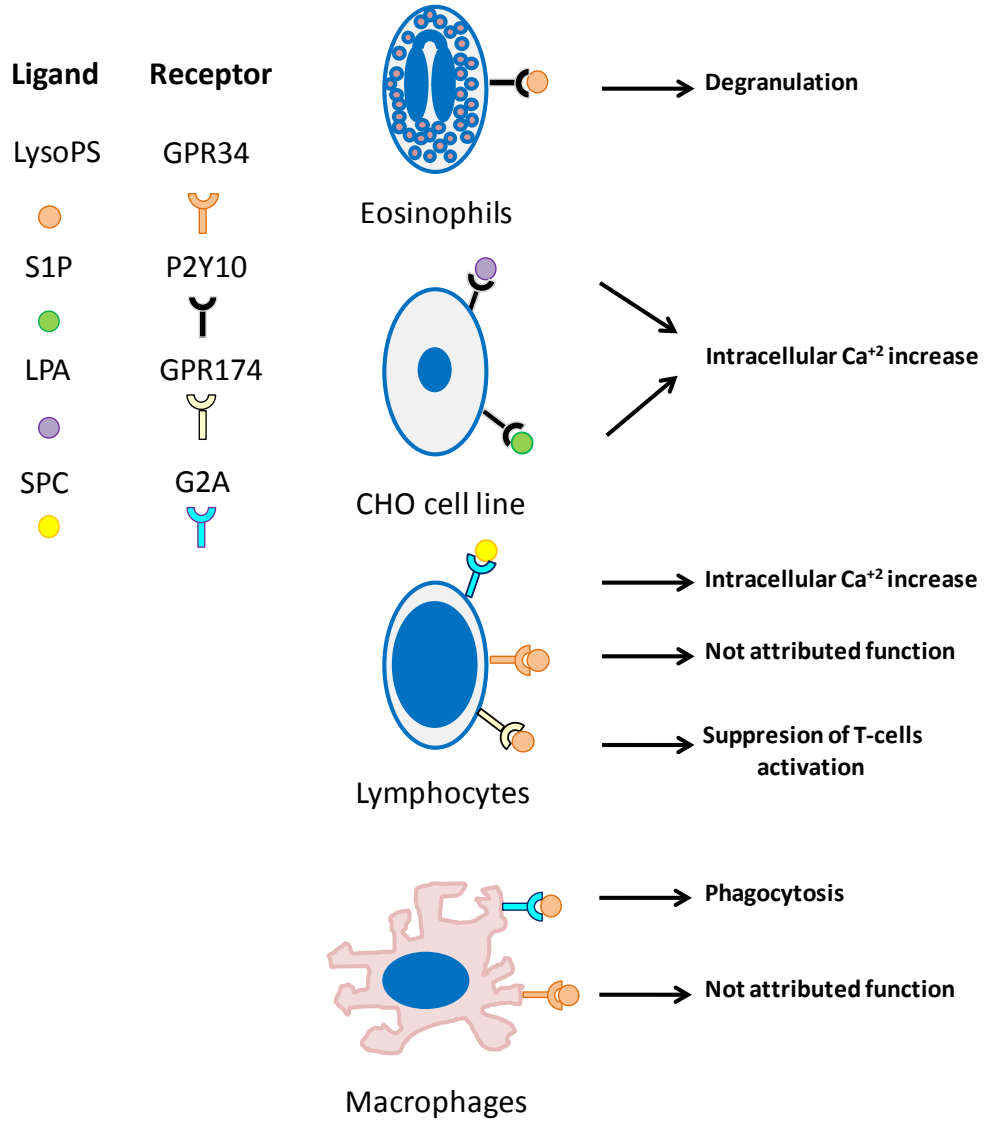

Figure 5. GPR34-related (lysoPS) receptors and their ligands. *Together with G protein-coupled receptor 34 (GPR34), three other receptors with affinity for lysophosphatidylserine (lysoPS) have been described: P2Y10, G protein-coupled receptor 174 (GPR174) and G2A. P2Y10 receptor interaction with lysoPS molecule leads to eosinophils degranulation [195]. However, P2Y10 interaction with their two other known ligands, sphingosine-1-phosphate (S1P) and lysophosphatidic acid (LPA), are linked to increases in intracellular calcium (Ca^{+2}) levels, observed in chinese hamster ovary (CHO) cells [196]. GPR174 receptor binding to lysoPS impedes the activation of T lymphocytes [197]. Lastly, G2A interaction with sphingosylphosphorylcholine (SPC) leads to increases in intracellular Ca^{+2} levels in lymphocytes [200]. On top of that, G2A receptor binding to lysoPS is related to the enhancement of phagocytosis of apoptotic neutrophils by macrophages [190, 191] . Apart from their role in microglia, GPR34 receptor, whose unique known ligand is lysoPS, is also known for being expressed in macrophages and lymphocytes, although their role in these cell types remains unknown. In the left, schematic representation of the different ligands (sphere-shaped) and receptors (Y-shaped).*

3.3.4. Methods to quantify phagocytosis of apoptotic cells.

The choice of reliable and consistent methods is fundamental in order to quantify phagocytosis properly. The assessment of microglial phagocytosis has been performed by both indirect and direct methods.

Indirect methods (in vivo and in vitro) may not reliably represent phagocytic efficiency. Some of them are based on the use of classical phagocytosis markers such as macrosialin (CD68); or microglial ameboid morphology [141]. The use of CD68 to quantify phagocytosis [17] seems misleading since it has been shown that microglia with impaired phagocytosis overexpress this protein, together with the fact that CD68-defective mice do not exhibit any alteration in phagocytosis [37]. Concerning microglial morphology, it is important to remark that phagocytosis can be performed by either ramified or hypertrophic microglia, thus it is not advisable to associate microglial morphology to their ability to execute the phagocytic response [28].

Fortunately, several methods have been developed to directly quantify microglial phagocytosis in vivo [141]. One of these methods is based on the quantification of engulfed artificial targets, such as latex beads. While widely used, latex beads have several limitations, since they do not manage to emit any signal to be recognized as a target by phagocytes. Thus, they do not activate the different phagocytic response mechanisms in microglia [163]. Another method relies on 3D electron microscopy reconstruction. This technique has been used for quantifying synaptic elements [202]. Other method involves the use of light microscopy and immunostaining [203]. This method allows the identification of phagocytic cups but does not ensure that cups contain apoptotic cells. Two other techniques can be mentioned: 2-photon microscopy and confocal microscopy. These are considered the best methods to directly assess microglial phagocytosis in vivo. 2-photon microscopy has been employed for quantifying phagocytosis of apoptotic cells in zebra fish [204]. In this PhD Thesis we have used confocal microscopy combined with immunofluorescence. Confocal microscope allows the definition of three dimensional phagocytic pouches and also to visualize whether these are empty or encapsulating an apoptotic cell [28]. Considering that we have focused on studying phagocytosis of apoptotic cells, the use of confocal microscopy results fundamental for distinguishing with precision any corpse engulfed by microglia in our samples.

3.3.5. Downstream consequences of phagocytosis of apoptotic cells

The removal of apoptotic cells via phagocytosis is essential to maintain tissue homeostasis. Whenever apoptotic cells are not phagocytosed properly, they give rise to secondary necrotic cells, involving the spillover of their intracellular contents, and triggering an inflammatory response [205] or autoimmune diseases [206]. Phagocytosis involves several benefits for the organism, apart from the removal of dead corpses or noxious agents [207]. It prevents the previously mentioned release of toxic cell components and importantly, exerts an anti-inflammatory function [208], thus maintaining tissue homeostasis. Several studies show that phagocytosis of apoptotic cells is anti-inflammatory in vitro [209, 210]. In microglial cells, it has been shown that upon phagocytosis, TNF-α secretion by microglia drops and TGF-β increased when compared to LPS-stimulated microglia [43]. Phagocytosis of apoptotic cells is a complex process which may impact on several cell processes. In this PhD Thesis we have focused on the consequences of phagocytosis on the microglial metabolism and their possible implications in neurogenesis.

The phagocyte metabolism is altered upon engulfment. The ingestion of apoptotic bodies by phagocytes is a tremendous metabolic load, involving the internalization of lipids, carbohydrates, proteins, nucleic acids or any other component belonging to target cells [211]. Nonetheless, the digestion of these materials remains the most unknown step of phagocytosis and the ultimate consequences for phagocytes have just begun to be unraveled. Related to this question, the novel concept of “trained immunity” has emerged in macrophages [212]. Upon engulfment of microbes, “trained” macrophages execute a metabolic shift from OXPHOS to aerobic glycolysis, the two main metabolic cell pathways for ATP production **(described in detail in Sections 3.4.1.1 and 3.4.1.2)**. This process is supported by epigenetic modifications in key genes of the glycolytic pathway, such as hexokinase and pyruvate kinase, via the master glycolysis transcription factor hypoxia induced factor-1 alpha (HIF-1α) [212]. Since most of metabolic studies have been performed in macrophages, very little is known about the possible metabolic adaptations in microglial cells upon phagocytosis. Interestingly, previous functional analysis of the microglial transcriptome in our laboratory evidence changes in glycolysis and OXPHOS pathways upon 24h of phagocytosis, suggesting a metabolic adaptation process **(Figure 6) (Data from Irune Díaz-Aparicio PhD Thesis, 2018)**. Therefore, the **Objective 4** of this PhD Thesis will be to study the possible metabolic adaptations in glycolysis and OXPHOS occurring in microglia upon phagocytosis.

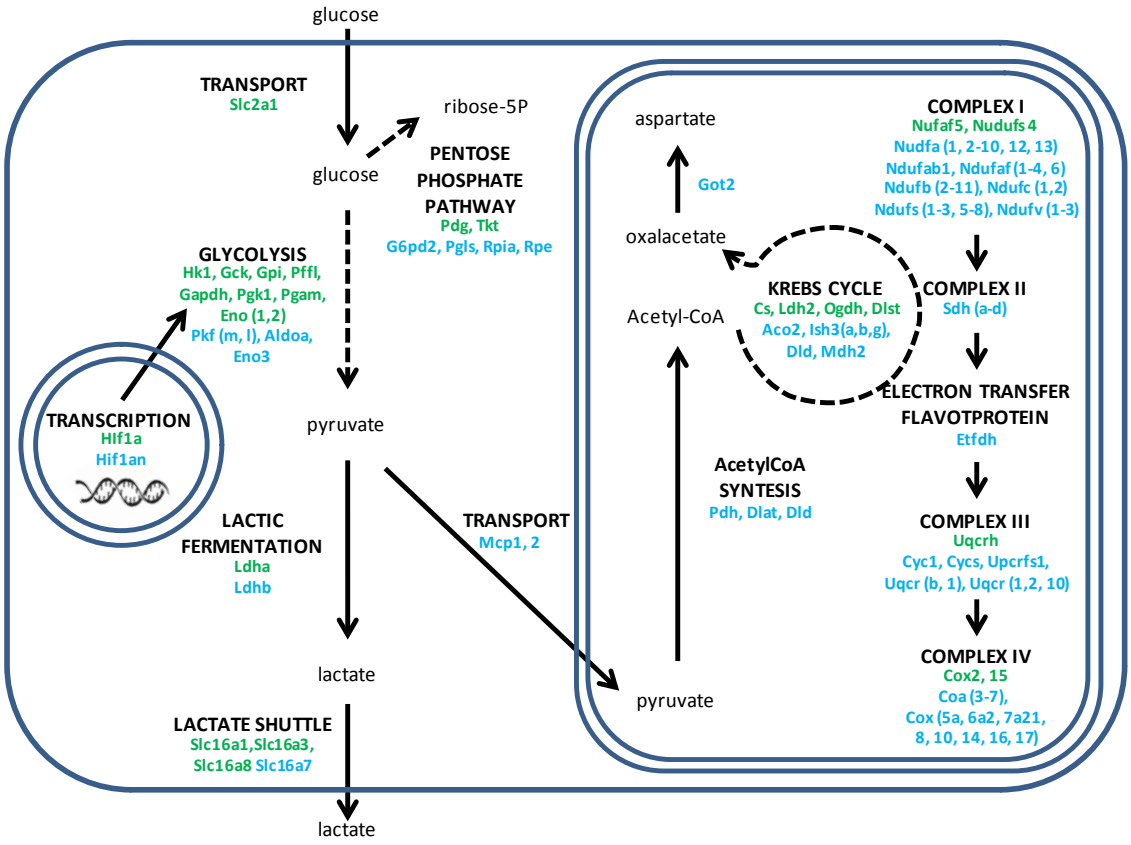

Figure 6. Metabolic adaptations of microglial cells upon phagocytosis. *Scheme reflecting the metabolic rearrangement in microglia upon 24h of phagocytosis via transcriptome analysis. Up-regulated genes are represented in green whereas down-regulated genes are represented in blue. Adapted from* ***Irune Díaz-Aparicio PhD Thesis (2018)*****.**

In addition to metabolic adaptations, phagocytosis may also serve to feed back into the surrounding cells and in this PhD Thesis we will study the adult neurogenic cascade. Specifically, we will focus on the SGZ of the hippocampus. In this region, the vast majority of newborns cells produced during neurogenesis become apoptotic and then are efficiently removed from the neurogenic niche by microglial cells via phagocytosis [28]. In addition, it has been shown that phagocytosis of apoptotic cells can trigger the secretion of trophic factors by microglia, such as TGF-β or NGF [43]. Moreover, vascular endothelial growth factor (VEGF) has been shown to be produced by hepatic macrophages upon phagocytosis. All these factors are identified as regulators of hippocampal neurogenesis in vivo [213, 214]. Thereby, the removal of dead corpses by microglia in the SGZ could be accompanied by the secretion of trophic factors which could help driving homeostasis in the neurogenic cascade, directly impacting on neurogenesis **(Figure 7)**. With the aim to test whether microglial phagocytosis of apoptotic cells may involve any changes in neurogenesis, our **Objective 5** is to assess whether phagocytosis impairment alters the hippocampal neurogenic cascade.

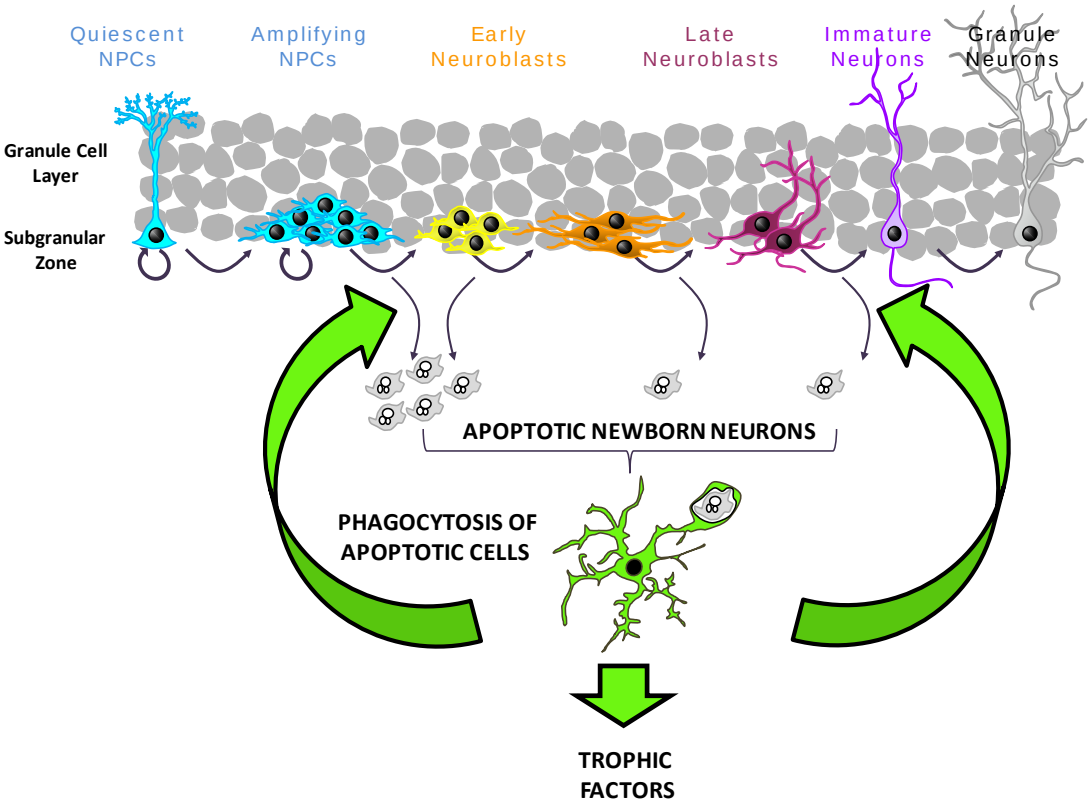

Figure 7. Microglial phagocytosis may involve benefits for the neurogenic cascade. *The removal of apoptotic cells by microglia in the SGZ of the hippocampus may give rise to the secretion of several trophic factors that could impact positively on neurogenesis (represented by green arrows). Adapted from [28].*

3.4. METABOLISM

Metabolism constitutes an essential set of chemical transformations within the cells which provides the energy required to elicit several functions such as mitosis or ATP synthesis [215]. The brain presents high metabolic demands and consumes nearby 20% of the available oxygen in the organism [216]. Whereas adult brain utilizes glucose as the absolute energy substrate, the developing brain can employ other molecules such as glycerol, lactate or amino acids [217]. When alternate molecules are used to produce energy, the brain still has an absolute requirement for glucose [217].

Glucose taken up by the brain serves as the fuel in a coordinated network of metabolic pathways including glycolysis, performed in the cytosol, followed by the tricarboxylic acid (TCA) cycle, the electron transport chain (ETC) and OXPHOS fundamentally, performed within

mitochondria [216]. In the next sections, we will delve into the description of these metabolic pathways just like the function and properties of mitochondria, known to exert a fundamental role in the metabolism of eukaryotic cells.

3.4.1. Metabolic pathways in eukaryotic cells

Two main metabolic pathways are responsible for the ATP production in eukaryotic cells: glycolysis and OXPHOS.

A complex network of metabolic reactions is triggered from the glucose uptake by cells to its conversion into pyruvate in the cytosol. After glycolysis, pyruvate is incorporated into the mitochondria and transformed to acetyl-coenzyme A (acetyl-CoA). Then, acetyl-CoA is converted into citrate in the TCA cycle, in which intermediate molecules such as nicotine adenine dinucleotide (NADH) and flavin adenine dinucleotide ($FADH_2$) are produced and employed as electron donors in the ETC of the inner mitochondrial membrane to initiate redox reactions which lead to the ATP production in the mitochondrial matrix in a process called OXPHOS. These metabolic pathways will be detailed below.

3.4.1.1. Cytosolic metabolic pathways

The cytosol is the liquid part of the cell cytoplasm. This cell site is responsible for signal transduction processes from the cell membrane to the nucleus [218] or organelles [219]. Additionally, the cytosol is the site of most prokaryote metabolism [220] and an important part of eukaryotic metabolism. Many important biochemical processes within eukaryotic cells take place in the cytosol, such as protein biosynthesis, glycolysis, the pentose phosphate pathway and gluconeogenesis, which will be introduced next.

Aerobic and anaerobic glycolysis

The glycolytic pathway is often referred to as Embden-Meyerhof pathway in honor of these two biochemists who made a major contribution to its knowledge in the 1930s. The glycolytic pathway was completely elucidated in 1940 [221]. Glycolysis is a major pathway for ATP production and very essential for brain, which is dependent on glucose as source of energy. Many glycolytic intermediates are taking part in other pathways since they are employed for amino acids or lipid synthesis [222]. Glycolysis can occur in presence or absence of oxygen (aerobic and anaerobic glycolysis, respectively). In aerobic conditions, pyruvate is carried into the mitochondria through a pyruvate carrier in a process called oxidative decarboxylation. Afterwards, pyruvate is converted into acetyl-CoA through the pyruvate dehydrogenase (PDH)

enzyme, and then metabolized in the TCA cycle [216] **(Figure 8)**. In anaerobic conditions, pyruvate is reduced by NADH to lactate via lactate dehydrogenase [223]. $NADH_2$ used in this step is obtained from that obtained in the reaction catalyzed by glyceraldehyde-3-phosphate dehydrogenase enzyme during aerobic glycolysis. The conversion to lactate allows regenerating NAD^+, which can be reused by glyceraldehyde-3-phosphate dehydrogenase, so glycolysis and thus ATP production can continue even without oxygen.

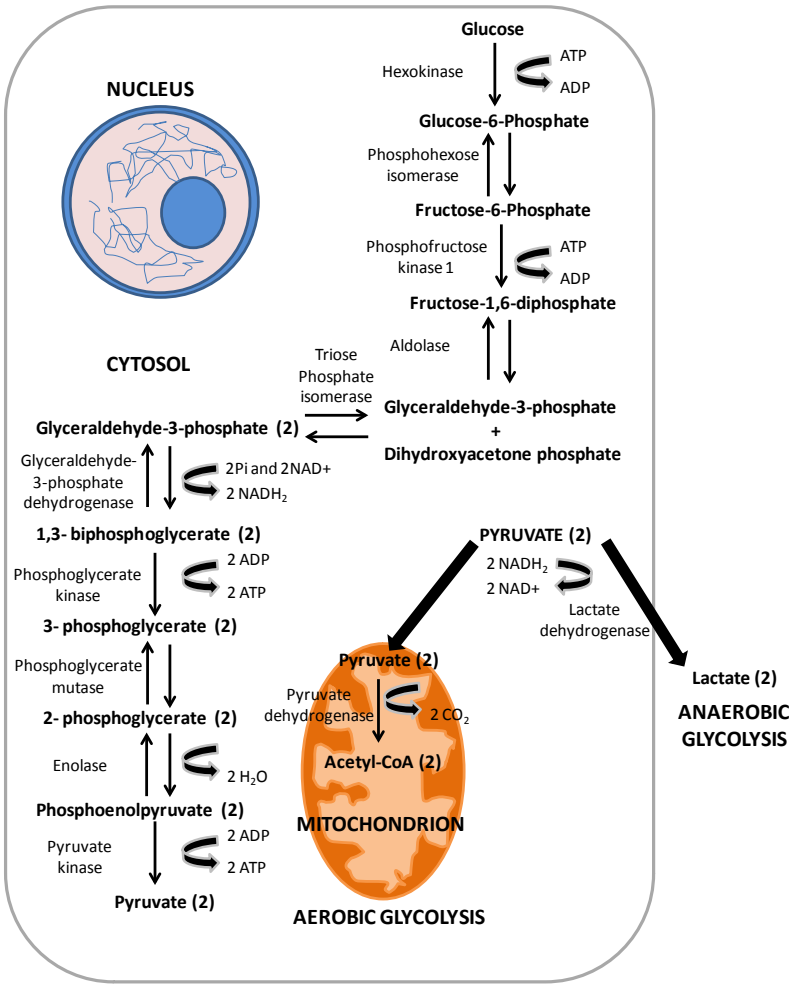

Figure 8. Aerobic and anaerobic glycolysis. *Scheme representing the biochemical reactions triggered in both routes. In aerobic glycolysis, pyruvate generated in the cytosol (from glucose) enters the mitochondrion and it is converted into acetyl-Coenzyme A (acetyl-CoA). Subsequently, the TCA cycle is initiated. In anaerobic glycolysis, pyruvate is extruded from the cell and converted to lactate. The number of molecules produced in each step is shown in brackets.*

Pentose phosphate pathway, gluconeogenesis and other cytosolic pathways

The pentose phosphate pathway (PPP) is an alternative route in which glucose-6-phosphate (G6P) is not driven to ATP synthesis, contrary to glycolytic pathway. The PPP comprises two phases: the oxidative phase and the non-oxidative phase.

During the oxidative phase, nicotine adenine dinucleotide phosphate (NADPH) and ribonucleotides are produced through three different biochemical reactions. First, G6P is dehydrogenated by glucose-6-phosphate dehydrogenase (G6PDH) to yield NADH and other product called 6-phosphogluconolactone. Second, 6-phosphogluconolactone is hydrolyzed into 6-phosphogluconate via 6-phosphogluconolactonase (6PGL). Third, 6-phosphogluconate is decarboxylated via 6-phosphogluconate dehydrogenase (6PGDH) to yield a second NADH and ribulose-5-phosphate (Ru5P), which is converted to ribose-5-phosphate (R5P). The non-oxidative phase involves a series of reversible reactions that recruit additional glycolytic intermediates, such as fructose-6-phosphate (F6P) and glyceraldehyde-3-phosphate (G3P), which can give rise to pentose phosphates and vice versa [224, 225].

Other metabolic pathways occur in cytosol, such as gluconeogenesis. Gluconeogenesis is a complex metabolic process in which glucose is synthesized from non-carbohydrate precursors, such as glycerol, lactate, pyruvate and glucogenic amino acids [226]. Contrary to glycolysis, it is an anabolic pathway, which comprises a series of reactions, some of them related to glycolytic pathway (reverse steps) and others exclusive of gluconeogenesis. These exclusive biochemical reactions involve: the conversion of pyruvate to phosphoenolpyruvate via pyruvate carboxylase (PC) and phosphoenolpyruvate carboxykinase (PEPCK); the conversion of fructose-1,6 biphosphate to fructose-6-phosphate through fructose biphosphatase (FBPase) activity; and the conversion of G6P to glucose via glucose-6-phosphatase (G6Pase). Other metabolic pathways present in the cytosol include serine biosynthesis, glyceroneogenesis, glutaminolysis, cataplerosis or anaplerosis [226] in which the enzymes PEPCK, FBPase or G6Pase participate as well.

3.4.1.2. Mitochondrial metabolic pathways

As the main organelle responsible for ATP production in eukaryotic cells, the mitochondrion houses a plethora of metabolic processes involving sugars, fats and proteins. The most relevant metabolic pathways produced in mitochondria are two: the TCA cycle, performed in mitochondrial matrix and OXPHOS, performed in the inner mitochondrial membrane (IMM) **(Figure 9)**. Furthermore, mitochondria are also able of exerting other remarkable processes

like the β-oxidation of fatty acids or Ca^{+2} handling [227]. Most of these biochemical reactions will be summarized below.

TCA cycle

The TCA cycle is the most important central pathway, since it connects almost all the metabolic pathways. It constitutes the final common pathway for the oxidation of carbohydrates, proteins and lipids. The reactions and components of the TCA cycle were established in 1930 [228] and it was firstly proposed by Hans Krebs in 1937.

The TCA consists of eight different phases. In the first phase or condensation phase, acetyl-CoA and oxalacetate are converted to citrate in a reaction catalyzed by citrate synthetase [216]. The second phase implies the isomerization of citrate molecule. Aconitase enzyme allows the conversion of citrate into *cis*-aconitate [229]. Later, *cis*-aconitate is converted to isocitrate. The third phase involves the conversion of isocitrate into alpha-ketoglutarate by isocitrate dehydrogenase, producing the cofactor $NADH_2$. In the fourth phase, a complex of enzymes leads to the formation of succinyl-coenzyme A (succinyl-CoA) from alpha-ketoglutarate via alpha-ketoglutarate dehydrogenase [230]. Afterwards, in the fifth phase, succinyl-CoA gives rise to succinate by succinic thiokinase. In the sixth phase, succinate will be converted to fumaric acid via succinate dehydrogenase [231]. This reaction is accompanied by the conversion of FAD into $FADH_2$. The seventh reaction consists of the hydration of the fumaric acid via fumarase enzyme [232] to form malate. Finally, in the eighth phase, malate is converted to oxalacetate by the malate hydrogenase enzyme. During the reaction, NAD is converted to $NADH_2$. This oxalacetate will be part of a new round of the TCA cycle when helps acetyl-CoA form a new molecule of citrate [233].

As a result of the TCA cycle, two molecules are used as electron donors in the ETC of the IMM to produce ATP via OXPHOS: these are the coenzymes NADH and $FADH_2$ [216]. These coenzymes are able to regenerate NAD^+ and FAD for the TCA cycle as well [216].

Oxidative phosphorylation (OXPHOS)

OXPHOS constitutes the biochemical process through which the energy released by the oxidation of substrates is used to drive ATP synthesis, a fundamental molecule for many biological processes in the organism.

OXPHOS process was unraveled by Peter Mitchell several decades ago. His chemiosmotic theory, still in force, established that the mitochondrial ETC is coupled to ATP synthesis through an electrochemical proton gradient [234, 235].

The ETC is composed of several carrier proteins in charge of the passage of the electrons given by NADH and $FADH_2$. The carriers of the ETC are organized into four protein complexes. The electrons, through several redox reactions across these complexes, are directed to oxygen and the energy released by these reactions drives the synthesis of ATP from ADP in a process called OXPHOS. This phenomenon occurs in a fifth complex, called ATP synthase, which couples the energy of redox reactions generated in the previous four to synthesize ATP.

Eventually, the breakdown of glucose via glycolysis allows the production of acetyl-CoA within mitochondria. Inside this organelle, acetyl-CoA enters the TCA cycle and gives rise to the production of NADH and $FADH_2$ in the mitochondrial matrix. Both molecules act as electron donors for the ETC, located in the IMM.

NADH donates electrons to complex I of the ETC. These electrons are then passed through the coenzyme Q (Q) to complex III. In complex III, electrons are transferred from cytochrome b to cytochrome c. Cytochrome c, located in the outer face of the IMM, carries the electrons to complex IV, where they are finally transferred to oxygen. Remarkably, a different complex, called complex II, receives electrons from succinate, produced in the TCA cycle. The electrons are then directed to $FADH_2$ instead of NADH. Afterwards, electrons reach Q, then pass to the complex III and finally to complex IV, as mentioned above. This complex constitutes an alternative route to the transfer of electrons from NADH to Q at complex I. The passage of electrons from $FADH_2$ to Q through complex II does not involve a drop in free energy. Therefore, it is not coupled to ATP synthesis.

The energy derived from the electron transport through complexes I, III and IV is coupled to the generation of a proton gradient which passes from the mitochondrial matrix to the intermembrane space (IMS). The electrochemical proton gradient created allows complex V (ATP synthase) to couple the flow of protons back across the membrane to the synthesis of ATP.

Other mitochondrial metabolic pathways

Together with TCA cycle and OXPHOS, other pathways are developed within these organelles such as Ca^{+2} handling or β-oxidation of fatty acids.

Ca^{+2} handling is produced in the mitochondrial matrix in order to balance the energy demands of the cell and the energy produced by OXPHOS. When the cytosolic Ca^{+2} concentration increases, mitochondria execute Ca^{+2} uptake through an uniporter channel located in the IMM [236]. The subsequent rise of Ca^{+2} levels in mitochondrial matrix then activates some enzymes

of TCA cycle: pyruvate dehydrogenase, α-ketoglutarate dehydrogenase and NAD-isocitrate dehydrogenase. As a consequence, the amount of NADH available to the start of the ETC increases, finally triggering a rise in the ATP synthesis via OXPHOS [237].

β-oxidation of fatty acids is initiated when cytosolic fatty acids are esterified to long chain acyl-coenzyme A (acyl-CoA). Then, the acyl group of the long chain acyl-CoA is transferred to carnitine by carnitine palmitoyltransferase-1 (CPT-1) in the outer membrane. The new molecule formed, acylcarnitine, is transported across the inner membrane via carnitine translocase (CAT) until reaching the matrix. When acylcarnitine reaches the mitochondrial matrix, it will be reconverted to long chain acyl-CoA and carnitine via CPT-2. Then, long chain acyl-CoA enters the β-oxidation pathway, leading to the production of acetyl-CoA, which will be driven to TCA cycle to produce NADH and $FADH_2$ [238].

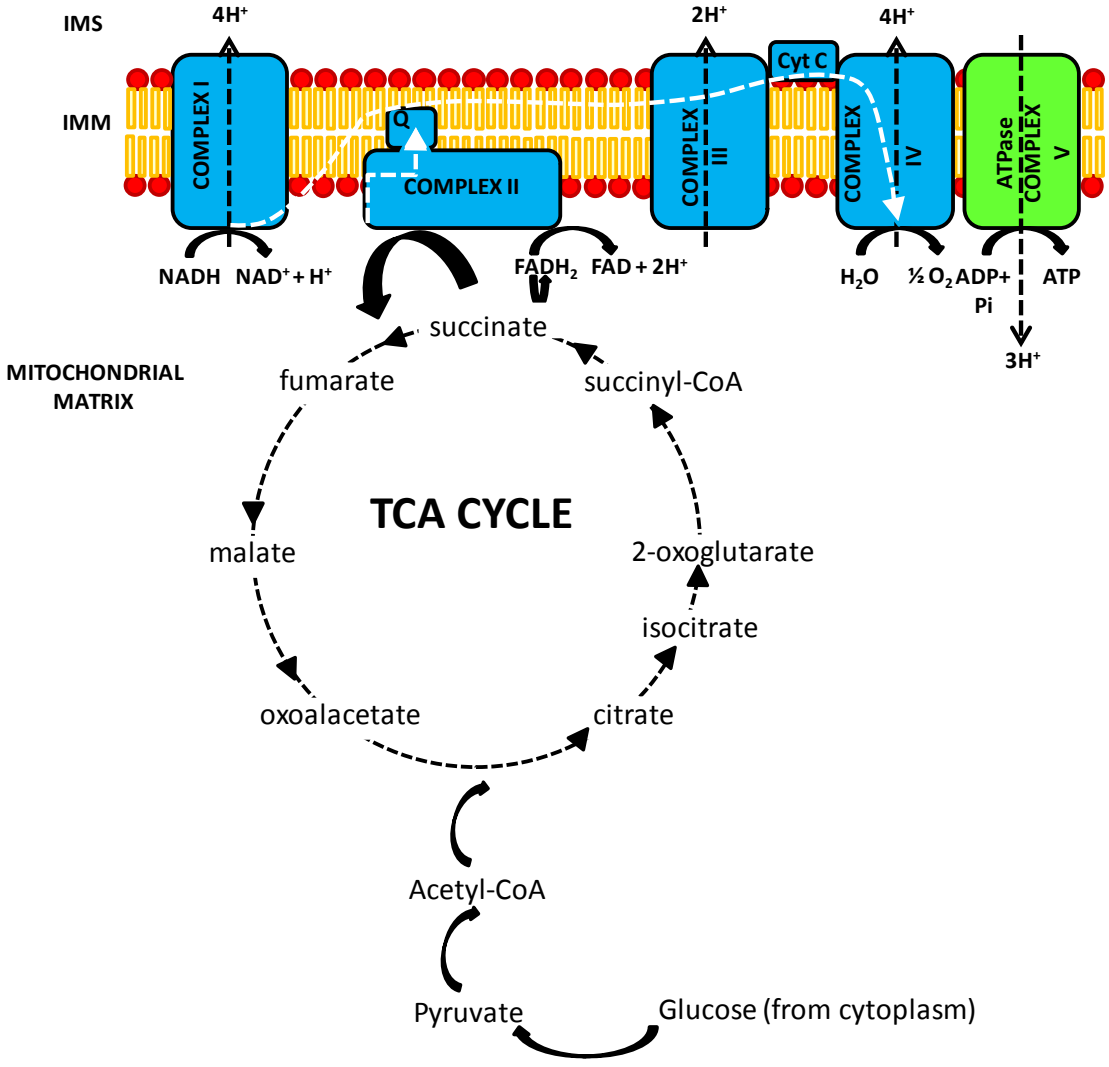

Figure 9. Main mitochondrial pathways in mammalian cells. *Glucose is converted to pyruvate in the cytoplasm via glycolysis. Then, pyruvate (in aerobic conditions) is carried to mitochondrion where it will be converted to acetyl-coenzyme A (acetyl-CoA). Acetyl-CoA allows the initiation of the tricarboxylic acid (TCA) cycle in the mitochondrial matrix, where several biochemical reactions are produced to finally obtain two electron donor molecules, such as nicotinamide adenine dinucleotide (NADH) and flavin adenine dinulceotide ($FADH_2$). These molecules give electrons to the electron transport chain (ETC) complexes, which generate an electron flow across the inner mitochondrial membrane (IMM). NADH give some electrons to complex I, which pass through the coenzyme Q (Q) to complex III. In complex III, electrons go through cytochrome c (Cyt C) to finally reach complex IV. The energy derived from the electron flow will be coupled to the generation of a proton gradient directed from the mitochondrial matrix to the intermembrane space (IMS). The electrochemical proton gradient created allows complex V (ATP synthase) to couple the flow of protons back across the membrane to the synthesis of ATP in a process called OXPHOS. Furthermore, there is an alternative route for the electron flow: complex II receives electrons from succinate. Electrons are directed to $FADH_2$ and reach Q, from where they will be directed to the complex III and thus to complex IV. Remarkably, this route is not coupled to ATP synthesis. White-dotted arrows indicate the electron flow and black-dotted arrows indicate the proton gradient.*

3.4.2. Mitochondria: definition, origin and functions

Mitochondria are double-membrane bound cell organelles, which act as powerhouses within eukaryotic cells to meet with any cellular demand. Many studies performed during the 20th century demonstrated that mitochondria evolved from endosymbiotic bacteria, thus having a prokaryotic origin [239-241]. As a consequence of this origin, they possess a residual genome known as mitochondrial DNA (mtDNA) encoding a total of 13 proteins, essential for the respiratory chain [242]. Defects in mtDNA have been associated to several diseases, such as Leigh syndrome, Leber's hereditary optic neuropathy or myoclonus epilepsy with ragged red fibers [243, 244]. Mitochondria are in charge of energy production via ATP, phospholipids synthesis and heme generation, a prosthetic group that is an essential component of hemoglobin but also found in other proteins and enzymes such as cytochromes, catalases or nitric oxide synthase [245, 246]. Mitochondria are also responsible for regulating Ca^{+2} homeostasis, apoptotic activation and cell death [247, 248]. Moreover, they constitute the location where very relevant processes such as OXPHOS, the TCA cycle and β-oxidation of fatty acids take place [227], detailed above **(Section 3.4.1.2)**.

3.4.2.1. Mitochondrial dynamics

Mitochondria are characterized for being very dynamic organelles. This dynamism is translated into several behaviors that include: fusion (the joining of two mitochondria into one) and

fission (the opposite process), whose balance determines the mitochondrial network morphology; transport (directed movement); and mitophagy (self-destruction via autophagy) [227] **(Figure 10)**. Interestingly, in the last several years many studies have focused on the possible link between mitochondrial metabolism and these dynamics, which will be described next.

Fusion

Mitochondrial fusion is a two-step process that requires fusion of the outer membrane followed by the inner-membrane. In mammals, this process is mediated by three GTP hydrolases (GTPases) that belong to the dynamin superfamily [249]. These GTPases are mitofusin 1 (Mfn1) and mitofusin 2 (Mfn2), involved in outer membrane fusion; and optic atrophy 1 (Opa1), involved in inner membrane fusion. Mitofusins loss of function gives rise to the fragmentation of mitochondrial network [250]. Fusion is very important for OXPHOS activity, especially because it can regulate the mtDNA levels. Furthermore, some studies stated that the addition of substrates which promote OXPHOS activity led to the stimulation of mitochondrial fusion [251].

Fission

Mitochondrial fission (division) is a complementary function to fusion. Mitochondrial division is crucial for cellular physiology [252], since it permits the removal of damaged mitochondria via a specialized form of autophagy, called mitophagy [253], which facilitates its degradation and recycling.

Mitochondrial fission is mediated by Dynamin-related protein 1 (Drp1). Drp1 exerts its function in a GTP-dependent manner in the outer mitochondrial membrane via aid of other proteins such as Mff, Fis1, MiD49 and MiD50 [227]. Several metabolic mechanisms have been proposed to regulate mitochondrial fission, being the phosphorylation of Drp1 one of the most characterized ones [254-256].

Transport

The location of mitochondria within cells results crucial. In neurons, mitochondria can move to the axon terminals in order to supply energy-demanding processes since they are the main source of ATP in cells. In many mammals, mitochondrial transport is possible due to the action of several motor proteins which work along the microtubule network of cells fundamentally [257]. These proteins, called kinesins, allow mitochondrial transport both towards the axon

terminals in the case of neurons (anterograde) whereas the transport towards cell soma (retrograde) is mediated by dyneins [258]. In order to direct the anterograde transport of mitochondria along the cell microtubules, kinesins need to be connected to mitochondria through GTPases Miro1 and Miro2. These GTPases interact with kinesin motor proteins via Milton proteins (Track1 and Track2), then constituting the Miro-Milton-kinesin complexes. In contrast, the retrograde transport of mitochondria requires a complex formed by dynein and the adaptor protein dynactin. Dynactin binds directly to cytoplasmic dynein and microtubules, and together with huntingtin-associate protein 1 (HAP1), is essential to the mitochondrial transport in the negative direction [259].

Mitophagy

The amount of mitochondria in a cell depends of a balance between biogenesis and degradation. When mitochondria are excessive or become defective, they suffer clearance via an autophagy process called mitophagy. The best studied model to understand mitophagy pathway involves Pink1 and Parkin, relevant genes in some cases of familial PD. Pink1 is often imported and degraded inside mitochondria. Cell stress induces mitochondria depolarization, triggering the accumulation of Pink1 on the outer mitochondrial membrane [260]. This is followed by Parkin recruitment and ubiquitination of outer membrane proteins and consequently, autophagy is initiated [261]. Interestingly, under glucose deprivation conditions, OXPHOS is increased, thus leading to the enhancement of mitophagy [262].

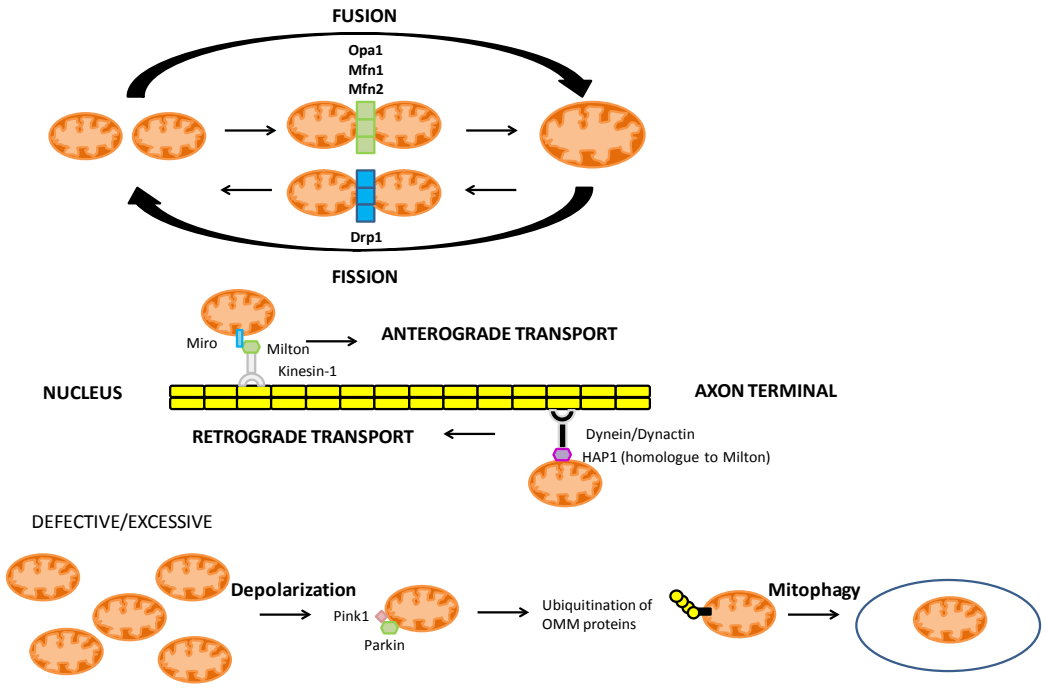

Figure 10. Mitochondria are very dynamic organelles. *Schematic representation of the four different dynamics performed by mitochondria. From the top to the bottom, mitochondrial joining (fusion), division (fission), transport along microtubules (anterograde and retrograde) and degradation via mitophagy. Mitochondrial fusion is mediated by three proteins: optic atrophy 1 (Opa1), mitofusin 1 (Mfn1) and mitofusin 2 (Mfn2). Fission is principally mediated by dynamin-related protein 1 (Drp1). Anterograde transport (towards axon terminal in the case of neurons) of mitochondria is possible thanks to the complex Miro-Milton-Kinesin-1. Retrograde transport (towards cell nucleus) involves the complex dynein/dynactin and huntingtin-associated protein 1 (HAP1) protein. Lastly, defective or excessive mitochondria undergo mitophagy through Pink1 and Parkin proteins.*

3.4.3. Cellular metabolism analysis methods

Traditionally, methods used to assess cell metabolism rely on extracellular flux analysis. Some of the classical extracellular flux analysis methods are: the Clark-type oxygen electrode (Hansatech Instruments), the Oroboros oxygraph-2k (Oroboros Instruments) or fiber optic oxygen sensors (Ocean Optic Sensors).

The Clark-type electrode measures oxygen dissolved in liquid or gas phase in the sample chamber by polarography [263], a process used to determine the oxygen content of electrolyte solutions (and of several tissues) by using solid microelectrodes. It is employed for intact and permeabilized cells as well as on isolated mitochondria. It has the advantage that many inhibitors and substrates can be added. However, large sample sizes are required and the chamber is stirred so cells cannot be adherent.

The Oroboros oxygraph is similar to the former method, although it uses a Clark-type electrode with high-resolution respirometry [264], based on the measurement of changes in oxygen concentration. In this case, small sample sizes are sufficient and it presents increased detection sensitivity. Nevertheless, the oxygraph is very expensive.

Finally, the fiber optic oxygen sensors measure the partial pressure of dissolved or gaseous oxygen in a sample by fluorescence [265]. In spite of existing more sophisticated methods (described next), the sensors have a prolonged lifetime and do not consume oxygen, so they permit extended measurements of samples.

These classical techniques have been gradually replaced by the use of modern methods, such as the XF Extracellular Flux Analyzer (Seahorse Bioscience), the most accurate method to assess cell metabolism at the moment. This is the first instrument which simultaneously

measures both cellular respiration (oxygen consumption rate (OCR)) and glycolysis (extracellular acidification rate (ECAR)). Remarkably, XF Extracellular Flux Analyzer presents an alternative method to assess glycolysis which relies on the proton efflux rate (PER) measurement. XF Extracellular Flux Analyzer method can be briefly explained: cells (or mitochondria) are plated in a 24 or 96 wells-microplate. Then, a small volume of cell medium is isolated above a monolayer of cells within the microplate, creating a "transient microchamber". Both respiration and glycolysis cause rapid and measurable changes to the concentrations of dissolved oxygen and free protons in this "microchamber", which are measured every few seconds by sensor probes above the cell monolayer. Once a measurement is completed, the probes lift, allowing the larger cell medium above to mix with the medium in the "microchamber", restoring cell values to baseline. Additionally, the analyzer presents an integrated drug delivery system which allows the injection of up to three compounds per well. Several combinations can be employed, depending on the kit chosen. The two main Seahorse kits employed are: XF Cell Mito Stress Test Kit and XF Glycolysis Stress Test Kit.

-XF Cell Mito Stress Test Kit, specific for assessing mitochondrial function, allows the sequential injection of oligomycin (ETC complex V inhibitor), which aids to estimate ATP production; carbonyl cyanide-p-trifluoromethoxyphenylhydrazone (FCCP), which disrupts the mitochondrial membrane potential and permits to estimate the maximal mitochondrial respiration; and a mix of rotenone/antimycin A (inhibitor of ETC complexes I and III), which blocks mitochondrial respiration, giving information about the respiration produced by processes outside mitochondria.

-XF Glycolysis Stress Test Kit, used for measuring glycolytic function, first injects glucose to generate pyruvate and estimate basal glycolysis; next, oligomycin is injected to inhibit the ETC complex V, revealing the maximum glycolytic capacity of cells; and finally an injection of 2-deoxy-glucose (2-DG), a glucose analog, inhibits the glycolytic pathway, determining the acidification of extracellular medium not attributed to glycolysis.

Furthermore, the XF Extracellular Flux Analyzer technology also employs indirect methods to study cell metabolism. For instance, we can mention the measurement of mitochondrial fuels oxidation. This method uses some inhibitors to evaluate the dependency and the capacity of cells to oxidize glucose, glutamine or fatty acids oxidation. Therefore, it provides some information about the contribution of these molecules to basal respiration. Other indirect methods, such as L-lactate assays (Abcam), are based on the lactate oxidation by the enzyme

lactate dehydrogenase, generating a product which interacts with a probe. Therefore, the amount of lactate in a sample is efficiently detected.

3.4.4. Metabolism regulation in macrophages and microglia

Energy demands exerted by cells are responsible for both their energetic production and the substrates influx inside them. In physiological conditions, immune cells, such as macrophages and microglia present a metabolic profile that depends on the energy substrate received. However, this metabolic profile can be altered upon cell activation state.

Metabolism regulation in macrophages

Several reports have shown that changes in the activation state of macrophages are linked to metabolic alterations. For instance, anti-inflammatory cytokine IL-4-stimulated macrophages exhibit increased OXPHOS [266, 267]. In contrast, studies performed in peripheral macrophages have stated that their activation via pro-inflammatory stimuli triggers a metabolic switch from OXPHOS to anaerobic glycolysis in order to increase ATP production [268]. Accordingly, LPS/IFN-γ-activated macrophages have shown increased glycolytic metabolism at the expense of OXPHOS, which is impaired [266, 269]. Besides, pro-inflammatory macrophages present a disrupted TCA cycle, allowing acetyl-CoA to generate fatty acids, lipids or even cytokines [270, 271].

Furthermore, the enhancement of glycolysis upon inflammation allows macrophages to generate sufficient ATP to perform important tasks such as inflammatory cytokines production, formerly mentioned, but also phagocytosis [272, 273]. Interestingly, it is known that upon engulfment of microbes, macrophages rely on aerobic glycolysis at the expense of OXPHOS [212] in a process called “trained immunity” **(see Section 3.3.5)**. The same phenomenon has been observed in macrophages upon phagocytosis of β-glucan [212]. Therefore, in both inflammatory and phagocytic contexts, macrophages increase glycolysis, suggesting a link between these processes.

Metabolism regulation in microglia

Initial works were performed in microglia cell lines. Several studies with BV2 microglia cell line have established that microglial activation via LPS or IFN-γ induction gives rise to a drop in mitochondrial function [274, 275]. Furthermore, it has been also shown that LPA-induced activation of C13NJ microglia cell line leads to alterations in glycolysis but also in motility and

morphology [276]. Additionally, LPS-stimulated BV2 microglia exhibit increased glycolysis via the suppression of mitochondrial function by glucose-regulated protein 75 (Gpr75) [277]. On top of that, LPS stimulation leads to an increase in the PPP pathway, leading to enhanced nucleic acid production for gene transcription [278].

Although these evidences reveal metabolic changes in microglial cells depending on their activation state, very little is known about the possible metabolic adaptations produced in microglia upon performance of one of their most important features, such as phagocytosis. Unfortunately, most of metabolic studies have been performed in macrophages. Therefore, our **Objective 4** will be to evaluate whether microglial phagocytosis of apoptotic cells give rise to any metabolic changes, particularly in glycolytic and OXPHOS pathways.

3.5. ADULT HIPPOCAMPAL NEUROGENESIS

Neurogenesis refers to the formation of newborn neurons in the brain. The first evidences of neurogenesis in the adult mammalian brain were detected many decades ago, thanks to the use of [^{3}H]-thymidine autoradiography, which allowed the visualization of newborn neurons in adult rat and cat brains [279, 280].

Neurogenesis has been described in several brain regions of many species. It has been identified in songbirds [281] and also in reptiles and fish [282]. In mammals, there are two brain regions in which the production of newborn neurons is maintained throughout adulthood: the SVZ, in which olfactory bulb neurons are produced and the SGZ of the hippocampus, which generates granule cells [283]. In this PhD Thesis, we focused on the DG of the SGZ, since it serves us as a good tool to assess microglial phagocytosis via the engulfment of apoptotic newborn neurons constantly produced in this neurogenic niche.

In humans, several studies have confirmed adult neurogenesis in the DG [284-286] whereas it remains controversial in the SVZ [287, 288]. In addition, controversy exists about the persistence of neurogenesis in adult humans. It has been recently published that the amount of proliferating progenitors and newborn neurons is greatly reduced in the DG of the SGZ after the first year and it is undetectable in adults [289, 290]. In contrast, other studies state that adult human neurogenesis continues in the DG until the eighth decade of life [291]. Therefore, more investigation is needed to elucidate the length of human adult neurogenesis.

3.5.1. Neurogenic cascade in the SGZ of the hippocampus

Adult hippocampal neurogenesis is complex and comprises several phases. The neurogenic cascade is maintained by the proliferation of NSCs located in the SGZ [292, 293]. These NSCs were first described as radial astrocytes [294]. They are characterized by the presence of an apical process extended towards the molecular layer, giving them one more name: radial neural stem cells (rNSCs). In addition, NSCs present expression of several proteins shown to be expressed by astrocytes as well, such as glial fibrillary acidic protein (GFAP), vimentin and brain lipid-binding protein (BLBP) [295]. They also express nestin and Sox2 [292, 296]. NSCs are usually maintained in mitotic quiescence, with a low rate of division [297]. NSCs divide asymmetrically, generating astrocytes [293] and a new cell population of called amplifying neural progenitors (ANPs), which divide several times before they differentiate into neuronal precursors [298].

ANPs are characterized for presenting low levels of GFAP, vimentin and nestin, even though they maintain similar levels of Sox2 and BLBP as NSCs [292]. In this differentiation step, up to 60% of ANPs undergo apoptosis and are efficiently removed by unchallenged microglia in physiological conditions [28]. The remaining viable ANPs give rise to neurons and maturate into granule cells [295]. ANPs stop dividing at 1 week-old giving rise to the next cell population, neuroblasts [297].

Neuroblasts express markers of immature neurons such as doublecortin (DCX) and polysialylated neuronal cell adhesion molecule (PSA-NCAM) and start extending neurites. Concomitantly, they start expressing several neurotransmitter receptors, first gamma-Aminobutyric acid (GABA) (inhibitory) and later glutamate (excitatory) [299, 300]. After a period of 3 weeks approximately, neuroblasts acquire a new morphology. Relying on these morphological characteristics, neuroblasts were divided in a total of six categories [301]. First, A-B cells, which are devoid or present short processes parallel to the granular cell layer. Second, C-D cells with medium processes, some of them able to reach the molecular layer of the hippocampus. Third and finally, E-F cells, which have one strong dendrite branching in the molecular layer or a dendritic tree branching in the granular cell layer of the hippocampus [301].

These cells start having very short processes and eventually evolve becoming cells clearly polarized. For this purpose, the axon extends towards the hilus. Once reached this region, the axon joins the mossy fibers that innervate CA region of the hippocampus and the main dendrite progresses across the granule cell layer until reaching the molecular layer.

Furthermore, dendritic spines start receiving synaptic input [299]. Then, newborn neurons with NMDA receptors expression are selected to integrate into the hippocampal circuitry [302] **(Figure 11)**. After several weeks, both morphology and electrophysiological properties of surviving newborn neurons are equivalent to those of granule cells [299].

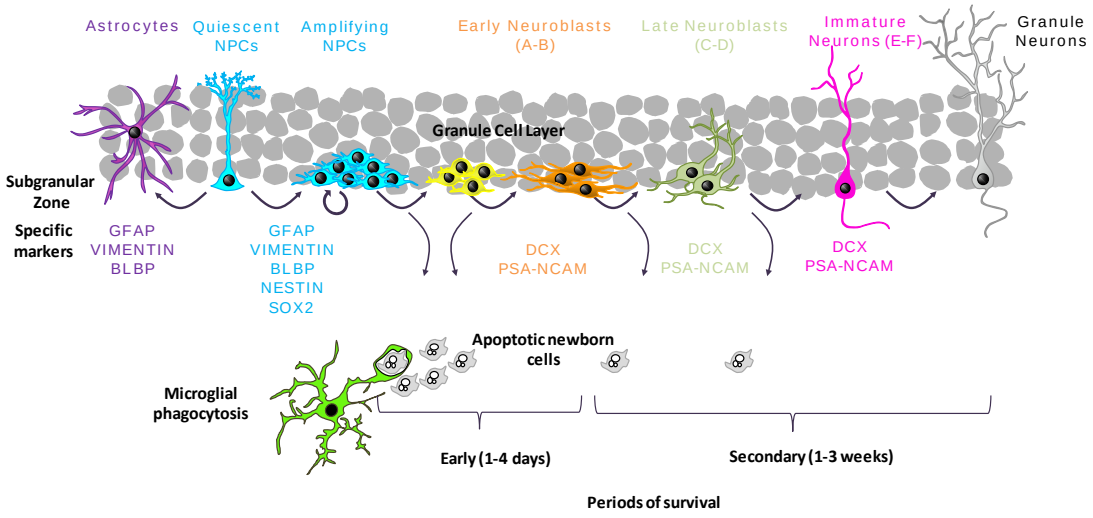

Figure 11. Adult hippocampal neurogenic cascade. *In the subgranular zone (SGZ) of the dentate gyrus (DG) of the hippocampus, we find quiescent neural progenitors (NPCs), also named radial neural stem cells (rNSCs). rNSCs, positive for nestin and Sox2 protein expression, divide asymmetrically giving rise to astrocytes, which express glial fibrillary acidic protein (GFAP), vimentin and brain lipid binding protein (BLBP) (rNSCs do express these three markers as well), and amplifying neural progenitors (ANPs). The majority of these ANPs will undergo apoptosis and be phagocytosed by surveillant microglia in their first 1-4 days of life. The rest of them will differentiate into neuroblasts, which express doublecortin (DCX) and polysialylated neuronal cell adhesion molecule (PSA-NCAM) as main markers. Neuroblasts are categorized in three groups: A-B, devoid or with short processes; C-D, with medium processes; and E-F, with at least one process branching in the molecular layer. Neuroblasts will extend their processes until becoming granule cells integrated in the hippocampal circuitry as mature neurons. Adapted from [295].*

3.5.2. Function of adult hippocampal neurogenesis

Adult newborn neurons integrated into the hippocampal network are susceptible of undergoing synaptic remodeling and activity-dependent plasticity [303]. These features suggest a possible role of adult hippocampal neurogenesis in processes related to cognition. Increasing evidences have postulated the role of adult hippocampal neurogenesis in learning [304] and memory [305], since these are functions dependent on neuroplasticity. Besides, it

has been stated that adult hippocampal neurogenesis can extent its influence to other brain tasks, such as pattern separation [306].

Learning and memory: several studies have postulated that adult hippocampal neurogenesis is crucial for learning and memory [307, 308]. In order to confirm this postulate, three very useful approaches relying on the ablation of neural progenitor cells have been employed: the use of anti-mitotic reagents, X-ray irraditation and genetic alterations.

First, it has been revealed that the ablation of adult neurogenesis by using temozolomide, an anti-mitotic reagent, was able to decrease the speed of learning and the flexibility of mice in the Morris water maze test [309]. Besides, the inhibition of neurogenesis via methylazoxymethanol (MAM) gives rise to defects in trace memory acquisition [304]. Second, it has been shown that the use of X-ray irradiation in adult mammals leads to the disruption of work memory in the Morris water maze test [310]. Other studies have revealed that irradiation also impairs learning in this test [311]. Third, experiments performed with transgenic mice treated with ganciclovir, which ablates neurogenesis, increases working memory in the radial maze task [312].

Furthermore, other procedures have been employed to study the implication of adult hippocampal neurogenesis in learning and memory tasks. It has been observed that surgical lesions in the cholinergic septohippocampal pathway decrease neurogenesis, thus affecting spatial learning [313]. In contrast, the administration of several drugs like ginseng, peptide 21 or neurotrophic factor VEGF induce an increase in neurogenesis, thus improving learning and memory [214, 314, 315].

Pattern separation: this concept refers the capacity of the DG to transform overlapping patterns of input from cortex into outputs to CA3 region [316]. Therefore, pattern separation within hippocampus has been proposed to rely on DG-CA3 circuit [317].

The role of adult hippocampal neurogenesis in pattern separation has been revealed by inhibiting neurogenic process and evaluating the ability of mice to distinguish similar fear conditioning contexts [318] and nearby locations on a radial arm maze as well [319]. Adult newborn neurons have a more pronounced influence in these tasks when new conditions, able to send overlapping patterns of input to DG and tax pattern separation, are introduced. Indeed, the inhibition of neurogenesis affects reversal learning on the Morris water maze [309] or active avoidance tasks [320].

Furthermore, lifestyle factors such as exercise, which positively regulates DG neurogenesis (briefly described in **Section 3.5.3**), has been shown to influence pattern separation. Human data have revealed that after six weeks of exercise, visual pattern separation was improved compared to individuals who do not perform any exercise [321] . Other studies state that humans suffer an age-dependent decline in patter separation, although recognitive memory performance is not affected [322].

In addition, adult hippocampal neurogenesis has been also related to other processes. In this sense, it has been proposed that adult hippocampal neurogenesis may regulate emotions, such as anxiety and depression. However, some studies in mice have shown that the ablation of adult newborn neurons does not impact on baseline levels of anxiety [312, 323]. In contrast, other authors state that the depletion of adult newborn neurons increases anxiety levels and depressive behaviors [324]. Concerning humans, it is thought that dysfunctions in neurogenesis are likely related to mood and psychiatric disorders. Studies in postmortem hippocampal tissue of patients of schizophrenia have shown that there is a remarkable drop in the amount of proliferating cells in the SGZ compared to control patients [325]. Nevertheless, adult human neurogenesis in the SVZ has been recently linked to play a relevant role in the development of psychiatric disorders. It has been suggested that increasing adult human neurogenesis in the SVZ may attenuate schizophrenia symptoms [326].

3.5.3. Regulation of adult hippocampal neurogenesis

The different stages of neurogenesis (proliferation, differentiation and survival) can be regulated by a plethora of both extrinsic and intrinsic factors [327].

Extrinsic regulation of neurogenesis

Concerning extrinsic factors, these include enriched environment, exercise or low-fat diets, considered positive regulators of hippocampal neurogenesis [328, 329]. The enriched environment involves a housing manipulation that provides sensory, social and motor stimulation [330]. Some studies have demonstrated that 4 weeks of this environment triggers an increase in the survival of newborn neurons in the hippocampus [331]. Furthermore, some authors have pointed towards an increase in neurogenesis attributed to physical exercise, since mice house with running wheels exhibit higher levels of neurogenesis than control mice [332]. Regarding the diet, some authors state that diets supplemented with omega 3 fatty acids increase hippocampal neurogenesis [333]. In contrast, mice diets without vitamins and minerals produce a negative effect in hippocampal neurogenesis [333].

Additionally, other extrinsic factors which regulate neurogenesis are aging and stress. However, these two are considered negative regulators of neurogenesis [334, 335]. Aging is related to great reductions in cell proliferation, survival and differentiation of neurons. Indeed, several studies have shown that aging leads to a persistent decline in neurogenesis in both rodents and humans [291, 336, 337], although the decrease is more dramatic and occurs later in mice than in humans [289, 290]. Furthermore, stress generally is associated with negative effects on cell proliferation, as shown by [338, 339]. Stress involves the response to any stimulus which generates environmental or physical pressure, constituting a great predictor of healthy aging and cognition [340]. Detrimental effects of stress on neurogenesis are linked to increased levels of glucocorticoids in the organism [341].

Intrinsic regulation of neurogenesis

Furthermore, the regulation of adult hippocampal neurogenesis is also related to several intrinsic factors, such as local activity exerted by mature neurons present in the neurogenic niche and the signaling of other cells taking part in this microenvironment.

Intrinsic regulation of adult hippocampal neurogenesis via mature neurons depends on neurotransmitters activity. In the adult SGZ, interneurons release GABA, the main inhibitory neurotransmitter in brain, which regulates cell proliferation, maturation, dendrite formation and synaptic integration of newborn neurons [342]. Furthermore, glutamate, the main excitatory neurotransmitter contributes to newborn cells survival in the SGZ as well [302]. On top of that, modulatory neurotransmitters also present a role in the intrinsic regulation of hippocampal neurogenesis. It has been found that one of these, serotonine, linked to depression and stress [332], induces proliferation of NSCs [343].

Apart from the role carried out by neurotransmitters, adult hippocampal neurogenesis can be modulated via the cell types present in the neurogenic niche of the SGZ. For instance, local signaling exerted by astrocytes can modulate neurogenesis in the SGZ. It has been established that astrocytic secretion of wingless/integrated 3a protein (Wnt3a) permits neuronal differentiation of NSCs [344]. Additionally, astrocytes are involved in synapse formation and integration of adult hippocampal newborn neurons [345-347]. Apart from astrocytes and NSCs, the neurogenic niche is composed of other cell types, such as endothelial cells and microglia [344, 348, 349]. Endothelial cells are known for releasing soluble factors that enhance NSCs proliferation and neurogenesis in the SGZ [350] but also in the SVZ [351]. One of the main

endogenous factors involved in neurogenesis regulation is microglial cells population. In the next section, we will delve into the role of microglial cells in neurogenesis regulation.

3.5.4. The role of microglia in adult hippocampal neurogenesis

Microglia are very relevant cells in the shaping of the CNS. During development, it is known that microglia are able to engulf apoptotic neurons and also prune synapses [16, 202, 352]. Subsequently, microglia secrete cytokines and other factors that support the differentiation of neural progenitors [353] and may regulate neuronal survival. Microglial cells have been shown to regulate the developmental neuronal production [354], but also exert a role in adult neurogenesis. As previously described in **Section 5**, together with SGZ of the hippocampus, the SVZ constitutes the unique region where neurogenesis persists throughout adulthood. Regarding the SVZ, microglia have been shown to exert some regulation in neurogenic process.

It is well established that SVZ microglia secrete factors which are relevant for SVZ neurogenesis [351]. Several reports have shown that SVZ and rostral migratory stream (RMS) microglia are able to support newborn cells survival and proliferation [355-357], thus influencing neurogenesis in this neurogenic niche. In addition, other authors have shown that conditioned media from microglial cultures promote SVZ newborn cells migration and differentiation [358]. On top of that, as the responsible cells for eliciting the inflammatory response in brain tissue [359], it has been shown that microglia can modulate neurogenesis in the SVZ via inflammatory stimuli, at least in the early postnatal brain [360]. However, the possible influence of microglia on SVZ neurogenesis does not seem to be related to apoptotic cells phagocytosis. Recent data have shown that in the neurogenic niche of the SVZ, microglial cells are devoid of newborn cells fragments and also lack of TREM2 expression, a receptor related to the activation of microglial phagocytosis [357]. Therefore, the role of microglia in SVZ neurogenesis is important but has a different impact on neurogenesis regulation than microglial role exerted on adult hippocampal neurogenesis in the neurogenic niche of the SGZ.

The microglial contribution to the SGZ neurogenic niche relies on two fundamental processes: inflammation and phagocytosis. Microglia are responsible for orchestrating the inflammatory response. The balance between pro-inflammatory and anti-inflammatory signaling results critical for supporting or inhibiting neurogenesis [361]. Furthermore, microglial cells exert an essential role in the neurogenic niche of the SGZ through the removal of apoptotic cells via phagocytosis, although the possible consequences of microglial phagocytosis for neurogenesis

in the SGZ have not been unraveled yet. Microglial roles in inflammation and phagocytosis and their link to neurogenesis in the niche of the SGZ of the hippocampus will be detailed next.

Microglial inflammation and adult hippocampal neurogenesis

It has been shown that inflammatory response involves negative consequences for neurogenesis [362, 363]. Several reports have exposed that LPS-induced inflammation inhibits the proliferation or survival of newborn cells in the adult rat hippocampus [364, 365]. These negative effects on neurogenesis are related to microglial release of pro-inflammatory cytokines such as IL-6, IL-β and TNF-α, known to inhibit neurogenesis both in vivo and in vitro [63, 347, 366]. Concerning TNF-α, some studies indicate that it can be pro-neurogenic as well [367]. It is important to remark that continuous release of pro-inflammatory cytokines due to inflammatory response can lead to apoptosis of both neurons and glial cells, and the secretion of neurotoxic factors [57] that could also negatively affect the neurogenic process. Remarkably, microglial secretion of the TGF-β cytokine can lead to the activation of pro-inflammatory and anti-inflammatory pathways, resulting in the induction [361] or inhibition of neurogenesis [213].

Microglial phagocytosis and adult hippocampal neurogenesis

Microglia constitute fundamental components of the neurogenic niche of the SGZ of the hippocampus. Related to this, it has been well suggested that ramified microglia of the SGZ may a critical role in adult neurogenesis regulation through the removal of newborn cells produced in the cascade. The vast majority of these newborn cells undergo apoptosis during their first days of proliferation through adulthood, and then microglia engulf and degrade them via phagocytosis very efficiently [28].

Some evidences demonstrate that after apoptotic cells phagocytosis, microglia are able to secrete several trophic factors. For instance, microglia are known to release TGF-β and NGF after phagocytosis in vitro [43, 44], which are negative and positive regulators of hippocampal neurogenesis, respectively [213, 368]. Therefore, the **Objective 5** in this PhD Thesis will be focused on assessing whether microglial phagocytosis is related to any changes in neurogenesis in our GPR34 KO mouse model in the SGZ of the hippocampus.

3.5.5. Methods to assess neurogenesis

The current knowledge about adult neurogenesis is mainly due to the numerous technical advances which have facilitated its characterization. These techniques comprise the use of

nucleotide analogs, the use of genetic tools and the employment of specific markers, fundamentally.

Nucleotide analogs: Among these compounds we can highlight [^{3}H]-thymidine, 5-bromo-2-deoxyuridine (BrdU), 5-iodo-2'-deoxyuridine (IdU) and 5-chloro-2'-deoxyuridine (CldU). These compounds are often injected intraperitoneally and they incorporate into DNA in place of thymidine in the S phase of cell cycle [369]. Cells that incorporate [^{3}H]-thymidine are detected by autoradiography, whereas cells which incorporate BrdU, IdU or CldU are visualized by immunochemistry. BrdU is the most used of these nucleotide analogs. It allows phenotypic analysis [370] and quantification of newly-produced cells [371]. Additionally, BrdU labeling can be combined with cell-specific markers and visualized via confocal microscopy [370]. Nevertheless, the use of BrdU has some disadvantages, as target tissue needs to be fixed and it can be mutagenic at high concentrations.

Genetic tools: the use of viral vectors is very common to study adult neurogenesis. These are injected in specific brain regions through stereotaxic surgery. Among them, retroviruses are frequently used because they specifically infect dividing cells [372], and this feature ensures the delivery of transgenes to proliferating cells in neurogenic niches [373] . Viral vectors usually carry a reporter gene, allowing the identification of those cells which have incorporated the vector [374]. However, their use is limited by the variability of the viral infection between animals [372].

Specific markers: endogenous cell markers are also used to study adult neurogenesis. Some of them are DCX, nestin or GFAP, used in this PhD Thesis to identify neuroblasts, NSCs and astrocytes in the neurogenic niche of the SGZ. Other markers are Ki67 or proliferating cell nuclear antigen (PCNA), which are only expressed in cells in division [375, 376]. Nonetheless, they are only useful to study proliferation but not survival or neuronal differentiation in adult neurogenesis [370].

4. HYPOTHESIS AND OBJECTIVES

4.HYPOTHESIS AND OBJECTIVES

As part of the immune system, microglia contribute to maintain brain homeostasis through phagocytosis of apoptotic cells. Together with phagocytosis, microglia also coordinate inflammation, thus controlling the first line of defense against damage in the organism. In this PhD Thesis, we hypothesize that several inflammatory mediators related to microglia could have also a role in apoptotic cell phagocytosis.

Microglial phagocytosis of apoptotic cells depends on many receptors attached to the microglial membrane. One of these receptors, GPR34, which binds to lysoPS, is highly expressed in microglia. Thus, we hypothesize that GPR34-lysoPS signaling may constitute a great regulator of microglial phagocytosis which help understand more deeply the complexity of phagocytic process.

Additionally, phagocytosis may involve intrinsic modifications in microglial cells upon engulfment of apoptotic bodies. In this PhD Thesis, we hypothesize that phagocytosis may impact on metabolism. Besides, considering the role of microglial phagocytosis on adult hippocampal neurogenesis, we hypothesize that alterations in phagocytosis could modify the role of microglial cells in neurogenic process.

Objective 1. To test the role of inflammatory mediators on microglial phagocytosis of apoptotic cells in vivo.

Objective 1.1. To test the possible role of cytokine TNF-α on microglial phagocytosis of apoptotic cells just as apoptotic cells numbers in vivo. For this purpose, we will use an in vivo mouse model of epilepsy by intrahippocampal KA injection in microglial-deficient TNF-α to induce excitotoxicity and apoptosis. Phagocytosis will be evaluated in the SGZ of the hippocampus and quantified by immunofluorescence in brain tissue sections imaged by confocal microscopy.

Objective 1.2. To test the possible role of chemokine CX3CL1 on microglial phagocytosis of apoptotic cells in vivo. For this purpose, we will use CX3CR1-deficient mice, thus impeding CX3CL1 interaction with microglial receptor. Phagocytosis will be evaluated in the SGZ of the hippocampus and quantified by immunofluorescence in brain tissue sections imaged by confocal microscopy.

Objective 2. To determine the role of GPR34 receptor on microglial phagocytosis of apoptotic cells in vivo. For this purpose, we will use young and adult GPR34-deficient mice, preventing its possible influence on phagocytosis. Phagocytosis will be evaluated in the SGZ of the hippocampus and quantified by immunofluorescence in brain tissue sections imaged by confocal microscopy.

Objective 3. To assess the role of GPR34 receptor ligand lysoPS on microglial phagocytosis of apoptotic cells in vitro and in vivo. For this purpose, we will first test the expression levels of lysoPS-associated receptors in fluorescence activated cell sorting (FACS)-sorted microglia by real time-quantitative polymerase chain reaction (RT-qPCR). Secondly, we will use microglial cells and hippocampal organotypic cultures treated with lysoPS as well as mice brains injected with lysoPS in the DG of the hippocampus. Phagocytosis will be quantified by immunofluorescence in brain tissue sections imaged by confocal microscopy.

Objective 4. To analyze the possible impact of apoptotic cells phagocytosis on microglial cells metabolism in vitro. For this purpose, we will first analyze the expression levels of several key transcripts in the two main metabolic pathways: OXPHOS and glycolysis by RT-qPCR in BV2 microglia after phagocytosis of apoptotic cells. Secondly, we will directly assess both metabolic pathways using an XF Extracellular Flux Analyzer. Next, we will assess mitochondrial morphology in mito7-GFP transfected BV2 cells by confocal imaging, followed by deconvolution and skeletonization of mitochondrial network with ImageJ. Finally, we will analyze several transcripts related to mitochondrial fusion and fission processes by RT-qPCR.

Objective 5. To study the possible link between the role of GPR34 receptor on microglial phagocytosis of apoptotic cells and microglia role on neurogenesis in vivo. For this purpose, we will use young and adult GPR34-deficient mice. Neurogenesis will be quantified by immunofluorescence in brain tissue sections imaged by confocal microscopy.

5. EXPERIMENTAL PROCEDURES

5. EXPERIMENTAL PROCEDURES

5.1. ANIMALS

Mice were maintained in 12:12h light cycle and fed with food and water *ad libitum*. All procedures followed the European Directive 2010/63/EU and were approved by the Ethics Committees of the University of the Basque Country (Leioa, Spain; CEBA/205/2011, CEBA/206/2011, CEIAB/82/2011, CEIAB/105/2012).

Several transgenic mouse lines were used, all of them in C57BL/6 background. Reporter mice CX3CR1-CreEGFP mice [87] and fms-eGFP (Macgreen) mice [377] were used for the analysis of microglial phagocytosis *in vivo* and *in vitro*, and to purify microglia by FACS. Inducible, microglial-specific TNF-α knockout mice were developed via Cre-loxP recombination by crossing CX3CR1-CreERT2 [378] and Rosa26-TNF-α floxed [379] mice in collaboration with Steffen Jung (Weizmann Institute of Science) and Knut Biber (Freiburg University, Germany). Inducible gene inactivation is produced by treatment with tamoxifen, which binds to the long-binding domain (LBD) of the estrogen receptor (ER), translocating the CreER recombinase into the nucleus where it can initiate Cre-loxP recombination [378]. Tamoxifen was solubilized in corn oil (Sigma) at 10 mg/ml and mice were injected three times, subcutaneously, at 48 h intervals at a dose of 100 mg/kg. These mice were used for the analysis of the effect of TNF-α cytokine on apoptosis and microglial phagocytosis. Constitutive knockout mice for GPR34 receptor [181] were used for the analysis of microglial phagocytosis and neurogenesis in collaboration with Angela Schulz, Leipzig University. For BrdU experiments, mice were intraperitoneally injected with a single dose of 150 mg/kg and later sacrificed at the interest time point depending on the experiment.

5.2. CELL AND ORGANOTYPIC CULTURES

5.2.1. Primary microglia cultures

Postnatal day 0-1 (PND0-1) fms-eGFP mice pups were decapitated. Brain meninges were removed in Hank's Balanced Solution (HBSS, Hyclone) with the aid of a magnifying scope. The cerebellum and olfactory bulb were cut and discarded. Once the meninges were removed, brains were diced and incorporated in a solution of papain (20U/ml, Sigma-Aldrich, St Louis,

MO, USA), a cysteine protease enzyme, and deoxyribonuclease (DNAse; 150U/ ul, Invitrogen) for 15 min at 37°C.

Afterwards, tissue was homogeneized by carefully pipetting and transferred to a 50ml collection tube (Falcon) through filtering with a 40 µm nylon cell strainer (Fisher) with 5ml of 20% Fetal Bovine Serum (FBS) in HBSS. The solution was then centrifuged at 200G for 5 min and pellet obtained was resuspended in 1ml of Dulbecco's Modified Eagle Medium (DMEM) supplemented with 10% Fetal Bovine Serum (FBS) and 1% antibiotic/antimycotic. The resuspended pellet was seeded in previously poli-L-lysine-coated (15 µl/ml, Sigma) culture flasks covered with 10ml of DMEM. Medium was replaced one day after and every 3 days with the incorporation of granulocyte-macrophage colony stimulating factor (5ng/ml, GM-CSF, Sigma-Aldrich, St Louis, MO, USA), which promotes microglial proliferation. At 14 days of culture, a well-defined microglial cell layer was grown over a layer of astrocytes. Microglial cells were harvested by shaking at 150 rpm for 4h at 37 °C, separating them from the lower astrocytic layer. Isolated microglial cells were plated at a density of 80.000 cells/well on poli-L-lysine coated glass cover slips in 24 well-plate wells and experiments were performed 1 day after plating.

5.2.2. BV2 cell line

BV2 murine microglial cells, generated by infecting primary microglial cell cultures with a v-raf/v-myc oncogen carrying retrovirus J2 [380], were obtained from the American Type Culture Collection (ATCC), and used to perform metabolism experiments, phagocytosis analysis, and gene expression analysis. BV2 cells were grown in 90mm Petri plates covered with 10ml of DMEM supplemented with 10% FBS and 1% antibiotic/antimycotic (all from Gibco). When confluency was reached, cells were trypsinized and replated at 1:3 each three days. Cells were used between passages P20 and P35.

5.2.3. SH-SY5Y cell line

SH-SY5Y cells (obtained from ATCC), a human neuroblastoma cell line derived from the bone marrow of 4 year-old female, was used as a model of apoptotic cells for phagocytosis assays. SH-SY5Y cells were grown in non-coated culture flasks covered with 15 ml of DMEM supplemented with 10% FBS and 1% antibiotic/antimycotic. When confluency was reached, cells were trypsinized and replated at 1:3 each three days.

5.2.4. Vampire-SH-SY5Y cell line

Vampire-SH-SY5Y cells (obtained from Innoprot, Zamudio, Spain), a variant of the human neuroblastoma cell line formerly mentioned, was developed through a stable transfection with the red reporter TurboFP602 (Vampire). Vampire-SH-SY5Y cells were grown in non-coated culture flasks covered with 15 ml of DMEM supplemented with 10% FBS, 1% antibiotic/antimycotic and 0.5 % geneticin. When confluency was reached, cells were trypsinized and replated at 1:3 each three days. Cells were used between passages P10 and P30.

5.2.5. Organotypic hippocampal slice cultures

7 day-old fms-eGFP mice were decapitated and brains removed and placed in a miniplate covered with HBSS. Both hippocampi were dissected out and subsequently cut in 350 µM slices with the aid of a tissue chopper (Mcllwain). Chopped slices with visible DG and CA were selected and used for the experiments. Slices were placed on 0.4 µM culture plate inserts (Millipore), four slices per insert. The inserts were placed in 6-well plates, each well containing 1ml of hippocampal organotypic culture medium composed of 50% Neurobasal Medium supplemented with 0.5% B27, 25% horse serum, 1% Glutamax, 1% penicillin/streptomycin (all from Gibco) and 1% glucose solution in HBSS. Medium was changed 24h after culture and every 2 days until reaching 1 week of culture.

5.3. IN VITRO PHAGOCYTOSIS ASSAY

5.3.1 Primary microglia

Primary microglia cells were plated in poly-L-lysine treated coverslips over 24-well plate wells and maintained for at least 24h before phagocytosis experiments. Then microglial cells were fed for 3h with apoptotic SH-SY5Y cells. SH-SY5Y cells were pre-treated with staurosporine (STP) 3µM for 4h (Sigma) to induce them apoptosis and then were added to microglia in a 1:1 proportion approximately.

Primary microglia cells were pre-treated with lysoPS (0.3 and 3 µM and Dimethyl Sulfoxide (DMSO) (lysoPS vehicle, 0.3 and 3 µM) for 2h. Coverslips were finally fixed with paraformaldehyde (PFA) 4% for 10 min and then replaced with Phosphate Buffer Solution (PBS) 1X and stored at 4°C until performing immunochemistry.

5.3.2. BV2 cells

BV2 cells were seeded in poly-L-lysine treated coverslips over 24 well-plate wells and after 2h fed with apoptotic vampire-SH-SY5Y cells (for 3h or 24h depending on the experiment), obtained by treatment with STP 3µM for 4h (Sigma-Aldrich, St Louis, MO, USA) at 37°C. For the metabolism experiments, the apoptotic cells were added to BV2 cells in a 1:1, 3:1 and 9:1 proportion approximately (BV2 cells: Vampire-SH-SY5Y cells). For the RT-qPCR analysis BV2 cells were fed with apoptotic vampire-SH-SY5Y cells in a 1:1 proportion approximately. For the mitochondrial dynamics experiments, previously transfected BV2 cells were fed with apoptotic vampire-SH-SY5Y cells in a 1:1 proportion approximately. In every experiment coverslips were fixed with PFA 4% for 10 min and then replaced with PBS 1X and stored at 4°C until performing immunochemistry.

5.4. INTRAHIPPOCAMPAL INJECTIONS

5.4.1. LysoPS administration

1 month-old fms-EGFP mice were intraperitoneally anesthetized with ketamine/xylazine (10/1 mg/kg) and were also treated with buprenorphine (1mg/kg) subcutaneously. Mice were shaved to exhibit the skin over the cranium and after applying povidone iodine, they were placed in the stereotaxic equipment by immobilization through ears and nose. Afterwards, an incision was cut with a scalpel in order to localize Bregma (intersection of the coronal suture and the sagital suture). Next, a 0.6mm whole was drilled at coordinates taken from Bregma: anteroposterior (AP) -1.7mm, laterolateral (LL) -1.6mm. A pooled glass microcapilary was inserted at -1.9mm dorsoventral (DV), and 1µL of saline, DMSO (36 µM), or lysoPS (36 µM) were injected into the dentate gyrus of the hippocampus using a microinjector (Nanoject II, Drummond Scientific, Broomal, PA, USA). Finally, the microcapillary was retracted and mice sutured and maintained in a thermal blanket until recovered from anesthesia.

5.4.2. Kainate administration

4 month-old wild type (WT) and Cre-TNF-α mice were intraperitoneally anesthetized with ketamine/xylazine (10/1 mg/kg) and were also treated with buprenorphine (1mg/kg) subcutaneously. Mice were shaved to exhibit the skin over the cranium and after applying povidone iodine, they were placed in the stereotaxic equipment by immobilization through ears and nose. Afterwards, an incision was cut with a scalpel in order to localize Bregma

(intersection of the coronal suture and the sagital suture). Next, a 0.6mm whole was drilled at coordinates taken from Bregma: AP -1.7mm, LL -1.6mm. A pooled glass microcapilary was inserted at -1.9mm DV and 20 (low dose) or 50 nL (high dose) of saline or KA (20mM) were injected into the dentate gyrus of the hippocampus using a microinjector (Nanoject II, Drummond Scientific, Broomal, PA, USA). Finally, the microcapillary was retracted and mice sutured and maintained in a thermal blanket until recovered from anesthesia [37].

5.5. IMMUNOFLUORESCENCE

5.5.1. Antibodies

The following antibodies were used for the different experiments: chicken anti-Green Fluorescent Protein (GFP) to label microglia in fms-eGFP mice (1:1000; Aves laboratories, Tigard, OR, USA); chicken anti-nestin for NSCs (1:1000; Aves laboratories); rabbit anti-calcium-binding adapter molecule 1 (Iba1) for microglia (1:1000; Wako Chemicals, Neuss, Germany); rabbit anti-DCX for neuroblasts (1:1000; Abcam, Cambridge, UK); rabbit anti-GFAP to label astrocytes and NSCs (1:1000; Abcam, Cambridge, UK); rat anti-BrdU to mark cell proliferation (1:300; AbD Serotec); and rat anti-Cluster of Differentiation Molecule 11b (Cd11b) to visualize BV2 cells (1:1000;AbD Serotec). Secondary antibodies coupled to Alexa Fluor 488, Rhodamine Red X or Alexa Fluor 647 were purchased for Molecular Probes or from Jackson Immunoresearch.

5.5.2. Primary microglia and BV2 cell cultures

Both primary microglia and BV2 cells were treated similarly. Seeded cells on coverslips in 24 well-plates were fixed with PFA 4% for 10 minutes. PFA was replaced by PBS 1X and plates stored at 4°C. Afterwards, coverslips were incubated in permeabilization solution composed of PBS 1X, 0,1% Triton X-100 and 0.5% Bovine Serum Albumine (BSA) (all from Sigma-Aldrich, St Louis, MO, USA) for 30 minutes and then incubated for 1 h with the primary antibodies diluted in the mentioned solution at room temperature (RT). Once the primary antibodies were removed, coverslips were washed with PBS 1X and then incubated with fluorochrome-conjugated secondary antibodies and 4’,6-diamidino-2-phenylindole (DAPI) (5 mg/ml; Sigma-Aldrich, St Louis, MO, USA) diluted in the permeabilization solution for 1h at RT and protected from light. After washing with PBS 1X, cell coverslips were mounted on glass slides with DakoCytomation Fluorescent Mounting Medium (DakoCytomation, Carpinteria, CA).

5.5.3. Hippocampal organotypic cultures immunostaining

Slices were fixed with formaldehyde (FA) for 40min and then kept in PBS at 4°C. Next, slices were incubated in permeabilization solution composed of PBS 1X, 0.3% Triton X-100 and 0.5% BSA, (Sigma-Aldrich, St Louis, MO, USA) and then incubated overnight (O/N) with the primary antibodies diluted in the mentioned solution at 4°C.

Once primary antibodies were removed from brain sections, these were washed with PBS 1X and then incubated with fluorochrome-conjugated secondary antibodies and DAPI (5 mg/ml; Sigma) diluted in the permeabilization solution for 2h at RT and protected from light. After washing with PBS 1X, sections were mounted on glass slides with DakoCytomation Fluorescent Mounting Medium (DakoCytomation, Carpinteria, CA).

5.5.4. Brain tissue sections immunostaining

Mice were anesthetized with 2.5% avertine and transcardially perfused with 25 ml of PBS 1X followed by 25 ml of 4% PFA. Afterwards, mice were decapitated and brains rapidly removed and maintained in PFA 4% until 3h postfixation at RT. Finally, brains were placed in PBS 1X and kept at 4°C. Next, six series of 50 µM-thick sections per brain hemisphere were sagitally cut using a Leica VT 1200S vibrating blade microtome (Leica Microsystems GmbH, Wetzlar, Germany). Free-floating vibratome sections were incubated in permeabilization solution composed of PBS 1X, 0.3% Triton X-100 and 0.5% BSA, (all from Sigma) for 3 hours and subsequently incubated O/N with the primary antibodies diluted in the mentioned solution at 4°C. For nestin and BrdU staining, an antigen retrieval step was needed. Briefly, sections were incubated in HCl 2N for 15 min at 37°C followed by two cycles of washing with 0.1M sodium tetraborate for 10 min at RT prior to the application of permeabilization solution which eliminates unspecific unions. Once primary antibodies were removed from brain sections, these were washed with PBS 1X and then incubated with fluorochrome-conjugated secondary antibodies and DAPI (5mg/ml; Sigma) diluted in the permeabilization solution for 2h at RT and protected from light. After washing with PBS 1X one more time to eliminate the excess of secondary antibodies, sections were mounted on glass slides from septal to temporal sections with DakoCytomation Fluorescent Mounting Medium (DakoCytomation, Carpinteria, CA).

5.6. PGFP-MITO-7 PLASMID GENERATION

pGFP-Mito-7 DNA plasmid was obtained by subcloning and combination of DsRed2-Mito-7 DNA plasmid (Addgene Plasmid # 55838) and pPB-CAG-MbGFP DNA plasmid [381]. In brief, replacement of the fluorescent proteins was performed with restriction enzymes AgeI and NotI (Thermofisher IVGN0074 and IVGN0014) following manufacturer's protocol (ANZA). These two enzymes were selected because they flank the restriction sites coding for the fluorescent protein in both plasmids. Enzymes were incubated (0.5 µl/enzyme) with 5 µg of plasmid for 1h at 37°C.

Later, the enzymatic reaction was inactivated for 15 min at 65°C and subsequently confirmed by DNA electrophoresis in agarose gel (0.8%) in Tris-acetate-EDTA (TAE) for 1h at 100V. Bands of interest, corresponding to the Mito-7 backbone (4 Kb) and GFP (1.2 Kb), were cut with a blade and DNA was purified with a DNA extraction kit (Qiagen 28704). Afterwards, the backbone and insert sticky ends were ligated with T4 ligase (Thermofisher IVGN2104) in a proportion 1:3 (backbone:insert) to avoid auto-ligation of the backbone. Ligated plasmids were transformed into competent bacteria and grown for miniprep.

5.6.1. Plasmid transformation

SIG10 5-α chemically competent cells (Sigma-Aldrich CMC0007) were thawed from -80°C. 2-4 µl of the plasmid DNA were added to the competent bacteria vial and gently mixed, resting on ice for 30 min to allow the plasmid to stick to the cell membrane. Later, the sample was heat-shocked at 42°C for 30 seconds, transiently opening the cell membrane and enabling the entrance of the plasmid in the cells, and brought back to ice for 5 min. Afterwards, 900 µl of Super Optimal Catabolite (SOC) medium were added close to flame of a Bunchen lighter to maintain sterility, gently swirling the tube. Transformed bacteria were grown in an incubator at 37°C for 1h at 250 rpm in SOC medium, and subsequently pelleted by centrifugation at 5000 rpm for 3 min. Supernatant was removed and the pellet resuspended with 100 µl of SOC medium by smooth pipetting. Bacteria were added to culture plate with 10 ml of solid Lysogeny Broth (LB) medium (Tryptone 1%, Yeast extract 0.5% and NaCl 1%, all from Sigma) agar supplemented with kanamycin (100 µl) to restrict the growth of bacteria to only those cells with a circular Mito-7 plasmid in. The plate was placed downside/down in order to attach cells to the agar for 5 min at RT. The plate was finally placed upside/down in an incubator O/N at 37°C. Next day, single bacterial colonies were selected and touched with a pipette tip. A tip was introduced in 5 ml of bacterial medium LB and tube shaken O/N at 37°C. DNA plasmid was finally purified with a Miniprep kit (Sigma-Aldrich PLN70). Final plasmid DNA concentration

was estimated by measuring absorbance with 1 µl of sample on Nanodrop 2000 (Thermo Fisher Scientific). The selected colony containing the successful pGFP-Mito-7 plasmid was grown using a Maxiprep (Zymo Research, Irvine, CA, USA).

Bacterial cultures were centrifuged at 3500G for 10 min to pellet the cells. The supernatant was discarded and the pellet was resuspended in 14 ml of ZymoPURE P1 solution. Afterwards, 14 ml of ZymoPURE P2 solution were added for 2-3 min to lysate the bacteria. Next, 14 ml of ZymoPURE P3 solution were added to neutralize the lysis reaction. The lysate was then loaded into a ZymoPURE Syringe Filter and clarified into a 50 ml Falcon tube. 14 ml of ZymoPURE Binding Buffer were added to the cleared lysate and mixed thoroughly. The mixture was loaded into a column and centrifuged at 500G for 2 min until the entire sample passed through the column. Next, the column was washed with ZymoPURE wash buffer and centrifuged at 500G for 2 min. Finally, the plasmid DNA was eluted from the column using 400 µl of ZymoPURE elution buffer. A total concentration of 3700 ng/µl of plasmid DNA was obtained by measuring in Nanodrop 2000.

5.7. TRANSFECTION

GFP-Mito-7 plasmid DNA (Addgene) was transfected into BV2 microglial cell line by using lipofectamine 2000 (ThermoFisher Scientific). Mito-7 corresponds to the mitochondrial targeting sequence from subunit VII of cytochrome C oxidase. BV2 cells were cultured in poli-L-lysine-treated coverslips in a 24-multiwell plate at a density of 50.000 cells per well. First, lipofectamine 2000 (Thermofischer Scientific) (1µl/well) was diluted in OPTI-MEM (250 µl/well) with no serum (Gibco) and incubated for 5 min at RT. Second, DNA (500 ng/well) was diluted in OPTI-MEM (250 µl/well) with no serum mixing gently. After combining both dilutions in a new tube, the mixture (500 µl/well) was incubated for 20 min at RT. DMEM low glucose 5% FBS (Gibco) (500 µl/well) was added to the tube maintaining a proportion 1:1 between OPTI-MEM and DMEM low glucose 5% medium. A total volume of 1ml/well was added to BV2 cells, which were incubated for 15-18h at 37°C. Transfection medium was then changed to DMEM 10% FBS, 1% antimycotic-antibiotic. Transfected cells were fed with apoptotic Vampire-SH-SY5Y cells for 24 h and finally fixed with PFA 4% for 10 min and then transferred to PBS 1X at 4°C until performing immunochemistry.

5.8. IMAGE ANALYSIS

All fluorescence immunostaining images were collected using a Leica SP8 laser scanning microscope using a 40X oil-immersion objective and a z-step of 0.7 µm. In contrast, images were collected using a 63X objective and a z-step of 0.3 µM for mitochondrial morphology analysis. All images were imported into LAS X program (Leica) in .lif format. Brightness, contrast, and background were adjusted equally for the entire image using the "process" tool. Quantitative analysis of apoptosis and phagocytosis was performed using unbiased stereology methods as previously described [28]. For mouse tissue sections, at least 3 15-20 µm-thick z-stacks located at random positions containing the DG were collected per hippocampal section, and a minimum of 6 sections per series were analyzed. Additionally, mean microglial volume was determined in the DG at all possible thresholds and divided by total image area using an in-house-made macro for the Fiji software [382]. For organotypic cultures, 2-3 10-20 µm-thick random z-stacks of the DG were collected per hippocampal slice. For cell cultures, 7 random z-stacks were obtained per coverslip.

5.8.1. Phagocytosis analysis

Cell nuclei were labeled with DAPI. Apoptotic cells were identified based on the condensation or fragmentation of the chromatin (pyknosis/karyorrhexis). Phagocytosis of apoptotic cells was established when microglial processes were shown to tridimensionally encapsulate an apoptotic cell through the formation of well-defined pouches using orthogonal projections of confocal z-stacks.

5.8.1.1. Phagocytosis in BV2 cells and primary microglial cultures

In primary microglia and BV2 cell cultures, several measurements were performed using LAS X (Leica) program. First, we quantified the number of microglial cells per image. Next, we determined the percentage of microglia phagocytosing apoptotic cells, apoptotic cell membrane fragments or both.

Finally, we quantified the percentage of phagocytic microglia per image (% of microglia phagocytosing apoptotic cells + % of microglia phagocytosing apoptotic cell membrane fragments (visualized as red inclusions) + % of microglia phagocytosing both apoptotic cells and apoptotic cell membrane fragments).

5.8.1.2. Phagocytosis in hippocampal sections and organotypic cultures

In brain tissue sections and organotypic cultures, the number of apoptotic cells, phagocytosed apoptotic cells and the density of microglial cells were quantified using LAS X (Leica) program. In both organotypic and tissue sections, the quantification was estimated per volume by using the DG contained in the z-stack (by multiplying the thickness of the stack by the area of the DG at the center of the stack). The estimation per hippocampus was only performed in brain tissue sections. For that purpose, the estimation per volume was multiplied by the volume of the septal hippocampus (spanning from -1mm to -2.5 in the AP axes, from Bregma), which was calculated by taking pictures of the last 6-7 brain slices cut with the vibratome, where the septal hippocampus is contained, with an epifluorescent microscope (Zeiss Axiovert) at 20X. Other measurements were determined, such as the percentage of apoptotic cells being phagocytosed by microglia (Ph index), the percentage of microglia which were phagocytosing at least one apoptotic cell (Ph capacity) and also the coupling ratio between apoptosis and phagocytosis processes (Ph/A coupling). The formulae used to estimate these three parameters are detailed below:

Ph index: percentage of apoptotic cells being phagocytosed by microglial cells.

$$\text{Ph index} = apo^{Ph} / apo^{tot} \times 100$$

apo^{Ph} is referred to the apoptotic cells phagocytosed and apo^{Tot} to the total number of apoptotic cells.

Ph capacity: percentage of microglial cells with one or more phagocytic pouches, each containing one apoptotic cell.

$$\text{Ph capacity} = mg^{Ph1} + 2 \times mg^{Ph2} + 3 \times mg^{Ph3} \ldots + n \times mg^{Phn} / mg \times 100$$

mg^{Phn} is the proportion of microglia with n phagocytic pouches and mg is the number of microglial cells.

Ph/A coupling: phagocytosis/apoptosis ratio.

$$\text{Ph/A coupling} = \text{Ph capacity} \times \text{microglia} / apo^{tot}$$

5.8.2. Mitochondrial morphology

Mitochondrial confocal images taken in naïve or phagocytic microglia were analyzed using a protocol developed by Mar Márquez (Master Thesis 2018), according to previous methods [383] with the aid of ImageJ (FIJI) program (https://fiji.sc/). Mitochondrial images were deconvoluted with Huygens professional program (Scientific Volume Imaging) by using the Classic Maximum Likelihood Estimation algorithm (CMLE). Deconvolution parameters were established as 40 maximum iterations, signal to noise ratio 20, 0.05 of quality threshold, and optimized iteration mode. Next, non-specific background was eliminated by using FIJI "Substract Background" tool. Additionally, cell-specific background was eliminated by substracting the cell nucleus intensity. Images were then converted to binary (black and white) by thresholding, where a foreground pixel is assigned the maximum value (255) and background pixels are assigned the minimum value (0). The "skeletonize" tool of FIJI allowed us to define the mitochondrial features of the original image ("skeleton") and it was analyzed using the plugin Analyze Skeleton 2D/3D [384]. This plugin classified the spatial distribution of each skeleton pixel to measure the length of each branch and the number of them.

Two types of mitochondrial structures were distinguished: individual mitochondria (unbranched) and mitochondria networks (branched). Individual mitochondria were defined as those objects in the image that did not contain junction pixels and were comprised of 1 or 0 branches (defined as a single point). Mitochondrial networks were defined as those objects which contained at least 1 junction pixel and were comprised of more than 1 branch. Based on this categorization, several parameters were determined in our images: the number of mitochondria and their length per cell; the number of branches per cell; and the number of junctions between branches per cell.

5.9. FACS SORTING

1 month-old Fms-eGFP mice were anesthetized with 2.5% avertine, perfused with saline and eventually decapitated to remove the hippocampi from the brain. After isolating the hippocampi they were placed in an enzymatic solution (116mM NaCl, 5.4mM KCl, 26mM $NaHCO_3$, 1mM NaH_2PO_4, 1.5mM $CaCl_2$, 1mM $MgSO_4$, 0.5mM EDTA, 25mM glucose, 1mM L-cysteine) with papain (20U/ml) and DNAse I (150U/µl, Invitrogen) at 37°C for 15 min. Once the solution was homogeneous, it was filtered by using a 40 µm nylon strainer to a 50ml collection tube (Falcon) containing 5ml of 20% FBS with HBSS. Afterwards, a Percoll gradient was used in order to remove the myelin. The cells were centrifuged at 200G for 5 min and then

resuspended in 20% Solution of Isotonic Percoll (20% SIP) in HBSS. HBSS was added carefully with a glass pipette in each sample. Gradients were centrifuged for 20 min at 200G with minimum acceleration and no brake to maintain the interphase, where myelin was trapped. The interphase was removed and cells were washed in HBSS by centrifuging at 200G for 5 min. The obtained pellet was resuspended in 500 µl of sorting buffer (25mM HEPES, 5mM EDTA, 1% BSA, in HBSS). Microglia sorting was performed by FACS using a FACS JAZZ (BD). The population of green fluorescent cells was selected, collected in Lysis Buffer (Qiagen) containing 0.7% β-mercaptoethanol, and stored at -80°C until processing.

5.10. RNA ISOLATION AND RETROTRANSCRIPTION

5.10.1. Primary microglia and BV2 cells

In both cases > 500.000 cells per well were scrapped from 6 well-plate wells removing the culture medium and including the same solution of lysis buffer with 0.7% β-Mercaptoethanol mentioned before. Sample was stored at -80°C until processing. Next, ribonucleic acid (RNA) was isolated from cell sample by using Qiagen RNeasy Mini Kit (Qiagen) according to manufacturer instructions which included a DNAse treatment step to eliminate genomic DNA. Total extracted RNA was quantified with 1 µl of sample in a Nanodrop 2000 and then a maximum of 5 µg of RNA were retrotranscribed with the aid of a mix of random primers (Invitrogen, Carisbad, CA, USA) and Superscript III Reverse Transcriptase Kit (Invitrogen, Carisbad, CA, USA) according to the manufacturer´s protocol in a Thermal Cycler (Applied Biosystems, Alcobendas, Spain).

5.10.2. Tissue

Several tissues were used as a positive control for RT-qPCR experiments. The tissue was directly obtained from mice previously anesthetized with 2.5% avertine. Once the tissue of interest was removed from the animal it was immediately disrupted with the aid of a roto-stator homogeneizer in a solution composed of RNA lysis buffer with 0.7% β-Mercaptoethanol (Qiagen). Sample was stored at -80°C until processing. Next, RNA was isolated from tissue sample by using Qiagen RNeasy Mini Kit (Alcobendas, Spain) according to manufacturer instructions which included a DNAse treatment step to eliminate genomic DNA.

Total extracted RNA was quantified with 1 µl of sample in a Nanodrop 2000 and then a maximum of 5 µg of RNA were retrotranscribed with the aid of a mix of random primers

(Invitrogen, Carisbad, CA, USA) and Superscript III Reverse Transcriptase Kit (Invitrogen, Carlsbad, CA, USA) according to the protocol in a Thermal Cycler (Applied Biosystems, Alcobendas, Spain).

5.10.3. FACS-sorted cells

FACS-sorted microglia (<500.000 cells) were collected in RNA lysis buffer with 0.7% β-Mercaptoethanol and stored at -80°C until processing. RNA was isolated by using RNeasy Plus Micro Kit (Qiagen) according to the manufacturer instructions which included a DNAse treatment step to eliminate genomic DNA. Total extracted RNA was quantified in a Nanodrop 2000. Finally, RNA was retrotranscribed by using an iScript Advanced complementary DNA (cDNA) Synthesis Kit (Biorad) according to the protocol in a Thermal Cycler (Applied Biosystems, Alcobendas, Spain).

5.11. qPCR

RT-qPCR was performed following MIQE guidelines (Minimal Information for Publication of Quantitative Real Time Experiments) [385].

Primers were designed to amplify exon-exon junctions using PrimerBlast (NIH) to avoid amplification of contaminating genomic DNA or were pre-designed by Sigma-Aldrich. First of all, their specificity and optimal concentration was tested with positive and negative controls by qPCR and corroborated by electrophoresis in 2% agarose gels. Two independent reference genes (or housekeeping genes) were compared each other for our analyses: ornithine decarboxylase antizyme 1 (OAZ-1), a rate-limiting enzyme in the biosynthesis of polyamines; and L27A, which encodes a ribosomal protein of the 60S subunit.

The following table **(Table 1)** shows all the reference genes analyzed in our experiments:

Gene	Gene ID	Gene name	Amplicon size (bp)	Sequence
Reference genes				
OAZ1	NM_008753	Ornithine decarboxylase antizyme 1	51	Fwd AGCGAGAGTTCTAGGGTTGCC Rev CCCCGGACCCAGGTTACTAC
L27A	BC086939	Ribosomal protein L27A	101	Fwd TGTTGGAGGTGCCTGTGTTCT Rev CATGCAGACAAGGAAGGATGC

LysoPS receptors				
GPR34	NM_011823.4	G Protein-Coupled Receptor 34	151	Fwd CTTCAGGAAAGCTTCAACTC Rev GTAACTATCAGGAGGAGAGC
P2Y10	NM_172435.3	P2Y Receptor Family member 10	80	Fwd ATGCCACAAAAGGAGCCATA Rev TGGTACTGTTGCTGCCCATC
G2A	NM_019925.4	G Protein-Coupled Receptor 132	145	Fwd AGGACTGGCTTGGGTCATTTT Rev GGTGCTCTGAAGAACGGAGG
GPR174	NM_001177781.1 (variant 1) NM_001033251.4 (variant 2) NM_001177782.1 (variant 3)	G Protein-Coupled Receptor 174	150	Fwd GCAAGCCTGAACTCCTGTCT Rev CACGGTAGAAGTGGCATGGT
Glycolisis genes				
HIF1α	NM_001313919.1 (variant 1) NM_010431.2 (variant 2) NM_001313920.1 (variant 3)	Hypoxia Inducible Factor 1 Alpha Subunit	93	Fwd CCTGATGTTTCTTTACTTTGCC Rev GCTGGAAGGTTTGTGGTG
PFKM	NM_001163487	Phosphofructokinase, Muscle	194	Fwd CAGACTTTGAACACCGAATC Rev CCATGGTCACATGATCTTTC
PFKFB3	NM_001177752	6-Phosphofructo-2-Kinase/Fructose-2,6-Biphosphatase 3	185	Fwd AGAGGTCAGAGAACATGAAG Rev CTTCTACTCTTCAACATGGC
Oxydative phosphorilation genes				
NDUFAF4	NM_026742.4	NADH:Ubiquinone Oxidoreductase Complex Assembly Factor 4	146	Fwd CACCGGAGTCAGTATCCAGAA Rev TCCTTTGGTTCTTGTCGTGGT
UQCRQ	NM_025352.3	Ubiquinol-Cytochrome C Reductase Complex III Subunit VII	80	Fwd TTCAGCAAAGGCATCCCCAA Rev TAGACCACTACAAACGGCGG
MPC1	NM_018819.4	Mitochondrial Pyruvate Carrier 1	142	Fwd AGCAAGGACTTCCGGGACTA Rev AGCAACAGAGGGCGAAAGTC
PDHB	NM_024221.3	Pyruvate Dehydrogenase E1 Beta Subunit	110	Fwd ACGGTGCATACAAGGTTAGC Rev AGCTGCACCAACAGCAATTC
IDH3G	NM_008323.1	Isocitrate Dehydrogenase 3 (NAD(+)) Gamma	81	Fwd TCAAGCCAACTCTCCTCTGC Rev TTTGTTGTGAGGAAATGCTCCTT
SDHB	NM_001355515.1	Succinate Dehydrogenase Complex Iron Sulfur Subunit B	94	Fwd AGAGAAGGCATCTGTGGCTC Rev AGACTTTGCTGAGGTCCGTG
Mitochondrial fission genes				
FIS1	NM_001163243	Fission,Mitochondrial 1	138	Fwd TCGAAGCAAATACAATGAGG Rev TTTTCATATTCCTTGAGCCG
DNM1L	NM_001025947	Dynamin 1 Like	103	FwdGATTCAATCCGTGATGAGTATG Rev TAAGTAACCTATTCAGGGTCC

MFF	NM_029409	Mitochondrial Fission Factor	130	Fwd AGAAACGATTCCATTGTGAC RevTACGAGTAGAAGACTGGATAAG
Mitochondrial fusion genes				
MFN1	NM_024200	Mitofusin 1	192	Fwd AACTTGCAGAAGGATTTCAAG Rev GAATAAACCCTCTTCTCTGC
MFN2	NM_133201	Mitofusin 2	102	Fwd GTCATACCACCAATTGCTTC Rev TCACAGTCTTGACACTCTTC
OPA1	NM_001199177	MItochondrial Dynamin Like GTPase	129	Fwd GGCAGAAGATCTCAAGAAAG Rev TTCAAATAAACGCAGAGGTG

Table 1. Primer sequences. *Primer sequences for mRNA expression analysis by RT-qPCR. From left to right, the GeneBank code, the gene name, the amplicon size and the primer sequence are indicated.*

Three replica of 1.5 µl of a 1:3 dilution of cDNA were amplified. Each cDNA sample (1.5 µl) was mixed with a solution of 8.5 µl composed of water (H_2O), forward primer (50 or 500nM), reverse primer (50 or 500nM) and DNA dye Power SyBrGreen (tissue and cell culture samples) or SsoFast Eva Green (for FACS-sorted microglia samples) (both from Biorad), pipetting a total volume of 10 µl per well in a Multiplate 96-well PCR plate (Biorad). The amplification protocol consisted on three steps: first of all, denaturalization of DNA strands by 3 min at 95°C, followed by the annealing of primers to DNA template by 30 seg at 60°C and 10 seg at 95°C for the DNA polymerization for at least 40 cycles. Next step was the performance of the melting curve through the progressive increase of temperature from 60 to 95°C (0.5°C each 5 seg) in a CFX96 Touch Real-Time PCR Detection System (Biorad). In the melting curve cDNA gets denaturated and the fluorescence of DNA dye is lost, obtaining the melting temperature (Tm), that in which 50 % of DNA is denatured. One single peak will indicates that one single product is amplified and quantification can be performed. Quantification of DNA was done by using threshold cycle (Ct) method.

For each set of primers, the amplification efficiency was calculated as described below. LinRegPCR sotware allowed us to make a linear regression considering the relative fluorescence unit (RFU) sample data of the interest set of primers (excluding positive and negative control samples from the analysis). Afterwards, a baseline was determined and the mean PCR efficiency value of the interest set of primers (mean of individual PCR efficiency

values, corresponding to each amplified sample) were obtained. Values were in a logarithmic scale from 1 (0% efficiency) to 2 (100% efficiency). The software LinRegPCR also allowed us to determine the relative amount using the following formula:

$$\Delta\Delta Ct = (1 + eff.target\ gene)\exp(Ct\ sample - Ct\ control)/(1 + eff.reference\ gene)\exp(Ct\ sample - Ct\ control)$$

5.12. METABOLISM ANALYSIS

Naïve and phagocytic BV2 cells grown in 90mm Petri plates were trypsinized and centrifuged at 200G for 5 min. Pellet was resuspended in 1ml of DMEM and 10 µl of cell solution was mixed with 10 µl of trypan blue solution 0.4% (Thermo Fisher Scientific, Waltham, MA, USA). Mixture was placed in a Neubauer Chamber in order to estimate the number of viable cells, those that have not internalized the trypan blue solution [386]. Later, 100 µl of cell suspension were plated in a Seahorse XFe96 Cell Culture Microplate (Agilent, Santa Clara, CA, USA) at a density of 15.000 BV2 cells per well for naive BV2 wells whereas 80 µl of the same cell suspension were plated for phagocytic BV2 wells. The four corner wells were no seeded so that they were used as background. Likewise, vampire-SH-SY5Y were induced to apoptosis for 4h as described above (**see Section 5.3**, In vitro phagocytosis assay). 1h after apoptotic cells were added, cell medium was changed to remove non-phagocytosed apoptotic cells.

5.12.1. OXPHOS analysis

The analysis of the mitochondrial function was done using the Seahorse XF Cell Mito Stress Kit (Agilent, Santa Clara, CA, USA), which targets several components of the mitochondrial ETC. The kit is composed of three drugs, which were sequentially injected. First, oligomycin (1 µM) inhibited ATPase synthase (ETC complex V), causing a decrease in the OCR of cells (pmol/min), which correlates with the mitochondrial respiration coupled to ATP production. Second, FCCP (1 µM) was injected and, as a consequence, oxygen was maximally consumed by complex IV of the ETC (mitochondrial membrane potential enhancement), producing an increase in the OCR that correlated with the maximal mitochondrial respiration. Third, a mix of rotenone (complex I inhibitor, 0.5 µM) and antimycin A (complex III inhibitor, 0.5 µM) was injected and mitochondrial respiration was shut down, permitting to estimate the non-mitochondrial respiration. Drugs were pipetted in a XFe96 Sensor Cartridge (Agilent), which was pretreated with XF Calibrant solution (200 µl/well) O/N at 37°C in a non-CO_2 incubator. DMEM 10% FBS, 1% Antimycotic/antibiotic was replaced by XF Seahorse Medium (1mM piruvate (Merck) ,

2mM glutamine (Sigma) and 10 mM glucose (Sigma)) in each well, including those at the corners (background correction or blank wells). The pH of the medium was adjusted to 7.4 with NaOH 1N and heated at 37°C. Cells were maintained with the supplemented medium 1h before assay in a non-CO_2 incubator (180 µl/ well).

5.12.2. Glycolysis analysis

The analysis of the glycolytic function was performed using the Seahorse XF Glycolysis Rate Assay Kit (Agilent, Santa Clara, CA, USA). Two drugs were sequentially injected in order to obtain an accurate measurement of the glycolytic proton efflux rate (glycoPER; pmol/min) in cells through the estimation of the OCR and the ECAR. First, a mix of rotenone and antimycin A (0.5 µM) was injected to block mitochondrial oxygen consumption.

Thereby, PER from mitochondrial respiration (produced by the extrusion of protons via the Krebs cycle) could be calculated and removed from the total PER, obtaining the glycoPER. Second, 2-DG 50 mM was injected. This is a glucose analog which inhibits glycolysis through competitive binding of glucose hexokinase, first enzyme in the glycolytic pathway. The consequence was a stop of glycolytic acidification, measuring the non-glycolytic acidification. Drugs were pipetted in a XFe96 Sensor Cartridge which was pretreated with XF Calibrant solution (200 µl/well) O/N at 37°C in a non-CO_2 incubator. DMEM 10% FBS, 1% Antimycotic/antibiotic was replaced by XF Seahorse Medium (1mM piruvate (Merck) , 2mM glutamine (Sigma), 10 mM glucose (Sigma), and HEPES buffer 5 mM for each well including background wells. The pH of the medium was adjusted to 7.4 with NaOH 1N and heated at 37°C. Cells were maintained with the supplemented medium 1h before assay in a non-CO_2 incubator (180 µl/ well).

5.13. STATISTICAL ANALYSIS

SigmaPlot (San Jose, CA, USA) was used for statistical analysis. Normality and homoscedasticity of the experimental conditions were checked prior to applying parametrical statistics. Student t-test was used to compare differences between two groups, whereas 1-way Analysis of Variance (ANOVA) was used to analyze differences between more than two groups. Holm-Sidak method was used as a posthoc test to determine the significance between groups in each factor. When data were not homoscedastic or do not follow a normal distribution, groups were compared using non-parametrical tests such as Mann-Whitney U test. Data reported as

significant were indicated in each figure legend. Data were shown as mean ± standard error of the mean (SEM).

6. RESULTS

6. RESULTS

6.1. MICROGLIAL PHAGOCYTOSIS IS NOT REGULATED BY IMMUNE MEDIATORS TNF-α AND CX3CL1

As the innate immune cells of the brain, microglia are involved in the initiation of an inflammatory response. Inflammation is a mechanism to protect the organism to infectious stimuli [32]. Together with phagocytosis, inflammation is the first line of defense against pathogens [35]. During inflammation and neurodegenerative diseases, microglia release several molecules, such as cytokines, chemokines and lipid mediators, which coordinate the microglial response against pathogens and debris in the brain. Microglial phagocytosis efficiency has been shown to be unaltered during an inflammatory challenge triggered by bacterial LPS administration [28] or omega-3 fatty acid deficiency [37]. Here we will focus on two major microglial inflammatory molecules: TNF-α and CX3CL1. TNF-α can be directly released by microglia, contributing to the initiation of the inflammatory response [71]. CX3CL1 facilitates the motility of microglia to the infection site (chemotaxis) through its interaction with CX3CR1 expressed in the microglial membrane [87]. Considering the role of both molecules on microglia, we decided to explore their possible regulation of phagocytosis. To study phagocytosis, we focused on the DG of the hippocampus, where there is a constant production of newborn cells throughout adulthood and the majority of them undergo apoptosis and are phagocytosed by "unchallenged" microglia in physiological conditions [28]. Thus, this region constitutes a perfect tool through which microglial phagocytosis can be assessed.

6.1.1. TNF-α microglial deficiency does not impair microglial phagocytosis nor reduces apoptosis in a mouse model of epilepsy

TNF-α is generally considered as detrimental, since it can mediate stroke or ischemic injury [73, 74]. However,, microglial-derived TNF-α has been shown to have neuroprotective effects in cerebral ischemia in mice [70] and acute excitotoxicity in vitro [68]. More recently, it was shown that microglia could be neuroprotective in a model of mouse organotypic slice cultures treated with NMDA, a glutamate agonist, to induce excitotoxicity. Slices chemically depleted of microglia showed an enhancement of NMDA-induced cell death, whereas their replenishment restored the resistance of neurons to the toxic [69]. One of the reasons behind this neuroprotective response was hypothesized to be the microglial release of TNF-α, as previously mentioned [68, 70]. With the aim to test the role of microglial-derived TNF-α in neuroprotection and microglial phagocytosis, we used an in vivo model of epilepsy, in which

seizures concur with excitotoxicity and inflammation, induced by the intrahippocampal injection of the glutamate analog KA [37]. In this model, the total number of apoptotic cells in the hippocampal DG was significantly decreased in saline mice compared to KA-injected mice at 1 day post injection (dpi) **(Figure 12A)**. The increased number of apoptotic cells was accompanied by a significant increase in the DG volume of KA-injected mice, related to the granule cell dispersion typical of this model and of human mesial temporal lobe epilepsy **(Figure 12B)**. Additionally, KA-injected mice showed a decreased Ph index **(Figure 12C)** [37].

To test the role of microglial TNF-α on KA-induced neurotoxicity, we used inducible microglial-specific TNF-α KO mice (via tamoxifen-induced Cre-loxP recombination) from our collaborators Stephen Jung from the Weizmann Institute of Science (Israel) and Knut Biber from Freiburg University (Germany). We restricted the analysis to the septal hippocampus, where the effect of KA is more consistent [37]. Our analysis in KA-injected WT and microglial TNF-α deficient mice revealed that the total number of apoptotic cells in the septal hippocampus remained very similar in both conditions at 1dpi (1,486 ± 165.5 vs 1,648.2 ± 190.3 in WT vs TNF-α KO mice, respectively; p=0.56) **(Figure 12D)**. This effect was not related to changes in the DG volume **(Figure 12E)**. Furthermore, the Ph index was 4.8 ± 1.5 % in WT mice whereas in TNF-α-deficient mice was 10.6 ± 2.9 % (p=0.18), reflecting non-significant differences **(Figure 12F).** These results indicated that microglial TNF-α did not play an active role in the maintenance of the microglial phagocytic efficiency after KA-induced seizures in vivo. Additionally, TNF-α did not affect cell survival, since apoptosis levels were unchanged in spite of its absence on microglia. Thus, TNF-α was not related to any type of neuroprotective microglial response in the hippocampus in vivo.

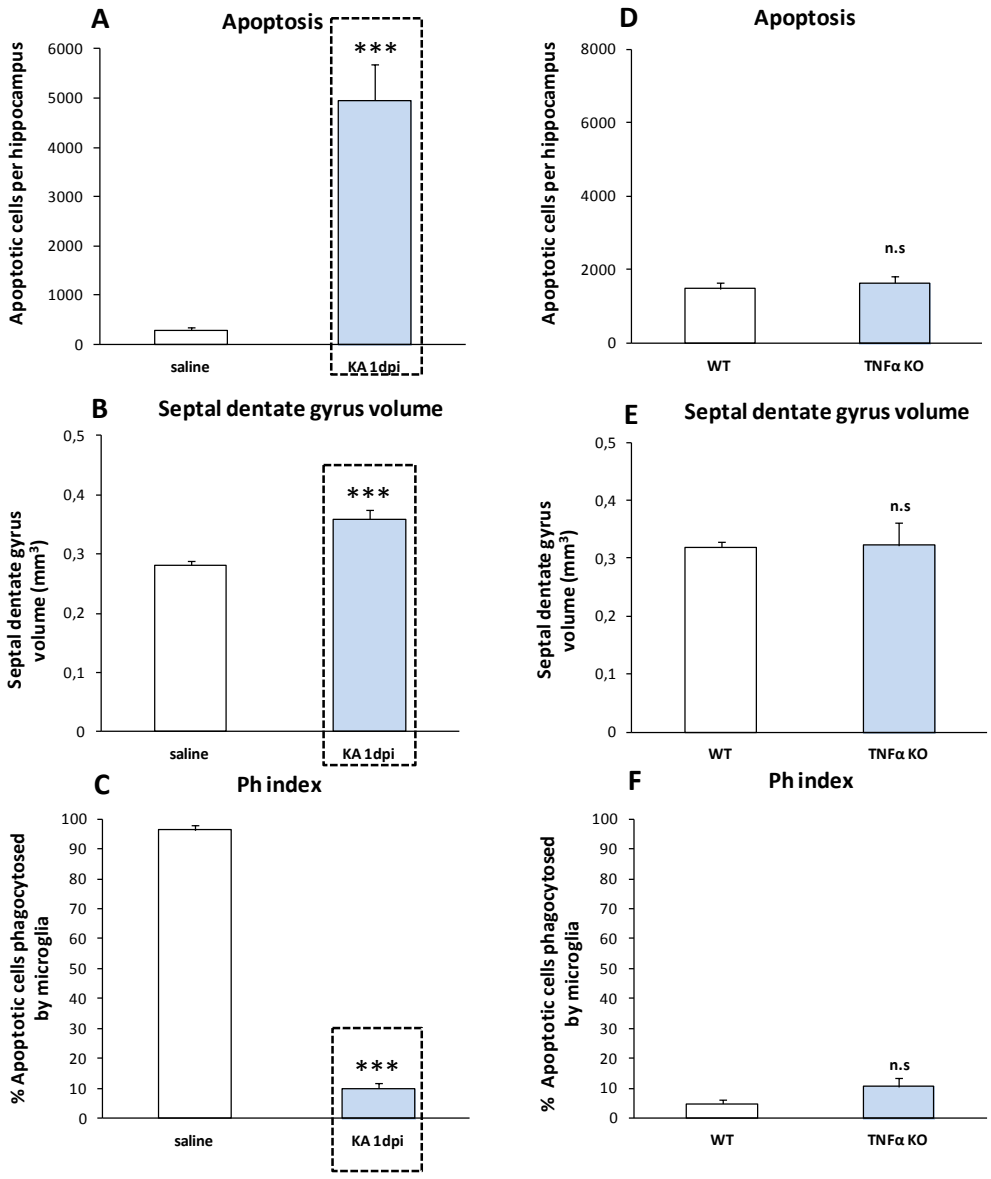

Figure 12. TNF-α microglial deficiency does not impair microglial phagocytosis nor reduce apoptosis in a mouse model of epilepsy in vivo. *Mice were treated with kainate (20 mM, 50nL) and sacrificed 1 day later. In the left side:* ***A.*** *Number of apoptotic cells per septal hippocampus of 2 month-old saline and Kainate (KA)-treated mice at 1 day post-injection (dpi). KA 1 dpi time point is highlighted.* ***B.*** *Septal dentate gyrus volume (in mm^3) in 2 month-old saline and KA-treated mice at 1dpi. KA 1dpi is highlighted.* ***C.*** *Ph index (in % of apoptotic cells) in the septal hippocampus of 2 month-old saline and KA-treated mice at 1 dpi. KA 1dpi is highlighted. In the right side:* ***D.*** *Number of apoptotic cells per septal hippocampus of 4 month-old KA-injected WT mice (n=3) and TNF-α deficient-microglia mice (TNF-α KO) (n=4) at 1 dpi.* ***E.*** *Septal dentate gyrus volume (in mm^3) in 4 month-old KA-injected WT and TNF-α KO mice at 1dpi.* ***F.*** *Ph index (in % of apoptotic cells) in the septal hippocampus of 4 month-old KA-injected WT mice and TNF-α KO mice at 1 dpi. Bars represent mean ± SEM. n.s. indicates non-significant differences and *** indicates p<0.001 by two tailed-Student's test. Figures* ***A, B and C*** *were originally published in [37].*

6.1.2 CX3CR1 deficiency does not impair microglial phagocytosis in physiological conditions

Neurons have been shown to inhibit microglial activity through its interaction by either membrane thethered or released CX3CL1 with CX3CR1 [87]. This leads us to propose that a glial-neuron crosstalk could influence microglial phagocytosis. With the aim to assess whether CX3CR1 could regulate the microglial phagocytosis of apoptotic cells, we analyzed the microglial behavior in young (1 month-old) CX3CR1 KO mice in the neurogenic niche of the hippocampal DG **(Figure 13)**. In physiological conditions, phagocytosis is very efficient and microglia engulf the vast majority of newborn cells, as determined by the Ph index, i.e, the percentage of apoptotic cells phagocytosed by microglia, which is about 90 % (91 ± 3.1 %) [28].

Our analysis in CX3CR1 KO mice showed that this percentage was only slightly reduced (80.2 ± 2.9 %), suggesting that the contribution of CX3CR1 to microglial phagocytosis through its interaction with CX3CL1 protein was residual. Thus, CX3CR1 microglial receptor was not a great candidate for the study and regulation of microglial phagocytosis in vivo.

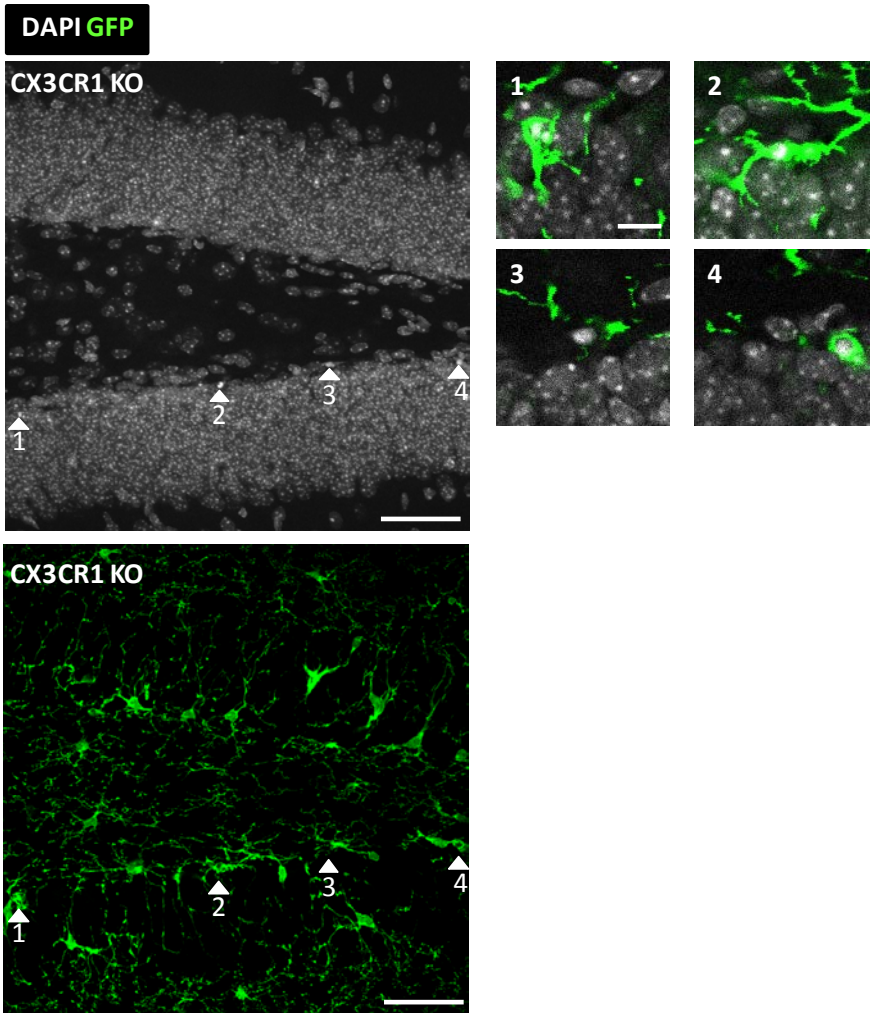

Figure 13. CX3CR1 does not regulate microglial phagocytosis in vivo. *Representative confocal z-stacks of the dentate gyrus of 1 month-old CX3CR1-deficient mice (n=4) and detailed images from a single focal plane of apoptotic cells. Nuclear morphology was visualized with DAPI (white) and microglia were visualized with GFP (green). Arrowheads point at apoptotic cells. Scale bars: 50µm (10 µm in high magnification images) Z=18,9 µm.*

6.2. PHAGOCYTOSIS RECEPTOR GPR34 IS SPECIFIC OF MICROGLIA IN VIVO AND IN VITRO

Next, we focused on another type of potential regulator of phagocytosis, GPR34, whose relevance in microglial cells has recently begun to be unraveled [181]. GPR34 has so far been described to respond to a single ligand, the lipid lysoPS [183]. Three other G-protein coupled receptors have been shown to bind to lysoPS: G2A [188], P2Y10 and GPR174 [189]. To test the role of GPR34 and related receptors on microglial phagocytosis, we first analyzed their expression in microglia both in vivo and in vitro.

6.2.1. GPR34 is highly expressed in microglia in vivo

With the purpose to assess which of the four described lysoPS-receptors (GPR34, G2A, P2Y10 and GPR174) were expressed by microglia in vivo, we performed an analysis of their mRNA expression levels by RT-qPCR. We used FACS-sorted in vivo microglia isolated from the hippocampus of 1 month-old fms-eGFP mice (in which the fluorescent reporter eGFP is exclusively expressed in microglia [387]) **(Figure 14A)**. The results clearly showed that GPR34 was highly enriched in FACS-sorted in vivo microglia (eGFP+ population) compared to non-microglial cells (eGFP-) ($p<0.001$) **(Figure 14B-C)**, in agreement with previous publications showing that GPR34 was highly expressed in microglial cells [177, 178]. In contrast, G2A had no expression in microglial cells compared to the remaining brain cells **(Figure 14B-C)**. Furthermore, both GPR174 and P2Y10 mRNA were also absent in microglia, in agreement with previous data showing that P2Y10 and GPR174 expression was restricted to lymphoid organs [192, 388] **(Figure 14B-C)**. Therefore, the main and unique lysoPS-receptor expressed in microglia in vivo was GPR34.

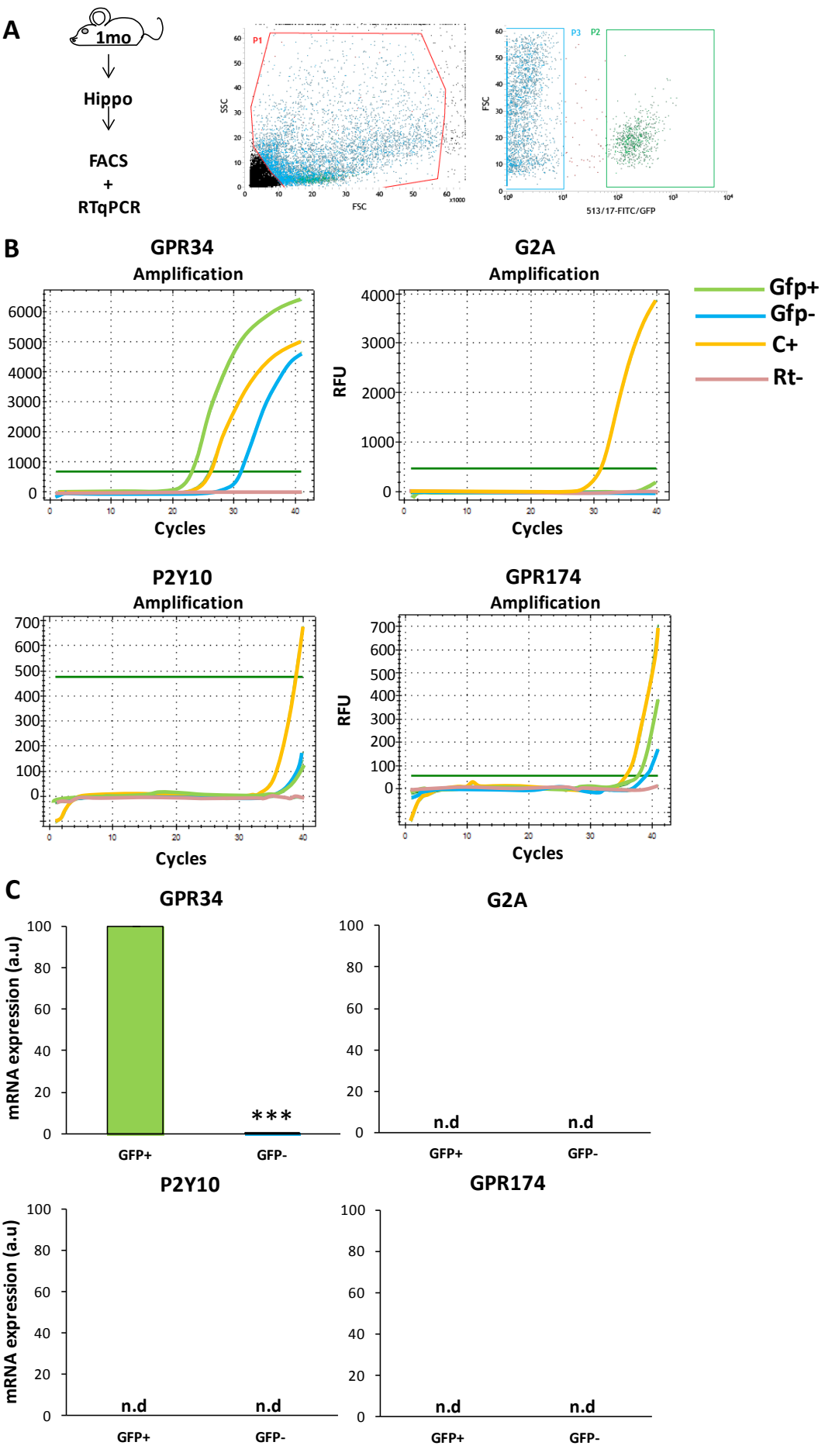
A
1mo
Hippo
FACS
+
RTqPCR
P1
SSC
FSC
P3
P2
FSC
513/17-FITC/GFP
B
GPR34
Amplification
RFU
Cycles
G2A
Amplification
RFU
Cycles
Gfp+
Gfp-
C+
Rt-
P2Y10
Amplification
RFU
Cycles
GPR174
Amplification
RFU
Cycles
C
GPR34
mRNA expression (a.u)
***
GFP+
GFP-
G2A
n.d
n.d
GFP+
GFP-
P2Y10
mRNA expression (a.u)
n.d
n.d
GFP+
GFP-
GPR174
n.d
n.d
GFP+
GFP-

Figure 14. GPR34 is specifically expressed in microglia in vivo. A. *Experimental design. 1 month-old fms-eGFP mice were sacrificed and hippocampi removed and processed by FACS (n=3 mice) to separate the eGFP$^+$ population (microglia) from eGFP$^-$ population (non-microglia).* ***B.*** *Amplification curves for GPR34, G2A, P2Y10, and GPR174 mRNA showing the RFU (relative fluorescent units) with increased amplification cycles.* ***C.*** *Quantification of mRNA expression of GPR34, G2A, P2Y10 and GPR174 genes in eGFP$^+$ and eGFP$^-$ populations. Each gene shows its normalized gene expression compared to OAZ1 gene (reference gene) in arbitrary units (a.u). KA-injected hippocampus at 3 days post-injection (dpi) was used as a positive control (C+). RT- was referred to non-retrotranscribed RNA and used as a negative control. n.d means non-detected and *** indicates p<0.001 by two-tailed Student's test.*

6.2.2. GPR34 is the predominant lysoPS-associated receptor in microglia in vitro

A similar mRNA expression analysis of these four lysoPS-receptors was performed in primary microglia and the BV2 microglia cell line in order to determine whether their expression patterns were different compared to those observed in FACS-sorted in vivo microglia. Results showed that GPR34 was highly expressed in primary microglia compared to BV2 microglia ($p<0.001$) **(Figure 15A-B)**. However, G2A expression was scarce in primary microglia whereas it was consistently expressed in BV2 microglia ($p=0.12$) **(Figure 15A-B)**. P2Y10 and GPR174 mRNA were not detected neither in primary microglia nor BV2 cells **(Figure 15A-B)**. Together, these results suggested that primary microglia showed a similar expression pattern compared to FACS-sorted microglia, since primary microglia presented a strong expression of GPR34 and G2A was scarcely expressed **(Figure 15A-B)**. In contrast, BV2 microglia had a very different expression pattern, showing high expression of G2A but residual expression of GPR34 **(Figure 15A-B)**. To sum up, both in vitro and in vivo microglia had a predominant expression of GPR34.

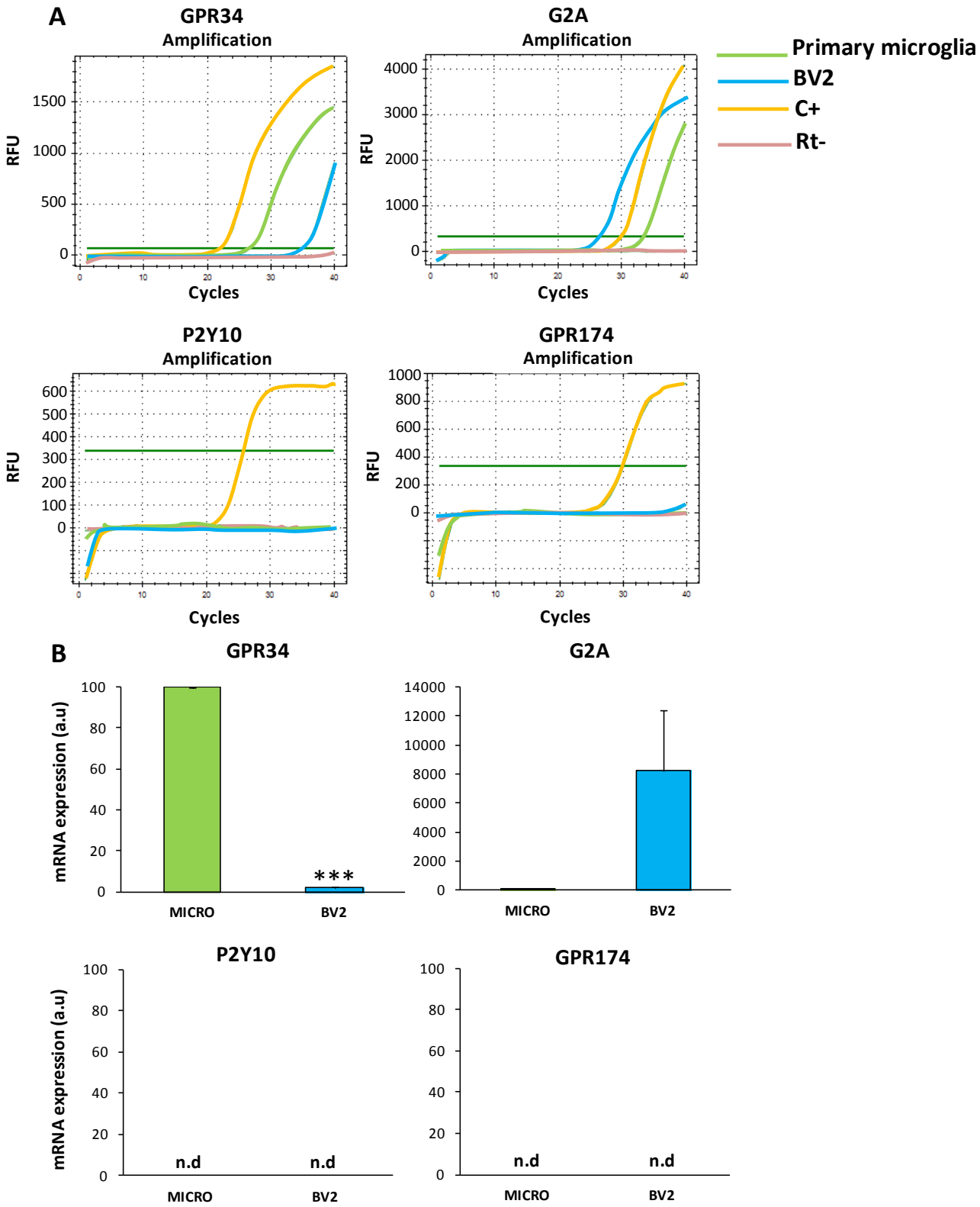
A
GPR34
Amplification
RFU
Cycles
G2A
Amplification
RFU
Cycles
Primary microglia
BV2
C+
Rt-
P2Y10
Amplification
RFU
Cycles
GPR174
Amplification
RFU
Cycles
B
GPR34
mRNA expression (a.u)
***
MICRO
BV2
G2A
MICRO
BV2
P2Y10
mRNA expression (a.u)
n.d
n.d
MICRO
BV2
GPR174
n.d
n.d
MICRO
BV2

Figure 15. GPR34 is the predominant lysoPS-receptor in primary microglia whereas G2A predominates in BV2 microglia. A. *Amplification curves for GPR34, G2A, P2Y10, and GPR174 mRNA in cultured primary microglia and BV2 microglia showing the RFU (relative fluorescent units) with increased amplification cycles.* ***B.*** *Quantification of mRNA expression of GPR34, G2A, P2Y10 and GPR174 genes in primary microglia (Micro, green) and BV2 microglia (BV2,blue). Each gene shows its normalized gene expression compared to OAZ1 gene (reference gene) in arbitrary units (a.u). Kainate (KA)-injected hippocampus at 3 days post-injection (dpi) was used as a positive control (C+). RT- was referred to non-retrotranscribed RNA and used as a negative control. n.d means non-detected and *** indicates p<0.001 by two-tailed Student's test.*

6.3. MICROGLIAL PHAGOCYTOSIS IS REGULATED BY GPR34 IN VIVO AND IN VITRO

Once we established that GPR34 was the main lysoPS-receptor expressed in microglia, our next task consisted on assessing the role of GPR34 on microglial phagocytosis. GPR34 was previously shown to be involved on microglial phagocytosis because GPR34-deficient microglia showed reduced phagocytosis of zymosan (a component of the yeast cell wall) particles or FBS-coated latex microbeads in acutely isolated retina and hippocampal cortical slices in vitro [182]. To directly test the role of GPR34 on phagocytosis of apoptotic cells in vivo, we first evaluated microglial phagocytosis in GPR34-deficient mice at different ages. Afterwards, we analyzed the role of lysoPS on microglial phagocytosis in primary microglia and BV2 microglia cultures. Next, we tested the effect of the addition of lysoPS to hippocampal slice cultures on microglial phagocytosis. Lastly, we injected lysoPS in the hippocampus of mice to observe its impact on microglial phagocytosis in vivo.

6.3.1. GPR34 deficiency leads to microglial phagocytosis impairment in young mice in vivo

As stated previously, GPR34 was postulated as a new regulator of microglial phagocytosis, at least in vitro [182]. Thus, in order to determine the relevance of GPR34 on microglial phagocytosis of apoptotic cells in vivo, we analyzed microglial phagocytosis in 1 month-old WT and GPR34 KO mice in the neurogenic niche of the hippocampus in collaboration with Dr. Angela Schulz from the University of Leipzig (Germany).

We first analyzed the number of apoptotic cells present in WT and GPR34 KO mice. In WT mice, the vast majority of the apoptotic cells in the DG was located in the SGZ of the DG, in agreement with previous findings where they were identified as newborn cells [28]. In GPR34 KO mice a similar pattern of location of apoptotic cells was observed **(Figure 16A-B)** suggesting that in the absence of GPR34 expression, the apoptotic cells might also be newborn cells.

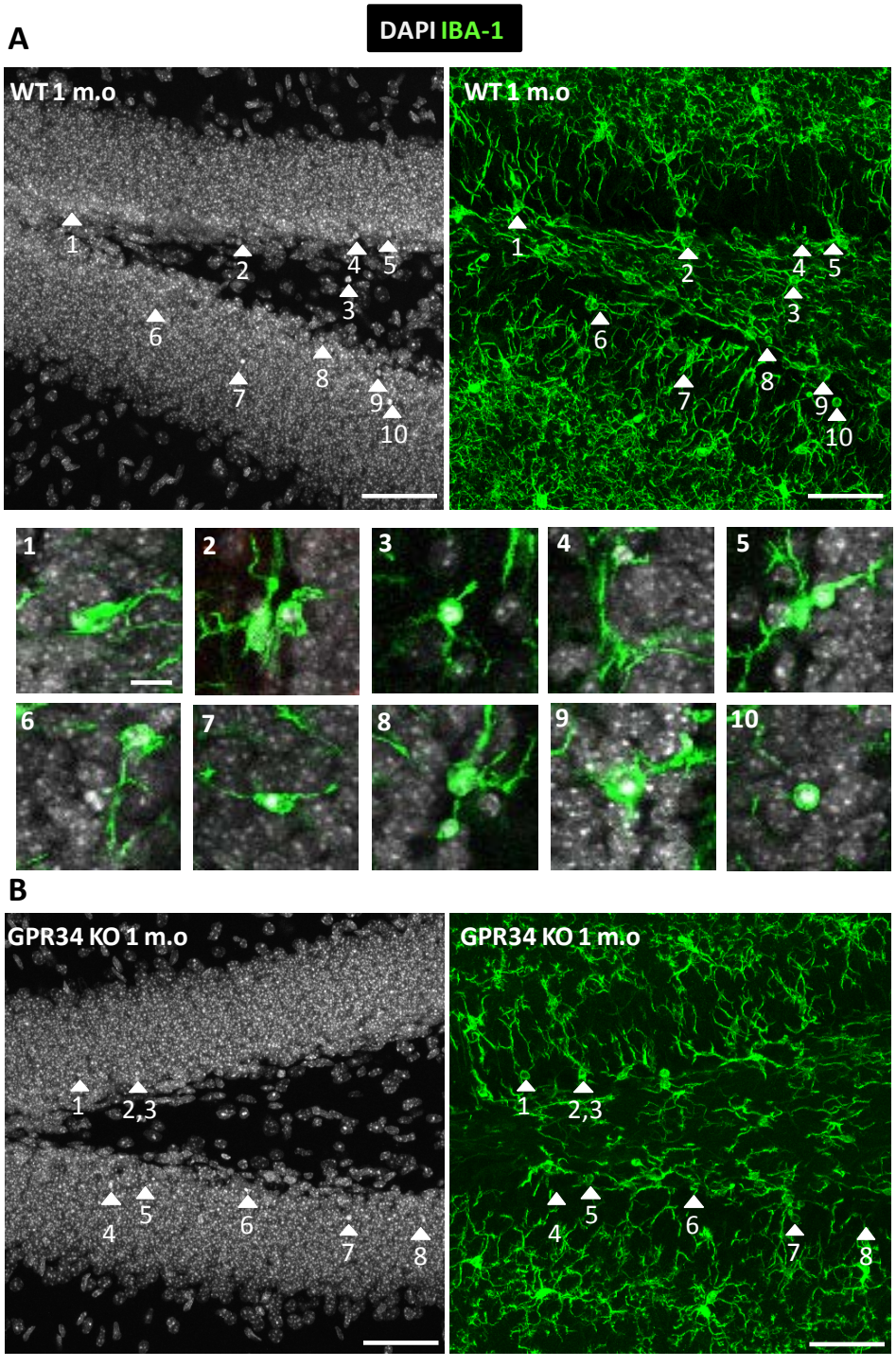
A
DAPI IBA-1
WT 1 m.o
WT 1 m.o
1
2
3
4
5
6
7
8
9
10
B
GPR34 KO 1 m.o
GPR34 KO 1 m.o
1
2,3
4
5
6
7
8

***Figure 16. Microglial phagocytosis in young GPR34 KO mice**. **A, B.** Representative confocal z-stacks of the dentate gyrus and detailed images from a single focal plane of apoptotic cells from 1 month-old (m.o) WT (n=3, **A**) and GPR34 KO mice (n=4, **B**). Nuclear morphology was visualized with DAPI (white) and microglia were visualized with Iba-1 (green). Arrowheads point at apoptotic cells. Scale bars: 50µm (10 µm in high magnification images) Z=29,4 µm (WT), Z=29,4 µm (KO).*

We did not find significant changes in the total number of apoptotic cells (1,429.3 ± 224.3 vs 1,012.4 ± 107.1 cells per septal hippocampus in WT and KO mice, respectively; p=0.12) **(Figure 17A)**, nor in the septal hippocampal volume (0.24 ± 0.03 vs 0.24 ± 0.01 mm^3 in WT and KO mice, respectively; p=0.86) **(Figure 17B)**, suggesting no major morphological defects. To assess the effect of GPR34 on microglial phagocytic efficiency we quantified the Ph index. The Ph index was over 90 % in WT mice (92.7 ± 1.8 %), in agreement with previous results [28]. In contrast, it was significantly lower in GPR34 KO mice (67.7 ± 3.1 %; p<0.001) **(Figure 17C)**. This partial decrease in the Ph index suggested that GPR34 could have a modulatory role in microglial phagocytosis**.** This phagocytic impairment observed in GPR34 KO mice could be caused by either a reduced number of microglial cells or by a decreased Ph capacity (percentage of microglia with phagocytic pouch(es), phagocytosing at least one apoptotic cell) of each microglial cell. To further delve into the mechanisms leading to a decreased microglial phagocytosis in GPR34 KO mice, we analyzed the amount of microglia per hippocampus and their Ph capacity. The quantification of the total number of microglia showed no differences in WT compared to GPR34 KO mice (3,756.6 ± 600 vs 3,639.6 ± 146.1 cells per hippocampus, respectively; p=0.83) **(Figure 17D)**. However, microglia occupied significantly more volume in the DG in WT mice (4.3 ± 0.1 %) than in GPR34 KO mice (2.7 ± 0.06 %; p<0.001) **(Figure 17E)**. This "shrinkage" of microglial processes in GPR34 KO mice may be related to a reduced motility [37], and would explain their reduced phagocytosis. We next quantified the Ph capacity. In WT mice we found 19.8 ± 1.2 % of microglial cells with one pouch whereas in GPR34 KO mice only 11.5 ± 1.8 % of microglia had a single pouch (p=0.018). Additionally, WT mice presented 2.9 ± 1.1 % microglial cells with two pouches and in GPR34 KO mice 0.8 ± 0.2 % microglia had two pouches (p=0.08). Finally, no microglial cells were observed with 3 or more pouches in WT or KO mice **(Figure 17F).** The weighted average of the Ph capacity was 0.27 ± 0.01 parts per unit (ppu) for WT and 0.13 ± 0.01 ppu for GP34 KO mice (p=0.008) **(Figure 17G)**. To sum up, the lack of GPR34 resulted in a decrease of phagocytic microglia **(Figure 17H)**.

Afterwards, we hypothesized that the impairment of phagocytosis (decreased Ph index and Ph capacity) observed in GPR34 KO mice would result in an uncoupling between apoptosis and

phagocytosis. These two processes are coupled in physiological conditions, excitotoxicity and inflammation because microglia reacts to an increase in the number of apoptotic cells with a proportional increase in phagocytosis [37]. To determine whether microglia was able to cope with the amount of apoptotic cells present in GPR34 KO mice, we quantified the Ph/A coupling ratio, that is, the ratio between the net phagocytosis and the net apoptosis between control and experimental conditions. As expected, we found that in GPR34 KO mice these processes were significantly uncoupled (1.00 ± 0.02 vs 0.67 ± 0.06 in WT and KO mice, respectively; $p<0.001$) **(Figure 17I).** All these showed results made us conclude that GPR34 KO mice suffered a microglial shrinkage and phagocytosis impairment in vivo which led to an uncoupling between phagocytosis and apoptosis processes.

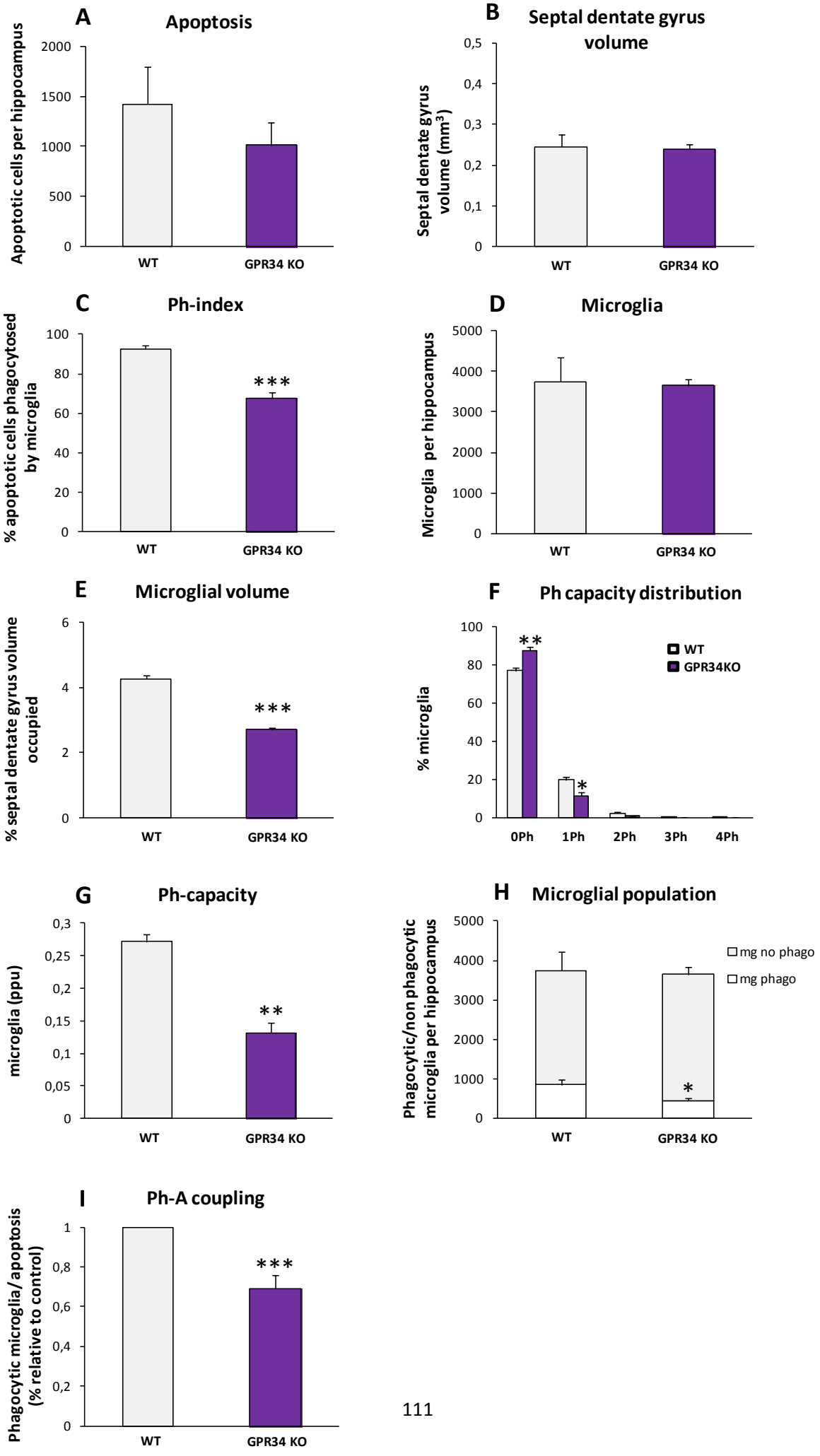
A
Apoptosis
Apoptotic cells per hippocampus
2000
1500
1000
500
0
WT
GPR34 KO
B
Septal dentate gyrus volume
Septal dentate gyrus volume (mm3)
0,5
0,4
0,3
0,2
0,1
0
WT
GPR34 KO
C
Ph-index
% apoptotic cells phagocytosed by microglia
100
80
60
40
20
0
***
WT
GPR34 KO
D
Microglia
Microglia per hippocampus
5000
4000
3000
2000
1000
0
WT
GPR34 KO
E
Microglial volume
% septal dentate gyrus volume occupied
6
4
2
0
***
WT
GPR34 KO
F
Ph capacity distribution
% microglia
100
80
60
40
20
0
**
*
WT
GPR34KO
0Ph
1Ph
2Ph
3Ph
4Ph
G
Ph-capacity
microglia (ppu)
0,3
0,25
0,2
0,15
0,1
0,05
0
**
WT
GPR34 KO
H
Microglial population
Phagocytic/non phagocytic microglia per hippocampus
5000
4000
3000
2000
1000
0
mg no phago
mg phago
*
WT
GPR34 KO
I
Ph-A coupling
Phagocytic microglia/apoptosis (% relative to control)
1
0,8
0,6
0,4
0,2
0
***
WT
GPR34 KO

Figure 17. GPR34 deficiency leads to an uncoupling between apoptosis and microglial phagocytosis in vivo*. **A.** Number of apoptotic cells (pyknotic/karyorrhectic) per septal hippocampus. **B**. Septal dentate gyrus volume (in mm^3). **C.** Ph index (in % of apoptotic cells) in the septal hippocampus. **D.** Total number of microglial cells ($Iba1^+$) per septal hippocampus. **E.** Percentage of septal dentate gyrus volume occupied by microglia. **F.** Histogram showing the Ph capacity of microglia (in % of cells). **G.** Weighted Ph capacity of microglia in parts per unit (ppu) in the septal hippocampus. **H.** Percentage of phagocytic and non phagocytic microglia per condition **I.** Ph-A coupling (in fold change). Bars represent mean ± SEM. * indicates p< 0.05, ** indicates p<0.01 and *** indicates p<0.001 by two-tailed Student's test.*

After observing the phagocytic impairment in 1 month-old mice caused by the lack of GPR34 receptor, we performed a brief analysis of apoptosis and phagocytosis in more mature mice, at 3 months of age **(Figure 18A-B)**.

Analysis of the total number of apoptotic cells per hippocampus showed no differences in 3 month-old WT mice versus GPR34 KO mice (211.3 ± 18.7 vs 187.6 ± 63.1 cells, respectively; p=0.79), **(Figure 19A)**, similar to 1 month-old mice. Remarkably, 3 month-old mice presented fewer apoptotic cells, presumably due to the progressive decline of neuroprogenitor cells and thus neurogenesis with age [295]. However, the Ph index decrease observed in younger 1 month-old mice was not reproduced in 3 month-old WT compared to GPR34 KO mice (97.5 ± 2.5 % vs 95 ± 3.6 %; p=0.64) **(Figure 19B)**. Quantification of the total number of microglia per hippocampus also reflected no differences between WT and GPR34 KO mice (4469.4 ± 166.6 vs 4323.9 ±214.1; p=0.65) **(Figure 19C)**. Likewise, analysis of the weighted average of the Ph capacity followed the same pattern, showing that mature 3 month-old mice did not present any differences in WT mice compared to GPR34 KO mice (0.024 ± 0.004 ppu vs 0.019 ± 0.003 ppu; p=0.40) **(Figure 19D)**, contrary to observed in 1 month-old mice. Consequently, the Ph/A coupling ratio in 3 month-old mice showed no alterations between WT and GPR34 KO mice (1.00 ± 0.24 vs 1.11 ±0.22; p=0.76) **(Figure 19E)**. These data obtained in 3 month-old mice suggested that microglial phagocytosis impairment due to the lack of GPR34 receptor was not maintained throughout adulthood.

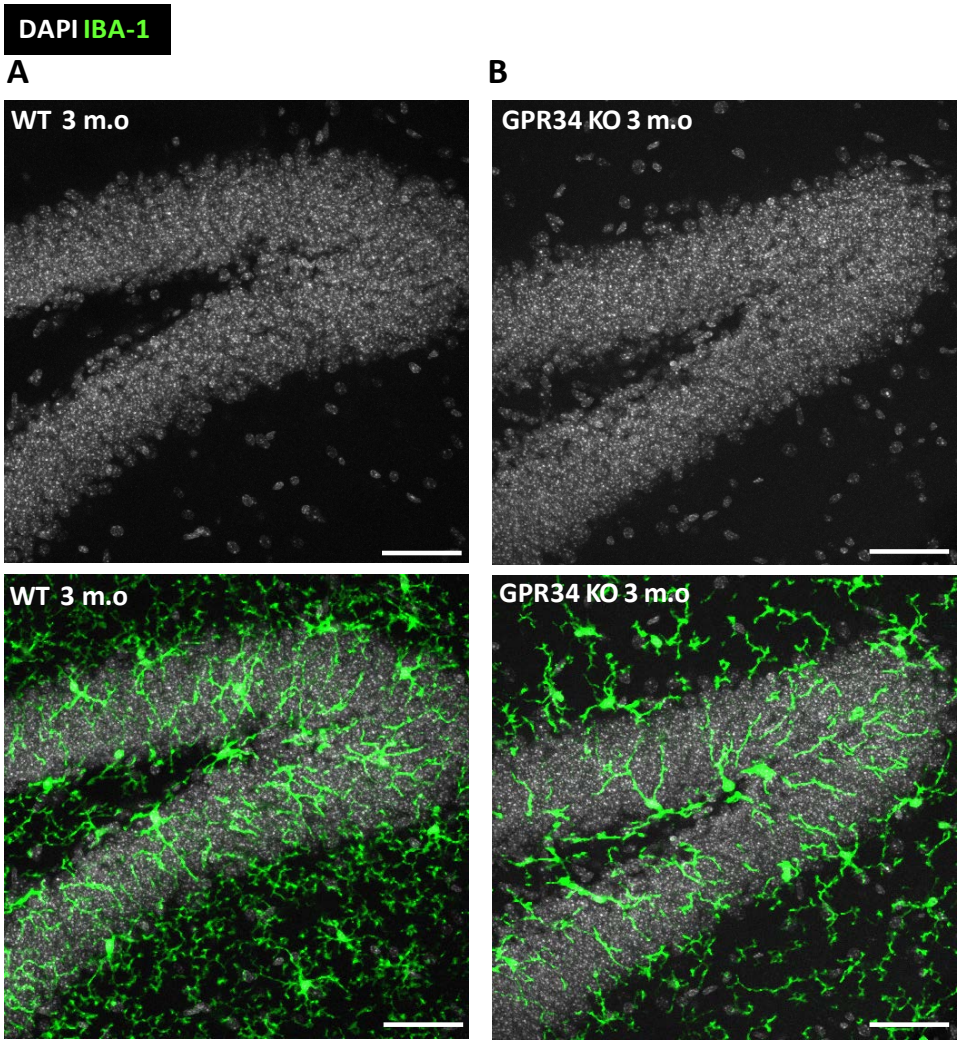

Figure 18. Microglial phagocytosis in adult GPR34 KO mice. A, B *Representative confocal z-stacks of 3 month-old WT mice (**A**; n=4) and GPR34 KO mice (**B**; n=7). Nuclear morphology was visualized with DAPI (white) and microglia were visualized with Iba-1 (green). Scale bars: 50 µm. Z=11,9 µm (WT) and Z=14,7 µm (KO).*

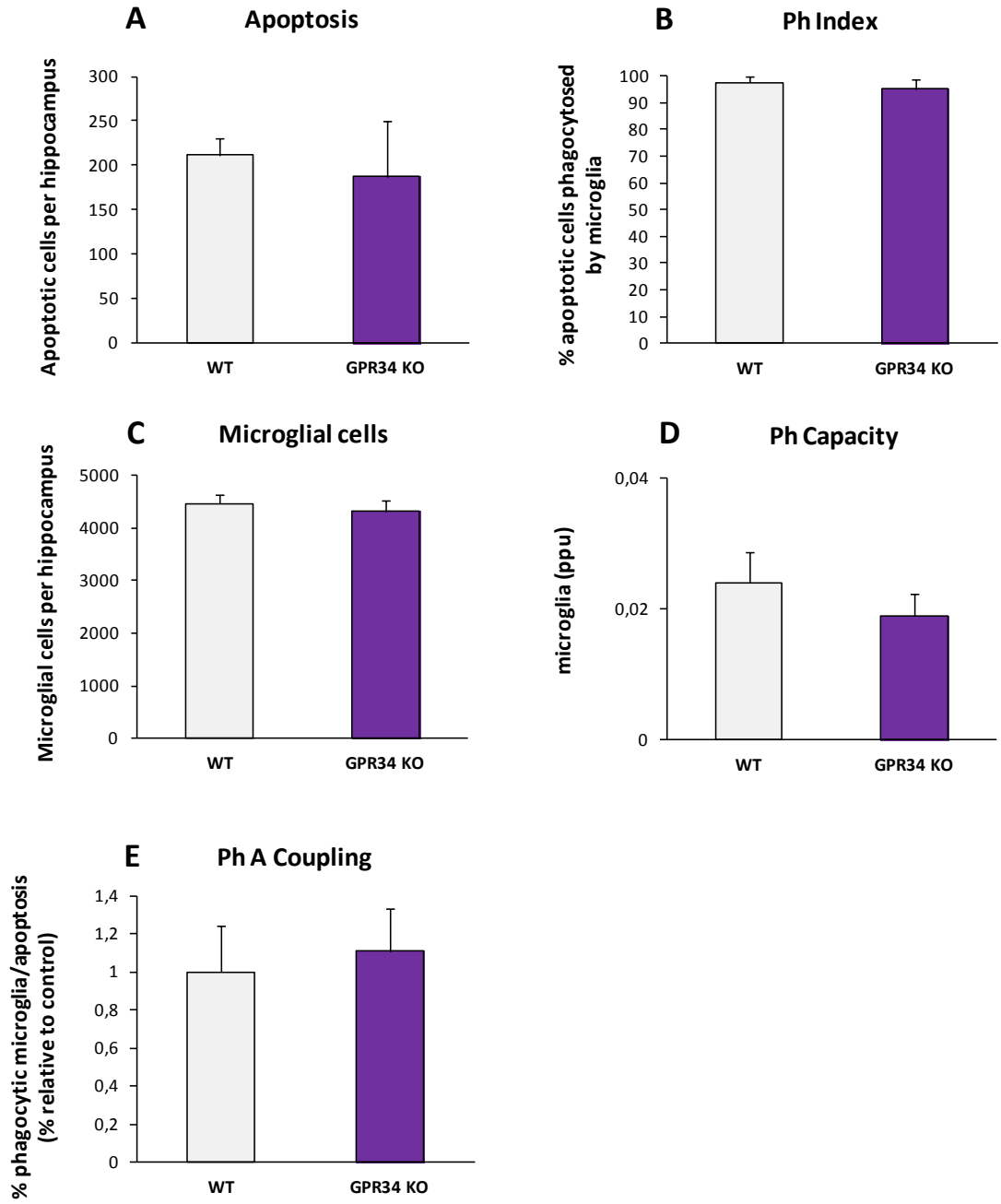

***Figure 19. GPR34 deficiency does not affect microglial phagocytosis in adult mice in vivo**. **A.** Total number of apoptotic cells per septal hippocampus. **B.** Ph index (in % apoptotic cells). **C.** Total number of microglial cells (Iba1^{+}) per septal hippocampus. **D.** Weighted Ph capacity (in ppu). **E.** Ph/A coupling ratio (in fold-change). Bars represent mean ± SEM. No significant differences were detected by two-tailed Student's test (**C**, **D** and **E**) or Mann-Whitney U test (**A** and **B**).*

6.3.2. GPR34 ligand lysoPS impairs microglial phagocytosis in vitro

The above results evidenced a role of GPR34 on microglial phagocytosis, the unique lysoPS-receptor expressed on microglia. To further test the role of GPR34 signaling on microglial phagocytosis, we resorted to a reductionist approach and utilized an in vitro model of phagocytosis using primary microglial cultures and the GPR34 ligand, lysoPS. Briefly, we pretreated microglia isolated from postnatal day 0-1 mice with lysoPS and DMSO (lysoPS vehicle) at a low dose (0.3 μM) and at a high dose (3 μM) for 2h prior to the addition of apoptotic cells for 3h **(Figure 20A).** The selected doses were based on a previous publication in which lysoPS 3 μM was shown to induce the activation of GPR34 in HEK293A cells transfected with a plasmid encoding this receptor [389].

The percentage of phagocytic microglia was unaltered by the low dose of DMSO compared to the low concentration of lysoPS (0.3 μM) (38.3 ± 3.7 % vs 37 ± 4.1 %; p=0.29) **(Figure 20B-C)**. However, the percentage was significantly higher in cultures treated with the high dose of DMSO compared to the high concentration of lysoPS (3 μM) (39.1 ± 3.7 % vs 29 ± 3.1 %; p<0.001) **(Figure 20D-E)**. Furthermore, DMSO treatments did not present any effect compared to basal conditions **(Data not shown)**. Thus, the effect of lysoPS on microglial phagocytosis was dose-dependent **(Figure 20F)**. LysoPS was originally described as a phagocytosis enhancer. It was shown that lysoPS generated in apoptotic neutrophils or supplied exogenously in liposomes along with lysoPS-negative (ultraviolet (UV)-irradiated) apoptotic neutrophils was shown to enhance the phagocytic response of peritoneal macrophages in vitro [188]. Nevertheless, our results suggested that in primary microglia cultures lysoPS blocked phagocytosis, presumably by binding to microglial GPR34, the major lysoPS-receptor expressed in vitro **(Figure 15B)**. These results suggested that lysoPS was a possible candidate to modulate microglial phagocytosis, at least in vitro.

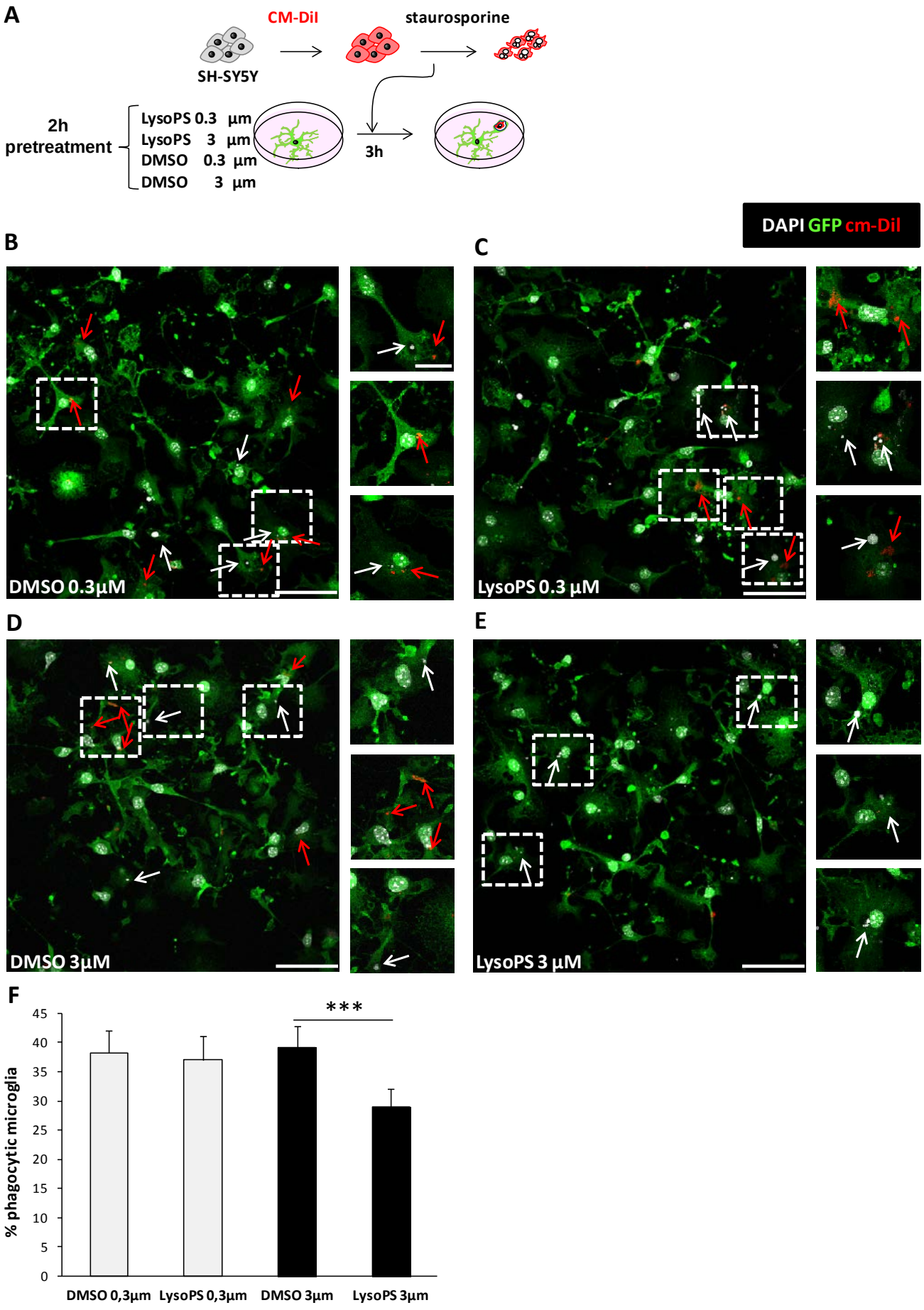
A
CM-DiI
staurosporine
SH-SY5Y
2h
pretreatment
LysoPS 0.3 µm
LysoPS 3 µm
DMSO 0.3 µm
DMSO 3 µm
3h
DAPI GFP cm-DiI
B
C
DMSO 0.3µM
LysoPS 0.3 µM
D
E
DMSO 3µM
LysoPS 3 µM
F
% phagocytic microglia
***
DMSO 0,3µm
LysoPS 0,3µm
DMSO 3µm
LysoPS 3µm

Figure 20. GPR34 ligand lysoPS impairs microglial phagocytosis in cultured microglia. A. *Experimental design. Microglia were pretreated with lysoPS and DMSO (0.3 and 3 µM) 2 h before adding apoptotic SH-SY5Y cells (pre-treated with STP 3 µM for 4h) for 3h.* ***B-E*** *are representative images of confocal z-stacks showing microglia (fms-EGFP, green), nuclei and apoptotic fragments (DAPI; white), and cm-dil (apoptotic cell membranes, red) in DMSO 0.3 and 3 µM (****B*** *and* ***D****, respectively), and lysoPS 0.3 and 3 µM (****C*** *and* ***E****, respectively). White and red arrows point at apoptotic cells and their membrane fragments, respectively. Scale bars: 50 µm (10 µm for high magnification images).* ***F.*** *Percentage of phagocytic microglia in every condition. Bars represent mean ± SEM (from 3 independent experiments). *** indicates p<0.001 by Holm-Sidak posthoc test (after one-Way ANOVA was significant at p<0.05).*

6.3.3. GPR34 ligand lysoPS impairs BV2 microglia phagocytosis in vitro

To further confirm the phagocytosis blockade observed in primary cultures, we used BV2 microglia, in which G2A was highly expressed whereas GPR34 was almost absent, contrary to primary microglia **(Figure 15B)**. In order to test whether the addition of lysoPS had a similar effect on BV2 microglia phagocytosis, we performed the same phagocytosis assay as described above **(Figure 20A)** comparing the phagocytic capacity of DMSO and lysoPS-treated BV2 microglia **(Figure 21A)**.

The percentage of phagocytic microglia was unaltered by the low dose of DMSO compared to the low concentration of lysoPS (0.3 µM) (23.1 ± 2.5 % vs 22.5 ± 1.9 %, respectively; p=0.94) **(Figure 21B-C)**. However, the percentage was significantly higher in cultures treated with the high dose of DMSO compared to the high concentration of lysoPS (3 µM) (18.9 ± 3 % vs 15.5 ± 2.8 %, respectively; p=0.02) **(Figure 21D-E)**. Like in primary microglia cultures, DMSO treatments did not present any effect compared to basal conditions **(Data not shown)**. Thus, the effect of lysoPS was dose-dependent **(Figure 21F)**, as in primary microglia **(Figure 20F)**. On top of that, the blocking effect of lysoPS on phagocytic capacity was weaker in BV2 microglia (18 ± 15 % reduction) compared to that observed in primary microglia cultures (26 ± 8 % reduction). As stated before, BV2 microglia expressed G2A and also GPR34 (almost absent expression) whereas primary microglia only expressed GPR34 as lysoPS-receptor **(Figure 15B)**. Therefore, in BV2 microglia, the blocking effect of lysoPS was principally mediated by G2A (with a scarce contribution of GPR34) whereas in primary microglia was exclusively mediated by GPR34. In brief, these results again showed the role of lysoPS in the regulation of microglial phagocytosis in vitro.

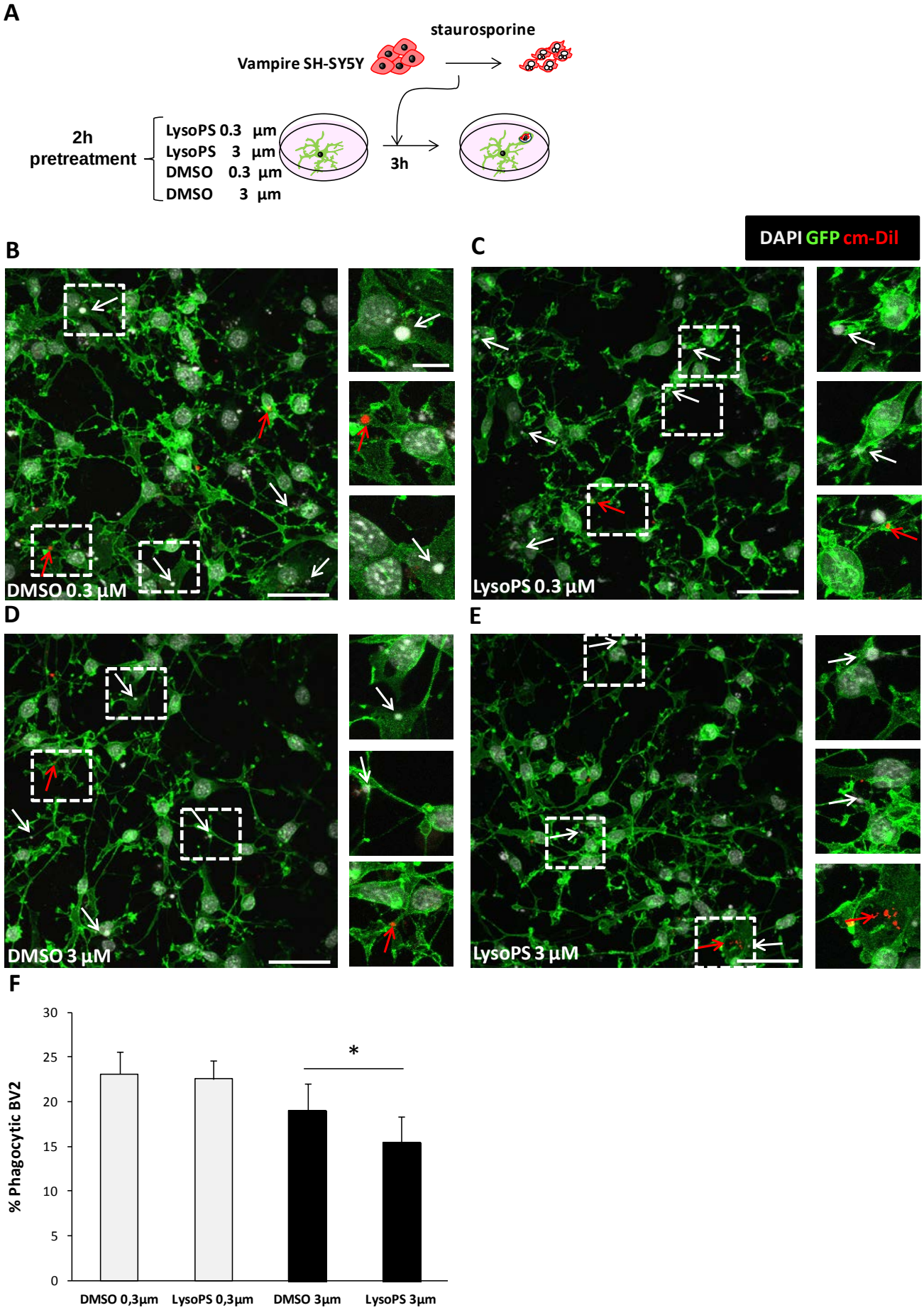
A
staurosporine
Vampire SH-SY5Y
2h
pretreatment
LysoPS 0.3 µm
LysoPS 3 µm
DMSO 0.3 µm
DMSO 3 µm
3h
B
C
DAPI GFP cm-Dil
DMSO 0.3 µM
LysoPS 0.3 µM
D
E
DMSO 3 µM
LysoPS 3 µM
F
% Phagocytic BV2
30
25
20
15
10
5
0
*
DMSO 0,3µm
LysoPS 0,3µm
DMSO 3µm
LysoPS 3µm

***Figure 21. GPR34 ligand lysoPS impairs BV2 microglia phagocytosis**. **A.** Experimental design. Microglia were pretreated with lysoPS and DMSO (0.3 and 3 µM) 2 h before adding apoptotic SH-SY5Y cells (pre-treated with STP 3 µM for 4h) for 3h. **B-E,** representative images of confocal z-stacks showing microglia (fms-EGFP, green), nuclei and apoptotic fragments (DAPI; white), and cm-dil (apoptotic cell membranes, red) in DMSO 0.3 and 3 µM (**B** and **D**, respectively), and LysoPS 0.3 and 3 µM (**C** and **E**, respectively). White and red arrows point at apoptotic cells and their membrane fragments, respectively. Scale bars: 50 µm (10 µm for high magnification images). **F.** Percentage of BV2 phagocytic microglia in every condition. Bars represent mean ± SEM (from 4 independent experiments). * indicates p<0.05 by Holm-Sidak posthoc test (after one-Way ANOVA was significant at p<0.05).*

6.3.4. GPR34 ligand lysoPS impairs microglial phagocytosis in hippocampal organotypic slice cultures

To delve into the role of lysoPS on microglial phagocytosis in more complex models, we tested its effect on hippocampal organotypic cultures from PND 7 fms-eGFP mice, treated with DMSO (lysoPS vehicle) or lysoPS 10 µM for 3h, and evaluated microglial phagocytosis **(Figure 22A-C)**.

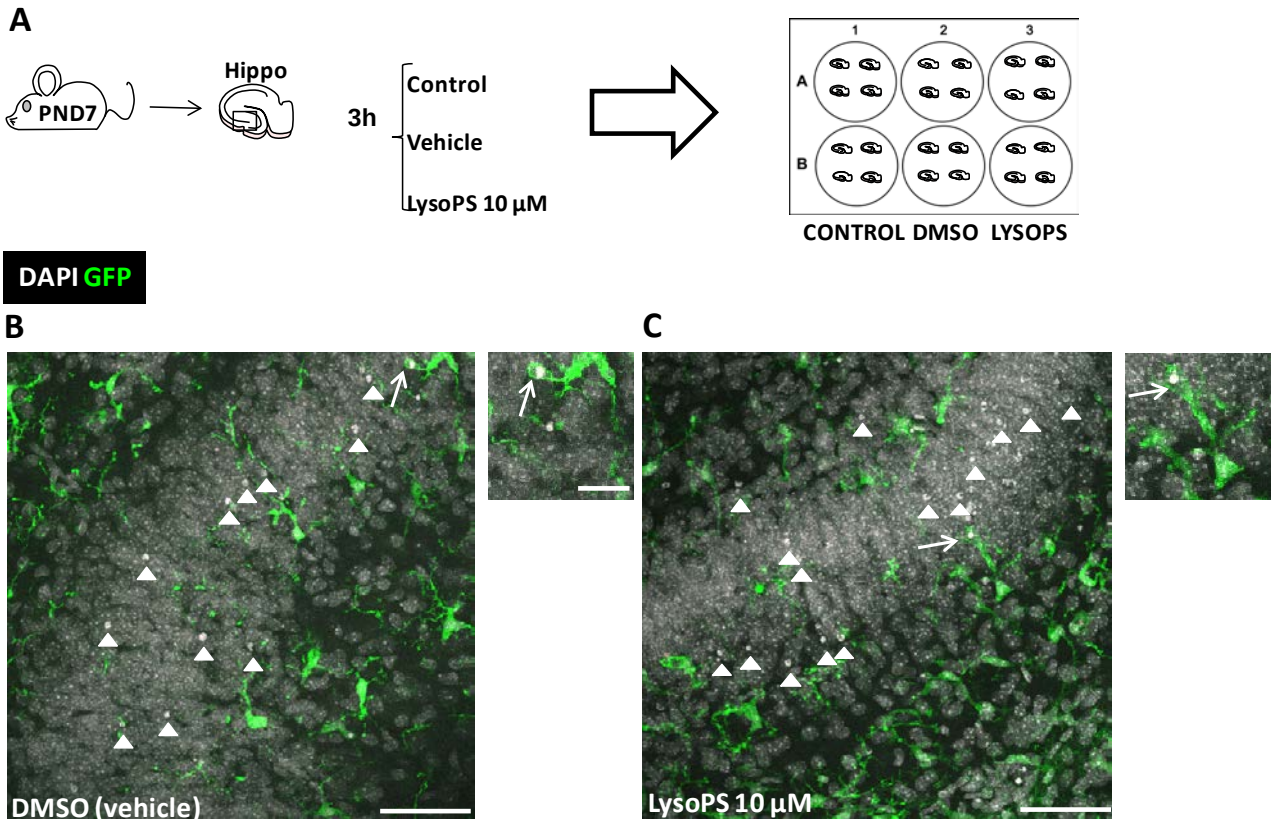

***Figure 22. Effect of GPR34 ligand lysoPS on microglial phagocytosis in hippocampal slice cultures. A.** Experimental design. Postnatal day 7 (PND7) fms-eFGP mice (n=2 per experiment, 3 experiments) were sacrificed, their hippocampi removed and chopped in slices. After 7 days in*

culture, slices were treated with lysoPS or DMSO (10 µM) for 3h. ***B.*** *Representative images of confocal z-stacks from DMSO-treated slices.* ***C.*** *Representative images of confocal z-stacks from lysoPS-treated slices. Arrowheads point at non-phagocytosed apoptotic cells whereas arrows point at phagocytosed apoptotic cells (showed in high magnification images). Scale bars: 50 µm (10 µm in high magnification images).*

First, we quantified the density of apoptotic cells, and found no significant differences between DMSO and lysoPS-treated slices (11 ± 0.9 vs 9.1 ± 0.9 apoptotic cells in 200,000 μm^3, (20µm thick, 100x100µm2 slice) respectively; p=0.18) **(Figure 23A)**. Afterwards, we analyzed the microglial phagocytic efficiency. In this case, DMSO-treated slices showed that microglia were significantly more efficient phagocytosing the apoptotic cells than in lysoPS-treated slices, as reflected by the drop in the Ph index (11.6 ± 0.5 % vs 7.9 ± 0.5 % in DMSO and lysoPS-treated slices, respectively; p<0.001) **(Figure 23B)**. This phagocytic impairment observed in lysoPS-treated slices could be caused by either a reduced number of microglial cells or by a decreased Ph capacity. For that reason, we continued analyzing the total amount of microglial cells and the Ph capacity. The number of microglia was similar in both DMSO and lysoPS-treated slices (4.4 ± 0.3 vs 3.8 ± 0.3 cells in 200,000 μm^3; p=0.25) **(Figure 23C)**. The phagocytosis impairment was then corroborated by observing the Ph capacity. DMSO-treated-slices presented 22.7 ± 2.1 % of microglia with one pouch whereas this percentage was significantly decreased to 17.3 ± 1.8 % in lysoPS-treated slices (p=0.08). Additionally, DMSO treatment generated 2.3 ± 1.1 % of microglia with two pouches, which was 1.6 ± 0.8 % in lysoPS-treated slices (p=0.56) **(Figure 23D)**. The weighted average of the Ph capacity was significantly higher in DMSO-treated slices compared to lysoPS-treated slices (0.27 ± 0.01 vs 0.20 ± 0.01 ppu; p=0.001) **(Figure 23E)**. Therefore, DMSO-treated slices showed a decreased percentage of non-phagocytic microglia compared to lysoPS-treated slices (74.9 ± 1.2 % vs 81.1 ± 1.4 % in DMSO and lysoPS treatment, respectively; p=0.007) **(Figure 23D)**.

Next, we postulated that the impairment of phagocytosis through a decreased Ph index and Ph capacity observed in lysoPS-treated slices could result in an uncoupling between apoptosis and phagocytosis, as previously observed in GPR34 KO mice. Thus, we quantified the Ph/A coupling ratio in our slices. Expectedly, results showed that these processes were significantly uncoupled in lysoPS-treated slices (1.00 ± 0.06 vs 0.76 ± 0.03 in DMSO and lysoPS treatment, respectively; p=0.017) **(Figure 23F)**. All these results showed that the addition of lysoPS to hippocampal slice cultures provoked an impairment in microglial phagocytosis leading to an

uncoupling between phagocytosis and apoptosis, similar to the effect in vivo caused by GPR34 deficiency. This again demonstrates the involvement of lysoPS in microglial phagocytosis.

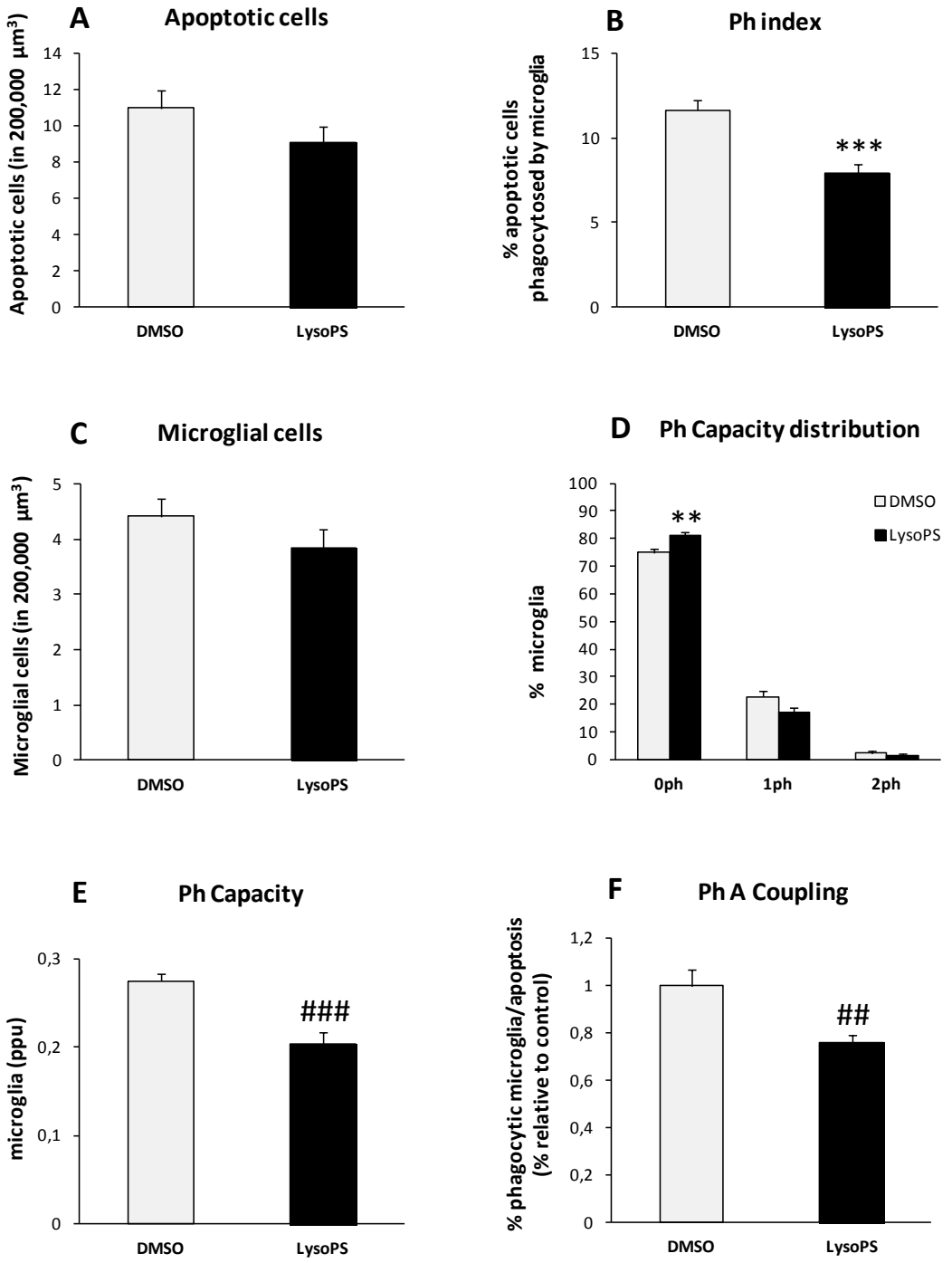

Figure 23. GPR34 ligand lysoPS uncouples apoptosis and microglial phagocytosis in hippocampal slice cultures. A. *Total number of apoptotic cells in 200.000 µm³ of the dentate gyrus (DG).* ***B.*** *Ph index (in % apoptotic cells) in each experimental condition.* ***C.*** *Total number of microglia in 200.000 µm³ of the DG.* ***D.*** *Histogram showing the Ph capacity of microglia (in % of*

cells). ***E.*** *Weighted Ph capacity (in ppu).* ***F.*** *Ph/A coupling ratio (in fold-change). Bars represent mean ± SEM from three independent experiments. ## indicates p=0.017, ** indicates p<0.01, ### indicates p=0.001 and *** indicates p<0.001 by two-tailed Student's test (**B** and **D**) or Mann-Whitney U test (**E** and **F**).*

6.3.5. GPR34 ligand lysoPS does not impair microglial phagocytosis in vivo

The next step was to determine the possible effect of lysoPS on microglial phagocytosis in vivo. Data obtained from in vitro experiments pointed towards a role of lysoPS in the regulation of microglial phagocytosis **(Figures 20-23)**. With the aim to assess its possible role on phagocytosis in vivo, DMSO (lysoPS vehicle) or lysoPS 36 µM were intrahippocampally injected in the DG of the hippocampus of 1 month-old fms-eGFP mice and microglial phagocytosis was analyzed **(Figure 24A-B)**.

We first observed that the amount of apoptotic cells in the hippocampus was similar between DMSO and lysoPS-injected mice (1,696.9 ± 233.7 vs 1,693.3 ± 258.1 apoptotic cells per septal hippocampus in DMSO and lysoPS-injected mice, respectively; p=0.94) **(Figure 25A)**. Regarding microglial phagocytic efficiency, Ph index was also similar in DMSO and lysoPS-injected mice (78.3 ± 3.1 % vs 75.5 ± 2.6 %; p=0.5) **(Figure 25B)**.

Furthermore, the number of microglia per hippocampus remained unchanged between DMSO and lysoPS-injected mice (4,081.1 ± 231.8 vs 4,098.5 ± 391.2; p=0.97) **(Figure 25C)**. Regarding the Ph capacity, DMSO-treated mice exhibited 24.2 ± 3.4 % of microglial cells with one single pouch whereas 19.2 ± 2.7 % of microglia with one pouch were observed in lysoPS-treated mice (p=0.27). Additionally, DMSO-treated mice presented 2.7 ± 0.7 % with two pouches whereas lysoPS-treated mice registered 0.8 ± 0.2 % of microglia with two pouches (p=0.02, although this difference is not reliable because only 5 microglial cells were visualized) **(Figure 25D).** The weighted average of the Ph capacity was slightly but not significantly higher in DMSO-treated mice compared to lysoPS-treated mice (0.31 ± 0.04 ppu vs 0.21 ± 0.02 ppu, respectively; p=0.09) **(Figure 25E)**. Finally, the quantification of the Ph/A coupling reflected a small but non-significant decrease in lysoPS-injected mice (1.00 ± 0.10 vs 0.73 ± 0.12; p=0.13) **(Figure 25F)**. As a conclusion, all these data did not give enough evidence of an impairing effect of the addition of lysoPS on microglial phagocytosis in vivo, as previously observed in microglia cultures.

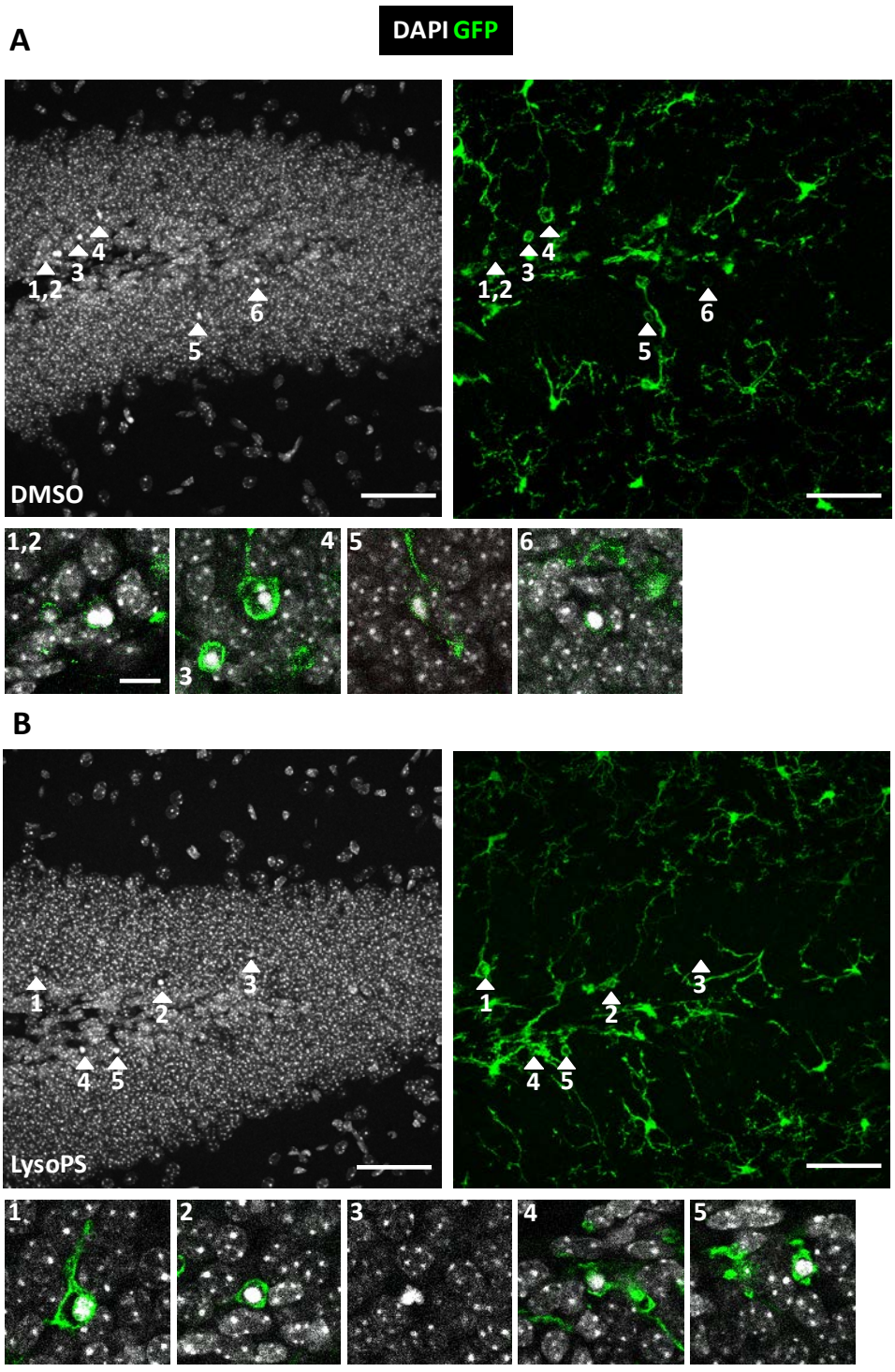

Figure 24. Effect of GPR34 ligand lysoPS on microglial phagocytosis in vivo. *1 month-old fms-eGFP mice were injected with DMSO (n=6) or lysoPS (n=7; 36 µM) into the right hippocampus and sacrificed 6h later.* ***A-B.*** *Representative confocal z-stacks of the dentate gyrus and detailed images from a single focal plane of apoptotic cells from 1 month-old fms-eGFP mice treated with DMSO (**A**) or lysoPS (**B**). Arrowheads point at apoptotic cells. Nuclear morphology was visualized with DAPI (white) and microglia were visualized with GFP (green). Scale bars: 50 µm (10 µm in high magnification images); Z=17 µm (DMSO), Z=20 µm (LysoPS).*

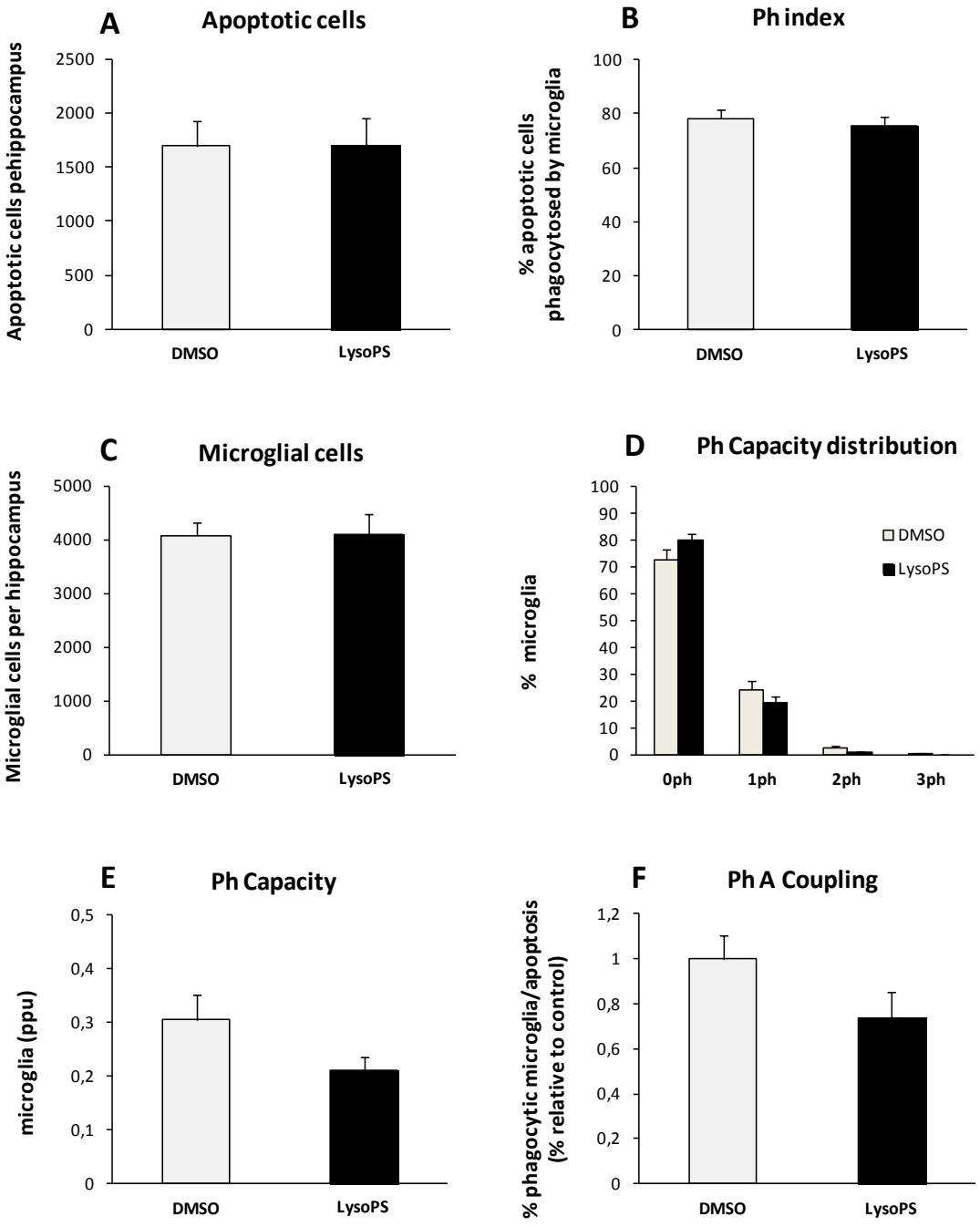

Figure 25. GPR34 ligand lysoPS does not affect microglial behavior in vivo. A. *Total number of apoptotic cells per septal hippocampus.* ***B.*** *Ph index (% apoptotic cells) per septal hippocampus.* ***C.*** *Total number of microglia cells per septal hippocampus.* ***D.*** *Histogram showing the Ph Capacity (in % of cells).* ***E.*** *Weighted Ph capacity (ppu).* ***F.*** *Ph/A coupling ratio. Bars represent mean ± SEM from n=7 (DMSO) and n=8 (LysoPS). No significant differences were detected by two-tailed Student's test.*

6.4. PHAGOCYTOSIS TRIGGERS METABOLIC ADAPTATIONS IN MICROGLIA IN VITRO

Once we had established the role of GPR34 on microglial phagocytosis, we focused on studying the consequences of phagocytosis on microglia through the analysis of microglial metabolism. Microglial phagocytosis is a complex process whose implications for the phagocyte are not fully understood yet. Engulfment and removal of apoptotic cells by microglia requires enough metabolic resources to meet such huge cellular demand [139]. Previous data of the laboratory comparing the transcriptional profile of cultured and phagocytic microglia 24h after engulfing apoptotic cells, pointed towards an upregulation of glycolytic pathway and a dowregulation of mitochondrial metabolic pathways through the phagocytic process **(Data of Irune Díaz-Aparicio Thesis; See introduction, Figure 6**). Glycolysis and OXPHOS are the main ATP production pathways in eukaryotic cells. Therefore, our aim was to study the possible metabolic changes affecting these pathways in microglia during phagocytosis. We used the BV2 microglia cell line as our model because of the low viability observed in metabolic analysis with primary microglia. First, we analyzed the mRNA expression pattern of key genes of glycolysis and OXPHOS metabolic pathways in search of alterations upon phagocytosis. Next, we studied deeply these two metabolic pathways at the cellular level. Afterwards, we assessed the mitochondrial morphology and dynamics (fusion, fission), which are usually linked to the energetic state of the cell [390] [391], and whose correct balance determines the mitochondrial network morphology [392]. Finally, we analyzed the mRNA expression of key genes involved in mitochondrial fusion and fission, whose expression could be related to mitochondrial morphology in BV2 microglia.

6.4.1. Glycolysis and OXPHOS genes are not altered in BV2 microglia after phagocytosis

We aimed to confirm whether an upregulation of genes involved in glycolysis occurred in BV2 microglia as a consequence of phagocytosis, as in primary microglia. For this purpose, we analyzed the mRNA expression profile of key genes encoding for glycolytic enzymes by RT-qPCR **(Genes are highlighted in Figure 26).** Encoding genes for these enzymes were selected according to their expression rate observed in the formerly mentioned array (upregulated for glycolysis genes and downregulated for OXPHOS genes, respectively).

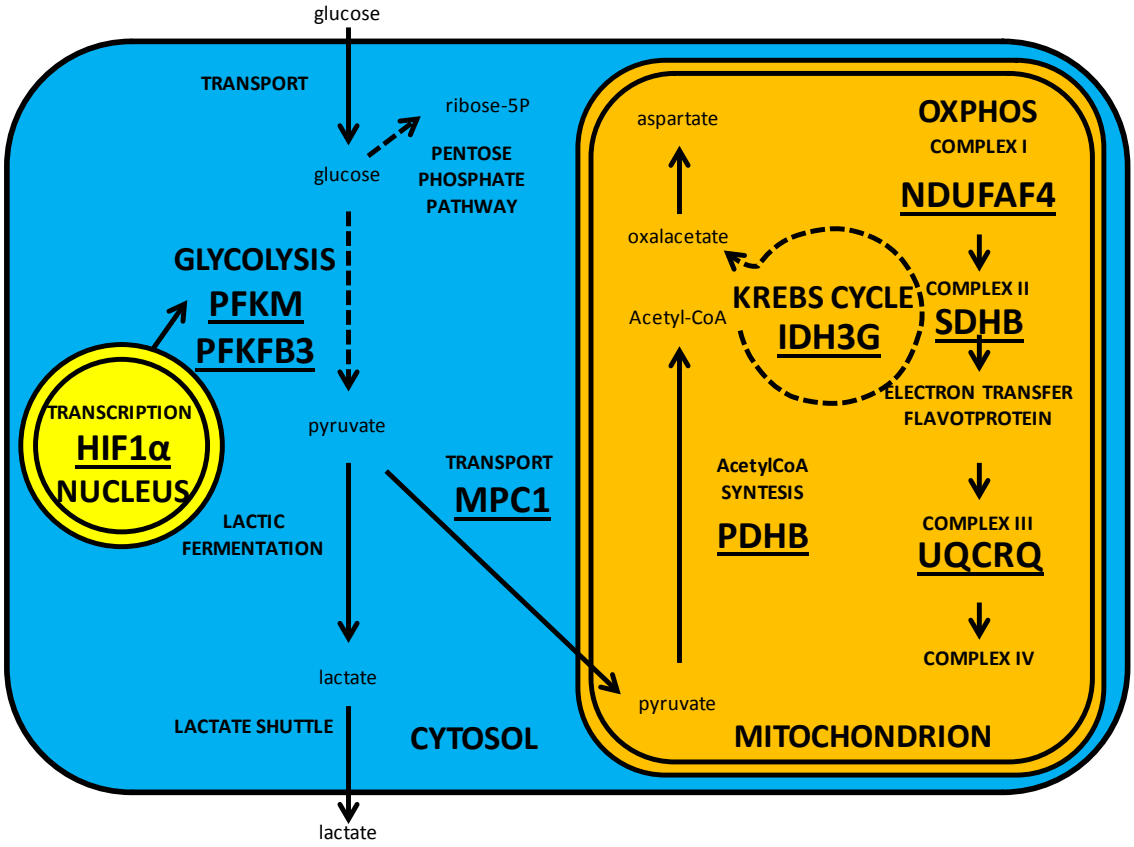

Figure 26. Scheme of the different metabolic pathways used for cell ATP production. *The mitochondrial metabolic pathway is illustrated in orange and the glycolytic pathway is illustrated in blue. Genes analyzed for each pathway are shown in capital letters.*

hif-1α was the first gene tested. It encodes the alpha subunit of transcription factor hypoxia-induced factor-1 (*hif-1*), a heterodimer protein which functions as a master regulator in glycolysis. *hif-1α* presented a non-significant decreased expression in naïve BV2 cells compared to phagocytic BV2 cells (increase of 31.4 ± 13 %; p=0.07) **(Figure 27A)**. Other two genes analyzed were 6-phosphofructokinase muscle (*pfkm*) and 6-phosphofructo-2-kinase/fructose-2,6-biphosphatase 3 (*pfkfb3*). *pfkm* encodes a subunit of the tetramer phosphofructokinase, which catalyzes the phosphorylation of fructose-6-phosphate into fructose 1,6-biphosphate. Naïve BV2 cells presented significantly increased expression compared to phagocytic BV2 cells (reduction until 43.6 ± 6.2 %, p<0.001) **(Figure 27B)**. *pfkfb3* encodes a protein that catalyzes the synthesis and degradation of fructose-2,6-biphosphate during glycolysis. *pfkfb3* did not experiment any changes in its expression in naïve BV2 cells compared to phagocytic BV2 cells (increase of 54.4 ± 53.6 %, p=0.36) **(Figure 27C)**. All these results were not consistent enough to confirm the gene expression changes in key glycolytic enzymes in BV2 cells, as observed in primary microglia after phagocytosis **(Table 2)**.

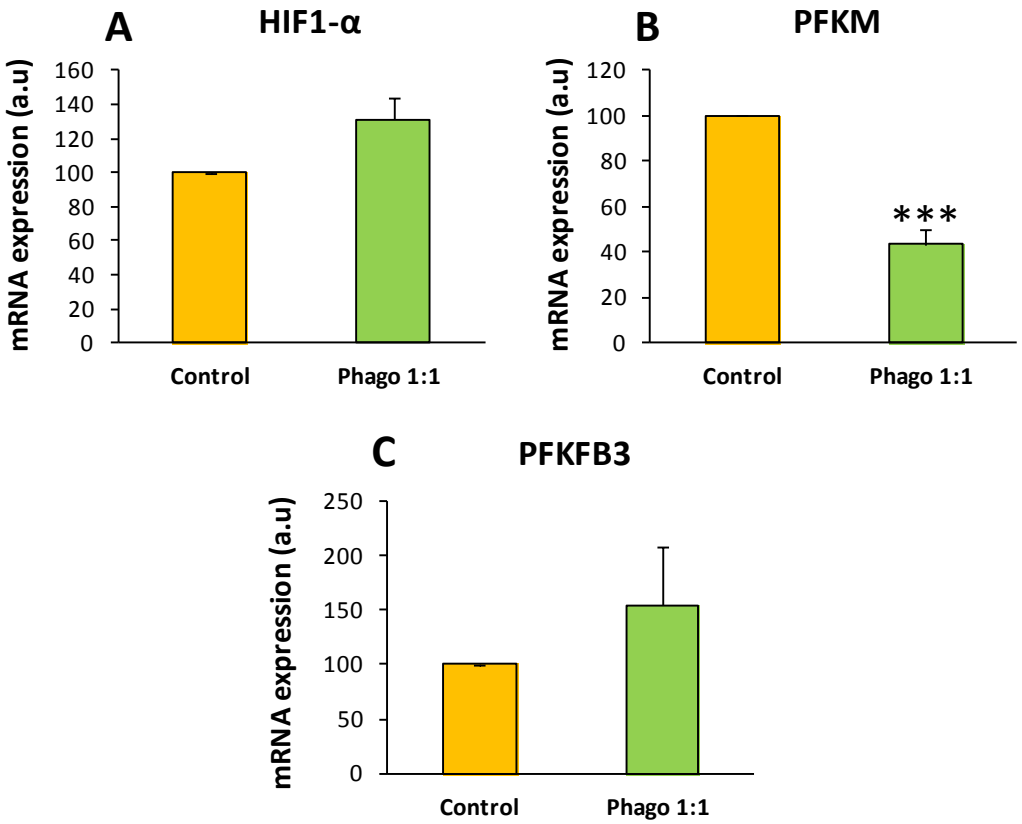

Figure 27. Glycolysis genes are not upregulated in BV2 microglia after phagocytosis*. Expression of HIF1-α (**A**), PFKM (**B**) and PFKFB3 (**C**) genes in naïve and high phagocytic (Phago 1:1) BV2 microglia (ratio 1:1; BV2; apoptotic cells). Each gene shows its gene expression normalized versus OAZ1 gene (reference gene) in arbitrary units (a.u). Bars represent mean ± SEM. *** indicates p<0.001 by two-tailed Student's test. N=3.*

Next, we tested whether there was a downregulation of mitochondrial metabolic pathways through phagocytosis in BV2 microglia. For this purpose, we analyzed the mRNA expression profile of key OXPHOS and TCA cycle enzymes by RT-qPCR **(Genes are highlighted in Figure 26).**

The OXPHOS pathway was tested by assessing three genes. We first tested NADH ubiquinone oxidoreductase complex assembly factor 4 (*ndufaf4)*, a gene which encodes for a protein involved in the assembly of the mitochondrial complex I, which catalyzes the transfer of electrons from NADH to ubiquinone in the first step of the respiratory chain. This gene showed very increased expression in naïve BV2 cells compared to phagocytic BV2 cells (reduction to 61.1 ± 8 %; p=0.008) **(Figure 28A)**. Next, ubiquinol-cytochrome C reductase Complex III Subunit VII (*uqcrq)*, a gene that encodes for a subunit that is a component of the ubiquinol-cytochrome

reductase complex III, part of the ETC, did not present significant changes in naïve BV2 cells compared to phagocytic BV2 cells (increase of 16.8 ± 13.5 %; p=0.28) **(Figure 28B).** Similarly, succinate dehydrogenase beta (*sdhb*), which encodes for a subunit of the mitochondrial respiratory chain complex II of the ETC, which carries electrons from FADH to Q, did not present any differences in naïve BV2 cells compared to phagocytic BV2 cells (reduction to 94.5 ± 9.4 %; p=0.59) **(Figure 28C)**.

Regarding other mitochondrial pathways, other three genes were tested. First we tested mitochondrial pyruvate carrier 1 (*mpc1*), which encodes for a protein which mediates the uptake of pyruvate into mitochondria, fundamental for the initiation of the TCA cycle and posterior OXPHOS process. It exhibited significantly decreased expression in naïve BV2 cells compared to phagocytic BV2 cells (increase of 73 ± 19.2 %; p=0.019) **(Figure 28D)**. However, the expression pattern was unaltered in the case of isocitrate dehydrogenase 3 gamma (*idh3g*), which encodes for a subunit of isocitrate dehydrogenase complex, involved in the decarboxylation of isocitrate into α-ketoglutarate in the TCA cycle, showing no differences between naïve BV2 cells and phagocytic BV2 cells (reduction to 90.2 ± 7.5 %; p=0.26) **(Figure 28E).** Lastly, pyruvate dehydroganse beta (*pdhb)*, which encodes for a subunit of the pyruvate dehydrogenase mitochondrial complex, in charge of the conversion of pyruvate to acetyl-CoA in the TCA cycle, did not present mRNA expression change either in naïve BV2 cells compared to phagocytic BV2 cells (reduction to 93.5 ± 9.2 %; p=0.51) **(Figure 28F)**. In conclusion, these results did not seem to be consistent enough to affirm that a negative regulation of mitochondrial metabolic pathways (OXPHOS and TCA cycle) through phagocytosis occurred in BV2 microglia as previously observed in phagocytic primary microglia **(Table 2)**.

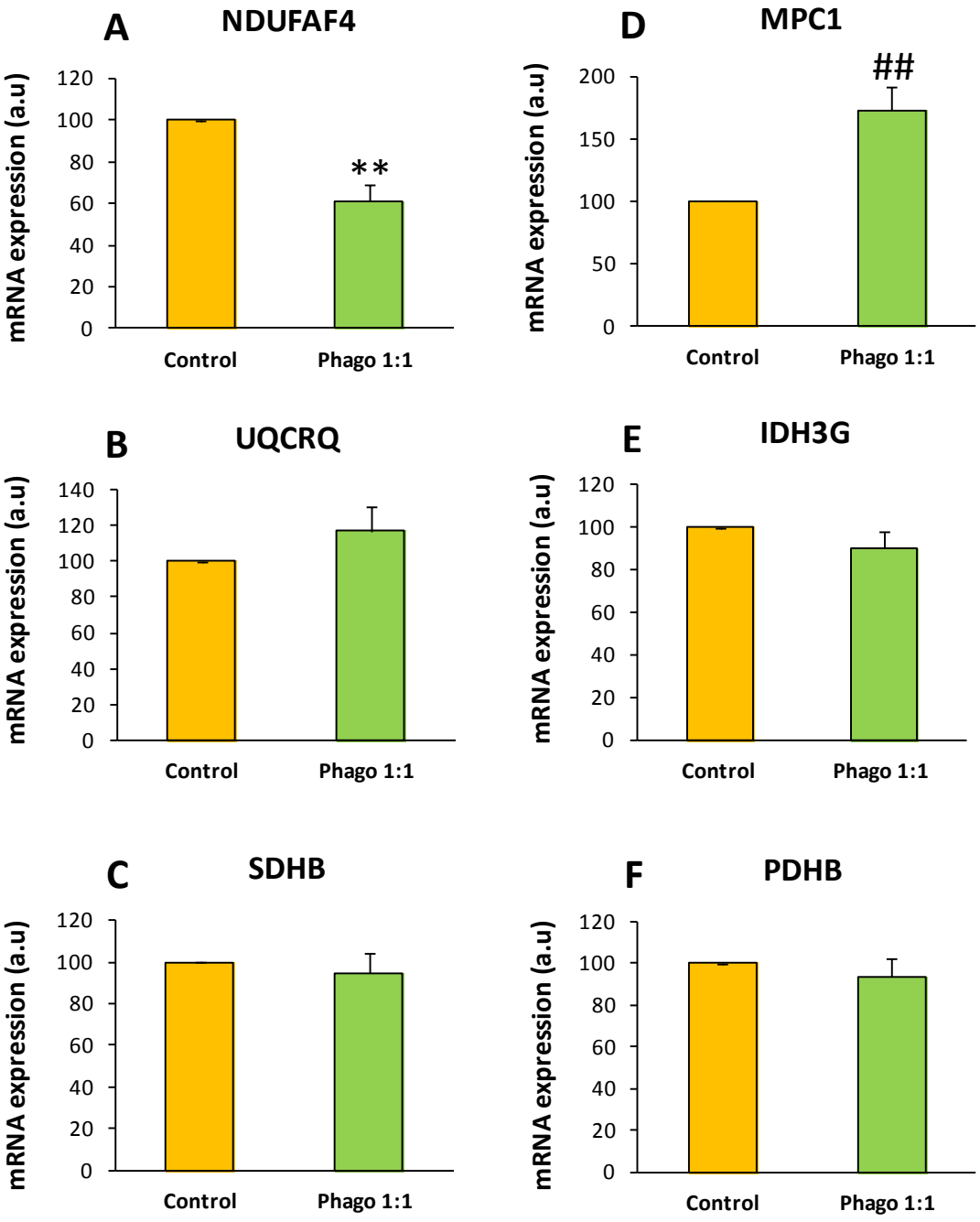

Figure 28. OXPHOS genes are not downregulated in BV2 microglia after phagocytosis. *In the left side: Expression of NDUFAF4 (**A**), UQCRQ (**B**) and SDHB (**C**) genes in naïve and high phagocytic (Phago 1:1) BV2 microglia (ratio 1:1; BV2; apoptotic cells). In the right side: Expression of MPC1 (**D**), IDH3G (**E**) and PDHB (**F**) genes in naïve and high phagocytic BV2 microglia. Each gene shows its gene expression normalized versus OAZ1 gene (reference gene) in arbitrary units (a.u). Bars represent mean ± SEM.* $^{\#\#}$ *indicates p=0.019 and ** indicates p<0.01 by two-tailed Student's test. N=3.*

CELL PROCESS	GENE	ARRAY (Ph 24H)	RTqPCR (Ph 24h)
GLYCOLISIS	HIF1α	2.77	0.07
GLYCOLISIS	PFKM	-1.5	0.0008
GLYCOLISIS	PFKFB3	2	n.s
OXIDATIVE PHOSPHORILATION	NDUFAF4	-1.9	0.008
OXIDATIVE PHOSPHORILATION	MPC1	-1.4	0.019
OXIDATIVE PHOSPHORILATION	IDH3G	-1.9	n.s
OXIDATIVE PHOSPHORILATION	UQCRQ	-1.5	n.s
OXIDATIVE PHOSPHORILATION	PDHB	-1.5	n.s
OXIDATIVE PHOSPHORILATION	SDHB	-1.7	n.s
FUSION	MFN1	-1.3	n.s
FUSION	MFN2	-1.4	n.s
FUSION	OPA1	-1.8	n.s
FISSION	FIS1	-1.05	0.0014
FISSION	MFF	-1.5	0.016
FISSION	DNM1L	NO DATA	n.s

	Array	RTqPCR
	Overexpression, F.C. > 1.5	**Upregulated < 0.05**
	Overexpression, F.C. 1.2-1.5	**Upregulated > 0.05**
	Underexpression. F.C. >1.5	**Downregulated < 0.05**
	Underexpression. F.C. 1.2-1.5	**Downregulated > 0.05**
	No changes	**No changes**

Table 2. Comparison of gene expression between primary microglia array and RT-qPCR analysis in BV2 microglia. *Glycolysis analyzed genes were indicated in yellow. Oxidative phosphorylation analyzed genes were indicated in orange. Fusion analyzed genes were indicated in blue. Fission analyzed genes were indicated in magenta. Legend indicates different levels of gene expression.*

6.4.2. Glycolysis is not increased whereas OXPHOS is decreased in BV2 microglia after phagocytosis

Although no consistent changes were observed in key glycolytic enzymes in BV2 phagocytic microglia **(Figure 27)**, we analyzed glycolytic pathway at cellular level.

The glycolytic pathway analysis was performed by measuring the PER (pmol/min). 5 experimental conditions were defined: naïve BV2 cells, high phagocytic BV2 cells (ratio 1:1 BV2: apoptotic cells), medium phagocytic BV2 cells (ratio 3:1), low phagocytic BV2 cells (ratio 9:1) and a negative control of apoptotic cells. The metabolic assays were performed 24h after the incorporation of apoptotic cells.

In eukaryotic cells, PER is supported by the contribution of glycolysis (through glycoPER) and mitochondrial Krebs Cycle (mitoPER), through de production of CO_2 (which acidifies the extracellular medium). We first analyzed the % of PER explained by glycolytic pathway (glycoPER) in naïve and phagocytic BV2 microglia. Mitochondrial-derived CO_2 contribution to the total PER is calculated by measuring the cell OCR. Then, it is substracted from total PER, obtaining the glycoPER. We observed that glycolysis was the main source driving PER in both naïve and phagocytic BV2 microglia. This glycoPER was similar in naïve (84.3 ± 4.1 %) and phagocytic BV2 microglia, tending to increase proportionally to the level of phagocytosis (86.3 ± 5.9 %, 90 ± 4.8 % and 94.9 ± 3.7 % in low, medium and high phagocytosis, respectively; p=0.45 (between groups ANOVA)). Next, we estimated the PER due to mitochondria (mitoPER), as the difference between basal PER (glycoPER+ mitoPER= 100 % PER) and glycoPER. MitoPER was similar in naïve (15.7 ± 4.1 %) and phagocytic BV2 microglia, tending to decrease proportionally to the level of phagocytosis (13.7 ± 5.9 %, 10 ± 4.8 % and 5.1 ± 3.7 % in low, medium and high phagocytosis, respectively; p=0.45 (between groups ANOVA)) **(Figure 29)**.

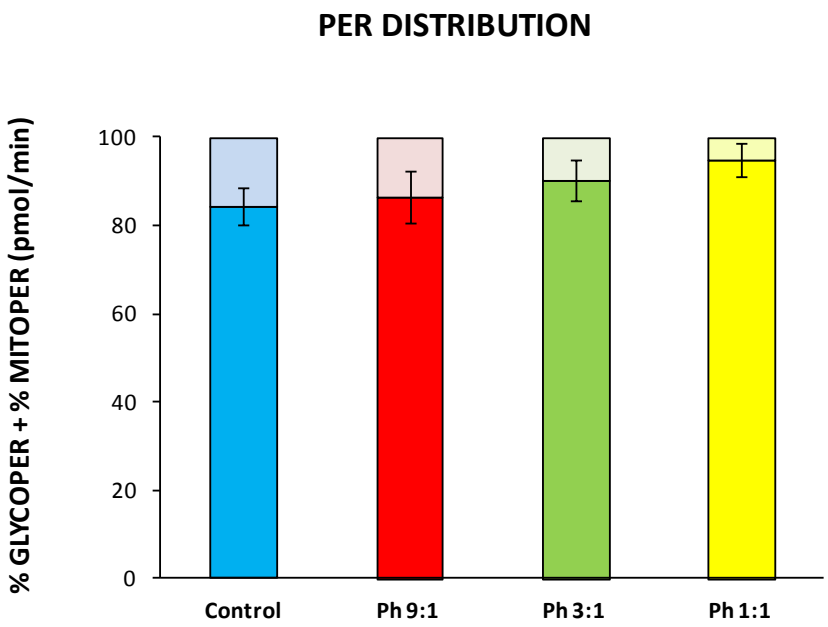

Figure 29. Glycolysis is the major catabolic pathway both in naïve and in phagocytic BV2 cells. *Representative graph of the proton efflux rate (PER) distribution. In blue, measurements of naive BV2 cells; in red, measurements of low phagocytic BV2 cells (ratio 9:1; (BV2: apoptotic cells)); in green, measurements of medium phagocytic BV2 cells (ratio 3:1), and in yellow measurements of high phagocytic BV2 cells (ratio 1:1). In dark colors, % PER due to glycolysis (glycoPER) and in light colors, % PER due to mitochondria (mitoPER). Bars represent mean ± SEM. No significant differences were detected by One-way ANOVA. N=3.*

Afterwards, we analyzed the PER corresponding to basal glycolysis, obtained after blocking mitochondrial activity via addition of rotenone (which blocks ETC complex I) and antimycin A (which blocks ETC complex III). We observed a significantly increased percentage in naïve BV2 cells compared to phagocytic BV2, with reductions down to 50 ± 7.9 %, 34 ± 6.3 %, and 23.9 ± 3 % in low, medium, and high phagocytosis, respectively ($p<0.001$ in each group vs naïve microglia by Holm-Sidak posthoc test (after ANOVA was significant at $p<0.05$)) **(Figure 30A)**. Next, we analyzed the PER corresponding to maximal glycolysis, referred to maximum PER reached by cells after blocking mitochondrial respiration (by addition of rotenone (ETC complex I blocker) and antimycin A (ETC complex III blocker)), as a percentage of the basal glycolysis in each group. Results showed no differences between naïve (142.3 ± 12.6 %) and phagocytic BV2 microglia (159.2 ± 20.2 %, 149.1 ± 20 % and 126.6 ± 12.1 % in low, medium and high phagocytosis respectively; $p=0.59$ (between groups ANOVA)) **(Figure 30B)**. Finally, we estimated the PER due to non-glycolytic acidification after treatment with 2-DG (a non-degradable analog of glucose), which reflected a non-significant but decreasing tendency in naïve BV2 microglia (18.7 ± 3.5 %) compared to phagocytic BV2 microglia, proportionally to the level of phagocytosis (21.4 ± 3.4 %, 29.7 ± 5.5 % and 43.3 ± 8.6 % in low, medium and high phagocytosis, respectively; $p=0.06$ (between groups ANOVA)) **(Figure 30B)**. In conclusion, our data do not support a metabolic reprogramming in BV2 microglia towards an increased glycolysis through phagocytosis, possible because BV2 microglia are highly glycolytic in basal conditions.

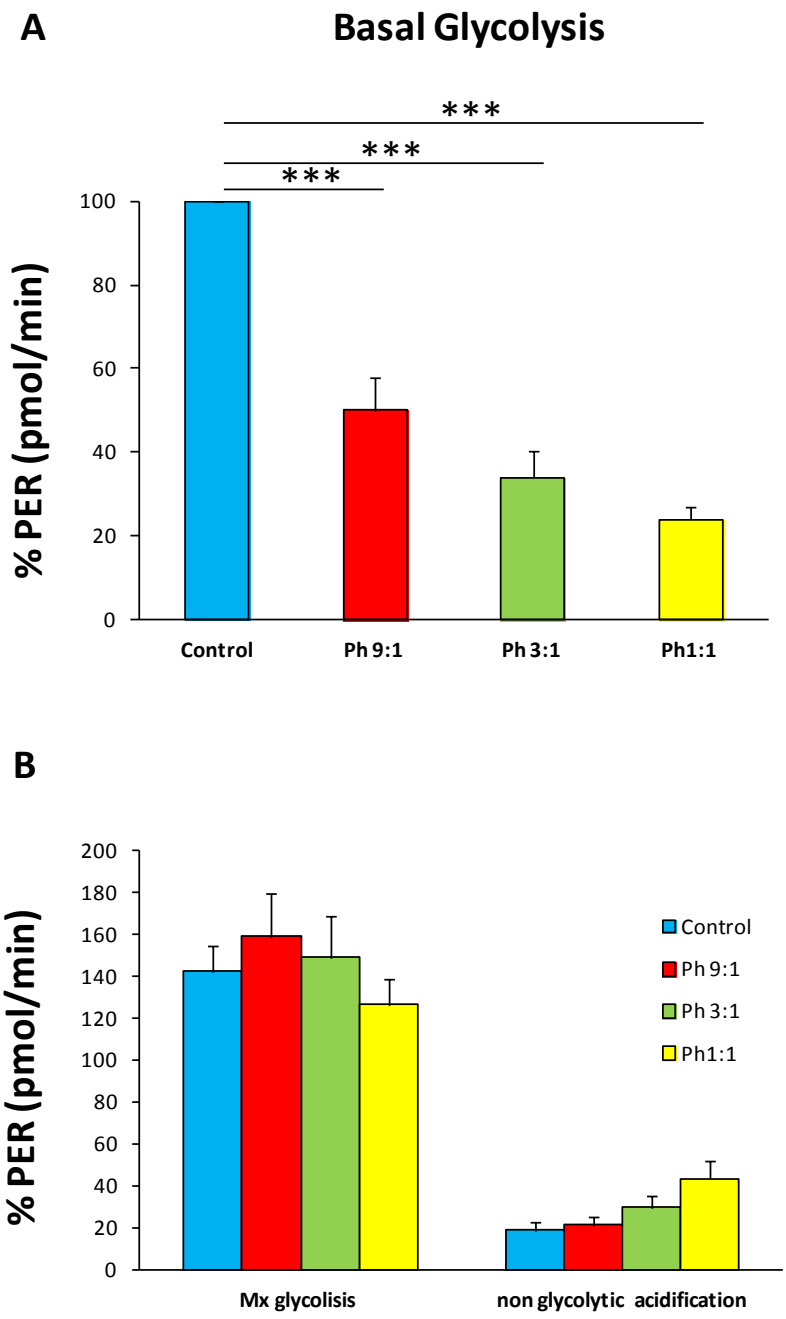

Figure 30. Glycolysis is not increased in BV2 microglia after phagocytosis. A. *Representative graph of the % proton efflux rate (PER) corresponding to basal glycolysis.* ***B.*** *Representative graph of the % PER corresponding to maximal glycolysis (mx glycolysis) and non-glycolytic acidification. In blue, measurements of naive BV2 cells; in red, measurements of low phagocytic BV2 cells (ratio 9:1; (BV2: apoptotic cells)); in green, measurements of medium phagocytic BV2 cells (ratio 3:1), and in yellow measurements of high phagocytic BV2 cells (ratio 1:1). Results were obtained from 3 independent experiments. Bars represent mean ± SEM. *** indicates p<0.001 by Holm-Sidak post-hoc test (after one-way ANOVA was significant at p<0.05).*

We next focused on OXPHOS. While no consistent changes were observed in key enzymes in BV2 phagocytic microglia **(Figure 28)**, we directly measured OXPHOS using the OCR (pmol/min). 5 experimental conditions were defined: naïve BV2 cells, high phagocytic BV2 cells (ratio 1:1(BV2: apoptotic cells)), medium phagocytic BV2 cells (ratio 3:1), low phagocytic BV2 cells (ratio 9:1) and a negative control of apoptotic cells. The metabolic assays were performed 24h after the engulfment of apoptotic cells.

Results of the OCR consumed in the basal mitochondrial respiration reflected a higher percentage in naïve BV2 cells compared to medium phagocytic BV2 cells (reduction down to 53.4 ± 12.7 %; p=0.015) and high phagocytic BV2 cells (reduction down to 55.1 ± 13.1 %; p=0.018) **(Figure 31A)**.

The % OCR consumed for ATP production (obtained after injecting oligomycin, an ATPase blocker) was higher in naïve BV2 than in phagocytic BV2 cells, and was significantly different in the case of high phagocytic BV2 microglia (40.9 ± 8.7 % for naïve BV2 vs 4.9 ± 6.1 % for high phagocytic BV2; p=0.013) **(Figure 31B)**. We next calculated the maximum respiration rate as a percentage of the basal respiration, in the presence of the ionophore FCCP, which collapses the proton gradient and disrupts mitochondrial membrane potential. As a consequence, the electron flow through the ETC is uninhibited and oxygen is maximally consumed by ETC complex IV. The maximum respiratory rate was higher in naïve BV2 cells (186.9 ± 3.5 %) compared to medium phagocytic BV2 microglia and high phagocytic BV2 microglia (79.9 ± 20.9 %; p=0.022 and 67.3 ± 28.1 %; p=0.013 in medium and high phagocytosis, respectively) **(Figure 31B)**. The % OCR consumed for maximal respiration gave rise to an estimation of the spare capacity (difference between maximal mitochondrial respiration and basal mitochondrial respiration). There was a tendency of a clear but non-significantly increased percentage in naïve BV2 cells (117.5 ± 32.9 %) compared to phagocytic BV2 cells (101.2 ± 18.2 %, 42.8 ± 14.3 % and 28.2 ± 17.9 % in low, medium and high phagocytosis, respectively; p=0.054 (between groups ANOVA)) **(Figure 31B)**. Finally, the % OCR for non-mitochondrial respiration, driven by processes outside the mitochondria and calculated as the percentage of oxygen consumed after blocking the respiratory chain by injecting a mix of rotenone and antimycin A, was non-significantly decreased in naïve BV2 cells (30.6 ± 4 %) compared to phagocytic BV2 cells (45.6 ± 9.9 %, 62.8 ± 6 % and 60.8 ± 10.7% in low, medium and high phagocytosis, respectively; p=0.11 (between groups ANOVA)) **(Figure 31B)**. To sum up, apoptotic cells phagocytosis in BV2 microglia generated a reduction of the OXPHOS in agreement with the transcriptional profile observed in primary microglia **(See introduction, Figure 6)**.

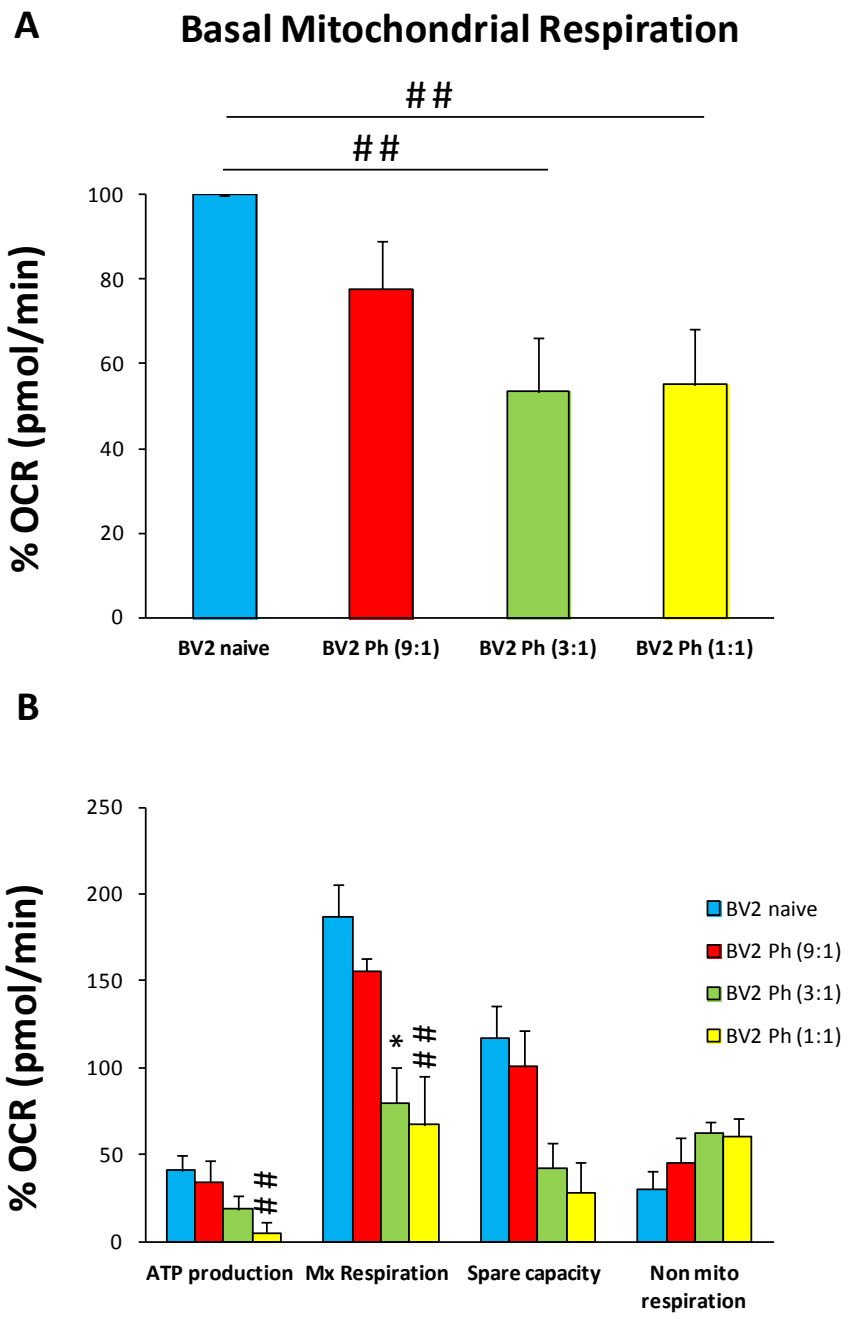

Figure 31. OXPHOS is reduced in BV2 microglia after phagocytosis. A. *Representative graph of the % oxygen consumption rate (OCR) corresponding to basal mitochondrial respiration.* ***B.*** *Representative graph of the % OCR consumed for ATP production, maximal respiration (mx respiration), spare capacity and non-mitochondrial respiration (from left to right). In blue, measurements of naive BV2 cells; in red, measurements of low phagocytic BV2 cells (ratio 9:1; (BV2: apoptotic cells)); in green, measurements of medium phagocytic BV2 cells (ratio 3:1), and in yellow measurements of high phagocytic BV2 cells (ratio 1:1). Results were obtained from 3 independent experiments. Bars represent mean ± SEM. * indicates p<0.05 and ## indicates p=0.015 and p=0.018, respectively (in* ***A****) and p=0.013 (in* ***B****) by Holm-Sidak posthoc test (after one-way ANOVA was significant at p<0.05).*

6.4.3. Mitochondrial morphology is affected in BV2 microglia after phagocytosis

The metabolic analysis at cellular level showed a reduction of the OXPHOS pathway in phagocytic BV2 microglia. In order to better understand if this metabolic change was related to mitochondrial structural alterations, we studied the mitochondrial morphology in phagocytic and naïve BV2 cells. To visualize mitochondria, cells were transfected with a mitochondrial-tagged reporter, pGFP-Mito-7 (Addgene). With the aim to analyze mitochondrial morphology, we developed an image analysis process which consisted in deconvolution and skeletonization of the mitochondrial network **(Figure 32A-D**).

The skeleton's analysis revealed that phagocytic BV2 microglia presented fewer mitochondria (decrease down to 47.2 ± 17.1 %, p=0.037), both in individual mitochondria (decrease down to 49.22 ± 20.1, p=0.06) and in those forming networks (reduction down to 40.4 ± 15.5 %, p=0.033). However, the mitochondrial length did not present any changes between naïve and phagocytic BV2 conditions, neither in the total length (decrease until 80.2 ± 38.2 %, p=0.59) nor in the length of those forming networks (reduction down to 80.51 ± 38.6 %, p=0.6). Mitochondria observed in phagocytic BV2 microglia were less ramified (decrease down to 64.43 ± 19.79 %, p=0.048) but the number of branches were similar in naïve and phagocytic BV2 (reduction down to 68.6 ± 22.02 %, p=0.083). The analysis of the number of mitochondrial network junctions revealed that phagocytic BV2 presented fewer junctions (decrease down to 55.52 ± 18.95 %, p=0.052). In brief, these results suggested that BV2 microglia phagocytosis reduced mitochondrial morphology complexity **(Figure 32E)**.

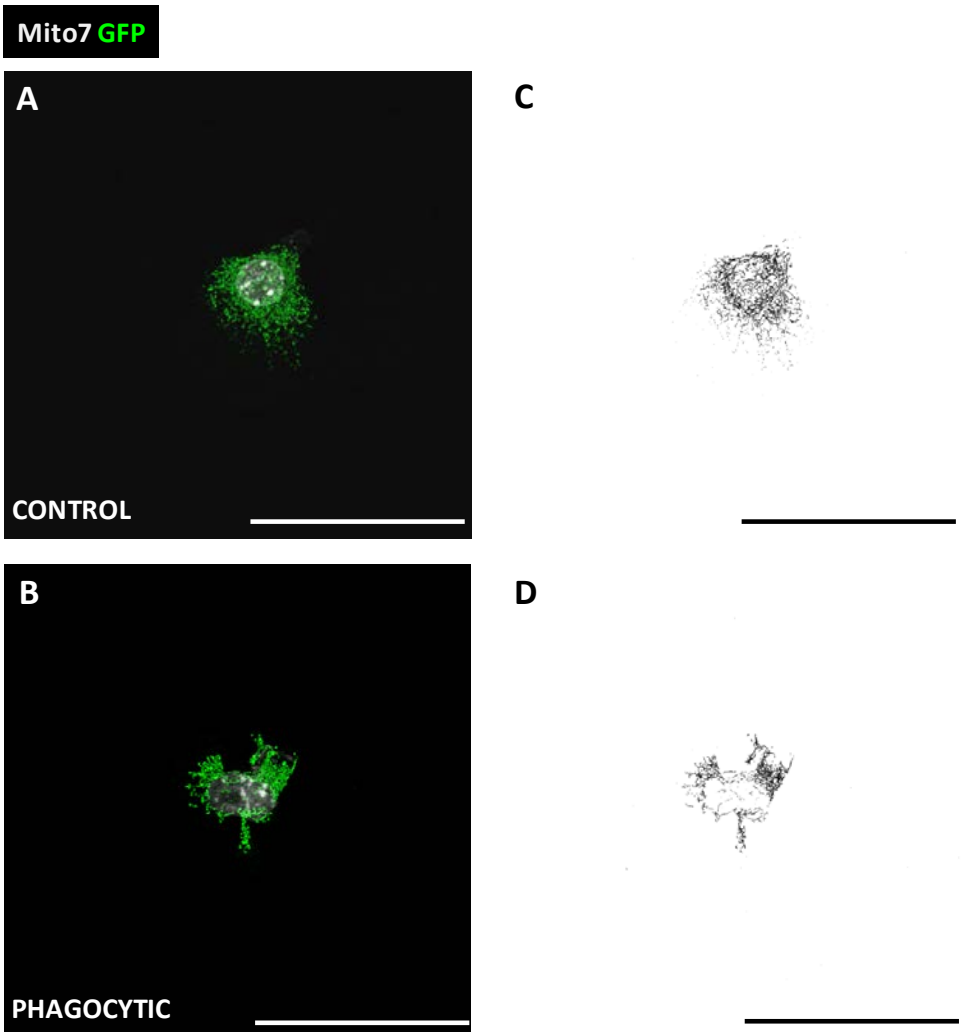
Mito7 GFP
A
CONTROL
C
B
PHAGOCYTIC
D

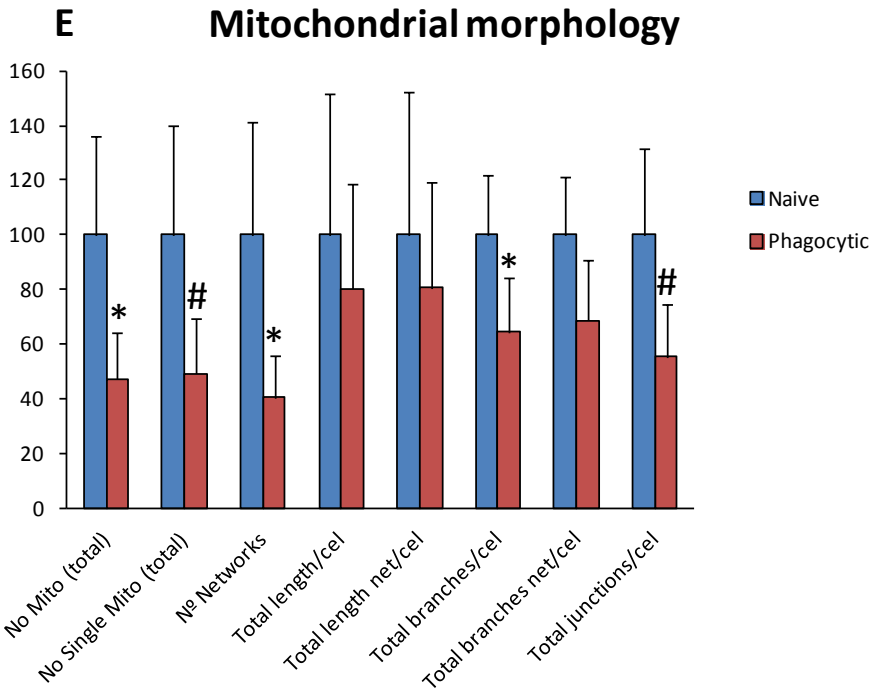
E
Mitochondrial morphology
160
140
120
100
80
60
40
20
0
*
#
*
*
#
No Mito (total)
No Single Mito (total)
Nº Networks
Total length/cel
Total length net/cel
Total branches/cel
Total branches net/cel
Total junctions/cel
Naive
Phagocytic

Figure 32. Mitochondrial morphology is altered in BV2 microglia after phagocytosis*. Representative confocal z-stacks of a naïve (**A**) and phagocytic (**B**) BV2 microglia cell showing the mitochondrial network (Mito7GFP, green) and the nuclei (DAPI, grey). Binary images (black and white) defining the skeleton of naïve cell (**C**) and phagocytic cell (**D**) showing the mitochondrial network (black) and the nuclei (grey). Scale bars: 50 µm. Z=5,8 µm (Control) Z=6,3 µm (Phagocytic)**. (**E**) Graph showing mitochondrial morphology analysis results. In blue, measurements of naïve BV2 microglia and in red measurements of high phagocytic BV2 microglia (ratio 1:1; BV2: apoptotic cells). From left to right, measurements of number of mitochondria per cell (single or mitochondrial networks), total length of mitochondria (single and mitochondrial networks) per cell, total branches in single mitochondria and in mitochondrial networks per cell and the total number of junctions between networks per cell. Bars represent mean ± SEM. Two independent experiments were performed with 5-6 cells analyzed per experiment.* indicates p<0.05 and # indicates p= 0.06 and p=0.052 by two-tailed Student's test.*

6.4.4. Mitochondrial fusion genes remain unaltered but mitochondrial fission genes are affected in BV2 microglia after phagocytosis

Mitochondrial remodeling via fusion/fission is well known to be relevant for OXPHOS [227]. The loss of fusion triggers a decrease in mtDNA and the membrane potential, implying a defective function of the respiratory chain both in vivo and in vitro [392, 393]. Furthermore, OXPHOS inhibition is generally linked to enhancement of fission [254]. Taking this into account, we decided to analyze several genes related to mitochondrial fusion and fission **(Figure 33)**, which could be modified in BV2 microglia through phagocytosis.

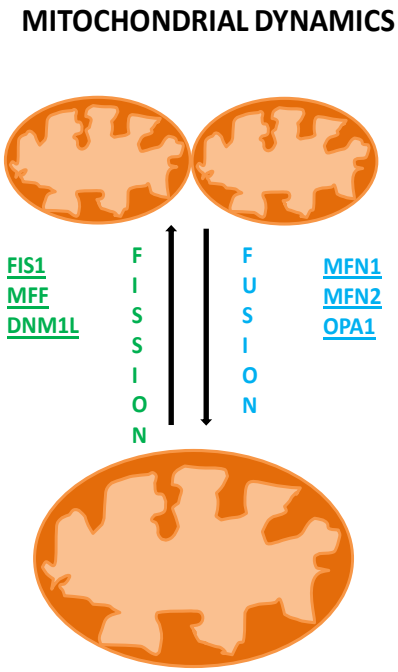

Figure 33. Mitochondrial fusion and fission processes. *Fusion genes analyzed are represented in blue and fission genes analyzed are represented in green.*

We first analyzed fusion genes. Genes were selected basing on previous publications pointing towards three fundamental protein-encoding genes involved in this process [249, 252]. On one hand, *mfn1* and *mfn2*. These genes encode for two outer-membrane GTPases that interact each other mediating outer mitochondrial membrane fusion. Neither *mfn1* (reduction down to 86.2 ± 11.9 %; p=0.31) **(Figure 34A)** nor *mfn2* (increase up to 9.6 ± 15.1 %; p=0.56) **(Figure 34B)** presented any significant changes in expression in naïve compared to phagocytic BV2 microglia. On the other hand *opa1*, a gene that encodes for a GTPase which mediates inner-membrane fusion and also regulates the balance between mitochondrial fusion and fission, did not present any change of expression either comparing naïve versus phagocytic BV2 microglia (reduction down to 96.7 ± 11.1 %; p=0.78) **(Figure 34C)**.

Next, we analyzed the main fission genes. Other three genes were tested: mitochondrial fission protein 1 (*fis1*), mitochondrial fission factor (*mff*) and dynamin 1-like (*dnm1l*). Both *fis1* and *mff* encode for receptor proteins which help recruiting *dnm1l* protein to the mitochondrial outer membrane, promoting fission. *fis1* showed decreased expression in naïve compared to phagocytic BV2 cells (increase up to 124.1 ± 15.9 %; p=0.0014) **(Figure 34D**). In contrast, *mff* presented increased expression in naïve BV2 compared to phagocytic BV2 cells (decrease down to 79.1 ± 5.3%, p=0.016) **(Figure 34E)**. *dnm1l*, which encodes for the main fission mediator protein, presented increased expression in naïve BV2 cells compared to phagocytic BV2 cells (decrease down to 73.5 ± 6.85 %, p=0.016) **(Figure 34F)**. Summing up, these results reflected an alteration in genes involved in mitochondrial fission process through phagocytosis in BV2 microglia.

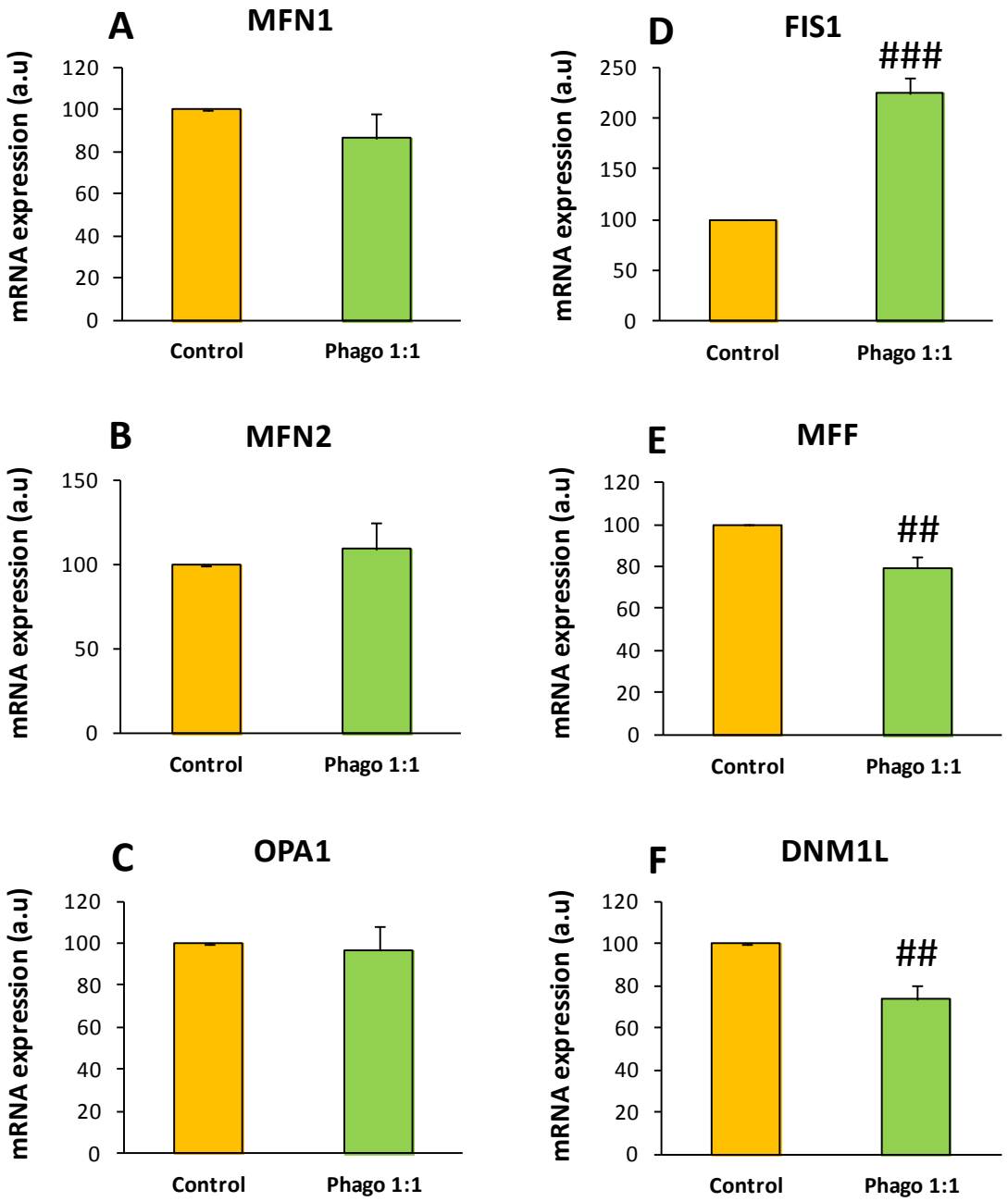

Figure 34. Mitochondrial fusion genes remain unaltered but mitochondrial fission genes and morphology are affected in BV2 phagocytic microglia in vitro. *Expression of MFN1 (**A**), MFN2 (**B**), OPA1 (**C**) fusion genes and FIS1 (**D**), MFF (**E**) and DNM1L (**F**) fission genes in naïve and high phagocytic BV2 microglia (ratio 1:1; BV2; apoptotic cells) (Phago 1:1). Each gene shows its gene expression normalized versus OAZ1 gene (reference gene) in arbitrary units (a.u). Bars represent mean ± SEM.* $^{##}$ *indicates p=0.016 and* $^{###}$ *indicates p=0.001 by two-tailed Student's test. N=3.*

6.5. PHAGOCYTOSIS IMPAIRMENT DOES NOT LEAD TO ALTERED NEUROGENESIS IN VIVO

Once we determined the metabolic profile of microglia upon phagocytosis, we studied the possible implications of microglial phagocytosis on their surrounding cells. Microglial crosstalk with neurons results crucial in the neurogenic niche of the hippocampus. Microglia phagocytose the excess of apoptotic newborn neurons [28] produced by neuroprogenitors generated from NSCs [292]. It has been suggested that microglia could influence adult neurogenesis, such as when activated by inflammation [354] or when neurogenesis is induced by an enriched environment [394]. However, it has not been elucidated the impact of microglial phagocytosis on adult hippocampal neurogenesis [28]. Previous work of the laboratory pointed towards a modulatory role of phagocytic microglia in the proliferation and differentiation of neural progenitors in vitro as well as in the proliferation of neuroblasts in vivo **(Data of Irune-Díaz Aparicio Thesis)**. Thus, with the aim to test whether it could exist a concomitant effect of the microglial phagocytosis impairment caused by GPR34 deficiency on the regulation of adult hippocampal neurogenesis in vivo, we analyzed whether the phagocytic impairment located in the DG could result in alterations in the neurogenic cascade (cell proliferation, NSCs and neuroblasts). Neurogenesis analysis was performed in several batches of 1 month and 3 month-old mice (Measured parameters are detailed in **Table 3)**.

1 month-old mice (BrdU-injected)	3 month-old mice (Non-injected)
Total cell proliferation Total NSCs and neuroblasts Proliferating NSCs and neuroblasts	Total NSCs and neuroblasts

Table 3. Neurogenesis-related analysis performed per mice age. *Brief description of parameters tested. Total cell proliferation, neural stem cells (NSCs) (total and proliferating) and neuroblasts (total and proliferating) were measured in 1 month-old WT and GPR34 KO mice (injected with BrdU). Total NSCs and neuroblasts were measured in 3 month-old WT and GPR34 KO mice (non-injected). NSCs were identified as double-positive for nestin and glial fibrilar acidic protein (GFAP) whereas neuroblasts were identified as positive for doublecortin (DCX).*

6.5.1. GPR34 deficiency does not affect newborn cells proliferation in 1 month-old mice

To delve into the changes in the neurogenic cascade induced by the lack of microglial GPR34, we analyzed the NSCs and neuroblasts in 1 month-old WT and GPR34 KO mice. These mice were intraperitoneally injected with BrdU (a thymidine analog which binds in the S-phase of cell cycle) and sacrificed 24h after the injection, allowing us to estimate cell proliferation.

Analyses were carried out in the septal hippocampus because the innervations in this region involve more neurogenic activity [395].

First, we quantified the total number of proliferating ($BrdU^+$) cells **(Figure 35A-B)**. Total proliferation analysis showed no differences in the number of $BrdU^+$ cells per hippocampus in WT compared to KO mice (2,425.6 ± 142.4 vs 2,533.6 ± 83.4 cells, respectively; p=0.54) **(Figure 35C)**. Afterwards, we analyzed total NSCs **(Figure 36A-B)**, defined as cells whose soma is located in the SGZ, are labeled with nestin and GFAP, and have an apical, radial process extending into the granular zone ($Nestin^+$, $GFAP^+$ cells) [295]. We found a trend of fewer NSCS in WT mice compared to GPR34 KO mice (14,140.5 ± 761.1 vs 16,256 ± 508.9 cells per septal hippocampus; p=0.08) **(Figure 36C)**. Finally, we analyzed proliferating NSCs by quantifying the number of $Nestin^+$, $GFAP^+$, $BrdU^+$ cells. Unfortunately, the low number of cells labeled (18 cells in WT mice (n=3) and 11 cells in KO mice (n=3)) did not allow us to obtain reliable data about NSC proliferation **(data not shown)**.

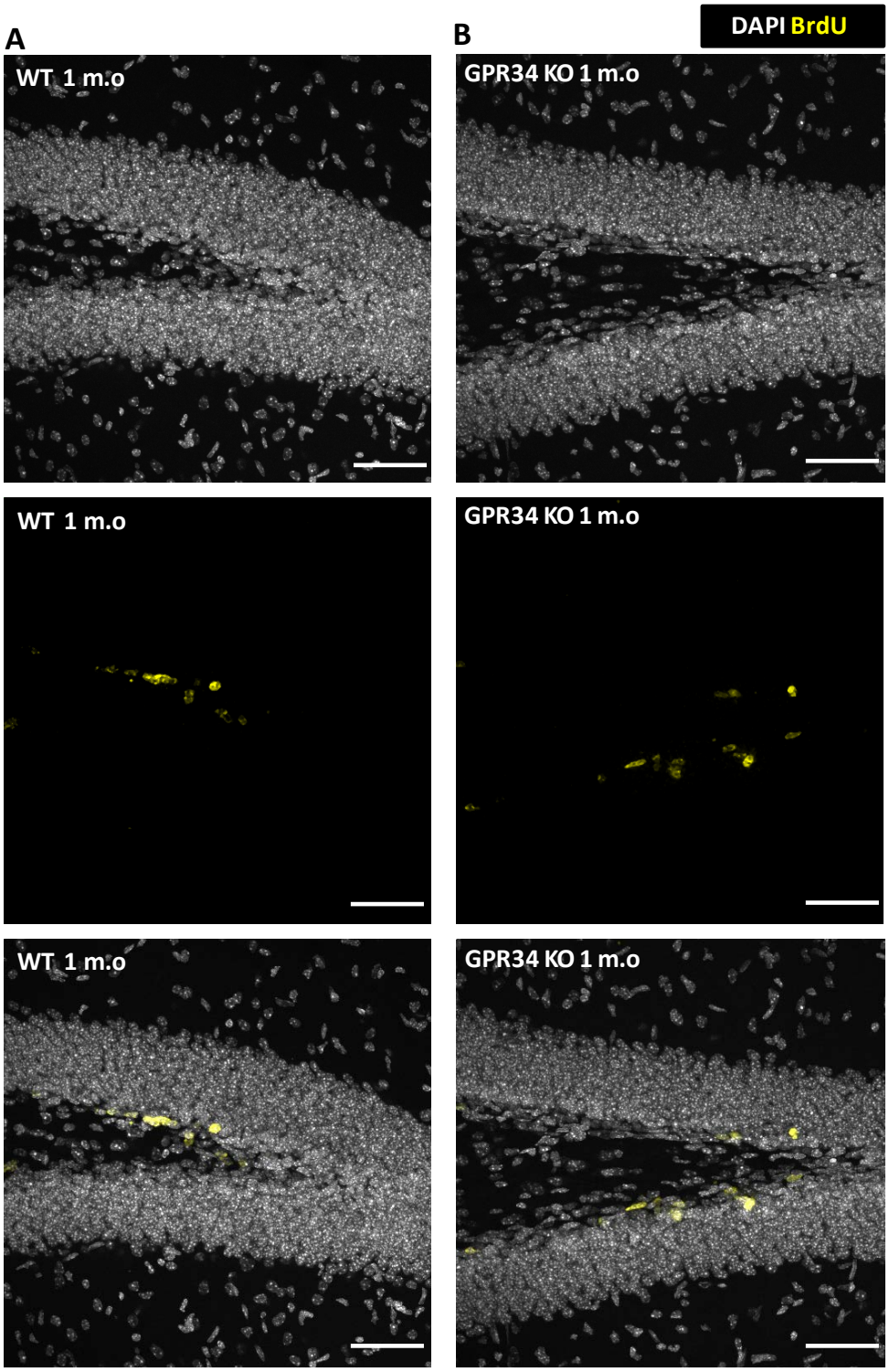
A
B
DAPI BrdU
WT 1 m.o
GPR34 KO 1 m.o
WT 1 m.o
GPR34 KO 1 m.o
WT 1 m.o
GPR34 KO 1 m.o

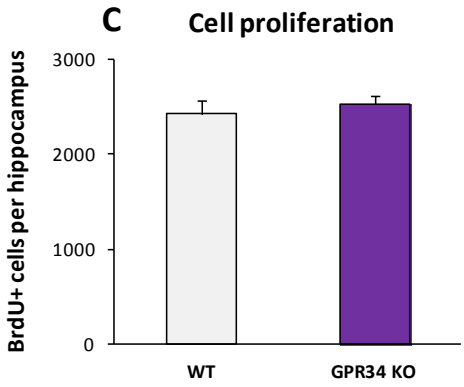
C
Cell proliferation
BrdU+ cells per hippocampus
3000
2000
1000
0
WT
GPR34 KO

Figure 35. GPR34 deficiency does not affect cell proliferation in 1 month-old mice. A, B *Representative confocal z-stacks of the dentate gyrus of 1 month-old WT (**A**) and KO mice (**B**) (n=3, each). Nuclei were visualized in DAPI (white) and BrdU+ cells were visualized in yellow. Scale bars: 50 µm Z=19 µm (WT) Z=21 µm (KO).* ***C.*** *Total proliferating (BrdU^{+}) cells per septal hippocampus. Bars represent mean ± SEM. No significant differences were observed by two-tailed Student's test.*

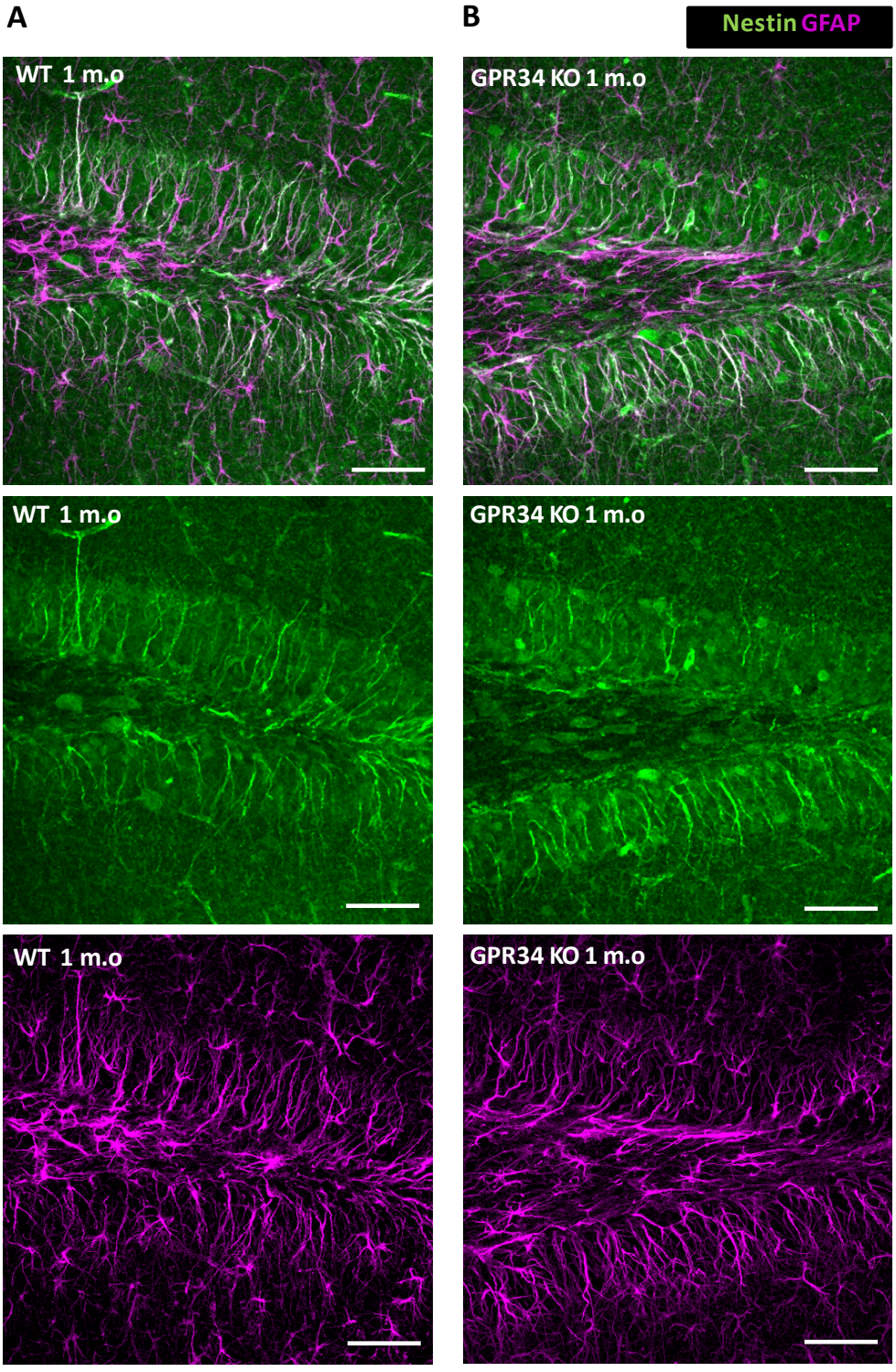

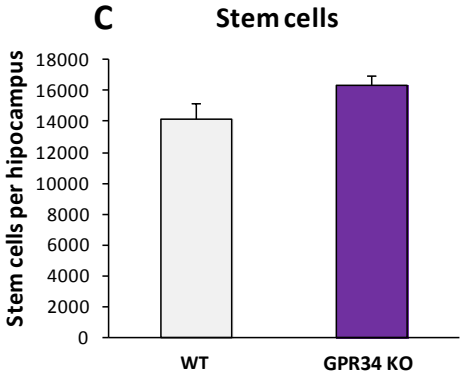

Figure 36. GPR34 deficiency does not alter neural stem cells population in 1 month-old mice. ***A, B*** *Representative confocal z-stacks of the dentate gyrus of 1 month-old WT (**A**) and KO mice (**B**) (n=3, each).* *Nestin was visualized in green and GFAP was visualized in magenta. Neural stem cells (NSCs) were double-positive for nestin and GFAP. Scale bars: 50 µm Z=19 µm (WT) Z=21 µm (KO).* ***C.*** *Total number of NSCs (Nestin$^+$, GFAP$^+$) per septal hippocampus. Bars represent mean ± SEM. No significant differences were observed by two-tailed Student's test.*

Next, we analyzed the neuroblasts population labeled with DCX **(Figure 37A-B).** We found no significant differences between WT and GPR34 KO mice in the total number of neuroblasts (DCX$^+$ cells) (53,952.3 ± 2,182.6 vs 54,963.9 ± 765.1 cells per septal hippocampus in WT and KO, respectively; p=0.76) **(Figure 38A)**. We also quantified the neuroblasts attending to their maturation stage. Three subpopulations can be distinguished basing on their maturation stage: A/B cells, which are devoid of processes or presented short ones; C/D cells, characterized by medium processes, some of them able to reach the molecular layer of the hippocampus; and E/F cells, which have one strong dendrite branching in the molecular layer or a dendritic tree branching in the granular cell layer of the hippocampus [301].

We observed similar amounts of A/B DCX$^+$ cells per hippocampus in both WT and GPR34 KO mice (19,665.3 ± 2053.5 vs 18,941.8 ± 729.5 cells; p=0.75) **(Figure 38B)** and a slight but non-significant decreased amount of C/D DCX$^+$ cells in WT versus GPR34 KO mice (2,219.6 ± 214.8 vs 2,693 ± 6.8; p=0.09) **(Figure 38C)**. Additionally, the quantification of E/F DCX$^+$ cells per hippocampus again showed no differences between WT and GPR34 KO mice (32,088.2 ± 2625.4 vs 33,305.9 ± 466.4; p=0.67) **(Figure 38D).** Furthermore, we found a similar distribution of the neuroblast types in WT and GPR34 KO mice **(Figure 38E)**. We also estimated the proliferation of neuroblasts (DCX$^+$BrdU$^+$ cells) and found similar percentages in WT and GPR34 KO mice (5.3 ± 0.9 % vs 4.5 ± 0.6 %; p=0.49) **(Figures 37A-B and 38F)**. Similarly, the total number of DCX$^+$BrdU$^+$ cells per hippocampus was not significantly different differences between WT and GPR34 KO mice (1,234.4 ± 126.7 vs 1,071.18 ± 131.1; p=0.42) **(Figure 38G).**

These results lead us to conclude that impaired microglial phagocytosis through the absence of GPR34 did not have an effect on neuroblasts proliferation in 1 month-old mice.

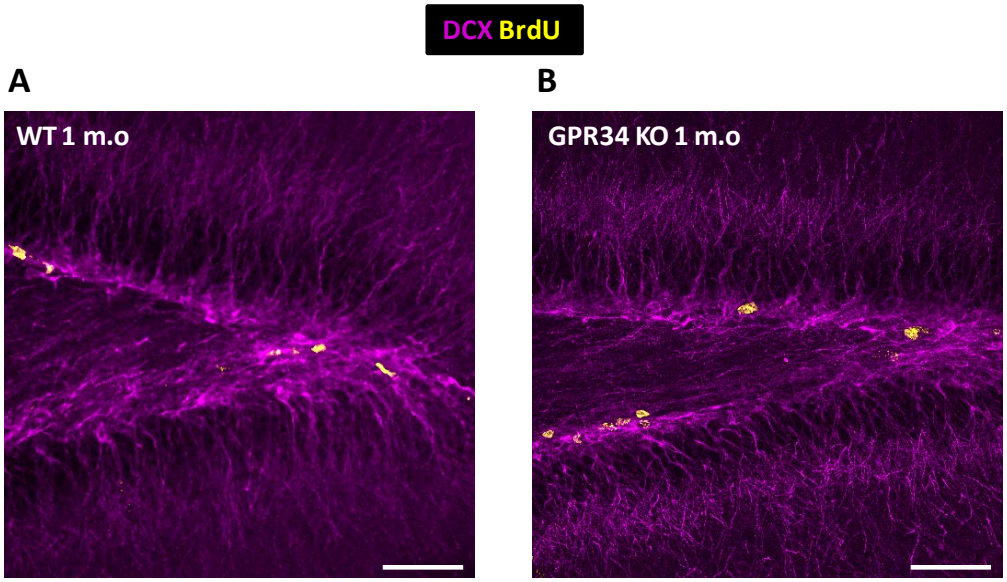

Figure 37. Effect of GPR34 on newborn cells in 1 month-old mice. *Representative confocal z-stacks of the dentate gyrus of 1 month-old WT mice* ***(A)*** *and GPR34 KO mice* ***(B)*** *(n=3, each). Neuroblasts were visualized with DCX (magenta) and BrdU was visualized in yellow. Scale bars: 50 µm. Z=23 µm (WT) Z=21 µm (KO).*

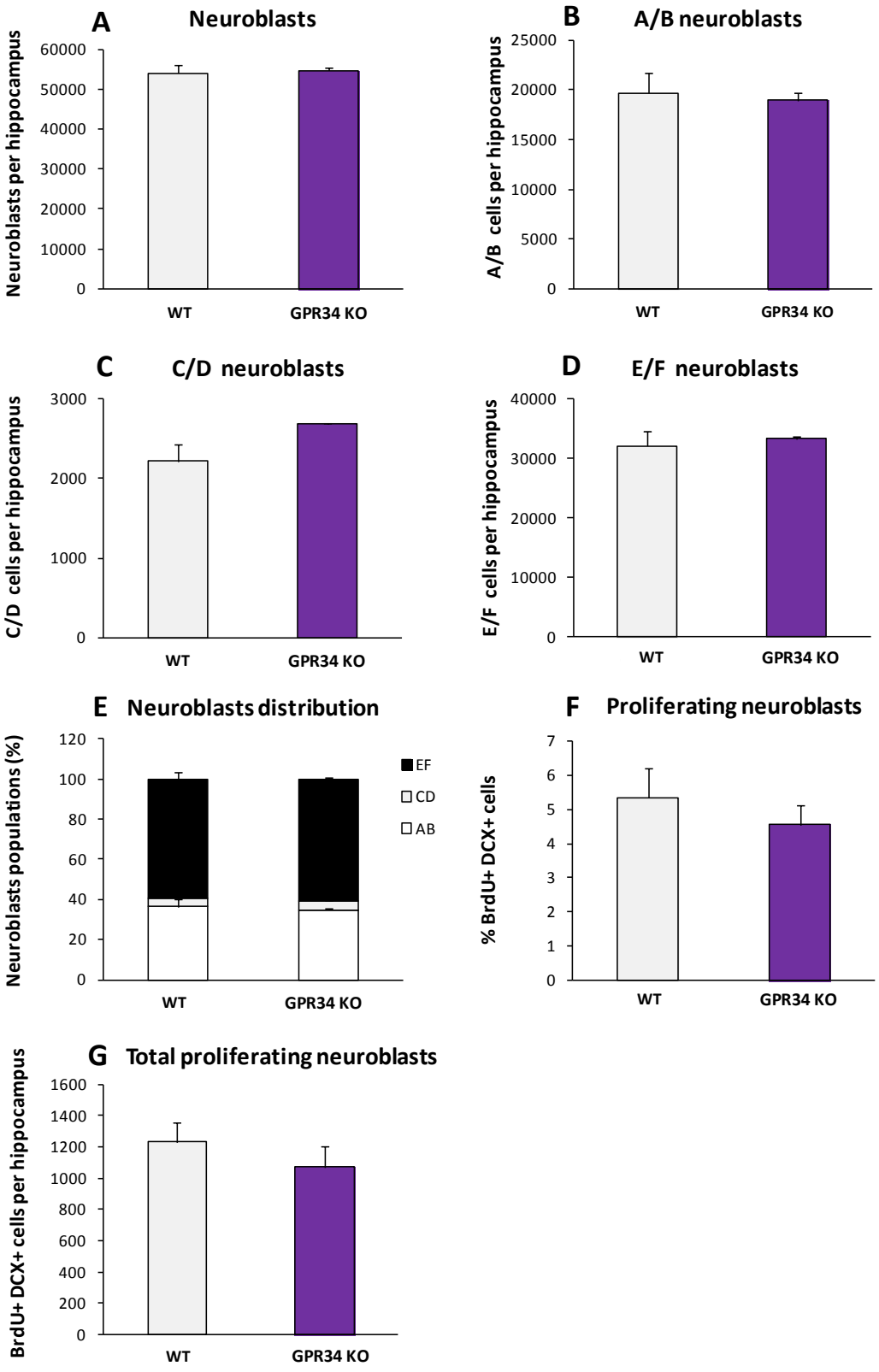

Figure 38. GPR34 deficiency does not alter newborn cells production in 1 month-old mice. A. *Total number of neuroblasts per septal hippocampus.* ***B.*** *Total number of A/B neuroblasts per septal hippocampus.* ***C.*** *Total number of C/D neuroblasts per septal hippocampus.* ***D.*** *Total number of E/F neuroblasts per septal hippocampus.* ***E.*** *Distribution of neuroblasts populations*

(in %). ***F.*** *Percentage of proliferative neuroblasts per septal hippocampus.* ***G.*** *Total number of proliferating neuroblasts per septal hippocampus. Bars represent mean ± SEM.* ***I.*** *No significant differences were observed by two-tailed Student's test.*

6.5.2. GPR34 deficiency decreases mature neuroblasts in 3 month-old mice

We extended our analysis of neurogenesis to older mice. For this purpose, we received from our collaborators another batch of 3 month-old GPR34 KO mice, although in this case they had not been injected with BrdU.

We first analyzed the NSCs population (nestin$^+$, GFAP$^+$ cells with radial morphology) **(Figure 39A-B).** Again, we observed no differences in the number of NSCs between WT and GPR34 KO mice (5,965.68 ± 145.9 vs 5,489.3 ± 370.9 cells per septal hippocampus, respectively; p=0.37) **(Figure 39C)**. Secondly, we analyzed neuroblasts (DCX$^+$ cells) **(Figure 40A-B)**, and observed an increased number in the total DCX$^+$ cells in WT compared to GPR34 KO mice (9,550.6 ± 527.2 vs 7,829.3 ± 491.4 cells per septal hippocampus; p=0.05) **(Figure 41A)**. No differences were observed in the number of A/B DCX$^+$ cells (3,318.2 ± 268.5 vs 3,148.6 ± 299.3 in WT and KO mice, respectively; p=0.71) **(Figure 41B)** or C/D DCX$^+$ cells (467.4 ± 216.1 vs 547.6 ± 58.4 in WT and KO mice, respectively; p=0.65) **(Figure 41C)**. However, there was a significant increased number of E/F DCX$^+$ cells in WT mice (5,720.9 ± 468.4) compared to GPR34 KO mice (4,097 ± 288.1; p=0.01) **(Figure 41D)**. As a consequence, we found a non-significant trend to increased percentage of E/F DCX$^+$ cells in the hippocampus in WT compared to GPR34 KO mice (59.7 ± 2.5 % vs 52.6 ± 2.6 %, respectively; p=0.1) **(Figure 41E)**. These evidences, together with the fact that 3 month-old GPR34 KO mice did not show any differences in microglial phagocytosis compared to WT mice, suggested that microglial phagocytosis was not presumably the underlying cause of fewer mature newborns neurons in 3 month-old adult mice.

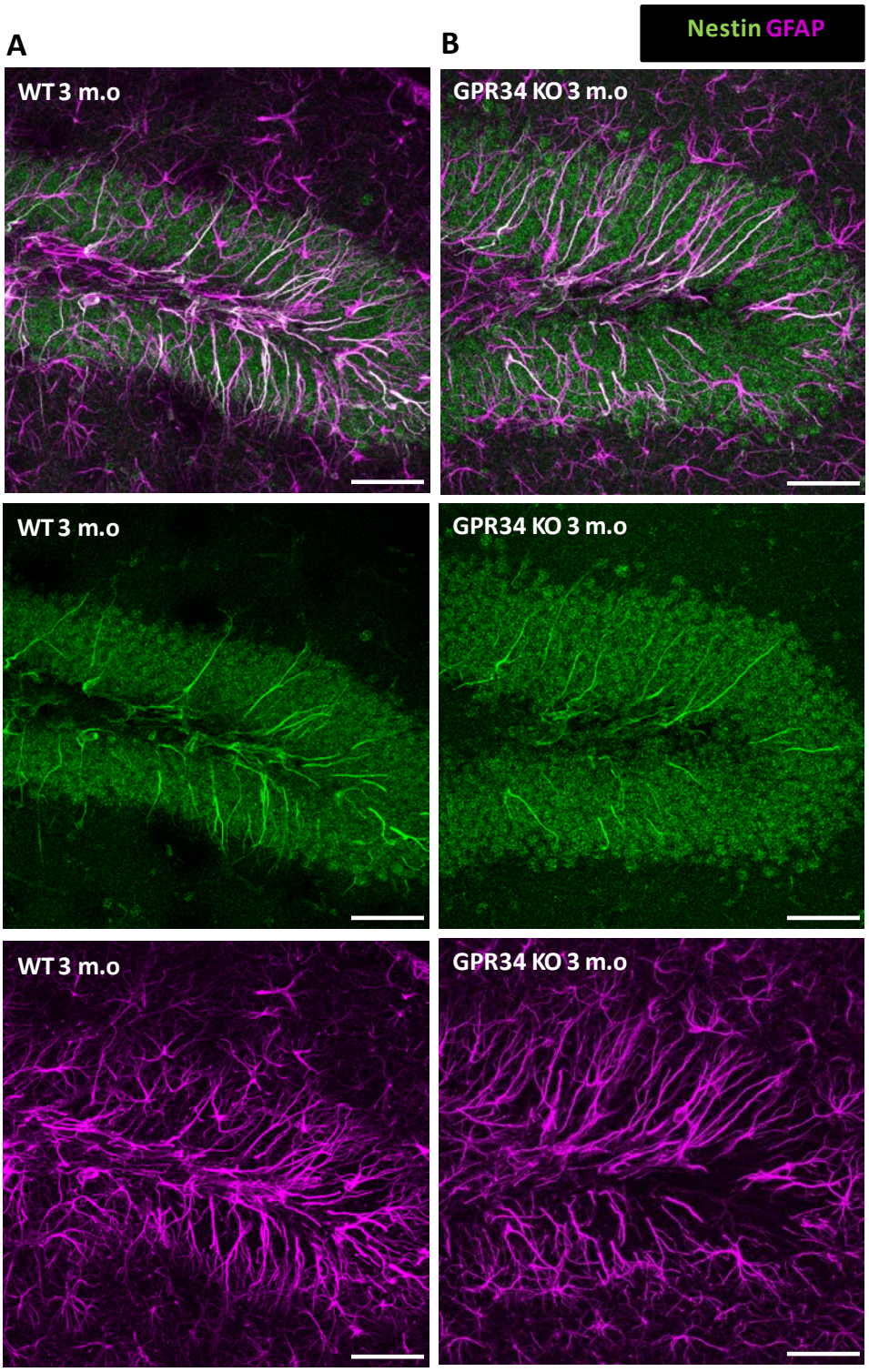
A
B
Nestin GFAP
WT 3 m.o
GPR34 KO 3 m.o
WT 3 m.o
GPR34 KO 3 m.o
WT 3 m.o
GPR34 KO 3 m.o

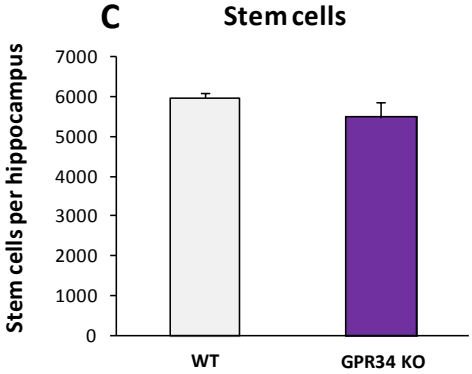
C
Stem cells
Stem cells per hippocampus
7000
6000
5000
4000
3000
2000
1000
0
WT
GPR34 KO

Figure 39. GPR34 deficiency remains stem cells population unaltered in 3 month-old mice. A. *Representative confocal z-stacks of the dentate gyrus of 3 month-old WT mice (n=4).* ***B.*** *Representative confocal z-stacsk of the dentate gyrus of 3 month-old GPR34 KO mice (n=7). Astrocytes were visualized with GFAP (magenta). Neural stem cells were positive for nestin (green) and GFAP (magenta). Scale bars: 50 µM, Z=19,5 µM (WT) Z=15,4 µM (KO).* ***C.*** *Total number of neural stem cells (Nestin^{+},GFAP^{+}) per septal hippocampus. Bars represent mean ± SEM. No significant differences were observed by two-tailed Student's test.*

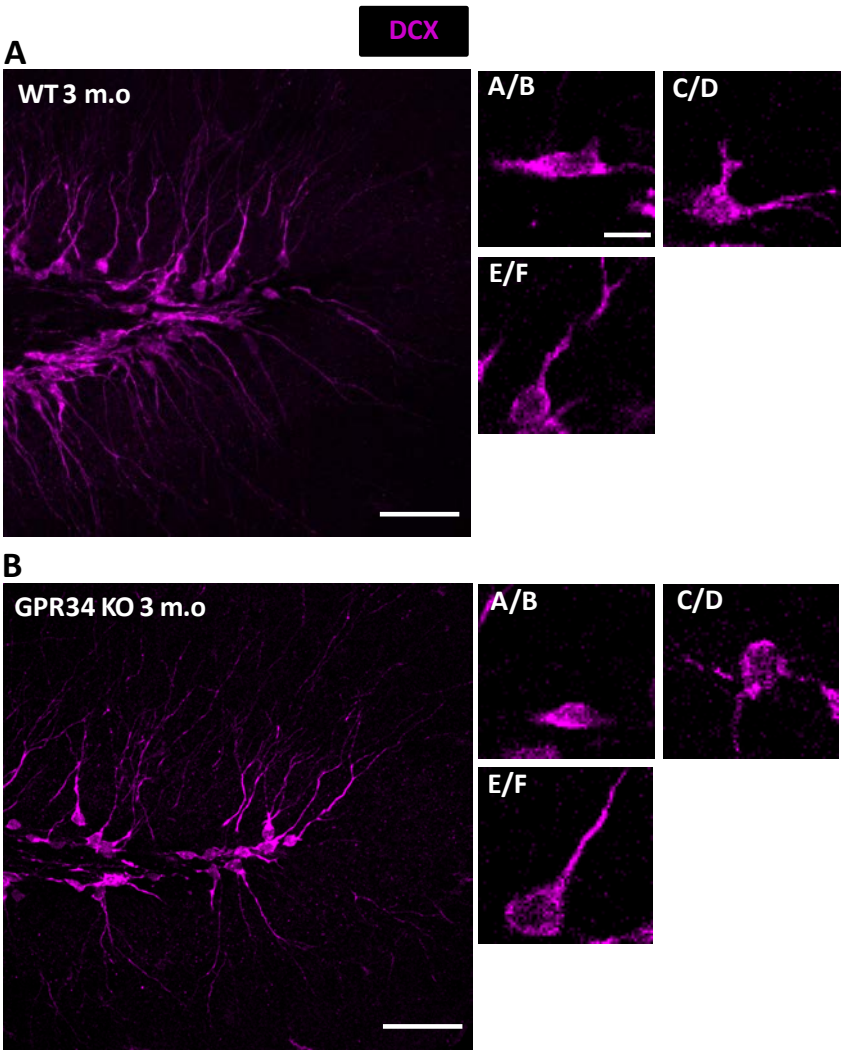

Figure 40. Effect of GPR34 deficiency on newborn neurons in 3 month-old mice. A, B. *Representative confocal z-stack of the dentate gyrus of 3 month-old WT mice (**A**, n=4) and GPR34 KO mice (**B**, n=7). Neuroblasts were visualized with DCX (magenta). Scale bars: 50 µM (10 µM in high magnification images). Detailed images from a single focal plane of A-B, C-D and E-F neuroblasts are shown. Z=18,2 µm (WT) Z=22,4 µm (KO).*

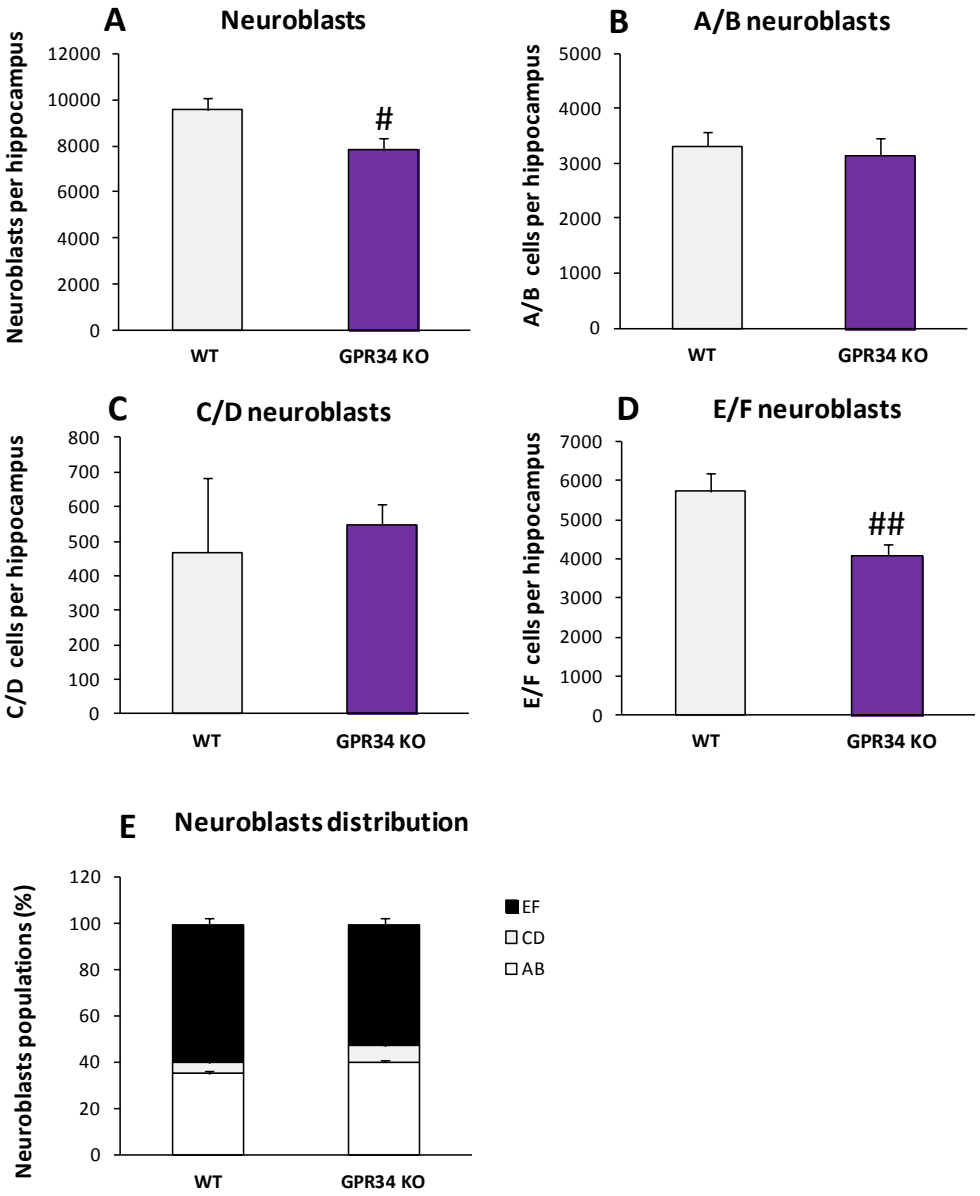

Figure 41. GPR34 deficiency decreases newborn neurons in 3 month-old mice. ***A.*** *Total number of neuroblasts per septal hippocampus.* ***B.*** *Total number of A-B neuroblasts per septal hippocampus.* ***C.*** *Total number of C-D neuroblasts per septal hippocampus.* ***D.*** *Total number of E-F neuroblasts per septal hippocampus.* ***E.*** *Distribution of neuroblasts populations (in %).* *Bars represent mean ± SEM. # indicates p=0.051 and ## indicates p=0.012 by two-tailed Student's test.*

7. DISCUSSION

7. DISCUSSION

Apoptosis or “programmed” cell death occurs during development and aging both in physiological and pathological conditions [142]. Dead cells need to be rapidly removed from the tissue to prevent the spillover of intracellular contents and to suppress the start of an inflammatory response [1]. The removal of cell debris is achieved through the recognition, engulfment and degradation of dead cells through a process called phagocytosis [104]. Together with inflammation, phagocytosis constitutes the first line of defense of the innate immune system [35]. In the mammalian CNS the innate immune response is performed by microglia, the resident macrophages.

In this PhD Thesis, we initially delved into the mechanisms regulating microglial phagocytosis efficiency. We first assessed the role of several inflammatory mediators in this process, such as TNF-α and CX3CL1. We found that they did not have a significant role in microglial phagocytosis regulation. We then focused on a novel postulated regulator of phagocytosis, the G-coupled receptor GPR34 and its ligand lysoPS. On one hand, our data revealed that GPR34 was an active participant in the regulation of phagocytic process in microglia since its absence produced a decrease in the phagocytosis of apoptotic cells in vivo. On the other hand, the addition of lysoPS to microglial cultures and organotypic cultures reduced the microglial phagocytic potential but this effect was not evidenced in vivo.

In the second part of this PhD Thesis, we studied downstream consequences of phagocytosis for microglia, focusing on metabolic adaptations; as well as on surrounding neurons, focusing on the adult neurogenic niche. Our results suggested that microglial phagocytosis triggered some metabolic adaptations in BV2 microglia, such as the downregulation of OXPHOS pathway accompanied by morphological changes in the mitochondria in vitro. Regarding neurogenesis, we observed that phagocytosis impairment due to GPR34 absence did not imply any changes in neurogenic cascade of young mice in vivo. Curiously, adult mice, which did not present impaired phagocytosis due to GPR34 absence, presented a decreased production of mature neurons in vivo. All these data seem to support that microglial phagocytosis constitutes a relevant process that not only contributes to brain homeostasis but also could influence other cellular processes such as metabolism, whereas further investigation is needed to demonstrate that microglial phagocytosis may influence neurogenesis. In the next sections all these observed results will be deeply discussed.

7.1. CROSSTALK INFLAMMATION-PHAGOCYTOSIS IN MICROGLIA

Inflammation is triggered as part of the innate immune system to protect the organism against any harmful stimulus, such as pathogens or excessive cell death [32]. Upon these stimuli, microglia respond by releasing several soluble factors, such as proteins of the complement cascade as well as chemokines or cytokines [12]. Chemokines help recruit microglia to the injury site [83], whereas cytokines, also released by astrocytes, endothelial cells and even neurons [47, 48] are in charge of executing the inflammatory response, which implies swelling, redness, heat, pain and fever in the affected tissue to initiate its repair [46].

Together with inflammation, phagocytosis constitutes the other fundamental component of the innate immune response [35], by rapidly removing invading microorganisms and cell debris, thus preventing the spillover of intracellular contents in response to infection or damage [1]. Thus, we analyzed the possible role in phagocytosis of two well-known inflammatory mediators: TNF-α and CX3CL1 (through its receptor CX3CR1).

7.1.1. TNF-α does not modulate neither apoptosis nor phagocytosis in vivo

TNF-α is one of the major pro-inflammatory cytokines (along with IL-6 and IL-β), mainly released by microglia [61] during the initiation of the inflammatory response [78]. TNF-α has been shown to be neurotoxic in vivo after focal cerebral ischemia [73, 74] and in vitro, where the addition of TNF-α to neuron-glial co-cultures induce neuronal loss [75]. Nevertheless, TNF-α has been also postulated as neuroprotective in excitotoxicity in vitro [68, 69]. TNF-α has been proposed to exert this neuroprotective effect through its interaction with TNFR2 [71] whereas its interaction with TNFR1 has been related with neurotoxicity [76].

Thus, we tested the role of microglial TNF-α on neuronal apoptosis and microglial phagocytosis in a mouse model of MTLE induced by intrahippocampal administration of KA. In this model, seizures and neuronal death are accompanied by tissue inflammation as well as microglial overpression of mRNA of several pro-inflammatory cytokines, including TNF-α [37]. We hypothesized that in addition to the excitotoxicity induced by seizures, TNF-α secreted by microglia could contribute to neuronal apoptosis. However, our experiments revealed that apoptosis was unchanged in microglial TNF-α-deficient mice compared to WT mice, suggesting that microglia TNF-α secretion was not linked to neuronal death in the experimental model tested. These results are in disagreement with the neurotoxic effect produced by this cytokine and postulated by [73, 74]. Moreover, our results did not allow us to observe either a neuroprotective role of microglial TNF-α, as reported by [70, 396, 397]. In any case, it is

important to remark that experimental models are different from that we have used. As shown by [70], microglial secretion of TNF-α protects neurons in a model of cerebral ischemia in mice. This neuroprotective role of TNF-α is in line with some in vitro studies performed by [68, 398]. Curiously, it has been shown that microglial TNF-α release and thus neuroprotection depends on previous stimulation of ATP-activated purine receptor P2X7 [399-401]. Our data suggested that microglial influence on neuronal survival does not depend on TNF-α secretion during excitotoxicity in the KA-induced epilepsy model. In brief, we can conclude that TNF-α secreted by microglia does not exert a neuroprotective response in KA-induced epilepsy.

As for microglial TNF-α impact on phagocytosis, we checked phagocytic capabilities of microglia by measuring the Ph index in TNF-α-deficient mice. Our results showed that microglial phagocytosis was unaltered in TNF-α-deficient mice, since the percentage of apoptotic cells engulfed by microglia was similar compared to WT mice. Therefore, our data suggested that TNF-α secreted by microglia does not either regulate microglial phagocytosis of apoptotic neurons. Contrary to this, [75] show that TNF-α addition to neuron-glial cultures produces neuronal loss via microglial activation and phagocytosis of viable neurons, causing neuronal death by phagoptosis. Phagoptosis has been shown to be produced by inflammation, triggering transient expression of PS in live neurons outer cell membrane, being recognized and engulfed by microglia [126].Therefore, neuronal loss is triggered by microglia and not by TNF-α, in line with our in vivo previous data referred to apoptosis, which show that neuronal health does not depend on TNF-α secreted by microglia. Despite its involvement in the microglial inflammatory response [78], neuronal death [73, 74] or survival [68, 70], microglial TNF-α does not act either as an autocrine mechanism to regulate the apoptotic cells phagocytosis in vivo.

7.1.2. CX3CL1 does not regulate phagocytosis of apoptotic cells in vivo

One of the most established “find-me” signals produced by apoptotic cells to enable the recruitment of microglia is the chemokine CX3CL1, cleaved from the apoptotic cell’s membrane [101, 144] by the enzyme ADAM17. According to this, some authors suggest that CX3CL1 released by apoptotic cells serves as a chemoattractant for microglia [102].

To directly test the role of CX3CL1 and its receptor CX3CR1 on phagocytosis in vivo, we analyzed microglial phagocytosis in 1 month-old CX3CR1-deficient mice. Our results showed that microglia were able to phagocytose up to 80 % of dead cells in CX3CR1-deficient mice. This percentage was similar to what our group have previously reported in WT mice in physiological conditions, where microglia have been shown to phagocytose up to 90 % of dead

cells [28]. Therefore, non-significant differences were observed in microglial phagocytosis in the absence of CX3CR1. These results were in apparent disagreement with [102], who showed that extracellular soluble components harvested from (ethanol-induced) apoptotic mice brains induce microglial migration towards apoptotic cells in a CX3CL1-dependent manner.

Several experimental differences may explain the discrepancy, such as the age of the animals, the region studied or the induction of apoptosis. While we studied physiological apoptosis in the DG of the hippocampus of 1 month-old mice, [102] studied ethanol-induced apoptosis in the cortex of PND7 mice. In addition, they focused on apoptotic cell-induced chemotaxis of microglial processes while we directly analyzed engulfment of apoptotic cells.

We directly quantified phagocytosis of apoptotic cells by determining the percentage of apoptotic cells engulfed in phagocytic pouches by microglia (Ph index), as defined by [28], and found no significant differences between WT and KO mice. In contrast, [102] analyzed chemotaxis by quantifying the apoptotic cells in contact (engulfed or not) with microglia, showing that microglial processes failed to associate with dead corpses in CX3CR1-deficient microglia. Besides, they determined that the percentage of microglia containing engulfed apoptotic cells was similar in WT and CX3CR1-deficient cells, reporting no significant differences in phagocytosis [102]. Thus, under ethanol-induced injury, CX3CL1 signals to microglia in a CX3CR1-dependent manner, evidencing a defect in the attraction of microglial processes to apoptotic cells (chemotaxis) but not in their phagocytosis. Summing up, despite its validated role as a chemotactic factor for microglia towards apoptotic cells during ethanol treatment, we conclude that CX3CL1 (through its receptor CX3CR1) does not act as a regulator of phagocytosis of apoptotic cells in vivo in physiological conditions in the adult hippocampus.

Despite the fact that both inflammation and phagocytosis constitute fundamental processes of the innate immune response, the data shown above highlight that neither TNF-α nor CX3CL1 inflammatory mediators exert a role in phagocytosis regulation. Therefore, in this PhD Thesis we have not found any evidences pointing towards a role of inflammation in regulating phagocytosis. Nevertheless, some studies have shown that inflammation and phagocytosis can regulate each other. Some in vitro studies have remarked that inflammatory stimuli induce multinucleated cultured microglia (primary rat microglia and BV2 microglia), increasing their capacity to phagocytose beads and PC12 cells [36], evidencing that inflammation can regulate phagocytosis. Furthermore, it has been also demonstrated that phagocytosis regulates inflammation. This is shown by [38], who state that defects in the clearance of apoptotic cells by macrophages are linked to the initiation of an inflammatory response. Besides, other

authors have stated that the clearance of apoptotic cells by macrophages inhibits the initiation of inflammatory or immune responses, in part through the release of anti-inflammatory cytokines [42, 402]. Other in vitro studies have shown that the anti-inflammatory role of phagocytosis in microglia involves the release of anti-inflammatory cytokines, such as TGF-β and trophic factors such as NGF [43, 44]. Consequently, an impairment in phagocytosis may be linked with an inflammatory response, as has been shown in a model of epilepsy [37] and in brain tumours [403]. Therefore, we can conclude that a direct dialogue and balance between inflammatory and phagocytic responses result essential to guarantee the accurate immune function of microglia and macrophages in order to preserve tissue homeostasis by preventing damage to the organism.

7.2. GPR34 AND LYSOPS ON MICROGLIAL PHAGOCYTOSIS

The correct engulfment of apoptotic cells by microglia is mediated by several receptors located in the microglial surface, which detect and bind to the "eat-me" signals produced by apoptotic cells [139]. Some of these engulfment receptors are TIM-4 [166], MERTK [168] and also TREM2 or VNR, which exert their role through their interaction with DAP12 [173] and MFG-E8 [170], respectively. Among this plethora of receptors, we focused on GPR34, which has been involved in chemotactic migration through lysoPS [404], its known ligand [176], a molecule derived from the classical "eat-me" signal PS.

7.2.1. GPR34 is the sole lysoPS receptor expressed in adult mouse microglia in vivo

GPR34 is highly expressed in immune cells such as mast cells, macrophages or immune system-derived cell lines [181]. However, GPR34 is preferentially expressed in (both human and mouse) microglial cells [177, 182, 405, 406] compared to astrocytes, oligodendrocytes and neurons [177, 178]. To confirm these evidences, we purified microglia from mice hippocampal tissue and found that GPR34 mRNA was highly expressed in microglia compared to non-microglial cells. On top of that, we found that GPR34 was the unique lysoPS receptor transcript expressed in this cell type, as other lysoPS-associated receptors (such as G2A, P2Y10 and GPR174) were undetectable in acutely purified microglia. Similarly, GPR34 mRNA, but not other lysoPS-associated receptors, was highly expressed in primary microglia cultures. These results were in agreement with previous analyses, in which GPR34 mRNA is highly expressed in cultured microglia compared to these three other receptors with affinity for lysoPS [193]. Thus,

we can state GPR34 is the unique lysoPS-receptor expressed in microglia in vivo, whereas it is predominant (but not exclusive) in vitro.

As previously mentioned, in addition to GPR34, other lysoPS receptors are G2A [188, 190], P2Y10 and GPR174 [189]. We found that transcripts for these receptors were not detectable in acutely isolated microglia and only G2A mRNA was (barely) expressed in primary cultures. In contrast, the microglial cell line BV2 expressed low levels of GPR34 and higher levels of G2A. Regarding P2Y10 and GPR174, they were both absent in microglia (in vivo and in vitro), in line with previous publications showing that both receptors (P2Y10 and GPR174) are restricted to the spleen and thymus [192, 388]. Since in vivo microglia are enriched in GPR34 whereas BV2 cells are enriched in G2A, our data suggested that in vivo microglia are a good model to study the effect of lysoPS on phagocytosis, since every possible phagocytic response involving lysoPS would be linked to its interaction with (our receptor of interest) GPR34. Furthermore, BV2 cells may constitute a better model to study the impact of G2A-lysoPS interaction on phagocytic response.

7.2.2. GPR34 contributes to apoptotic cells clearance in young but not in adult mice

To study the role of GPR34 on microglial phagocytosis we used a constitutive KO model [181]. We observed decreased microglial phagocytosis in 1 month-old GPR34 KO mice, demonstrated through a decreased microglial Ph index and Ph capacity. Additionally, the phagocytic impairment was accompanied by an uncoupling between phagocytosis and apoptosis. These results were in agreement with in vitro phagocytosis assays performed in isolated retina and cortical slices from adult GPR34-deficient mice [182]. Microglial cells of GPR34-deficient mice showed fewer zymosan particles and/or latex microbeads phagocytosed than microglia from control mice [182]. Curiously, recent reports establish that GPR34-deficient mice are also characterized by presenting alterations in immune functions. For instance, pulmonary infection with the yeast-like fungus *Cryptococcus neoformans* triggers an increased number of colonies in the brain (lungs and spleen as well) compared to WT mice at 60 days post-infection [181]. This is possibly related to an imbalance between T helper (Th)1 and Th2 cytokines, both involved in the response against this pathogen [407]. It has been also speculated that the increased brain pathogen burden may be related to altered microglial phagocytosis via GPR34, which may impede the clearance of pathogens [182].

We also analyzed older 3 month-old GPR34-deficient mice, finding that the microglial phagocytic impairment observed in 1 month-old mice was not maintained and suggesting that the control of phagocytosis by GPR34 was not produced throughout adulthood. This

suggestion is in line with recent reports that state that GPR34 expression is reduced in aged human brains [408]. Considering our data, although mice are not aged at 3 months, we can speculate that GPR34 expression and thus its effect on microglial phagocytosis may be gradually reduced with increased age. The reduction of GPR34 expression may prevent its contribution to microglial phagocytosis. In brief, our data suggested that GPR34 is a regulator of microglial phagocytosis of apoptotic cells in vivo in the young hippocampus.

Several mechanisms could explain the deficiency in microglial phagocytosis registered in 1 month-old GPR34 KO mice. For instance, we observed that GPR34-deficient microglia showed morphological changes, as they occupied a smaller territory in the DG of the hippocampus. Microglial processes retraction has been previously linked to phagocytosis impairment during seizures [37]. Thus, the "shrinkage" of microglia we observed in GPR34-deficient mice may explain the phagocytic impairment produced. In line with this hypothesis, microglia from GPR34-deficient mice have larger somata, fewer branches and occupy a smaller area [182]. Thereby, we speculate that microglial processes retraction may be related to a decreased motility, thus influencing the phagocytic response.

Another mechanism that may explain the altered phagocytosis in 1 month-old GPR34-deficient mice is their altered expression of several genes related to phagocytosis [182]. For instance, receptor for activated C kinase 1 (*rack1*) is upregulated, whereas dedicator of cytokinesis 4 (*dock4*) is downregulated [182]. *rack1* gene encodes for an anchoring protein which enables the translocation of protein kinase C (PKC) from the cytosol to the membrane [409]. PKC activity is crucial for phagocytosis since its two isozymes (α and β) have been shown to interact with F-actin cytoskeleton [410], implied in the engulfment of particles in several cell types. PKCα has been associated with phagosomal membranes, suggesting a role in phagocytosis [411], whereas PKCβ, along with isozyme α, has been implied in phagocytosis of latex beads by THP1 cells [412]. *rack1* results fundamental for phagocytosis because in human monocytes infected with Epstein-Barr virus (EBV), the immediate-early protein ZEBRA of EBV is able to interact with *rack1*, disrupting the translocation of PKC isozymes α and β to the monocytes membrane, thus affecting phagocytosis [413]. On the other hand, *dock4* modulates dynamics of actin cytoskeleton activity [414], since it encodes for a protein that regulates Rac1 GTPase activity, which involves the reorganization of the phagocyte cytoskeleton leading to the formation of the phagocytic pouch in charge of engulfing corpses, visualized in human kidney epithelial 293T cells and LR73 CHO cell line [158, 159]. Therefore, the phagocytosis impairment observed in vitro [182] and (in young mice) in vivo (this PhD Thesis) is possibly related to the reduced expression of key cytoskeletal proteins, such as dock4.

7.2.3. LysoPS inhibits microglial phagocytosis in cultures

Once corroborated the role of microglial receptor GPR34 on phagocytosis, we tested the involvement of its ligand: LysoPS. GPR34, as a member of P2Y12-like receptors group [415], is associated to lipids and nucleotides as its possible physiological ligands [416, 417]. Specifically, lysoPS has been identified as the endogenous ligand for GPR34 [176]. This finding is supported by [418], but other authors initially argued against the conclusion that lysoPS constitutes a ligand for GPR34 [181]. However, this controversy can be explained by differences in the lipid moiety used: subsequent studies observed that GPR34 is more attracted to 2-acyl-lysoPS, produced by PS-PLA1, than to 1-acyl-lysoPS, produced by PS-PLA2 [183]. Thus, GPR34 has been defined to have high and predominant affinity for lysoPS with a fatty acid at the sn-2 position in its glycerol backbone [175]. Despite its great affinity for GPR34, lysoPS can bind at least to other three receptors: G2A, P2Y10 and GPR174.

We directly tested the role of lysoPS in phagocytosis of apoptotic cells using primary microglia and BV2 cells cultures, finding an impairment. We observed a phagocytic impairment in primary microglia ($GPR34^{high}$) that was slightly higher than in BV2 cells ($G2A^{high}$), suggesting a stronger role of GRP34 than G2A in lysoPS-induced regulation of microglial phagocytosis. No roles were attributed to P2Y10 and GPR174 in this regulation since, based on our previous results, they were both absent in microglia. We then validated these results in more complex models, such as hippocampal organotypic cultures. We found fewer apoptotic cells phagocytosed by microglia (decreased Ph index) and an increase of non-phagocytic microglia (decreased Ph capacity). These results suggested that lysoPS addition involved an uncoupling between apoptosis and phagocytosis in primary cultures and organotypic cultures, similar to the effect of genetic depletion of GPR34 in vivo. This role is opposed to what was postulated by [188, 190], who stated that lysoPS enhances the phagocytosis of dying neutrophils by macrophages. This apparent disagreement could result from differences arising on lysoPS production, its mode of presentation, or its concentration, as we will now discuss.

The mechanism of lysoPS production has not been well studied in cells other than platelets and neutrophils [188], where it appears to be generated via NADPH oxidase and phospholipase-mediated mechanisms, respectively [191, 419]. Given the ubiquitous presence of oxidases and phospholipases, together with the fact that SHSY5Y cells have been shown to express NADPH oxidase mRNA [420], it is likely that lysoPS may be generated and exposed in the membrane of our apoptotic SHSY5Y neurons via some of these enzymatic pathways. The added lysoPS may compete for microglial GPR34 with the lysoPS produced by the apoptotic

cells used in our experiments, triggering an impairing effect on microglial phagocytosis, contrary to the enhancer role of lysoPS observed in macrophages [188].

Another reason that may explain the discrepancy with postulated effect of lysoPS on phagocytosis by [188] relies on the mode of presentation of lysoPS. When bound to a cell membrane or to a liposome, lysoPS acts as an enhancer of phagocytosis [188]. However, when lysoPS was added to the culture media in our experiments, it impaired phagocytosis. Similarly, lysoPS bound to albumin protein or solved in methanol, was not able to enhance phagocytosis [190]. Thereby, the mode of presentation of lysoPS to microglia seems crucial for the phagocytic response to apoptotic cells.

Finally, the efficient concentration of lysoPS reached in the cultures and in vivo may have an impact on phagocytosis. While we have reported that microglial phagocytosis was impaired in primary cultures at 3 μM lysoPS, many microglial processes follow U-shaped curves and it is possible that higher or lower concentrations may enhance phagocytosis. For instance, 10 μM lysoPS induces a ramified morphology in cultured microglia, with long processes whose tips are cone-like shaped [193], very similar to in vivo surveillant microglia [9]. We speculate that a ramified morphology may be related to the motility of the processes, which in turn is necessary for microglia to extend their processes towards the apoptotic cells and engulf them. Therefore, increasing lysoPS concentration may increase microglial motility and thus phagocytic response.

Furthermore, hippocampal organotypic cultures are more complex models, as they maintain the connectivity between neurons as well as the endogenous populations of microglia and astrocytes. Initial approaches with lysoPS (3 μM) did not impact on phagocytosis at all, contrary to the phagocytosis impairment seen in microglia cultures. However, increasing lysoPS (10 μM) led to a blockade of microglial phagocytosis, although increasing lysoPS dose did not change microglial morphology compared to initial lysoPS (3 μM) treatment tested. Thus, we speculate that the more complex in vitro model is a higher lysoPS concentration may be needed to influence microglial phagocytosis.

7.2.4. Microglia do not respond to lysoPS in vivo

Lastly, we directly tested the role of lysoPS injection into the hippocampus. Initial approaches with 10 μM lysoPS did not show any effect on microglial phagocytosis in vivo, contrary to what was observed in organotypic cultures. We resorted to a higher lysoPS concentration (36 μM, 1:100 from lysoPS stock), observing non-significant alterations neither in the Ph index nor in

the Ph capacity of microglial cells. This result was in disagreement with our results in vitro, in which lysoPS addition was shown to alter microglial phagocytosis. Some issues need to be considered in order to explain this lack of microglial response to lysoPS in vivo.

On one hand, we propose that intrinsic properties of lysoPS could be the underlying cause of this unaltered microglial phagocytic behavior. All phospholipids have a head and a tail group [421]. The head group, attracted by water, may facilitate lysoPS diffusion over the extracellular space in brain tissue, which is an advantage for its diffusion over the hippocampal region. However, an effective diffusion of drug could reduce its local effect on microglia.

On the other hand, metabolic processes involving phospholipids could explain the lack of response of lysoPS in vivo. For instance, it is known that lysoPS incorporates into the membrane of living cells [422] and then flip to the inner monolayer turning into PS via acyltransferases in a process called Lands cycle [423, 424]. In vitro data show that exogenously applied lysoPS triggers this phenomenon in primary microglia [193]. Given that in our primary microglia (and organotypic cultures) lysoPS addition produced an impairing effect on microglial phagocytosis, it is not likely that Lands cycle was produced. Nevertheless, we can speculate that exogenously applied lysoPS in the mice hippocampus could trigger this phenomenon in microglia and other living cells membrane, avoiding any possible effect on microglial phagocytosis.

Furthermore, it is likely that technical issues may explain the unaltered microglial response to lysoPS, so it would be advisable to test different drug concentrations and treatment times in order to faithfully assess whether lysoPS manages to regulate microglial phagocytosis in vivo. Summing up, we can conclude that lysoPS exerts a modulating role in microglial phagocytosis in vitro. Furthermore, more investigation is needed to completely discard lysoPS as a candidate to modulate microglial phagocytosis in vivo.

7.3. MICROGLIAL METABOLIC REWIREMENT UPON PHAGOCYTOSIS

Another goal of this PhD Thesis was to test whether phagocytosis could entail some metabolic changes or adaptations in microglia. All phagocytes, including microglia, possess downstream mechanisms which permit the degradation of cell debris or pathogens [425]. In macrophages, it is known that a metabolic shift from OXPHOS to aerobic glycolysis is produced upon phagocytosis of microbial targets [212]. Nevertheless, very little is known about metabolic processes triggered by microglial phagocytosis.

7.3.1. Phagocytosis does not trigger a metabolic switch to glycolysis in BV2 microglia

Cytosolic glycolysis constitutes one of the two main metabolic pathways responsible for ATP production in eukaryotic cells, together with mitochondrial OXPHOS. Our results showed that phagocytosis was not accompanied by changes in the glycolytic pathway in BV2 microglia. In contrast, upon engulfment of microbes, macrophages undergo a metabolic reprogramming ("trained immunity") [212]. The basis of this training in macrophages has been recently proposed as a shift from OXPHOS to aerobic glycolisis, supported by epigenetic modifications in key genes of the glycolysis pathway controlled by the master glycolysis transcription factor HIF-1α [212, 426]. Nevertheless, it is important to remark that "trained immunity" performed by macrophages was seen at 7 days post-phagocytosis whereas our experiments were evaluated at 24h upon phagocytosis. Thus, we speculate that more prolonged time after phagocytosis might make possible to observe an upregulation of glycolysis in BV2 phagocytic microglia. Our data, which showed no shift from OXPHOS to glycolysis upon BV2 microglia phagocytosis, were also contrary to stated by some other authors [427]. They state that after engulfment of dead cells by phagocytosis, several genes are upregulated promoting glycolysis in insulin-responsive CHO-derived cell line LR73 phagocytes [142]. After corpse uptake, several genes of the solute carrier family are activated, promoting glucose uptake and lactate release whereas a concurrent suppression of the OXPHOS pathway is produced [427].

The origin of the discrepancy between [427] and our experiments may rely on several aspects that need to be considered. First of all, the metabolic analysis of glycolysis by [427] was performed with a less reliable method than the one used in this PhD Thesis. Their method includes the measurement of the ECAR generated by glycolysis and also by mitochondrial OXPHOS, but did not take into account that the mitochondrial Krebs Cycle produces CO_2, which acidifies the extracellular medium and contributes to ECAR. In contrast, our method removes mitochondrial contribution to the ECAR, by blocking mitochondrial activity with specific blockers of complexes I and III of the mitochondrial respiratory chain. As a result, we obtained a more reliable measurement of glycolytic activity of phagocytes upon the engulfment of cargo.

In addition, it is important to remark that [427] state that the activation of glycolysis occurs early on, in the first hour after engulfment, and glycolysis pathway activity is analyzed only for 2h upon phagocytosis. Considering that our analysis of glycolytic pathway is performed at 24h after engulfment and no changes are detected in glycolysis, we speculate that glycolysis upregulation via phagocytosis observed by [427] may be transient. In addition to this,

experiments performed by [427] use the LR73 CHO cell line [428] as phagocyte model whereas we employed a microglial cell line (BV2). It is likely that BV2 microglia respond in a different (and possibly better) way to a phagocytic challenge due its similarities to microglial cells (considered as professional phagocytes) than CHO cells could do. These originate from ovaries and thus are not specialized in phagocytosis, although its rapid growth in suspension has extended their use in vitro. Thus, it is likely that the effect of cell type used as phagocyte model constitutes another source of discrepancy.

The choice of BV2 cell line as the microglial model for our biochemical studies was due to technical limitations with primary microglia. Immortalized microglia cell lines, such as BV2, are commonly used due to their highly proliferative nature, a typical feature of cancer cells. Cancer cells present an uncontrolled proliferation since they consume much larger quantities of glucose than normal cells and metabolize it principally through glycolysis [429, 430]. As shown in our results, highly proliferative BV2 cells present high basal glycolysis, so these cells could suppose a disadvantage for studying glycolytic pathway behavior upon phagocytosis compared to primary microglia, maybe explaining the unaltered glycolytic activity in BV2 microglia upon phagocytosis of apoptotic cells. However, several studies report that BV2 microglial glycolysis increases under different stimuli, such as LPS or NO. LPS increases lactate production in BV2 microglia and primary microglia [431], while decreases both oxygen and ATP production at the mitochondrial level [277, 278]. In this way, Volobоueva et al. suggest that a switch to glycolysis could maintain the ATP production in BV2 cells, since NO gives rise to OXPHOS inhibition [274, 275], in line with observed in dendritic cells [432]. On the other hand, Bernhart et al. reported that LPA, a phospholipid recognized as a relevant signaling molecule, is able to promote some changes in glycolysis in C13NJ cells, another microglial cell line [276]. Considering that upon LPS stimulation, glycolysis is increased in both BV2 and primary microglia, we speculate that both cell types could have a similar metabolic behavior upon apoptotic cells phagocytosis. Nonetheless, gene expression analyses of key enzymes in glycolysis in BV2 phagocytic microglia were not consistent with the upregulation of glycolytic genes in primary microglia upon 24 h of phagocytosis **(Data from Irune Díaz-Aparicio PhD Thesis, 2018)**. Thereby, we can conclude that microglia BV2 cell line and primary microglia regulate differently the glycolytic pathway and the phagocytosis.

In summary, our data suggest that microglia BV2 cells phagocytose apoptotic cells in a glycolysis independent-manner, contrary to observed in macrophages and other phagocytes, in which phagocytic activity on apoptotic cells is directly related to glycolysis [212, 427].

7.3.2. Phagocytosis disrupts mitochondrial metabolism in BV2 microglia

Phagocytosis has high metabolic demands that rely mostly on the mitochondria, which play an essential role in cellular metabolism [163]. We analyzed the mitochondrial function (focusing on OXPHOS) upon phagocytosis. Our results showed a downregulation of OXPHOS upon phagocytosis in BV2 microglia which was not related to changes in gene expression, except for *ndufaf4* (coding for a protein involved in the assembly of mitochondrial complex I). These data did not match with preliminary data of the laboratory using gene expression arrays comparing naïve and phagocytic cultures of primary microglia, which pointed towards a downregulation of key genes of mitochondrial metabolic pathways, including OXPHOS, in primary microglia upon 24h after phagocytosis **(Data from Irune Díaz-Aparicio PhD Thesis, 2018)**.

One explanation for the discrepancy is that arrays analyze all genes involved in OXPHOS (and other mitochondrial pathways) whereas our analyses (via RT-qPCR) were focused on a minimal group of genes involved in OXPHOS. On top of that, our analyses were performed in BV2 microglia [380], whose features are different from those of primary microglia, as explained above.

The reduced OXPHOS triggered by phagocytosis could be related to altered mitochondrial morphology. Our data reflected a decreased number and less ramified mitochondria upon phagocytosis in BV2 microglia. In the last few years, it has been proposed a link between mitochondrial metabolism and mitochondrial dynamics. It was shown that mitochondrial fusion and fission dynamics are intimately related to metabolic changes [433]. Thereby, we speculate that OXPHOS decrease upon phagocytosis is linked to mitochondrial morphology changes, which may be triggered by an unbalance between mitochondrial fusion and fission dynamics. In fact, Chen et al. have linked disruption in fusion to a decrease in OXPHO5 in fusion-defective mouse embryonic fibroblasts (MEFs) [392]. However, analyzing the expression of key fusion genes by RT-qPCR analyses, we have shown that those expression genes remained unaltered, independiently of OXPHOS. Furthermore, all key fission genes examined presented altered expression in BV2 phagocytic microglia. *Mff* and *dnm1l* were downregulated whereas *fis1* was upregultated upon phagocytosis. These findings are in agreement with the results reported by [254, 434], in which OXPHOS inhibition (via mitochondrial uncouplers, such as FCCP or CCCP) was linked to enhancement of fission. Therefore, OXPHOS reduction in BV2 microglia upon phagocytosis leads to changes in fission processes. Additionally, based on our data, we could also speculate that OXPHOS reduction in phagocytic BV2 microglia could decrease mitochondrial mitophagy, since it has been shown that increased OXPHOS is linked to

increased mitophagy [262]. In summary, OXPHOS decrease in phagocytic BV2 cells is accompanied by alterations in mitochondrial fission genes and could suggest alterations in mitophagy.

Overall, we can conclude that mitochondrial metabolic disruption, reflected by decreased OXPHOS, is accompanied by morphological changes in these organelles upon phagocytosis of apoptotic cells. However, the fact that this mitochondrial impairment is not compensated by an increase in glycolysis, lead us to speculate that other metabolic pathways, which have not been analyzed, such as β-oxidation of fatty acids or purine metabolism, could present some alterations. Related to purine metabolism, [278] show that increase in glucose uptake in BV2 microglia involves the rise in PPP pathway, so that we speculate that this pathway is not altered in our BV2 microglia experiments. Furthermore, these results could suggest that BV2 phagocytic microglia enter in a metabolic quiescence period in which their mitochondria suffer a blockade after the engulfment of dead cells. We speculate that a mitochondrial blockade could interfere with important microglial features, like their scanning capacity in the brain parenchyma [8, 9], since this surveillance state in microglia is likely to rely in OXPHOS [435]. As a summary, we can conclude that phagocytic response and thus maintaining of brain homeostasis is tightly associated with biochemical modifications produced within microglial cells in order to develop their functions properly.

7.4. MICROGLIA AND NEUROGENESIS

The SGZ of the hippocampus constitutes one of the major sites for the birth of new neurons from radial NSCs [299, 436]. Neurogenesis in the SGZ is produced throughout life, including senescence in mice [437], although its existence in humans is under strong discussion, since recent reports support that neurogenesis persists across lifespan [290, 291] but on the contrary, other publications claim that is limited to childhood [289] .

Microglial cells are regulators in the neurogenic niche of the SGZ. They phagocytose the excess of newborn cells undergoing apoptosis, maintaining the homeostasis of the baseline neurogenic cascade in the young adult SGZ [28]. However, the role of microglia in neurogenesis may not be limited to removal of dead cells. Other mechanisms allow microglia to regulate neurogenesis, such as the secretion of soluble factors. When treated with IL-4 or IFN-γ, cultured microglia promote neurogenesis via reduction of TNF-α and increased production of insulin growth factor 1 (IGF-1) [354], a well-known inducer of neurogenesis

[438]. Another growth factor such as brain-derived neurotrophic factor (BDNF) has been shown to be expressed by microglia, also promoting neurogenesis [439].

7.4.1. Phagocytosis does not regulate newborn cells production in the niche of the SGZ

Microglia have acquired relevance on neurogenesis since they determine inflammation rates in the cellular environment, which influences the survival of the newborn neurons in the adult hippocampus. Some authors have shown that inflammation via LPS administration inhibits neurogenesis in the adult rat hippocampus via microglial release of pro-inflammatory cytokines IL-6 and TNF-α [366]. Other authors also established that microglial activation, induced by an inflammatory stimulus, impairs neurogenesis in adult rats [364]. Nonetheless, other inflammatory cells such as astrocytes can also exert a role in neurogenesis regulation. For instance, chronic astrocytic release of IL-6 in transgenic mice reduces proliferation, survival and differentiation of newborn neurons, thus decreasing neurogenesis [347]. Thus, inflammation can regulate neurogenesis through the activation of glial cells.

In addition to inflammation, phagocytosis may also regulate neurogenesis. Some in vitro studies have linked microglial phagocytosis to the secretion of several factors by microglia, which may help regulating neurogenic process. For example, microglia have been shown to release higher levels of TGF-β and NGF after phagocytosis in vitro [43], which are negative and positive regulators of hippocampal neurogenesis, respectively [213, 368]. Furthermore, in vitro approaches in our laboratory have revealed that conditioned media from phagocytic microglia alters the proliferation and differentiation of cultured neural progenitors in vitro and in vivo **(Data from Irune Díaz-Aparicio PhD Thesis, 2018)**, evidencing the role of microglial phagocytosis secretome on neurogenesis.

To directly test the role of microglial phagocytosis on neurogenesis in vivo, we used the GPR34 KO mice as a genetic model of phagocytosis impairment [181]. The analyses were focused on analyzing the populations of neuroblasts (newborn cells) and radial NSCs (in charge of the newborn cells production in the neurogenic cascade) in young (1 month-old) and adult (3 months-old) mice in the neurogenic niche of the SGZ. We found that impaired phagocytosis observed in 1 month-old GPR34 KO mice did not imply any changes in neuroblasts population. This is contrary to results obtained in other in vivo 1 month-old mice models of phagocytosis impairment tested in our laboratory **(Data from Iñaki Paris PhD Thesis)**. On one hand, mice deficient in P2Y12, another phagocytic receptor highly expressed in microglia [177], showed decreased neuroblasts numbers. On the other hand, double KO mice for MertK and Axl receptors, both related to phagocytosis [168, 440], also registered decreased amount of

neuroblasts **(Data from Irune Díaz-Aparicio PhD Thesis, 2018)**. This discrepancy could be produced as a result of the different contribution of each receptor to phagocytosis process in young mice. Surprisingly, 3 month-old GPR34 KO mice, which did not show any phagocytosis impairment, registered a reduction in the E-F neuroblasts, the most mature newborn neurons in the neurogenic cascade. Importantly, 3 month-old mice registered a scarce number of apoptotic cells compared to young 1 month-old mice. This was expected considering that neurogenesis is dramatically reduced with age [295]. This point, in conjunction with the fact that the vast majority of apoptotic cells produced during neurogenesis in the SGZ are removed by microglia [28], triggers a minor apoptotic activity throughout adulthood. Consequently, microglial phagocytosis results observed in 3 month-old mice need to be cautiously interpreted. We speculate that fewer apoptotic cells may prevent us from observing a regulation of microglial phagocytosis via GPR34 in adult mice (as clearly shown in young mice), which may explain the decreased number of neuroblasts. Thus, further investigation is needed to rule out the role of GPR34 on microglial phagocytosis in adult mice.

Since microglial cells seem to regulate neuroblasts population via phagocytosis, they may also control the rNSCs population, in charge of the production of these newborn cells in the SGZ. Nonetheless, no changes were detected in rNSCs in our GPR34 KO mice model in the SGZ. Besides, young GPR34 KO mice did not show any changes in cell proliferation. Together with the fact that very few rNSCS were labeled with BrdU, we could suggest that microglial phagocytosis impairment observed in GPR34 KO mice is not linked to rNSCS behavior.

Altogether, these data do not suggest that there is a link between microglial phagocytosis and newborn cells production in the neurogenic niche of the SGZ. This is contrary to previous studies, in which toxin-induced microglial reduction in the DG of the SGZ is sufficient to disrupt hippocampal neurogenesis due to reduced survival of neuroblasts [441]. Remarkably, microglial reduction is reversed via induction of VEGF, a well-known angiogenic factor, which increases microglial population and also induces a strong neurogenic response exclusively in the DG [214, 442, 443]. However, VEGF-induced neurogenesis by DG microglia can be abolished by inhibiting tyrosine kinase Axl, which has been shown to play a role in adult hippocampal neurogenesis [444, 445]. The latter, in conjunction with the fact that DG microglia express Axl receptor [441] support the idea that DG microglia are able to influence neurogenesis and that Axl receptor, linked to phagocytosis, and maybe other phagocytosis-related receptors expressed in DG microglia, such as GPR34, could have a modulatory effect on neurogenesis through their role in the phagocytosis of apoptotic cells by microglia. However, our data do not allow us to assign this modulatory role in neurogenesis to GPR34. Therefore,

we conclude that we have no evidences pointing towards the role of microglia on neurogenesis regulation through phagocytosis of dead newborn neurons in the DG of the SGZ.

The regulation of neurogenesis by microglia via phagocytosis of apoptotic newborn cells may extend to other neurogenic niches. Together with the SGZ of the hippocampus, the SVZ of the lateral ventricles constitute the two only brain regions where neurogenesis is produced throughout adulthood [446]. Despite our data do not show that microglial phagocytosis is involved in neurogenesis regulation in the SGZ, the engulfment of dead cells exerted by these phagocytes might be a mechanism to modulate neurogenesis in the SVZ. It is known that microglial cells in the SVZ produce soluble factors which are essential for SVZ neurogenesis [351]. However, according to [357], the neurogenic role of microglia in the SVZ does not seem to be related to phagocytic activity, since microglia within the SVZ are largely nonphagocytic, although these microglial cells are essential for neuroblast survival and migration to the olfactory bulb (OB). Remarkably, other authors highlight the role of SVZ microglia in neurogenesis via inflammatory stimuli. Studies performed by [360] show that activated microglia (via LPS treatment) in the early postnatal SVZ increase neurogenesis (and oligodendrogenesis) via cytokines release. Moreover, other authors have shown that LPS-stimulated microglia are able to phagocytose live neural precursor cells (phagoptosis) in the primate SVZ during the development of cerebral cortex [27]. This is consistent with the concept that microglia are able to engulf live cells during inflammation [105] and suggests that both inflammation and phagocytosis processes could influence the role of microglial cells on neurogenesis. Curiously, periventricular microglia, another microglial population located within the ventricular zone (VZ), near the lateral ventricles, are also able to contact with neural precursor cells in primates [447], thus impacting on prenatal cortical neurogenesis [448], remarking that microglia manage to regulate neural precursor cells population, in line with [27]. In short, we can say that both inflammation and phagocytosis seem to exert a role in regulating neurogenesis by microglia in the SVZ (and also in the VZ) whereas our data cannot link microglial phagocytosis process to neurogenesis regulation in the SGZ.

Finally, in addition to the role here described of microglial cells on neurogenesis, other immune cells are also part in stem cell niches. For instance, macrophages and T cells are also key components of stem cell niches [449], which are located in diverse sites other than brain tissue, such as the bone marrow or the intestine, among others [450]. Specifically, these two cell types have emerged as important regulators of stem cells under physiological conditions [451, 452]. In the bone marrow, macrophages retain hematopoietic stem cells (HSCs) in the mesenchymal stem cell niche [453], whereas T cells, located close to HSCs, secrete IL-10 and

adenosine to control HSC quiescence and pool size [454]. In the intestine, macrophages express colony stimulating factor 1 receptor (CSF1R), promoting the differentiation of intestinal stem cells (ISCs), which is abolished when mice are treated with blocking antibodies against CSF1R [455]. Furthermore, depletion of T cells leads to a reduction in ISCs [456], remarking a crucial role of these cells in ISC pool size. As a conclusion, the role of immune cells in the stem cell niches regulation is shared by many cell types other than microglia, whose communication with stem cells may be fundamental in health and disease [450].

8. CONCLUSIONS

8. CONCLUSIONS

1. MICROGLIAL PHAGOCYTOSIS IS NOT REGULATED BY INFLAMMATORY MEDIATORS TNF-α AND CX3CL1 IN VIVO

-Granule neuron apoptosis and microglial phagocytosis in KA-induced epilepsy are not regulated by microglial TNF-α.

-Microglial phagocytosis in physiological conditions is not regulated by genetic deficiency of CX3CR1.

2. GPR34 IS A POTENTIAL REGULATOR OF MICROGLIAL PHAGOCYTOSIS IN VIVO

-GPR34 mRNA is highly expressed in microglia in vivo and in vitro whereas G2A, GPR174 and P2Y10 are not expressed.

-Microglial phagocytosis is uncoupled from apoptosis in 1 month-old mice lacking GPR34 because fewer apoptotic cells are phagocytosed and non-phagocytic microglia increase.

-GPR34-deficient microglia occupy fewer volume in the DG, which could be explained by the retraction of their processes, explaining the phagocytic impairment produced.

-Microglial phagocytic impairment caused by GPR34 deficiency in 1 month-old mice is not maintained at 3 months of age.

3. LYSOPS HAS A MODULATORY ROLE IN PHAGOCYTOSIS IN VITRO BUT NOT IN VIVO

-The addition of lysoPS to microglia cultures exerts a blocking effect on phagocytosis since it increases non-phagocytic microglia, contrary to its previously stated role as an enhancer of phagocytosis in macrophages.

-The addition of lysoPS to hippocampal slice cultures leads to an uncoupling between apoptosis and phagocytosis because fewer apoptotic cells are phagocytosed and non-phagocytic microglia increase, similar to the effect of genetic depletion of GPR34 in vivo.

-The injection of lysoPS into the hippocampus of mice does not affect microglial phagocytosis.

4. PHAGOCYTOSIS IS LINKED TO METABOLIC CHANGES IN BV2 MICROGLIA IN VITRO

-BV2 cells are highly glycolytic, and phagocytosis does not significantly increase glycolysis as shown by *hif-1α, pfkm* and *pfkfb3* gene expression.

-BV2 microglial phagocytosis of apoptotic cells involves the downregulation of mitochondrial OXPHOS as shown by *ndufaf4* gene expression.

-The downregulation of mitochondrial metabolism in phagocytic BV2 microglia is accompanied by morphological changes in mitochondrial network as well as alterations in genes involved in mitochondrial fission.

5. MICROGLIAL PHAGOCYTOSIS IS NOT LINKED TO NEUROGENESIS IN VIVO

-Microglial phagocytic impairment caused by GPR34 deficiency does not imply changes neither in newborn cells nor NSCs population in young mice.

-There is a decreased number of mature newborn cells in adult GPR34-deficient mice, although there are no evidences of microglial phagocytic impairment, thus a link between microglial phagocytosis and the neuronal production in the DG of the hippocampus cannot be confirmed.

9. BIBLIOGRAPHY

9. BIBLIOGRAPHY

1. Sierra, A., et al., *Janus-faced microglia: beneficial and detrimental consequences of microglial phagocytosis.* Front Cell Neurosci, 2013. **7**: p. 6.
2. Tremblay, M.E., et al., *From the Cajal alumni Achucarro and Rio-Hortega to the rediscovery of never-resting microglia.* Front Neuroanat, 2015. **9**: p. 45.
3. Gomez-Nicola, D. and V.H. Perry, *Microglial dynamics and role in the healthy and diseased brain: a paradigm of functional plasticity.* Neuroscientist, 2015. **21**(2): p. 169-84.
4. Ajami, B., et al., *Local self-renewal can sustain CNS microglia maintenance and function throughout adult life.* Nat Neurosci, 2007. **10**(12): p. 1538-43.
5. Ginhoux, F., et al., *Fate mapping analysis reveals that adult microglia derive from primitive macrophages.* Science, 2010. **330**(6005): p. 841-5.
6. Aguzzi, A., B.A. Barres, and M.L. Bennett, *Microglia: scapegoat, saboteur, or something else?* Science, 2013. **339**(6116): p. 156-61.
7. Ginhoux, F. and M. Prinz, *Origin of microglia: current concepts and past controversies.* Cold Spring Harb Perspect Biol, 2015. **7**(8): p. a020537.
8. Davalos, D., et al., *ATP mediates rapid microglial response to local brain injury in vivo.* Nat Neurosci, 2005. **8**(6): p. 752-8.
9. Nimmerjahn, A., F. Kirchhoff, and F. Helmchen, *Resting microglial cells are highly dynamic surveillants of brain parenchyma in vivo.* Science, 2005. **308**(5726): p. 1314-8.
10. Kettenmann, H., F. Kirchhoff, and A. Verkhratsky, *Microglia: new roles for the synaptic stripper.* Neuron, 2013. **77**(1): p. 10-8.
11. Ginhoux, F., et al., *Origin and differentiation of microglia.* Front Cell Neurosci, 2013. **7**: p. 45.
12. Nayak, D., T.L. Roth, and D.B. McGavern, *Microglia development and function.* Annu Rev Immunol, 2014. **32**: p. 367-402.
13. Katz, L.C. and C.J. Shatz, *Synaptic activity and the construction of cortical circuits.* Science, 1996. **274**(5290): p. 1133-8.
14. Hua, J.Y. and S.J. Smith, *Neural activity and the dynamics of central nervous system development.* Nat Neurosci, 2004. **7**(4): p. 327-32.
15. Huberman, A.D., M.B. Feller, and B. Chapman, *Mechanisms underlying development of visual maps and receptive fields.* Annu Rev Neurosci, 2008. **31**: p. 479-509.
16. Paolicelli, R.C., et al., *Synaptic pruning by microglia is necessary for normal brain development.* Science, 2011. **333**(6048): p. 1456-8.
17. Schafer, D.P., et al., *Microglia sculpt postnatal neural circuits in an activity and complement-dependent manner.* Neuron, 2012. **74**(4): p. 691-705.
18. Weinhard, L., et al., *Microglia remodel synapses by presynaptic trogocytosis and spine head filopodia induction.* Nat Commun, 2018. **9**(1): p. 1228.
19. Vilalta, A. and G.C. Brown, *Neurophagy, the phagocytosis of live neurons and synapses by glia, contributes to brain development and disease.* FEBS J, 2018. **285**(19): p. 3566-3575.
20. Park, S.K., D. Solomon, and T. Vartanian, *Growth factor control of CNS myelination.* Dev Neurosci, 2001. **23**(4-5): p. 327-37.
21. Kotter, M.R., et al., *Myelin impairs CNS remyelination by inhibiting oligodendrocyte precursor cell differentiation.* J Neurosci, 2006. **26**(1): p. 328-32.
22. Domingues, H.S., et al., *Oligodendrocyte, Astrocyte, and Microglia Crosstalk in Myelin Development, Damage, and Repair.* Front Cell Dev Biol, 2016. **4**: p. 71.

23. Pang, Y., Z. Cai, and P.G. Rhodes, *Effects of lipopolysaccharide on oligodendrocyte progenitor cells are mediated by astrocytes and microglia.* J Neurosci Res, 2000. **62**(4): p. 510-20.
24. Rezaie, P., et al., *Microglia in the cerebral wall of the human telencephalon at second trimester.* Cereb Cortex, 2005. **15**(7): p. 938-49.
25. Kubota, Y., et al., *M-CSF inhibition selectively targets pathological angiogenesis and lymphangiogenesis.* J Exp Med, 2009. **206**(5): p. 1089-102.
26. Zhao, X., et al., *Microglial interactions with the neurovascular system in physiology and pathology.* Dev Neurobiol, 2018. **78**(6): p. 604-617.
27. Cunningham, C.L., V. Martinez-Cerdeno, and S.C. Noctor, *Microglia regulate the number of neural precursor cells in the developing cerebral cortex.* J Neurosci, 2013. **33**(10): p. 4216-33.
28. Sierra, A., et al., *Microglia shape adult hippocampal neurogenesis through apoptosis-coupled phagocytosis.* Cell Stem Cell, 2010. **7**(4): p. 483-95.
29. Fourgeaud, L., et al., *TAM receptors regulate multiple features of microglial physiology.* Nature, 2016. **532**(7598): p. 240-244.
30. Sierra, A., M.E. Tremblay, and H. Wake, *Never-resting microglia: physiological roles in the healthy brain and pathological implications.* Front Cell Neurosci, 2014. **8**: p. 240.
31. Kreutzberg, G.W., *Microglia: a sensor for pathological events in the CNS.* Trends Neurosci, 1996. **19**(8): p. 312-8.
32. Ferrero-Miliani, L., et al., *Chronic inflammation: importance of NOD2 and NALP3 in interleukin-1beta generation.* Clin Exp Immunol, 2007. **147**(2): p. 227-35.
33. MacLeod, A.S. and J.N. Mansbridge, *The Innate Immune System in Acute and Chronic Wounds.* Adv Wound Care (New Rochelle), 2016. **5**(2): p. 65-78.
34. Garden, G.A. and T. Moller, *Microglia biology in health and disease.* J Neuroimmune Pharmacol, 2006. **1**(2): p. 127-37.
35. Litman, G.W., J.P. Cannon, and L.J. Dishaw, *Reconstructing immune phylogeny: new perspectives.* Nat Rev Immunol, 2005. **5**(11): p. 866-79.
36. Hornik, T.C., U. Neniskyte, and G.C. Brown, *Inflammation induces multinucleation of Microglia via PKC inhibition of cytokinesis, generating highly phagocytic multinucleated giant cells.* J Neurochem, 2014. **128**(5): p. 650-61.
37. Abiega, O., et al., *Correction: Neuronal Hyperactivity Disturbs ATP Microgradients, Impairs Microglial Motility, and Reduces Phagocytic Receptor Expression Triggering Apoptosis/Microglial Phagocytosis Uncoupling.* PLoS Biol, 2016. **14**(9): p. e1002554.
38. Lauber, K., et al., *Clearance of apoptotic cells: getting rid of the corpses.* Mol Cell, 2004. **14**(3): p. 277-87.
39. Botto, M., et al., *Homozygous C1q deficiency causes glomerulonephritis associated with multiple apoptotic bodies.* Nat Genet, 1998. **19**(1): p. 56-9.
40. Botto, M. and M.J. Walport, *C1q, autoimmunity and apoptosis.* Immunobiology, 2002. **205**(4-5): p. 395-406.
41. Rosen, A. and L. Casciola-Rosen, *Autoantigens as substrates for apoptotic proteases: implications for the pathogenesis of systemic autoimmune disease.* Cell Death Differ, 1999. **6**(1): p. 6-12.
42. Savill, J., et al., *A blast from the past: clearance of apoptotic cells regulates immune responses.* Nat Rev Immunol, 2002. **2**(12): p. 965-75.
43. De Simone, R., et al., *Apoptotic PC12 cells exposing phosphatidylserine promote the production of anti-inflammatory and neuroprotective molecules by microglial cells.* J Neuropathol Exp Neurol, 2003. **62**(2): p. 208-16.
44. Fraser, D.A., K. Pisalyaput, and A.J. Tenner, *C1q enhances microglial clearance of apoptotic neurons and neuronal blebs, and modulates subsequent inflammatory cytokine production.* J Neurochem, 2010. **112**(3): p. 733-43.

45. Amor, S., et al., *Inflammation in neurodegenerative diseases.* Immunology, 2010. **129**(2): p. 154-69.
46. Lucas, S.M., N.J. Rothwell, and R.M. Gibson, *The role of inflammation in CNS injury and disease.* Br J Pharmacol, 2006. **147 Suppl 1**: p. S232-40.
47. Benveniste, E.N., *Inflammatory cytokines within the central nervous system: sources, function, and mechanism of action.* Am J Physiol, 1992. **263**(1 Pt 1): p. C1-16.
48. Camara-Lemarroy, C.R., F.J. Guzman-de la Garza, and N.E. Fernandez-Garza, *Molecular inflammatory mediators in peripheral nerve degeneration and regeneration.* Neuroimmunomodulation, 2010. **17**(5): p. 314-24.
49. Zhang, J., et al., *Inhibitory receptors of the immune system: functions and therapeutic implications.* Cell Mol Immunol, 2009. **6**(6): p. 407-14.
50. Brocker, C., et al., *Evolutionary divergence and functions of the human interleukin (IL) gene family.* Hum Genomics, 2010. **5**(1): p. 30-55.
51. Tisoncik, J.R., et al., *Into the eye of the cytokine storm.* Microbiol Mol Biol Rev, 2012. **76**(1): p. 16-32.
52. Fensterl, V. and G.C. Sen, *Interferons and viral infections.* Biofactors, 2009. **35**(1): p. 14-20.
53. Jeannin, P., et al., *The roles of CSFs on the functional polarization of tumor-associated macrophages.* FEBS J, 2018. **285**(4): p. 680-699.
54. Sun, M. and P.J. Fink, *A new class of reverse signaling costimulators belongs to the TNF family.* J Immunol, 2007. **179**(7): p. 4307-12.
55. Vezzani, A. and T. Granata, *Brain inflammation in epilepsy: experimental and clinical evidence.* Epilepsia, 2005. **46**(11): p. 1724-43.
56. Smith, J.A., et al., *Role of pro-inflammatory cytokines released from microglia in neurodegenerative diseases.* Brain Res Bull, 2012. **87**(1): p. 10-20.
57. Sastre, M., T. Klockgether, and M.T. Heneka, *Contribution of inflammatory processes to Alzheimer's disease: molecular mechanisms.* Int J Dev Neurosci, 2006. **24**(2-3): p. 167-76.
58. Su, F., F. Bai, and Z. Zhang, *Inflammatory Cytokines and Alzheimer's Disease: A Review from the Perspective of Genetic Polymorphisms.* Neurosci Bull, 2016. **32**(5): p. 469-80.
59. Wajant, H., K. Pfizenmaier, and P. Scheurich, *Tumor necrosis factor signaling.* Cell Death Differ, 2003. **10**(1): p. 45-65.
60. Lau, L.T. and A.C. Yu, *Astrocytes produce and release interleukin-1, interleukin-6, tumor necrosis factor alpha and interferon-gamma following traumatic and metabolic injury.* J Neurotrauma, 2001. **18**(3): p. 351-9.
61. Hanisch, U.K., *Microglia as a source and target of cytokines.* Glia, 2002. **40**(2): p. 140-55.
62. Klintworth, H., G. Garden, and Z. Xia, *Rotenone and paraquat do not directly activate microglia or induce inflammatory cytokine release.* Neurosci Lett, 2009. **462**(1): p. 1-5.
63. Keohane, A., et al., *Tumour necrosis factor-alpha impairs neuronal differentiation but not proliferation of hippocampal neural precursor cells: Role of Hes1.* Mol Cell Neurosci, 2010. **43**(1): p. 127-35.
64. Bernardino, L., et al., *Tumor necrosis factor-alpha modulates survival, proliferation, and neuronal differentiation in neonatal subventricular zone cell cultures.* Stem Cells, 2008. **26**(9): p. 2361-71.
65. Obregon, E., et al., *HIV-1 infection induces differentiation of immature neural cells through autocrine tumor necrosis factor and nitric oxide production.* Virology, 1999. **261**(2): p. 193-204.
66. Beattie, E.C., et al., *Control of synaptic strength by glial TNFalpha.* Science, 2002. **295**(5563): p. 2282-5.

67. Steinmetz, C.C. and G.G. Turrigiano, *Tumor necrosis factor-alpha signaling maintains the ability of cortical synapses to express synaptic scaling.* J Neurosci, 2010. **30**(44): p. 14685-90.
68. Marchetti, L., et al., *Tumor necrosis factor (TNF)-mediated neuroprotection against glutamate-induced excitotoxicity is enhanced by N-methyl-D-aspartate receptor activation. Essential role of a TNF receptor 2-mediated phosphatidylinositol 3-kinase-dependent NF-kappa B pathway.* J Biol Chem, 2004. **279**(31): p. 32869-81.
69. Vinet, J., et al., *Neuroprotective function for ramified microglia in hippocampal excitotoxicity.* J Neuroinflammation, 2012. **9**: p. 27.
70. Lambertsen, K.L., et al., *Microglia protect neurons against ischemia by synthesis of tumor necrosis factor.* J Neurosci, 2009. **29**(5): p. 1319-30.
71. Iosif, R.E., et al., *Tumor necrosis factor receptor 1 is a negative regulator of progenitor proliferation in adult hippocampal neurogenesis.* J Neurosci, 2006. **26**(38): p. 9703-12.
72. Montgomery, S.L. and W.J. Bowers, *Tumor necrosis factor-alpha and the roles it plays in homeostatic and degenerative processes within the central nervous system.* J Neuroimmune Pharmacol, 2012. **7**(1): p. 42-59.
73. Barone, F.C., et al., *Tumor necrosis factor-alpha. A mediator of focal ischemic brain injury.* Stroke, 1997. **28**(6): p. 1233-44.
74. Wang, X., et al., *Inhibition of tumor necrosis factor-alpha-converting enzyme by a selective antagonist protects brain from focal ischemic injury in rats.* Mol Pharmacol, 2004. **65**(4): p. 890-6.
75. Neniskyte, U., A. Vilalta, and G.C. Brown, *Tumour necrosis factor alpha-induced neuronal loss is mediated by microglial phagocytosis.* FEBS Lett, 2014. **588**(17): p. 2952-6.
76. Cacci, E., J.H. Claasen, and Z. Kokaia, *Microglia-derived tumor necrosis factor-alpha exaggerates death of newborn hippocampal progenitor cells in vitro.* J Neurosci Res, 2005. **80**(6): p. 789-97.
77. Hofman, F.M., et al., *Tumor necrosis factor identified in multiple sclerosis brain.* J Exp Med, 1989. **170**(2): p. 607-12.
78. Vezzani, A., S. Balosso, and T. Ravizza, *The role of cytokines in the pathophysiology of epilepsy.* Brain Behav Immun, 2008. **22**(6): p. 797-803.
79. Opal, S.M. and V.A. DePalo, *Anti-inflammatory cytokines.* Chest, 2000. **117**(4): p. 1162-72.
80. Vezzani, A., A. Friedman, and R.J. Dingledine, *The role of inflammation in epileptogenesis.* Neuropharmacology, 2013. **69**: p. 16-24.
81. Loftis, J.M., M. Huckans, and B.J. Morasco, *Neuroimmune mechanisms of cytokine-induced depression: current theories and novel treatment strategies.* Neurobiol Dis, 2010. **37**(3): p. 519-33.
82. Wu, A., et al., *Glioma cancer stem cells induce immunosuppressive macrophages/microglia.* Neuro Oncol, 2010. **12**(11): p. 1113-25.
83. Hughes, C.E. and R.J.B. Nibbs, *A guide to chemokines and their receptors.* FEBS J, 2018.
84. Miller, M.C. and K.H. Mayo, *Chemokines from a Structural Perspective.* Int J Mol Sci, 2017. **18**(10).
85. Lehnardt, S., *Innate immunity and neuroinflammation in the CNS: the role of microglia in Toll-like receptor-mediated neuronal injury.* Glia, 2010. **58**(3): p. 253-63.
86. Bazan, J.F., et al., *A new class of membrane-bound chemokine with a CX3C motif.* Nature, 1997. **385**(6617): p. 640-4.
87. Jung, S., et al., *Analysis of fractalkine receptor CX(3)CR1 function by targeted deletion and green fluorescent protein reporter gene insertion.* Mol Cell Biol, 2000. **20**(11): p. 4106-14.
88. Mizutani, M., et al., *The fractalkine receptor but not CCR2 is present on microglia from embryonic development throughout adulthood.* J Immunol, 2012. **188**(1): p. 29-36.

89. Liang, K.J., et al., *Regulation of dynamic behavior of retinal microglia by CX3CR1 signaling.* Invest Ophthalmol Vis Sci, 2009. **50**(9): p. 4444-51.
90. Ragozzino, D., et al., *Chemokine fractalkine/CX3CL1 negatively modulates active glutamatergic synapses in rat hippocampal neurons.* J Neurosci, 2006. **26**(41): p. 10488-98.
91. Scianni, M., et al., *Fractalkine (CX3CL1) enhances hippocampal N-methyl-D-aspartate receptor (NMDAR) function via D-serine and adenosine receptor type A2 (A2AR) activity.* J Neuroinflammation, 2013. **10**: p. 108.
92. Sheridan, G.K., et al., *CX3CL1 is up-regulated in the rat hippocampus during memory-associated synaptic plasticity.* Front Cell Neurosci, 2014. **8**: p. 233.
93. Rogers, J.T., et al., *CX3CR1 deficiency leads to impairment of hippocampal cognitive function and synaptic plasticity.* J Neurosci, 2011. **31**(45): p. 16241-50.
94. Maggi, L., et al., *CX(3)CR1 deficiency alters hippocampal-dependent plasticity phenomena blunting the effects of enriched environment.* Front Cell Neurosci, 2011. **5**: p. 22.
95. Cardona, A.E., et al., *Control of microglial neurotoxicity by the fractalkine receptor.* Nat Neurosci, 2006. **9**(7): p. 917-24.
96. Biber, K., et al., *Neuronal 'On' and 'Off' signals control microglia.* Trends Neurosci, 2007. **30**(11): p. 596-602.
97. Zujovic, V., et al., *Fractalkine modulates TNF-alpha secretion and neurotoxicity induced by microglial activation.* Glia, 2000. **29**(4): p. 305-15.
98. Sheridan, G.K. and K.J. Murphy, *Neuron-glia crosstalk in health and disease: fractalkine and CX3CR1 take centre stage.* Open Biol, 2013. **3**(12): p. 130181.
99. Lee, S., et al., *CX3CR1 deficiency alters microglial activation and reduces beta-amyloid deposition in two Alzheimer's disease mouse models.* Am J Pathol, 2010. **177**(5): p. 2549-62.
100. Denes, A., et al., *Role of CX3CR1 (fractalkine receptor) in brain damage and inflammation induced by focal cerebral ischemia in mouse.* J Cereb Blood Flow Metab, 2008. **28**(10): p. 1707-21.
101. Noda, M., et al., *Fractalkine attenuates excito-neurotoxicity via microglial clearance of damaged neurons and antioxidant enzyme heme oxygenase-1 expression.* J Biol Chem, 2011. **286**(3): p. 2308-19.
102. Sokolowski, J.D., et al., *Fractalkine is a "find-me" signal released by neurons undergoing ethanol-induced apoptosis.* Front Cell Neurosci, 2014. **8**: p. 360.
103. Zabel, M.K., et al., *Microglial phagocytosis and activation underlying photoreceptor degeneration is regulated by CX3CL1-CX3CR1 signaling in a mouse model of retinitis pigmentosa.* Glia, 2016. **64**(9): p. 1479-91.
104. Mukherjee, S., R.N. Ghosh, and F.R. Maxfield, *Endocytosis.* Physiol Rev, 1997. **77**(3): p. 759-803.
105. Fricker, M., et al., *MFG-E8 mediates primary phagocytosis of viable neurons during neuroinflammation.* J Neurosci, 2012. **32**(8): p. 2657-66.
106. Jones, R.S., et al., *Amyloid-beta-induced astrocytic phagocytosis is mediated by CD36, CD47 and RAGE.* J Neuroimmune Pharmacol, 2013. **8**(1): p. 301-11.
107. Magnus, T., et al., *Astrocytes are less efficient in the removal of apoptotic lymphocytes than microglia cells: implications for the role of glial cells in the inflamed central nervous system.* J Neuropathol Exp Neurol, 2002. **61**(9): p. 760-6.
108. Lu, Z., et al., *Phagocytic activity of neuronal progenitors regulates adult neurogenesis.* Nat Cell Biol, 2011. **13**(9): p. 1076-83.
109. Parnaik, R., M.C. Raff, and J. Scholes, *Differences between the clearance of apoptotic cells by professional and non-professional phagocytes.* Curr Biol, 2000. **10**(14): p. 857-60.

110. Baldwin, A.C. and T. Kielian, *Persistent immune activation associated with a mouse model of Staphylococcus aureus-induced experimental brain abscess.* J Neuroimmunol, 2004. **151**(1-2): p. 24-32.
111. Esen, N. and T. Kielian, *Central role for MyD88 in the responses of microglia to pathogen-associated molecular patterns.* J Immunol, 2006. **176**(11): p. 6802-11.
112. Blasi, E., et al., *Role of nitric oxide and melanogenesis in the accomplishment of anticryptococcal activity by the BV-2 microglial cell line.* J Neuroimmunol, 1995. **58**(1): p. 111-6.
113. Jin, X. and T. Yamashita, *Microglia in central nervous system repair after injury.* J Biochem, 2016. **159**(5): p. 491-6.
114. Hosmane, S., et al., *Toll/interleukin-1 receptor domain-containing adapter inducing interferon-beta mediates microglial phagocytosis of degenerating axons.* J Neurosci, 2012. **32**(22): p. 7745-57.
115. Rawji, K.S. and V.W. Yong, *The benefits and detriments of macrophages/microglia in models of multiple sclerosis.* Clin Dev Immunol, 2013. **2013**: p. 948976.
116. Safaiyan, S., et al., *Age-related myelin degradation burdens the clearance function of microglia during aging.* Nat Neurosci, 2016. **19**(8): p. 995-8.
117. Hamley, I.W., *The amyloid beta peptide: a chemist's perspective. Role in Alzheimer's and fibrillization.* Chem Rev, 2012. **112**(10): p. 5147-92.
118. Xu, J. and T. Ikezu, *The comorbidity of HIV-associated neurocognitive disorders and Alzheimer's disease: a foreseeable medical challenge in post-HAART era.* J Neuroimmune Pharmacol, 2009. **4**(2): p. 200-12.
119. Daria, A., et al., *Young microglia restore amyloid plaque clearance of aged microglia.* EMBO J, 2017. **36**(5): p. 583-603.
120. Krabbe, G., et al., *Functional impairment of microglia coincides with Beta-amyloid deposition in mice with Alzheimer-like pathology.* PLoS One, 2013. **8**(4): p. e60921.
121. Liu, Y., et al., *LPS receptor (CD14): a receptor for phagocytosis of Alzheimer's amyloid peptide.* Brain, 2005. **128**(Pt 8): p. 1778-89.
122. Liu, S., et al., *TLR2 is a primary receptor for Alzheimer's amyloid beta peptide to trigger neuroinflammatory activation.* J Immunol, 2012. **188**(3): p. 1098-107.
123. Hellwig, S., et al., *Forebrain microglia from wild-type but not adult 5xFAD mice prevent amyloid-beta plaque formation in organotypic hippocampal slice cultures.* Sci Rep, 2015. **5**: p. 14624.
124. Bolmont, T., et al., *Dynamics of the microglial/amyloid interaction indicate a role in plaque maintenance.* J Neurosci, 2008. **28**(16): p. 4283-92.
125. Brown, G.C. and J.J. Neher, *Eaten alive! Cell death by primary phagocytosis: 'phagoptosis'.* Trends Biochem Sci, 2012. **37**(8): p. 325-32.
126. Brown, G.C. and J.J. Neher, *Microglial phagocytosis of live neurons.* Nat Rev Neurosci, 2014. **15**(4): p. 209-16.
127. Neher, J.J., et al., *Inhibition of microglial phagocytosis is sufficient to prevent inflammatory neuronal death.* J Immunol, 2011. **186**(8): p. 4973-83.
128. Neniskyte, U., J.J. Neher, and G.C. Brown, *Neuronal death induced by nanomolar amyloid beta is mediated by primary phagocytosis of neurons by microglia.* J Biol Chem, 2011. **286**(46): p. 39904-13.
129. McArthur, S., et al., *Annexin A1: a central player in the anti-inflammatory and neuroprotective role of microglia.* J Immunol, 2010. **185**(10): p. 6317-28.
130. Neher, J.J., et al., *Phagocytosis executes delayed neuronal death after focal brain ischemia.* Proc Natl Acad Sci U S A, 2013. **110**(43): p. E4098-107.
131. Wang, Y. and H. Neumann, *Alleviation of neurotoxicity by microglial human Siglec-11.* J Neurosci, 2010. **30**(9): p. 3482-8.
132. Poon, I.K., et al., *Unexpected link between an antibiotic, pannexin channels and apoptosis.* Nature, 2014. **507**(7492): p. 329-34.

133. Barber, G.N., *Host defense, viruses and apoptosis.* Cell Death Differ, 2001. **8**(2): p. 113-26.
134. Taylor, R.C., S.P. Cullen, and S.J. Martin, *Apoptosis: controlled demolition at the cellular level.* Nat Rev Mol Cell Biol, 2008. **9**(3): p. 231-41.
135. Zaman, S., R. Wang, and V. Gandhi, *Targeting the apoptosis pathway in hematologic malignancies.* Leuk Lymphoma, 2014. **55**(9): p. 1980-92.
136. Eidet, J.R., et al., *Objective assessment of changes in nuclear morphology and cell distribution following induction of apoptosis.* Diagn Pathol, 2014. **9**: p. 92.
137. Krysko, D.V., et al., *Apoptosis and necrosis: detection, discrimination and phagocytosis.* Methods, 2008. **44**(3): p. 205-21.
138. Peter, C., S. Wesselborg, and K. Lauber, *Molecular suicide notes: last call from apoptosing cells.* J Mol Cell Biol, 2010. **2**(2): p. 78-80.
139. Ravichandran, K.S. and U. Lorenz, *Engulfment of apoptotic cells: signals for a good meal.* Nat Rev Immunol, 2007. **7**(12): p. 964-74.
140. Kinchen, J.M., et al., *A pathway for phagosome maturation during engulfment of apoptotic cells.* Nat Cell Biol, 2008. **10**(5): p. 556-66.
141. Diaz-Aparicio, I., et al., *Clearing the corpses: regulatory mechanisms, novel tools, and therapeutic potential of harnessing microglial phagocytosis in the diseased brain.* Neural Regen Res, 2016. **11**(10): p. 1533-1539.
142. Arandjelovic, S. and K.S. Ravichandran, *Phagocytosis of apoptotic cells in homeostasis.* Nat Immunol, 2015. **16**(9): p. 907-17.
143. Elliott, M.R., et al., *Nucleotides released by apoptotic cells act as a find-me signal to promote phagocytic clearance.* Nature, 2009. **461**(7261): p. 282-6.
144. Truman, L.A., et al., *CX3CL1/fractalkine is released from apoptotic lymphocytes to stimulate macrophage chemotaxis.* Blood, 2008. **112**(13): p. 5026-36.
145. Gude, D.R., et al., *Apoptosis induces expression of sphingosine kinase 1 to release sphingosine-1-phosphate as a "come-and-get-me" signal.* FASEB J, 2008. **22**(8): p. 2629-38.
146. Lauber, K., et al., *Apoptotic cells induce migration of phagocytes via caspase-3-mediated release of a lipid attraction signal.* Cell, 2003. **113**(6): p. 717-30.
147. Peter, C., et al., *Migration to apoptotic "find-me" signals is mediated via the phagocyte receptor G2A.* J Biol Chem, 2008. **283**(9): p. 5296-305.
148. Xu, J., et al., *Microglia Colonization of Developing Zebrafish Midbrain Is Promoted by Apoptotic Neuron and Lysophosphatidylcholine.* Dev Cell, 2016. **38**(2): p. 214-22.
149. O'Sullivan, S.A., et al., *Sphingosine 1-phosphate receptors regulate TLR4-induced CXCL5 release from astrocytes and microglia.* J Neurochem, 2018. **144**(6): p. 736-747.
150. Chekeni, F.B., et al., *Pannexin 1 channels mediate 'find-me' signal release and membrane permeability during apoptosis.* Nature, 2010. **467**(7317): p. 863-7.
151. Fadok, V.A., et al., *Exposure of phosphatidylserine on the surface of apoptotic lymphocytes triggers specific recognition and removal by macrophages.* J Immunol, 1992. **148**(7): p. 2207-16.
152. Vermes, I., et al., *A novel assay for apoptosis. Flow cytometric detection of phosphatidylserine expression on early apoptotic cells using fluorescein labelled Annexin V.* J Immunol Methods, 1995. **184**(1): p. 39-51.
153. Segawa, K., et al., *Caspase-mediated cleavage of phospholipid flippase for apoptotic phosphatidylserine exposure.* Science, 2014. **344**(6188): p. 1164-8.
154. Suzuki, J., et al., *Xk-related protein 8 and CED-8 promote phosphatidylserine exposure in apoptotic cells.* Science, 2013. **341**(6144): p. 403-6.
155. Obeid, M., et al., *Calreticulin exposure is required for the immunogenicity of gamma-irradiation and UVC light-induced apoptosis.* Cell Death Differ, 2007. **14**(10): p. 1848-50.

156. Gregory, C.D. and A. Devitt, *The macrophage and the apoptotic cell: an innate immune interaction viewed simplistically?* Immunology, 2004. **113**(1): p. 1-14.
157. Moffatt, O.D., et al., *Macrophage recognition of ICAM-3 on apoptotic leukocytes.* J Immunol, 1999. **162**(11): p. 6800-10.
158. Albert, M.L., J.I. Kim, and R.B. Birge, *alphavbeta5 integrin recruits the CrkII-Dock180-rac1 complex for phagocytosis of apoptotic cells.* Nat Cell Biol, 2000. **2**(12): p. 899-905.
159. Gumienny, T.L., et al., *CED-12/ELMO, a novel member of the CrkII/Dock180/Rac pathway, is required for phagocytosis and cell migration.* Cell, 2001. **107**(1): p. 27-41.
160. Jahraus, A., et al., *In vitro fusion of phagosomes with different endocytic organelles from J774 macrophages.* J Biol Chem, 1998. **273**(46): p. 30379-90.
161. Garin, J., et al., *The phagosome proteome: insight into phagosome functions.* J Cell Biol, 2001. **152**(1): p. 165-80.
162. Kinchen, J.M., et al., *Two pathways converge at CED-10 to mediate actin rearrangement and corpse removal in C. elegans.* Nature, 2005. **434**(7029): p. 93-9.
163. Park, D., et al., *Continued clearance of apoptotic cells critically depends on the phagocyte Ucp2 protein.* Nature, 2011. **477**(7363): p. 220-4.
164. Wu, Q., et al., *Beta-amyloid activated microglia induce cell cycling and cell death in cultured cortical neurons.* Neurobiol Aging, 2000. **21**(6): p. 797-806.
165. Peri, F. and C. Nusslein-Volhard, *Live imaging of neuronal degradation by microglia reveals a role for v0-ATPase a1 in phagosomal fusion in vivo.* Cell, 2008. **133**(5): p. 916-27.
166. Miyanishi, M., et al., *Identification of Tim4 as a phosphatidylserine receptor.* Nature, 2007. **450**(7168): p. 435-9.
167. Nishi, C., et al., *Tim4- and MerTK-mediated engulfment of apoptotic cells by mouse resident peritoneal macrophages.* Mol Cell Biol, 2014. **34**(8): p. 1512-20.
168. Scott, R.S., et al., *Phagocytosis and clearance of apoptotic cells is mediated by MER.* Nature, 2001. **411**(6834): p. 207-11.
169. Wu, Y., et al., *A role for Mer tyrosine kinase in alphavbeta5 integrin-mediated phagocytosis of apoptotic cells.* J Cell Sci, 2005. **118**(Pt 3): p. 539-53.
170. Hanayama, R., et al., *Identification of a factor that links apoptotic cells to phagocytes.* Nature, 2002. **417**(6885): p. 182-7.
171. Mazaheri, F., et al., *Distinct roles for BAI1 and TIM-4 in the engulfment of dying neurons by microglia.* Nat Commun, 2014. **5**: p. 4046.
172. Hickman, S.E. and J. El Khoury, *TREM2 and the neuroimmunology of Alzheimer's disease.* Biochem Pharmacol, 2014. **88**(4): p. 495-8.
173. Hsieh, C.L., et al., *A role for TREM2 ligands in the phagocytosis of apoptotic neuronal cells by microglia.* J Neurochem, 2009. **109**(4): p. 1144-56.
174. Atagi, Y., et al., *Apolipoprotein E Is a Ligand for Triggering Receptor Expressed on Myeloid Cells 2 (TREM2).* J Biol Chem, 2015. **290**(43): p. 26043-50.
175. Makide, K., et al., *Novel lysophosphoplipid receptors: their structure and function.* J Lipid Res, 2014. **55**(10): p. 1986-95.
176. Sugo, T., et al., *Identification of a lysophosphatidylserine receptor on mast cells.* Biochem Biophys Res Commun, 2006. **341**(4): p. 1078-87.
177. Butovsky, O., et al., *Identification of a unique TGF-beta-dependent molecular and functional signature in microglia.* Nat Neurosci, 2014. **17**(1): p. 131-43.
178. Bedard, A., et al., *Identification of genes preferentially expressed by microglia and upregulated during cuprizone-induced inflammation.* Glia, 2007. **55**(8): p. 777-89.
179. Schoneberg, T., et al., *The G protein-coupled receptor GPR34 - The past 20years of a grownup.* Pharmacol Ther, 2018. **189**: p. 71-88.
180. Ikubo, M., et al., *Structure-activity relationships of lysophosphatidylserine analogs as agonists of G-protein-coupled receptors GPR34, P2Y10, and GPR174.* J Med Chem, 2015. **58**(10): p. 4204-19.

181. Liebscher, I., et al., *Altered immune response in mice deficient for the G protein-coupled receptor GPR34.* J Biol Chem, 2011. **286**(3): p. 2101-10.
182. Preissler, J., et al., *Altered microglial phagocytosis in GPR34-deficient mice.* Glia, 2015. **63**(2): p. 206-15.
183. Kitamura, H., et al., *GPR34 is a receptor for lysophosphatidylserine with a fatty acid at the sn-2 position.* J Biochem, 2012. **151**(5): p. 511-8.
184. Martin, T.W. and D. Lagunoff, *Interactions of lysophospholipids and mast cells.* Nature, 1979. **279**(5710): p. 250-2.
185. Lourenssen, S. and M.G. Blennerhassett, *Lysophosphatidylserine potentiates nerve growth factor-induced differentiation of PC12 cells.* Neurosci Lett, 1998. **248**(2): p. 77-80.
186. Bellini, F. and A. Bruni, *Role of a serum phospholipase A1 in the phosphatidylserine-induced T cell inhibition.* FEBS Lett, 1993. **316**(1): p. 1-4.
187. Lee, S.Y., et al., *Lysophosphatidylserine stimulates chemotactic migration in U87 human glioma cells.* Biochem Biophys Res Commun, 2008. **374**(1): p. 147-51.
188. Frasch, S.C. and D.L. Bratton, *Emerging roles for lysophosphatidylserine in resolution of inflammation.* Prog Lipid Res, 2012. **51**(3): p. 199-207.
189. Inoue, A., et al., *TGFalpha shedding assay: an accurate and versatile method for detecting GPCR activation.* Nat Methods, 2012. **9**(10): p. 1021-9.
190. Frasch, S.C., et al., *Signaling via macrophage G2A enhances efferocytosis of dying neutrophils by augmentation of Rac activity.* J Biol Chem, 2011. **286**(14): p. 12108-22.
191. Frasch, S.C., et al., *NADPH oxidase-dependent generation of lysophosphatidylserine enhances clearance of activated and dying neutrophils via G2A.* J Biol Chem, 2008. **283**(48): p. 33736-49.
192. Rao, S., et al., *The Ets factors PU.1 and Spi-B regulate the transcription in vivo of P2Y10, a lymphoid restricted heptahelical receptor.* J Biol Chem, 1999. **274**(48): p. 34245-52.
193. Tokizane, K., et al., *Phospholipid localization implies microglial morphology and function via Cdc42 in vitro.* Glia, 2017. **65**(5): p. 740-755.
194. Hwang, S.M., et al., *Olig2 is expressed late in human eosinophil development and controls Siglec-8 expression.* J Leukoc Biol, 2016. **100**(4): p. 711-723.
195. Hwang, S.M., et al., *Lysophosphatidylserine receptor P2Y10: A G protein-coupled receptor that mediates eosinophil degranulation.* Clin Exp Allergy, 2018. **48**(8): p. 990-999.
196. Murakami, M., et al., *Identification of the orphan GPCR, P2Y(10) receptor as the sphingosine-1-phosphate and lysophosphatidic acid receptor.* Biochem Biophys Res Commun, 2008. **371**(4): p. 707-12.
197. Barnes, M.J. and J.G. Cyster, *Lysophosphatidylserine suppression of T-cell activation via GPR174 requires Galphas proteins.* Immunol Cell Biol, 2018. **96**(4): p. 439-445.
198. Parks, B.W., et al., *Loss of G2A promotes macrophage accumulation in atherosclerotic lesions of low density lipoprotein receptor-deficient mice.* J Lipid Res, 2005. **46**(7): p. 1405-15.
199. Murakami, N., et al., *Transcriptional regulation of human G2A in monocytes/ macrophages: involvement of c/EBPs, Runx and Pu.1.* Genes Cells, 2009. **14**(12): p. 1441-55.
200. Kabarowski, J.H., et al., *Lysophosphatidylcholine as a ligand for the immunoregulatory receptor G2A.* Science, 2001. **293**(5530): p. 702-5.
201. Radu, C.G., et al., *Differential proton sensitivity of related G protein-coupled receptors T cell death-associated gene 8 and G2A expressed in immune cells.* Proc Natl Acad Sci U S A, 2005. **102**(5): p. 1632-7.
202. Tremblay, M.E., R.L. Lowery, and A.K. Majewska, *Microglial interactions with synapses are modulated by visual experience.* PLoS Biol, 2010. **8**(11): p. e1000527.

203. Perez-Pouchoulen, M., J.W. VanRyzin, and M.M. McCarthy, *Morphological and Phagocytic Profile of Microglia in the Developing Rat Cerebellum.* eNeuro, 2015. **2**(4).
204. Sieger, D., et al., *Long-range Ca2+ waves transmit brain-damage signals to microglia.* Dev Cell, 2012. **22**(6): p. 1138-48.
205. Poon, I.K., et al., *Apoptotic cell clearance: basic biology and therapeutic potential.* Nat Rev Immunol, 2014. **14**(3): p. 166-80.
206. Nagata, S., R. Hanayama, and K. Kawane, *Autoimmunity and the clearance of dead cells.* Cell, 2010. **140**(5): p. 619-30.
207. Gordon, S. and A. Pluddemann, *Macrophage Clearance of Apoptotic Cells: A Critical Assessment.* Front Immunol, 2018. **9**: p. 127.
208. Stern, M., J. Savill, and C. Haslett, *Human monocyte-derived macrophage phagocytosis of senescent eosinophils undergoing apoptosis. Mediation by alpha v beta 3/CD36/thrombospondin recognition mechanism and lack of phlogistic response.* Am J Pathol, 1996. **149**(3): p. 911-21.
209. Voll, R.E., et al., *Immunosuppressive effects of apoptotic cells.* Nature, 1997. **390**(6658): p. 350-1.
210. Fadok, V.A., et al., *Macrophages that have ingested apoptotic cells in vitro inhibit proinflammatory cytokine production through autocrine/paracrine mechanisms involving TGF-beta, PGE2, and PAF.* J Clin Invest, 1998. **101**(4): p. 890-8.
211. Han, C.Z. and K.S. Ravichandran, *Metabolic connections during apoptotic cell engulfment.* Cell, 2011. **147**(7): p. 1442-5.
212. Cheng, S.C., et al., *mTOR- and HIF-1alpha-mediated aerobic glycolysis as metabolic basis for trained immunity.* Science, 2014. **345**(6204): p. 1250684.
213. Buckwalter, M.S., et al., *Chronically increased transforming growth factor-beta1 strongly inhibits hippocampal neurogenesis in aged mice.* Am J Pathol, 2006. **169**(1): p. 154-64.
214. Cao, L., et al., *VEGF links hippocampal activity with neurogenesis, learning and memory.* Nat Genet, 2004. **36**(8): p. 827-35.
215. McKenna, M.C., S. Scafidi, and C.L. Robertson, *Metabolic Alterations in Developing Brain After Injury: Knowns and Unknowns.* Neurochem Res, 2015. **40**(12): p. 2527-43.
216. McKenna, M.C., *Substrate competition studies demonstrate oxidative metabolism of glucose, glutamate, glutamine, lactate and 3-hydroxybutyrate in cortical astrocytes from rat brain.* Neurochem Res, 2012. **37**(11): p. 2613-26.
217. Brekke, E., T.S. Morken, and U. Sonnewald, *Glucose metabolism and astrocyte-neuron interactions in the neonatal brain.* Neurochem Int, 2015. **82**: p. 33-41.
218. Kholodenko, B.N., *Four-dimensional organization of protein kinase signaling cascades: the roles of diffusion, endocytosis and molecular motors.* J Exp Biol, 2003. **206**(Pt 12): p. 2073-82.
219. Pesaresi, P., et al., *Interorganellar communication.* Curr Opin Plant Biol, 2007. **10**(6): p. 600-6.
220. Hoppert, M. and F. Mayer, *Principles of macromolecular organization and cell function in bacteria and archaea.* Cell Biochem Biophys, 1999. **31**(3): p. 247-84.
221. Kresge, N., R.D. Simoni, and R.L. Hill, *Otto Fritz Meyerhof and the elucidation of the glycolytic pathway.* J Biol Chem, 2005. **280**(4): p. e3.
222. Akram, M., *Mini-review on glycolysis and cancer.* J Cancer Educ, 2013. **28**(3): p. 454-7.
223. Goldblatt, H. and G. Cameron, *Induced malignancy in cells from rat myocardium subjected to intermittent anaerobiosis during long propagation in vitro.* J Exp Med, 1953. **97**(4): p. 525-52.
224. Horecker, B.L., *The pentose phosphate pathway.* J Biol Chem, 2002. **277**(50): p. 47965-71.
225. Kruger, N.J. and A. von Schaewen, *The oxidative pentose phosphate pathway: structure and organisation.* Curr Opin Plant Biol, 2003. **6**(3): p. 236-46.

226. Wang, Z. and C. Dong, *Gluconeogenesis in Cancer: Function and Regulation of PEPCK, FBPase, and G6Pase.* Trends Cancer, 2019. **5**(1): p. 30-45.
227. Mishra, P. and D.C. Chan, *Metabolic regulation of mitochondrial dynamics.* J Cell Biol, 2016. **212**(4): p. 379-87.
228. Krebs, H.A., *The history of the tricarboxylic acid cycle.* Perspect Biol Med, 1970. **14**(1): p. 154-70.
229. Costello, L.C. and R.B. Franklin, *Aconitase activity, citrate oxidation, and zinc inhibition in rat ventral prostate.* Enzyme, 1981. **26**(6): p. 281-7.
230. Guffon, N., et al., *2-Ketoglutarate dehydrogenase deficiency, a rare cause of primary hyperlactataemia: report of a new case.* J Inherit Metab Dis, 1993. **16**(5): p. 821-30.
231. Briere, J.J., et al., *Succinate dehydrogenase deficiency in human.* Cell Mol Life Sci, 2005. **62**(19-20): p. 2317-24.
232. Akiba, T., K. Hiraga, and S. Tuboi, *Intracellular distribution of fumarase in various animals.* J Biochem, 1984. **96**(1): p. 189-95.
233. Srere, P.A., *The enzymology of the formation and breakdown of citrate.* Adv Enzymol Relat Areas Mol Biol, 1975. **43**: p. 57-101.
234. Mitchell, P., *Coupling of phosphorylation to electron and hydrogen transfer by a chemi-osmotic type of mechanism.* Nature, 1961. **191**: p. 144-8.
235. Mitchell, P., *Vectorial chemistry and the molecular mechanics of chemiosmotic coupling: power transmission by proticity.* Biochem Soc Trans, 1976. **4**(3): p. 399-430.
236. Baughman, J.M., et al., *Integrative genomics identifies MCU as an essential component of the mitochondrial calcium uniporter.* Nature, 2011. **476**(7360): p. 341-5.
237. Jouaville, L.S., et al., *Regulation of mitochondrial ATP synthesis by calcium: evidence for a long-term metabolic priming.* Proc Natl Acad Sci U S A, 1999. **96**(24): p. 13807-12.
238. Zhang, L., et al., *Role of fatty acid uptake and fatty acid beta-oxidation in mediating insulin resistance in heart and skeletal muscle.* Biochim Biophys Acta, 2010. **1801**(1): p. 1-22.
239. Sagan, L., *On the origin of mitosing cells.* J Theor Biol, 1967. **14**(3): p. 255-74.
240. Schwartz, R.M. and M.O. Dayhoff, *Origins of prokaryotes, eukaryotes, mitochondria, and chloroplasts.* Science, 1978. **199**(4327): p. 395-403.
241. Yang, D., et al., *Mitochondrial origins.* Proc Natl Acad Sci U S A, 1985. **82**(13): p. 4443-7.
242. Osellame, L.D., T.S. Blacker, and M.R. Duchen, *Cellular and molecular mechanisms of mitochondrial function.* Best Pract Res Clin Endocrinol Metab, 2012. **26**(6): p. 711-23.
243. Santorelli, F.M., et al., *The mutation at nt 8993 of mitochondrial DNA is a common cause of Leigh's syndrome.* Ann Neurol, 1993. **34**(6): p. 827-34.
244. Wallace, D.C., et al., *Mitochondrial DNA mutation associated with Leber's hereditary optic neuropathy.* Science, 1988. **242**(4884): p. 1427-30.
245. Paoli, M., J. Marles-Wright, and A. Smith, *Structure-function relationships in heme-proteins.* DNA Cell Biol, 2002. **21**(4): p. 271-80.
246. Alderton, W.K., C.E. Cooper, and R.G. Knowles, *Nitric oxide synthases: structure, function and inhibition.* Biochem J, 2001. **357**(Pt 3): p. 593-615.
247. Duchen, M.R., *Mitochondria and calcium: from cell signalling to cell death.* J Physiol, 2000. **529 Pt 1**: p. 57-68.
248. Susin, S.A., et al., *Molecular characterization of mitochondrial apoptosis-inducing factor.* Nature, 1999. **397**(6718): p. 441-6.
249. Labbe, K., A. Murley, and J. Nunnari, *Determinants and functions of mitochondrial behavior.* Annu Rev Cell Dev Biol, 2014. **30**: p. 357-91.
250. Chen, H., et al., *Mitofusins Mfn1 and Mfn2 coordinately regulate mitochondrial fusion and are essential for embryonic development.* J Cell Biol, 2003. **160**(2): p. 189-200.
251. Mishra, P., et al., *Proteolytic cleavage of Opa1 stimulates mitochondrial inner membrane fusion and couples fusion to oxidative phosphorylation.* Cell Metab, 2014. **19**(4): p. 630-41.

252. Chan, D.C., *Fusion and fission: interlinked processes critical for mitochondrial health.* Annu Rev Genet, 2012. **46**: p. 265-87.
253. Kim, I., S. Rodriguez-Enriquez, and J.J. Lemasters, *Selective degradation of mitochondria by mitophagy.* Arch Biochem Biophys, 2007. **462**(2): p. 245-53.
254. Cereghetti, G.M., et al., *Dephosphorylation by calcineurin regulates translocation of Drp1 to mitochondria.* Proc Natl Acad Sci U S A, 2008. **105**(41): p. 15803-8.
255. Serasinghe, M.N., et al., *Mitochondrial division is requisite to RAS-induced transformation and targeted by oncogenic MAPK pathway inhibitors.* Mol Cell, 2015. **57**(3): p. 521-36.
256. Toyama, E.Q., et al., *Metabolism. AMP-activated protein kinase mediates mitochondrial fission in response to energy stress.* Science, 2016. **351**(6270): p. 275-281.
257. Saxton, W.M. and P.J. Hollenbeck, *The axonal transport of mitochondria.* J Cell Sci, 2012. **125**(Pt 9): p. 2095-104.
258. Pilling, A.D., et al., *Kinesin-1 and Dynein are the primary motors for fast transport of mitochondria in Drosophila motor axons.* Mol Biol Cell, 2006. **17**(4): p. 2057-68.
259. Sheng, Z.H. and Q. Cai, *Mitochondrial transport in neurons: impact on synaptic homeostasis and neurodegeneration.* Nat Rev Neurosci, 2012. **13**(2): p. 77-93.
260. Matsuda, N., et al., *PINK1 stabilized by mitochondrial depolarization recruits Parkin to damaged mitochondria and activates latent Parkin for mitophagy.* J Cell Biol, 2010. **189**(2): p. 211-21.
261. Sarraf, S.A., et al., *Landscape of the PARKIN-dependent ubiquitylome in response to mitochondrial depolarization.* Nature, 2013. **496**(7445): p. 372-6.
262. Melser, S., et al., *Rheb regulates mitophagy induced by mitochondrial energetic status.* Cell Metab, 2013. **17**(5): p. 719-30.
263. Clark, L.C., Jr., et al., *Monitor and control of blood oxygen tension and pH during total body perfusion.* J Thorac Surg, 1958. **36**(4): p. 488-96.
264. Pesta, D. and E. Gnaiger, *High-resolution respirometry: OXPHOS protocols for human cells and permeabilized fibers from small biopsies of human muscle.* Methods Mol Biol, 2012. **810**: p. 25-58.
265. Weegman, B.P., et al., *Continuous real-time viability assessment of kidneys based on oxygen consumption.* Transplant Proc, 2010. **42**(6): p. 2020-3.
266. Van den Bossche, J., L.A. O'Neill, and D. Menon, *Macrophage Immunometabolism: Where Are We (Going)?* Trends Immunol, 2017. **38**(6): p. 395-406.
267. Van den Bossche, J., J. Baardman, and M.P. de Winther, *Metabolic Characterization of Polarized M1 and M2 Bone Marrow-derived Macrophages Using Real-time Extracellular Flux Analysis.* J Vis Exp, 2015(105).
268. Kelly, B. and L.A. O'Neill, *Metabolic reprogramming in macrophages and dendritic cells in innate immunity.* Cell Res, 2015. **25**(7): p. 771-84.
269. Pearce, E.L. and E.J. Pearce, *Metabolic pathways in immune cell activation and quiescence.* Immunity, 2013. **38**(4): p. 633-43.
270. Tannahill, G.M., et al., *Succinate is an inflammatory signal that induces IL-1beta through HIF-1alpha.* Nature, 2013. **496**(7444): p. 238-42.
271. Jha, A.K., et al., *Network integration of parallel metabolic and transcriptional data reveals metabolic modules that regulate macrophage polarization.* Immunity, 2015. **42**(3): p. 419-30.
272. O'Neill, L.A. and E.J. Pearce, *Immunometabolism governs dendritic cell and macrophage function.* J Exp Med, 2016. **213**(1): p. 15-23.
273. Rodriguez-Prados, J.C., et al., *Substrate fate in activated macrophages: a comparison between innate, classic, and alternative activation.* J Immunol, 2010. **185**(1): p. 605-14.

274. Moss, D.W. and T.E. Bates, *Activation of murine microglial cell lines by lipopolysaccharide and interferon-gamma causes NO-mediated decreases in mitochondrial and cellular function.* Eur J Neurosci, 2001. **13**(3): p. 529-38.
275. Chenais, B., H. Morjani, and J.C. Drapier, *Impact of endogenous nitric oxide on microglial cell energy metabolism and labile iron pool.* J Neurochem, 2002. **81**(3): p. 615-23.
276. Bernhart, E., et al., *Lysophosphatidic acid receptor activation affects the C13NJ microglia cell line proteome leading to alterations in glycolysis, motility, and cytoskeletal architecture.* Proteomics, 2010. **10**(1): p. 141-58.
277. Voloboueva, L.A., et al., *Inflammatory response of microglial BV-2 cells includes a glycolytic shift and is modulated by mitochondrial glucose-regulated protein 75/mortalin.* FEBS Lett, 2013. **587**(6): p. 756-62.
278. Gimeno-Bayon, J., et al., *Glucose pathways adaptation supports acquisition of activated microglia phenotype.* J Neurosci Res, 2014. **92**(6): p. 723-31.
279. Altman, J., *Are new neurons formed in the brains of adult mammals?* Science, 1962. **135**(3509): p. 1127-8.
280. Altman, J., *Autoradiographic investigation of cell proliferation in the brains of rats and cats.* Anat Rec, 1963. **145**: p. 573-91.
281. Nottebohm, F., *Why are some neurons replaced in adult brain?* J Neurosci, 2002. **22**(3): p. 624-8.
282. Zupanc, G.K., *A comparative approach towards the understanding of adult neurogenesis.* Brain Behav Evol, 2001. **58**(5): p. 246-9.
283. Ehninger, D. and G. Kempermann, *Neurogenesis in the adult hippocampus.* Cell Tissue Res, 2008. **331**(1): p. 243-50.
284. Eriksson, P.S., et al., *Neurogenesis in the adult human hippocampus.* Nat Med, 1998. **4**(11): p. 1313-7.
285. Knoth, R., et al., *Murine features of neurogenesis in the human hippocampus across the lifespan from 0 to 100 years.* PLoS One, 2010. **5**(1): p. e8809.
286. Roy, N.S., et al., *In vitro neurogenesis by progenitor cells isolated from the adult human hippocampus.* Nat Med, 2000. **6**(3): p. 271-7.
287. Bergmann, O., et al., *The age of olfactory bulb neurons in humans.* Neuron, 2012. **74**(4): p. 634-9.
288. Curtis, M.A., et al., *Human neuroblasts migrate to the olfactory bulb via a lateral ventricular extension.* Science, 2007. **315**(5816): p. 1243-9.
289. Sorrells, S.F., et al., *Human hippocampal neurogenesis drops sharply in children to undetectable levels in adults.* Nature, 2018. **555**(7696): p. 377-381.
290. Spalding, K.L., et al., *Dynamics of hippocampal neurogenesis in adult humans.* Cell, 2013. **153**(6): p. 1219-1227.
291. Boldrini, M., et al., *Human Hippocampal Neurogenesis Persists throughout Aging.* Cell Stem Cell, 2018. **22**(4): p. 589-599 e5.
292. Kempermann, G., et al., *Milestones of neuronal development in the adult hippocampus.* Trends Neurosci, 2004. **27**(8): p. 447-52.
293. Encinas, J.M., et al., *Division-coupled astrocytic differentiation and age-related depletion of neural stem cells in the adult hippocampus.* Cell Stem Cell, 2011. **8**(5): p. 566-79.
294. Seri, B., et al., *Astrocytes give rise to new neurons in the adult mammalian hippocampus.* J Neurosci, 2001. **21**(18): p. 7153-60.
295. Encinas, J.M. and A. Sierra, *Neural stem cell deforestation as the main force driving the age-related decline in adult hippocampal neurogenesis.* Behav Brain Res, 2012. **227**(2): p. 433-9.
296. Seri, B., et al., *Cell types, lineage, and architecture of the germinal zone in the adult dentate gyrus.* J Comp Neurol, 2004. **478**(4): p. 359-78.

297. Encinas, J.M., A. Vaahtokari, and G. Enikolopov, *Fluoxetine targets early progenitor cells in the adult brain.* Proc Natl Acad Sci U S A, 2006. **103**(21): p. 8233-8.
298. Encinas, J.M., et al., *Neurogenic hippocampal targets of deep brain stimulation.* J Comp Neurol, 2011. **519**(1): p. 6-20.
299. van Praag, H., et al., *Functional neurogenesis in the adult hippocampus.* Nature, 2002. **415**(6875): p. 1030-4.
300. Toni, N., et al., *Neurons born in the adult dentate gyrus form functional synapses with target cells.* Nat Neurosci, 2008. **11**(8): p. 901-7.
301. Plumpe, T., et al., *Variability of doublecortin-associated dendrite maturation in adult hippocampal neurogenesis is independent of the regulation of precursor cell proliferation.* BMC Neurosci, 2006. **7**: p. 77.
302. Tashiro, A., et al., *NMDA-receptor-mediated, cell-specific integration of new neurons in adult dentate gyrus.* Nature, 2006. **442**(7105): p. 929-33.
303. Bruel-Jungerman, E., C. Rampon, and S. Laroche, *Adult hippocampal neurogenesis, synaptic plasticity and memory: facts and hypotheses.* Rev Neurosci, 2007. **18**(2): p. 93-114.
304. Shors, T.J., et al., *Neurogenesis in the adult is involved in the formation of trace memories.* Nature, 2001. **410**(6826): p. 372-6.
305. Deng, W., et al., *Adult-born hippocampal dentate granule cells undergoing maturation modulate learning and memory in the brain.* J Neurosci, 2009. **29**(43): p. 13532-42.
306. Sahay, A., et al., *Increasing adult hippocampal neurogenesis is sufficient to improve pattern separation.* Nature, 2011. **472**(7344): p. 466-70.
307. Leuner, B., E. Gould, and T.J. Shors, *Is there a link between adult neurogenesis and learning?* Hippocampus, 2006. **16**(3): p. 216-24.
308. Koehl, M. and D.N. Abrous, *A new chapter in the field of memory: adult hippocampal neurogenesis.* Eur J Neurosci, 2011. **33**(6): p. 1101-14.
309. Garthe, A., J. Behr, and G. Kempermann, *Adult-generated hippocampal neurons allow the flexible use of spatially precise learning strategies.* PLoS One, 2009. **4**(5): p. e5464.
310. Winocur, G., et al., *Inhibition of neurogenesis interferes with hippocampus-dependent memory function.* Hippocampus, 2006. **16**(3): p. 296-304.
311. Fan, Y., et al., *Environmental enrichment enhances neurogenesis and improves functional outcome after cranial irradiation.* Eur J Neurosci, 2007. **25**(1): p. 38-46.
312. Saxe, M.D., et al., *Ablation of hippocampal neurogenesis impairs contextual fear conditioning and synaptic plasticity in the dentate gyrus.* Proc Natl Acad Sci U S A, 2006. **103**(46): p. 17501-6.
313. Mohapel, P., et al., *Forebrain acetylcholine regulates adult hippocampal neurogenesis and learning.* Neurobiol Aging, 2005. **26**(6): p. 939-46.
314. Qiao, C., et al., *Ginseng enhances contextual fear conditioning and neurogenesis in rats.* Neurosci Res, 2005. **51**(1): p. 31-8.
315. Li, B., et al., *Neurotrophic peptides incorporating adamantane improve learning and memory, promote neurogenesis and synaptic plasticity in mice.* FEBS Lett, 2010. **584**(15): p. 3359-65.
316. Rolls, E.T. and R.P. Kesner, *A computational theory of hippocampal function, and empirical tests of the theory.* Prog Neurobiol, 2006. **79**(1): p. 1-48.
317. Treves, A. and E.T. Rolls, *Computational analysis of the role of the hippocampus in memory.* Hippocampus, 1994. **4**(3): p. 374-91.
318. Nakashiba, T., et al., *Young dentate granule cells mediate pattern separation, whereas old granule cells facilitate pattern completion.* Cell, 2012. **149**(1): p. 188-201.
319. Clelland, C.D., et al., *A functional role for adult hippocampal neurogenesis in spatial pattern separation.* Science, 2009. **325**(5937): p. 210-3.
320. Park, E.H., et al., *Experience-Dependent Regulation of Dentate Gyrus Excitability by Adult-Born Granule Cells.* J Neurosci, 2015. **35**(33): p. 11656-66.

321. Dery, N., et al., *Adult hippocampal neurogenesis reduces memory interference in humans: opposing effects of aerobic exercise and depression.* Front Neurosci, 2013. **7**: p. 66.
322. Stark, S.M., et al., *A task to assess behavioral pattern separation (BPS) in humans: Data from healthy aging and mild cognitive impairment.* Neuropsychologia, 2013. **51**(12): p. 2442-9.
323. Kitamura, T., et al., *Adult neurogenesis modulates the hippocampus-dependent period of associative fear memory.* Cell, 2009. **139**(4): p. 814-27.
324. Snyder, J.S., et al., *Adult hippocampal neurogenesis buffers stress responses and depressive behaviour.* Nature, 2011. **476**(7361): p. 458-61.
325. Allen, K.M., S.J. Fung, and C.S. Weickert, *Cell proliferation is reduced in the hippocampus in schizophrenia.* Aust N Z J Psychiatry, 2016. **50**(5): p. 473-80.
326. Inta, D., et al., *Postnatal neurogenesis and dopamine alterations in early psychosis.* Recent Pat CNS Drug Discov, 2012. **7**(3): p. 236-42.
327. Aimone, J.B., et al., *Regulation and function of adult neurogenesis: from genes to cognition.* Physiol Rev, 2014. **94**(4): p. 991-1026.
328. Morris, A.M., et al., *Selective lesions of the dentate gyrus produce disruptions in place learning for adjacent spatial locations.* Neurobiol Learn Mem, 2012. **97**(3): p. 326-31.
329. Olah, M., et al., *Enhanced hippocampal neurogenesis in the absence of microglia T cell interaction and microglia activation in the murine running wheel model.* Glia, 2009. **57**(10): p. 1046-61.
330. Diamond, M.C., et al., *Effects of environment on morphology of rat cerebral cortex and hippocampus.* J Neurobiol, 1976. **7**(1): p. 75-85.
331. Kempermann, G., H.G. Kuhn, and F.H. Gage, *More hippocampal neurons in adult mice living in an enriched environment.* Nature, 1997. **386**(6624): p. 493-5.
332. Gould, E., *Serotonin and hippocampal neurogenesis.* Neuropsychopharmacology, 1999. **21**(2 Suppl): p. 46S-51S.
333. Stangl, D. and S. Thuret, *Impact of diet on adult hippocampal neurogenesis.* Genes Nutr, 2009. **4**(4): p. 271-82.
334. Gould, E., et al., *Neurogenesis in the neocortex of adult primates.* Science, 1999. **286**(5439): p. 548-52.
335. Maxwell, I.H., F. Maxwell, and L.M. Glode, *Regulated expression of a diphtheria toxin A-chain gene transfected into human cells: possible strategy for inducing cancer cell suicide.* Cancer Res, 1986. **46**(9): p. 4660-4.
336. Kuhn, H.G., H. Dickinson-Anson, and F.H. Gage, *Neurogenesis in the dentate gyrus of the adult rat: age-related decrease of neuronal progenitor proliferation.* J Neurosci, 1996. **16**(6): p. 2027-33.
337. Manganas, L.N., et al., *Magnetic resonance spectroscopy identifies neural progenitor cells in the live human brain.* Science, 2007. **318**(5852): p. 980-5.
338. Czeh, B., et al., *Stress-induced changes in cerebral metabolites, hippocampal volume, and cell proliferation are prevented by antidepressant treatment with tianeptine.* Proc Natl Acad Sci U S A, 2001. **98**(22): p. 12796-801.
339. Czeh, B., et al., *Chronic social stress inhibits cell proliferation in the adult medial prefrontal cortex: hemispheric asymmetry and reversal by fluoxetine treatment.* Neuropsychopharmacology, 2007. **32**(7): p. 1490-503.
340. Moreno-Villanueva, M. and A. Burkle, *Molecular consequences of psychological stress in human aging.* Exp Gerontol, 2015. **68**: p. 39-42.
341. Cameron, H.A. and E. Gould, *Adult neurogenesis is regulated by adrenal steroids in the dentate gyrus.* Neuroscience, 1994. **61**(2): p. 203-9.
342. Ge, S., et al., *GABA regulates synaptic integration of newly generated neurons in the adult brain.* Nature, 2006. **439**(7076): p. 589-93.

343. Malberg, J.E., et al., *Chronic antidepressant treatment increases neurogenesis in adult rat hippocampus.* J Neurosci, 2000. **20**(24): p. 9104-10.
344. Song, H., C.F. Stevens, and F.H. Gage, *Astroglia induce neurogenesis from adult neural stem cells.* Nature, 2002. **417**(6884): p. 39-44.
345. Toni, N. and S. Sultan, *Synapse formation on adult-born hippocampal neurons.* Eur J Neurosci, 2011. **33**(6): p. 1062-8.
346. Sultan, S., et al., *Synaptic Integration of Adult-Born Hippocampal Neurons Is Locally Controlled by Astrocytes.* Neuron, 2015. **88**(5): p. 957-972.
347. Vallieres, L., et al., *Reduced hippocampal neurogenesis in adult transgenic mice with chronic astrocytic production of interleukin-6.* J Neurosci, 2002. **22**(2): p. 486-92.
348. Zhao, C., W. Deng, and F.H. Gage, *Mechanisms and functional implications of adult neurogenesis.* Cell, 2008. **132**(4): p. 645-60.
349. Bonaguidi, M.A., et al., *In vivo clonal analysis reveals self-renewing and multipotent adult neural stem cell characteristics.* Cell, 2011. **145**(7): p. 1142-55.
350. Shen, Q., et al., *Endothelial cells stimulate self-renewal and expand neurogenesis of neural stem cells.* Science, 2004. **304**(5675): p. 1338-40.
351. Walton, N.M., et al., *Microglia instruct subventricular zone neurogenesis.* Glia, 2006. **54**(8): p. 815-25.
352. Marin-Teva, J.L., et al., *Microglia promote the death of developing Purkinje cells.* Neuron, 2004. **41**(4): p. 535-47.
353. Ueno, M., et al., *Layer V cortical neurons require microglial support for survival during postnatal development.* Nat Neurosci, 2013. **16**(5): p. 543-51.
354. Butovsky, O., et al., *Microglia activated by IL-4 or IFN-gamma differentially induce neurogenesis and oligodendrogenesis from adult stem/progenitor cells.* Mol Cell Neurosci, 2006. **31**(1): p. 149-60.
355. Zhao, C., et al., *Distinct morphological stages of dentate granule neuron maturation in the adult mouse hippocampus.* J Neurosci, 2006. **26**(1): p. 3-11.
356. Platel, J.C., K.A. Dave, and A. Bordey, *Control of neuroblast production and migration by converging GABA and glutamate signals in the postnatal forebrain.* J Physiol, 2008. **586**(16): p. 3739-43.
357. Ribeiro Xavier, A.L., et al., *A Distinct Population of Microglia Supports Adult Neurogenesis in the Subventricular Zone.* J Neurosci, 2015. **35**(34): p. 11848-61.
358. Aarum, J., et al., *Migration and differentiation of neural precursor cells can be directed by microglia.* Proc Natl Acad Sci U S A, 2003. **100**(26): p. 15983-8.
359. Jeong, H.K., et al., *Brain inflammation and microglia: facts and misconceptions.* Exp Neurobiol, 2013. **22**(2): p. 59-67.
360. Shigemoto-Mogami, Y., et al., *Microglia enhance neurogenesis and oligodendrogenesis in the early postnatal subventricular zone.* J Neurosci, 2014. **34**(6): p. 2231-43.
361. Battista, D., et al., *Neurogenic niche modulation by activated microglia: transforming growth factor beta increases neurogenesis in the adult dentate gyrus.* Eur J Neurosci, 2006. **23**(1): p. 83-93.
362. Sierra, A., et al., *Surveillance, phagocytosis, and inflammation: how never-resting microglia influence adult hippocampal neurogenesis.* Neural Plast, 2014. **2014**: p. 610343.
363. Terrando, N., et al., *Resolving postoperative neuroinflammation and cognitive decline.* Ann Neurol, 2011. **70**(6): p. 986-995.
364. Ekdahl, C.T., et al., *Inflammation is detrimental for neurogenesis in adult brain.* Proc Natl Acad Sci U S A, 2003. **100**(23): p. 13632-7.
365. Fujioka, H. and T. Akema, *Lipopolysaccharide acutely inhibits proliferation of neural precursor cells in the dentate gyrus in adult rats.* Brain Res, 2010. **1352**: p. 35-42.
366. Monje, M.L., H. Toda, and T.D. Palmer, *Inflammatory blockade restores adult hippocampal neurogenesis.* Science, 2003. **302**(5651): p. 1760-5.

367. Chen, Z. and T.D. Palmer, *Differential roles of TNFR1 and TNFR2 signaling in adult hippocampal neurogenesis.* Brain Behav Immun, 2013. **30**: p. 45-53.
368. Frielingsdorf, H., et al., *Nerve growth factor promotes survival of new neurons in the adult hippocampus.* Neurobiol Dis, 2007. **26**(1): p. 47-55.
369. Miller, M.W. and R.S. Nowakowski, *Use of bromodeoxyuridine-immunohistochemistry to examine the proliferation, migration and time of origin of cells in the central nervous system.* Brain Res, 1988. **457**(1): p. 44-52.
370. Lieberwirth, C. and Z. Wang, *The social environment and neurogenesis in the adult Mammalian brain.* Front Hum Neurosci, 2012. **6**: p. 118.
371. Scharfman, H., et al., *Increased neurogenesis and the ectopic granule cells after intrahippocampal BDNF infusion in adult rats.* Exp Neurol, 2005. **192**(2): p. 348-56.
372. Christie, B.R. and H.A. Cameron, *Neurogenesis in the adult hippocampus.* Hippocampus, 2006. **16**(3): p. 199-207.
373. Enikolopov, G., L. Overstreet-Wadiche, and S. Ge, *Viral and transgenic reporters and genetic analysis of adult neurogenesis.* Cold Spring Harb Perspect Biol, 2015. **7**(8): p. a018804.
374. Ming, G.L. and H. Song, *Adult neurogenesis in the mammalian central nervous system.* Annu Rev Neurosci, 2005. **28**: p. 223-50.
375. Galand, P. and C. Degraef, *Cyclin/PCNA immunostaining as an alternative to tritiated thymidine pulse labelling for marking S phase cells in paraffin sections from animal and human tissues.* Cell Tissue Kinet, 1989. **22**(5): p. 383-92.
376. Kee, N., et al., *The utility of Ki-67 and BrdU as proliferative markers of adult neurogenesis.* J Neurosci Methods, 2002. **115**(1): p. 97-105.
377. Sasmono, R.T. and E. Williams, *Generation and characterization of MacGreen mice, the Cfs1r-EGFP transgenic mice.* Methods Mol Biol, 2012. **844**: p. 157-76.
378. Feil, S., N. Valtcheva, and R. Feil, *Inducible Cre mice.* Methods Mol Biol, 2009. **530**: p. 343-63.
379. Grivennikov, S.I., et al., *Distinct and nonredundant in vivo functions of TNF produced by t cells and macrophages/neutrophils: protective and deleterious effects.* Immunity, 2005. **22**(1): p. 93-104.
380. Blasi, E., et al., *Immortalization of murine microglial cells by a v-raf/v-myc carrying retrovirus.* J Neuroimmunol, 1990. **27**(2-3): p. 229-37.
381. Garcia-Moreno, F., et al., *CLoNe is a new method to target single progenitors and study their progeny in mouse and chick.* Development, 2014. **141**(7): p. 1589-98.
382. Schindelin, J., et al., *Fiji: an open-source platform for biological-image analysis.* Nat Methods, 2012. **9**(7): p. 676-82.
383. Valente, A.J., et al., *A simple ImageJ macro tool for analyzing mitochondrial network morphology in mammalian cell culture.* Acta Histochem, 2017. **119**(3): p. 315-326.
384. Arganda-Carreras, I., et al., *3D reconstruction of histological sections: Application to mammary gland tissue.* Microsc Res Tech, 2010. **73**(11): p. 1019-29.
385. Bustin, S.A., et al., *The MIQE guidelines: minimum information for publication of quantitative real-time PCR experiments.* Clin Chem, 2009. **55**(4): p. 611-22.
386. Strober, W., *Trypan Blue Exclusion Test of Cell Viability.* Curr Protoc Immunol, 2015. **111**: p. A3 B 1-3.
387. Sierra, A., et al., *Microglia derived from aging mice exhibit an altered inflammatory profile.* Glia, 2007. **55**(4): p. 412-24.
388. Sugita, K., et al., *Expression of orphan G-protein coupled receptor GPR174 in CHO cells induced morphological changes and proliferation delay via increasing intracellular cAMP.* Biochem Biophys Res Commun, 2013. **430**(1): p. 190-5.
389. Uwamizu, A., et al., *Lysophosphatidylserine analogues differentially activate three LysoPS receptors.* J Biochem, 2015. **157**(3): p. 151-60.

390. Egner, A., S. Jakobs, and S.W. Hell, *Fast 100-nm resolution three-dimensional microscope reveals structural plasticity of mitochondria in live yeast.* Proc Natl Acad Sci U S A, 2002. **99**(6): p. 3370-5.
391. Rossignol, R., et al., *Energy substrate modulates mitochondrial structure and oxidative capacity in cancer cells.* Cancer Res, 2004. **64**(3): p. 985-93.
392. Chen, H., A. Chomyn, and D.C. Chan, *Disruption of fusion results in mitochondrial heterogeneity and dysfunction.* J Biol Chem, 2005. **280**(28): p. 26185-92.
393. Chen, H., et al., *Mitochondrial fusion is required for mtDNA stability in skeletal muscle and tolerance of mtDNA mutations.* Cell, 2010. **141**(2): p. 280-9.
394. Ziv, Y., et al., *Immune cells contribute to the maintenance of neurogenesis and spatial learning abilities in adulthood.* Nat Neurosci, 2006. **9**(2): p. 268-75.
395. de Hoz, L. and S.J. Martin, *Double dissociation between the contributions of the septal and temporal hippocampus to spatial learning: the role of prior experience.* Hippocampus, 2014. **24**(8): p. 990-1005.
396. Chertoff, M., et al., *Neuroprotective and neurodegenerative effects of the chronic expression of tumor necrosis factor alpha in the nigrostriatal dopaminergic circuit of adult mice.* Exp Neurol, 2011. **227**(2): p. 237-51.
397. Biber, K., et al., *Interleukin-6 upregulates neuronal adenosine A1 receptors: implications for neuromodulation and neuroprotection.* Neuropsychopharmacology, 2008. **33**(9): p. 2237-50.
398. Shieh, C.H., et al., *P2X7-dependent, but differentially regulated release of IL-6, CCL2, and TNF-alpha in cultured mouse microglia.* Glia, 2014. **62**(4): p. 592-607.
399. Masuch, A., et al., *Mechanism of microglia neuroprotection: Involvement of P2X7, TNFalpha, and valproic acid.* Glia, 2016. **64**(1): p. 76-89.
400. Friedle, S.A., et al., *The P2X7-Egr pathway regulates nucleotide-dependent inflammatory gene expression in microglia.* Glia, 2011. **59**(1): p. 1-13.
401. Hide, I., et al., *Extracellular ATP triggers tumor necrosis factor-alpha release from rat microglia.* J Neurochem, 2000. **75**(3): p. 965-72.
402. Serhan, C.N. and J. Savill, *Resolution of inflammation: the beginning programs the end.* Nat Immunol, 2005. **6**(12): p. 1191-7.
403. Jinushi, M., et al., *MFG-E8-mediated uptake of apoptotic cells by APCs links the pro- and antiinflammatory activities of GM-CSF.* J Clin Invest, 2007. **117**(7): p. 1902-13.
404. Iida, Y., et al., *Lysophosphatidylserine stimulates chemotactic migration of colorectal cancer cells through GPR34 and PI3K/Akt pathway.* Anticancer Res, 2014. **34**(10): p. 5465-72.
405. Bennett, M.L., et al., *New tools for studying microglia in the mouse and human CNS.* Proc Natl Acad Sci U S A, 2016. **113**(12): p. E1738-46.
406. Hickman, S.E., et al., *The microglial sensome revealed by direct RNA sequencing.* Nat Neurosci, 2013. **16**(12): p. 1896-905.
407. Koguchi, Y. and K. Kawakami, *Cryptococcal infection and Th1-Th2 cytokine balance.* Int Rev Immunol, 2002. **21**(4-5): p. 423-38.
408. Olah, M., et al., *A transcriptomic atlas of aged human microglia.* Nat Commun, 2018. **9**(1): p. 539.
409. Mochly-Rosen, D. and A.S. Gordon, *Anchoring proteins for protein kinase C: a means for isozyme selectivity.* FASEB J, 1998. **12**(1): p. 35-42.
410. Allen, L.H. and A. Aderem, *A role for MARCKS, the alpha isozyme of protein kinase C and myosin I in zymosan phagocytosis by macrophages.* J Exp Med, 1995. **182**(3): p. 829-40.
411. Zheleznyak, A. and E.J. Brown, *Immunoglobulin-mediated phagocytosis by human monocytes requires protein kinase C activation. Evidence for protein kinase C translocation to phagosomes.* J Biol Chem, 1992. **267**(17): p. 12042-8.

412. Dieter, P. and H. Schwende, *Protein kinase C-alpha and -beta play antagonistic roles in the differentiation process of THP-1 cells.* Cell Signal, 2000. **12**(5): p. 297-302.
413. Tardif, M., et al., *Impaired protein kinase C activation/translocation in Epstein-Barr virus-infected monocytes.* J Biol Chem, 2002. **277**(27): p. 24148-54.
414. Xiao, Y., et al., *The atypical guanine nucleotide exchange factor Dock4 regulates neurite differentiation through modulation of Rac1 GTPase and actin dynamics.* J Biol Chem, 2013. **288**(27): p. 20034-45.
415. Schoneberg, T., et al., *Structural and functional evolution of the P2Y(12)-like receptor group.* Purinergic Signal, 2007. **3**(4): p. 255-68.
416. Nonaka, Y., T. Hiramoto, and N. Fujita, *Identification of endogenous surrogate ligands for human P2Y12 receptors by in silico and in vitro methods.* Biochem Biophys Res Commun, 2005. **337**(1): p. 281-8.
417. Tabata, K., et al., *The orphan GPCR GPR87 was deorphanized and shown to be a lysophosphatidic acid receptor.* Biochem Biophys Res Commun, 2007. **363**(3): p. 861-6.
418. Iwashita, M., et al., *Synthesis and evaluation of lysophosphatidylserine analogues as inducers of mast cell degranulation. Potent activities of lysophosphatidylthreonine and its 2-deoxy derivative.* J Med Chem, 2009. **52**(19): p. 5837-63.
419. Hosono, H., et al., *Phosphatidylserine-specific phospholipase A1 stimulates histamine release from rat peritoneal mast cells through production of 2-acyl-1-lysophosphatidylserine.* J Biol Chem, 2001. **276**(32): p. 29664-70.
420. Nikolova, S., et al., *Rac1-NADPH oxidase-regulated generation of reactive oxygen species mediates glutamate-induced apoptosis in SH-SY5Y human neuroblastoma cells.* Free Radic Res, 2005. **39**(12): p. 1295-304.
421. Swain, S., S. Beg, and S.M. Babu, *Liposheres as a Novel Carrier for Lipid Based Drug Delivery: Current and Future Directions.* Recent Pat Drug Deliv Formul, 2016. **10**(1): p. 59-71.
422. Arouri, A. and O.G. Mouritsen, *Membrane-perturbing effect of fatty acids and lysolipids.* Prog Lipid Res, 2013. **52**(1): p. 130-40.
423. Lands, W.E., *Metabolism of glycerolipides; a comparison of lecithin and triglyceride synthesis.* J Biol Chem, 1958. **231**(2): p. 883-8.
424. Shindou, H. and T. Shimizu, *Acyl-CoA:lysophospholipid acyltransferases.* J Biol Chem, 2009. **284**(1): p. 1-5.
425. Dale, D.C., L. Boxer, and W.C. Liles, *The phagocytes: neutrophils and monocytes.* Blood, 2008. **112**(4): p. 935-45.
426. Arts, R.J., et al., *Glutaminolysis and Fumarate Accumulation Integrate Immunometabolic and Epigenetic Programs in Trained Immunity.* Cell Metab, 2016. **24**(6): p. 807-819.
427. Morioka, S., et al., *Efferocytosis induces a novel SLC program to promote glucose uptake and lactate release.* Nature, 2018.
428. Pollard, J.W. and C.P. Stanners, *Characterization of cell lines showing growth control isolated from both the wild type and a leucyl-tRNA synthetase mutant of Chinese hamster ovary cells.* J Cell Physiol, 1979. **98**(3): p. 571-85.
429. Warburg, O., *On the origin of cancer cells.* Science, 1956. **123**(3191): p. 309-14.
430. Warburg, O., *[Origin of cancer cells].* Oncologia, 1956. **9**(2): p. 75-83.
431. Orihuela, R., C.A. McPherson, and G.J. Harry, *Microglial M1/M2 polarization and metabolic states.* Br J Pharmacol, 2016. **173**(4): p. 649-65.
432. Everts, B., et al., *Commitment to glycolysis sustains survival of NO-producing inflammatory dendritic cells.* Blood, 2012. **120**(7): p. 1422-31.
433. Youle, R.J. and A.M. van der Bliek, *Mitochondrial fission, fusion, and stress.* Science, 2012. **337**(6098): p. 1062-5.

434. Cribbs, J.T. and S. Strack, *Reversible phosphorylation of Drp1 by cyclic AMP-dependent protein kinase and calcineurin regulates mitochondrial fission and cell death.* EMBO Rep, 2007. **8**(10): p. 939-44.
435. Cherry, J.D., J.A. Olschowka, and M.K. O'Banion, *Are "resting" microglia more "m2"?* Front Immunol, 2014. **5**: p. 594.
436. Eckenhoff, M.F. and P. Rakic, *Nature and fate of proliferative cells in the hippocampal dentate gyrus during the life span of the rhesus monkey.* J Neurosci, 1988. **8**(8): p. 2729-47.
437. Kempermann, G., H.G. Kuhn, and F.H. Gage, *Experience-induced neurogenesis in the senescent dentate gyrus.* J Neurosci, 1998. **18**(9): p. 3206-12.
438. O'Kusky, J.R., P. Ye, and A.J. D'Ercole, *Insulin-like growth factor-I promotes neurogenesis and synaptogenesis in the hippocampal dentate gyrus during postnatal development.* J Neurosci, 2000. **20**(22): p. 8435-42.
439. Ziv, Y. and M. Schwartz, *Immune-based regulation of adult neurogenesis: implications for learning and memory.* Brain Behav Immun, 2008. **22**(2): p. 167-76.
440. Zagorska, A., et al., *Diversification of TAM receptor tyrosine kinase function.* Nat Immunol, 2014. **15**(10): p. 920-8.
441. Kreisel, T., et al., *Unique role for dentate gyrus microglia in neuroblast survival and in VEGF-induced activation.* Glia, 2018.
442. Jin, K., et al., *Vascular endothelial growth factor (VEGF) stimulates neurogenesis in vitro and in vivo.* Proc Natl Acad Sci U S A, 2002. **99**(18): p. 11946-50.
443. Licht, T., et al., *Reversible modulations of neuronal plasticity by VEGF.* Proc Natl Acad Sci U S A, 2011. **108**(12): p. 5081-6.
444. Ji, R., et al., *TAM receptors affect adult brain neurogenesis by negative regulation of microglial cell activation.* J Immunol, 2013. **191**(12): p. 6165-77.
445. Zelentsova, K., et al., *Protein S Regulates Neural Stem Cell Quiescence and Neurogenesis.* Stem Cells, 2017. **35**(3): p. 679-693.
446. Lledo, P.M., M. Alonso, and M.S. Grubb, *Adult neurogenesis and functional plasticity in neuronal circuits.* Nat Rev Neurosci, 2006. **7**(3): p. 179-93.
447. Barger, N., et al., *Microglia: An Intrinsic Component of the Proliferative Zones in the Fetal Rhesus Monkey (Macaca mulatta) Cerebral Cortex.* Cereb Cortex, 2018.
448. Noctor, S.C., et al., *Periventricular Microglial Cells Interact with Dividing Precursor Cells in the Nonhuman Primate and Rodent Prenatal Cerebral Cortex.* J Comp Neurol, 2018.
449. Fan, X. and A.Y. Rudensky, *Hallmarks of Tissue-Resident Lymphocytes.* Cell, 2016. **164**(6): p. 1198-1211.
450. Naik, S., et al., *Two to Tango: Dialog between Immunity and Stem Cells in Health and Disease.* Cell, 2018. **175**(4): p. 908-920.
451. Davies, L.C., et al., *Tissue-resident macrophages.* Nat Immunol, 2013. **14**(10): p. 986-95.
452. Burzyn, D., C. Benoist, and D. Mathis, *Regulatory T cells in nonlymphoid tissues.* Nat Immunol, 2013. **14**(10): p. 1007-13.
453. Chow, A., et al., *Bone marrow CD169+ macrophages promote the retention of hematopoietic stem and progenitor cells in the mesenchymal stem cell niche.* J Exp Med, 2011. **208**(2): p. 261-71.
454. Fujisaki, J., et al., *In vivo imaging of Treg cells providing immune privilege to the haematopoietic stem-cell niche.* Nature, 2011. **474**(7350): p. 216-9.
455. Sehgal, A., et al., *The role of CSF1R-dependent macrophages in control of the intestinal stem-cell niche.* Nat Commun, 2018. **9**(1): p. 1272.
456. Biton, M., et al., *T Helper Cell Cytokines Modulate Intestinal Stem Cell Renewal and Differentiation.* Cell, 2018. **175**(5): p. 1307-1320 e22.